

CLEAN FILAMENT WINDING:
PROCESS OPTIMISATION

by

NICHOLAS EDWARD HARRY
SHOTTON-GALE

A thesis submitted to
The University of Birmingham
for the degree of
DOCTOR OF PHILOSOPHY

School of Metallurgy and Materials
Sensors and Composites Group
The University of Birmingham
Dec 2012

UNIVERSITY OF
BIRMINGHAM

University of Birmingham Research Archive

e-theses repository

This unpublished thesis/dissertation is copyright of the author and/or third parties. The intellectual property rights of the author or third parties in respect of this work are as defined by The Copyright Designs and Patents Act 1988 or as modified by any successor legislation.

Any use made of information contained in this thesis/dissertation must be in accordance with that legislation and must be properly acknowledged. Further distribution or reproduction in any format is prohibited without the permission of the copyright holder.

ABSTRACT

This thesis reports on a modified wet-filament winding method, termed 'clean filament winding', which was developed to address multiple issues associated with the conventional method. The modified method comprised of a resin dispensing unit, static mixer and resin impregnation unit; these were incorporated to replace the practice of commonly used resin baths. Adaptations and developments of this method, such as impregnation modelling, fibre spreading and composite recycling were also used to further enhance the process.

It was shown that the modified method was able to produce filament wound tubes with comparable (or superior) mechanical properties when compared the conventional technique. It was also shown that the modified method had considerable economic viability whilst providing substantial environmental impact reductions. These results were attributed to the use of a patented resin impregnation method which reduced the amount of waste resin, solvent for cleaning and production-time needed to fabricate filament wound components.

This thesis concludes with details of a closed-loop composites recycling site-trial. Here, waste-fibre materials were used to manufacture filament wound tubes as replacements for cardboard tubes for the storage of glass-fibre fabrics.

DEDICATION

On completing this thesis, I would like to thank my mother for her passion, my father for his drive, my sister for her support and my girlfriend for her companionship. It was all truly appreciated.

ACKNOWLEDGEMENTS

The author wishes to offer his gratitude to Professor Gerard F Fernando for his continued support and drive throughout this research project. It was also truly appreciated.

This research would also not have been possible without the considerable support provided by Dr Surya Pandita, Mark Paget, Dr Venkata Machavaram, Sebastian Ballard, Dr Ramani Mahendran, Dr Liwei Wang, Frank Biddlestone and Dr Stephen Kukureka.

The financial and technical support provided by the Engineering and Physical Sciences Research Council (EPSRC), Technology Strategy Board (TSB) and E3 Comp (Halyard Precision Composites, Pultrex, Dispensing Liquid, Huntsman Advanced Materials, PPG and PD-Interglas) is also duly acknowledged.

TABLE OF CONTENTS

	Page
Table of Contents	iv
List of Figures	ix
List of Tables	xvii
List of Publications	xix
Glossary	xxi
1 Introduction	1
1.1 Introduction to Filament Winding	1
1.2 Issues and Constraints Associated with Conventional Filament Winding	5
1.3 Aims and Objectives	7
2 Literature Review	10
2.1 Filament Winding	11
2.2 Impregnation Modelling	25
2.2.1 Impregnation Modelling: Permeability	27
2.2.2 Impregnation Modelling: Dimensions of Fibre Bundles	30
2.2.3 Impregnation Modelling: Viscosity of Resin	31
2.2.4 Impregnation Modelling: Pressure	31
2.3 Fibre Spreading	34
2.3.1 Patent Review on Fibre Spreading Techniques	36

2.3.1.1	Mechanical Techniques for Fibre Spreading	37
2.3.1.2	Gas-based Techniques for Fibre Spreading	41
2.3.2	Summary of Fibre Spreading Review	43
2.4	EU Directives and Waste Disposal Legislation	44
2.5	Review of Thermoset Composite Recycling Methods	46
2.5.1	Thermal Composite Recycling Methods	46
2.5.2	Mechanical Composite Recycling Methods	50
2.5.3	Chemical Composite Recycling Methods	51
2.5.4	Re-use Composite Recycling Methods	52
2.6	Life Cycle Assessment (LCA)	53
2.6.1	Development of LCA as an Assessment Tool	53
2.6.2	Review of LCA studies	55
2.7	Conclusion of the Literature Review	62
3.	Experimental	64
3.1	Materials and Equipment	64
3.1.1	Reinforcing Fibres	64
3.1.2	Resin and Hardener	69
3.1.3	Manufacturing Equipment	70
3.1.3.1	Clean Filament Winding (CFW)	70
3.1.3.2	Conventional Filament Winding	78
3.1.4	Analysis Equipment	79
3.2	Calibration of the Resin Dispensing Unit	80
3.3	Development of a Clean Filament Winding Resin Impregnation Unit	81

3.3.1	Application of Impregnation Modelling	83
3.4	Fibre Spreading during Clean Filament Winding	86
3.5	Filament Winding Trials	89
3.5.1	In-house Clean Filament Winding	90
3.5.2	On-site Clean Filament Winding	90
3.5.3	Conventional Filament Winding	91
3.5.4	In-house Recycled-Clean Filament Winding	92
3.5.5	On-site Recycled-Clean Filament Winding	93
3.5.6	Manufacture of Composite Overwrapped Pressure Vessels (COPVs)	94
3.6	Evaluation Methods	97
3.6.1	Image Analysis	97
3.6.2	Resin Burn-off: Fibre Volume Fraction and Void Content	97
3.6.3	Hoop Tensile (Split-Disk) Strength	98
3.6.4	Inter-laminar Shear Strength	99
3.6.5	Lateral Compression Strength	100
3.6.6	Pressure Burst Strength of COPV's	101
3.6.7	Life Cycle Assessment (LCA)	102
3.6.7.1	Filament Winding LCA Template	105
3.6.8	Life Cycle Cost (LCC)	109
3.6.8.1	Life Cycle Cost of Filament Winding Methods	109
4.	Results and Discussion	112
4.1	Materials	112
4.1.1	Reinforcing Fibres	112

4.1.2	Resin and Hardener	121
4.2	Clean Filament Winding	122
4.3	Recycled-Clean Filament Winding	124
4.4	Calibration of the Resin Dispensing Unit	127
4.5	Development of a Clean Filament Winding Resin Impregnation Unit	131
4.5.1	Application of Impregnation Modelling	133
4.6	Fibre Spreading during Clean Filament Winding	136
4.7	Filament Winding Trials	140
4.7.1	In-house Clean Filament Winding	140
4.7.2	On-site Clean Filament Winding	142
4.7.3	Conventional Filament Winding	146
4.7.4	In-house Recycled-Clean Filament Winding	149
4.7.5	On-site Recycled-Clean Filament Winding	153
4.7.6	Manufacture of Composite Overwrapped Pressure Vessels (COPVs)	157
4.8	Evaluation Methods	159
4.8.1	Resin Burn-off: Fibre Volume Fraction and Void Content	159
4.8.2	Hoop Tensile (Split-disk) Strength	166
4.8.3	Inter-laminar Shear Strength	173
4.8.4	Lateral Compression Strength	179
4.8.5	Pressure Burst Strength of Composite Overwrapped Pressure Vessels (COPVs)	188
4.8.6	Life Cycle Assessment (LCA)	191

4.8.7	Life Cycle Cost (LCC)	197
4.8.8	Site-trial of Waste-fibre Tubes	205
5.	Conclusions	207
5.1	Recommendations for Future Research	210
6.	Appendix	212
6.1	Appendix A: Alternative Mechanical Spreading Methods	212
6.2	Appendix B: Testing Load/Displacement Curves	217
7.	List of Definitions and/or Abbreviations	219
8.	References	223

LIST OF FIGURES

Figure 1. Schematic illustration of the conventional filament winding process.

Figure 2. Multi-component filament winding. Here, four carbon fibre pressure vessels (A) are filament wound simultaneously.

Figure 3. A schematic view of meniscus shaped flow advancement.

Figure 4. A diagram showing void formation caused by differential macropore and micropore flow.

Figure 5. Image of a composite test piece after hoop tensile (split-disk) strength testing.

Figure 6. Image showing the hoop tensile (split-disk) testing procedure employed by Sobrinho et al.

Figure 7. Image of a failed hoop tensile (split-disk) testing sample presented by Sobrinho et al.

Figure 8. Schematic illustration presenting an overview of the various models that were considered for the design of the resin impregnation unit.

Figure 9. Capillary pressure plotted against fibre volume fraction.

Figure 10. Regions of behaviour in pin impregnation: (1) entry; (2) impregnation; (3) contact; and (4) exit.

Figure 11. An illustration of fibre spreading. (A) An un-spread fibre bundle; and (B) a spread fibre bundle. Here w and T_0 are the fibre bundle width and thickness respectively.

Figure 12. Simulation of the effect of fibre spreading on fibre bundle thickness.

Figure 13. Schematic illustration of mechanical fibre spreading (transverse view). (A) fibre tow; and (B) spreading pin.

Figure 14. Schematic illustration of mechanically-induced fibre spreading (idealised view): (a) before fibre spreading; and (b) after fibre spreading.

Figure 15. Schematic illustration of an 'S-wrap' fibre spreading set-up.

Figure 16. Schematic illustration of gas-based fibre spreading. The highlighted components are: (A) spreading fixtures; and (B) spread fibres.

Figure 17. Schematic diagram of side-vacuum gas-based fibre spreading.

Figure 18. Overview of recycling processes.

Figure 19. Photograph of the as-received E-glass fibres on conventional bobbins.

Figure 20. Photograph of the waste slittings showing the relative dimensions of the warp and weft fibres.

Figure 21. Photograph of a fibre bobbin with waste slittings.

Figure 22. Photograph of direct-loom waste fibres showing the relative dimensions of the warp and weft fibres.

Figure 23. Photograph of a bobbin with direct-loom waste.

Figure 24. Schematic illustration of the clean filament winding process.

Figure 25. Photograph of: (A) a static mixer; and (B) a static mixing element.

Figure 26. Schematic illustration of the clean filament winding resin delivery system.

Figure 27. Photographs of: (a) the air circulating oven; and (b) the mandrel extraction system used during the in-house CFW trials.

Figure 28. Photograph of the conventional 2-axis filament winding machine used during the industrial site trials in Portsmouth, UK.

Figure 29. Photograph of the retrofitted CFW equipment onto the conventional 2-axis filament winding machine.

Figure 30. Photographs of: (a) the oven; and (b) the mandrel extraction unit used during the site trials.

Figure 31. Photograph of the conventional filament winding resin bath.

Figure 32. Schematic illustration of the resin impregnation unit.

Figure 33. Mechanical fibre spreading station.

Figure 34. Photograph of the custom-made bobbins used during the industrial site-trials.

Figure 35. Photograph of aluminium COPV liners.

Figure 36. Photographs of: (a) custom-made end-fittings; and (b) an aluminium liner held in-place on the in-house filament winding machine.

Figure 37. Photograph of the hoop-tensile test fixture.

Figure 38. Photograph of the inter-laminar shear test fixture.

Figure 39. Photograph of the lateral compression test fixture with a cardboard tube ring in-situ.

Figure 40. Schematic illustration of the COPV pressure burst test method.

Figure 41. Photographs of: (a) a steel end-nozzle mounted on a COPV; (b) the controlling unit for the high-pressure hydrostatic water pump; and (c) the underground water chamber.

Figure 42. Schematic illustration of the LCA template developed during this study.

Figure 43. LCA Level-3 plan: Input transportation.

Figure 44. LCA Level-2 plan: Filament winding.

Figure 45. LCA Level-2 plan: Cleaning operation.

Figure 46. LCA Top-level plan: Filament winding.

Figure 47. Image analysis micrographs of in-house CFW tube sections.

Figure 48. Image analysis micrographs of conventional filament wound tube sections.

Figure 49. Image analysis micrographs of on-site CFW tube sections (7 m/min).

Figure 50. Image analysis micrographs of on-site CFW tube sections (21 m/min).

Figure 51. Image analysis micrographs of in-house R-CFW (waste slittings) tube sections.

Figure 52. SEM micrographs of the waste slittings (x50 magnification).

Figure 53. SEM micrographs of the waste slittings (x100 magnification).

Figure 54. SEM micrographs of the waste slittings (x500 magnification).

Figure 55. Photographs of varying quality waste slittings.

Figure 56. Image analysis micrographs of R-CFW (direct-loom waste) tube sections.

Figure 57. SEM micrographs of the direct-loom waste (x50 magnification).

Figure 58. SEM micrographs of the direct-loom waste (x100 magnification).

Figure 59. SEM micrographs of the direct-loom waste (x500 magnification).

Figure 60. Photographs of varying quality direct-loom waste fibres.

Figure 61. Cardboard tube in-use.

Figure 62. Photographs of end-of-life deformed cardboard tubes.

Figure 63. Comparison of measured and “predicted” volumes of the epoxy resin (LY3505) at four dispensing rates.

Figure 64. Comparison of measured and “predicted” volumes of the amine hardener (XB3403) at four dispensing rates.

Figure 65. Comparison of measured and “predicted” volumes of the epoxy/amine resin system (LY3505/XB3403) at 12.5 rpm.

Figure 66. Simulation of the model proposed by Foley and Gillespie.

Figure 67. Simulation of the model proposed by Gaymans and Wevers.

Figure 68. A response plot showing the influence of Level 1 and Level 2 variations on the four input parameters.

Figure 69. Photograph showing: (A) an as-received fibre tow; and (B) a fibre tow after fibre spreading.

Figure 70. A graph showing the effect of fibre tow thickness variations on the transverse impregnation rates.

Figure 71. Photographs of: (a) a filament wound tube in production via the in-house CFW method; and (b) an example CFW tube.

Figure 72. Photographs of: (a) the spreading station and resin impregnation unit in-use during the on-site trials; (b) impregnated fibre tows being applied to a rotating mandrel (106 mm diameter); and (c) a 1.5 m on-site CFW tube.

Figure 73. Photographs of: (a) the resin-bath used during conventional filament winding; (b) the impregnated fibres being wound on to the rotating mandrel; and (c) a 1.5 m conventional filament wound tube.

Figure 74. Photographs highlighting the issues associated with conventional filament winding.

Figure 75. Photographs of: (a) a 100 mm inner-diameter waste slittings tube manufactured by the in-house R-CFW method; and (b) two 100 mm inner-diameter direct-loom waste tubes manufactured by the in-house R-CFW method.

Figure 76. Photographs of the hoop-wound waste slittings tube during on-site production.

Figure 77. Photographs of the hoop-wound waste slittings tube.

Figure 78. Photographs of the angle-wound waste slittings tube during on-site production.

Figure 79. Photographs of the angle-wound waste slittings tube.

Figure 80. Comparison of hoop-wound and angle-wound wall thickness dimensions of on-site R-CFW tubes.

Figure 81. Photograph of the COPVs manufactured with the in-house CFW method.

Figure 82. Fibre volume fraction and void content results.

Figure 83. Conventional filament wound tube sections with an outer surface resin film present.

Figure 84. Summary of hoop tensile (split-disk) strength results.

Figure 85. Photographs of hoop tensile (split-disk) failed samples manufactured by the in-house CFW process.

Figure 86. Photographs of hoop tensile (split-disk) failed samples.

Figure 87. Photograph and SEM images of a failed waste slittings hoop tensile (split-disk) test sample.

Figure 88. Photograph and typical SEM images of a failed direct-loom waste hoop tensile (split-disk) test sample.

Figure 89. Summary of inter-laminar shear strength results.

Figure 90. Photographs of inter-laminar shear failed samples; in-house CFW samples.

Figure 91. Photographs of inter-laminar shear failed samples.

Figure 92. Photographs of inter-laminar shear failed samples; R-CFW (waste slittings) and R-CFW (direct-loom waste).

Figure 93. Summary of lateral compression strength results.

Figure 94. Photographs of failed lateral compression samples; in-house CFW.

Figure 95(a). Photographs of failed lateral compression samples: conventional filament winding.

Figure 95(b). Photographs of failed lateral compression samples: on-site CFW (7 m/min).

Figure 95(c). Photographs of lateral compression failed samples: on-site CFW (21 m/min).

Figure 96. Photographs of lateral compression failed samples.

Figure 97. Photograph of the lateral compression test fixture.

Figure 98. Pressure burst strengths of overwrapped COPVs.

Figure 99. Photographs of burst COPV's.

Figure 100. Radar plot comparing the environmental impact potentials of conventional and CFW.

Figure 101. Radar plot comparing the environmental impact potentials of conventional, CFW and R-CFW (waste slittings).

Figure 102. Radar plot comparing the environmental impact potentials of conventional, CFW and R-CFW (DLW).

Figure 103. Overall environmental impact reductions achieved by the CFW and R-CFW methods in comparison to conventional filament winding.

Figure 104. Life cycle cost output data.

Figure 105. Life cycle cost simulations for R-CFW (WS): 'expensive'.

Figure 106. Life cycle cost simulations for R-CFW (WS): 'intermediate'.

Figure 107. Life cycle cost simulations for R-CFW (WS): 'cheap'.

LIST OF TABLES

- Table 1.** Overview of filament winding components and manufacturers.
- Table 2.** Summary of mandrel systems used during filament winding.
- Table 3.** A summary of test methods used to assess filament wound composites.
- Table 4.** Comparison of fibre volume fractions produced by composite manufacturing methods.
- Table 5.** An overview of selected publications on hoop tensile strengths.
- Table 6.** Summary of selected models reported in the literature that considered axial permeability.
- Table 7.** Selection of models which predict transverse permeability.
- Table 8.** Summary of selected papers and patents on fibre spreading methods.
- Table 9.** A summary of thermal recycling methods and references.
- Table 10.** Summary of chemical recycling methods and references.
- Table 11.** Summary of natural fibre LCA studies and references.
- Table 12.** Summary of selected papers that have discussed the LCA of materials in the automotive industry.
- Table 13.** Overall ratings from 'Green guide to Composites'.
- Table 14.** Properties of E-glass fibres (EC15 1200 Tex).
- Table 15.** Input factors for the L₁₆ Taguchi analysis.
- Table 16.** L₁₆ Taguchi array.
- Table 17.** LCA input and output data for the production of 10 tubes.
- Table 18.** LCC input and output data for the production of 10 tubes.
- Table 19.** Dispensed volumes of the epoxy resin, amine hardener and mixed epoxy resin (LY3505/XB3403).

Table 20. Summary results of impregnation modelling.

Table 21. Calculation of the average spreading values from the L₁₆ Taguchi analysis.

Table 22. ANOVA analysis with a confidence level of 95%.

Table 23. Waste slittings wall thickness data.

Table 24. Relative wall thickness dimensions of the on-site waste-fibre filament wound tubes.

Table 25. Fibre volume fraction and void content results.

Table 26. Hoop tensile (split-disk) strength results.

Table 27. Inter-laminar shear strength results.

Table 28. Lateral compression strength results.

Table 29. Summary of COPV pressure burst strength results.

Table 30. Potential environmental impact data.

Table 31. Life cycle cost output data for the manufacture of a 3 meter filament wound tube via: (i) in-house CFW; (ii) conventional filament winding; and (iii) in-house R-CFW.

Table 32. Simulated life cycle cost output data for On-site R-CFW (WS) with three winding conditions: (i) 'expensive'; (ii) 'intermediate'; and (iii) 'cheap'.

Table 33. LCC output data for cardboard tubes.

LIST OF PUBLICATIONS

Book chapter:

Shotton-Gale, N., Harris, D., Pandita, S.D., Paget, M.A., Allen, J.A. and Fernando, G.F. (2010) 'Clean and environmentally friendly wet-filament winding' *Management, Recycling and Reuse of Waste Composites*. Woodhead Publishing in Materials, Chapter 13, pp. 329-368.

Journal papers:

Pandita, S.D., Irfan, M.S., Machavaram, V.R., **Shotton-Gale, N.**, Mahendran, R.S., Wait, C.F., Paget, M.A., Harris, D., Leek, C. and Fernando, G.F. (2012) . (2012) ns: (house CFW; (ii) conventional filament winding; and (iii) *Journal of Composite Materials*, pp 1-12.

Irfan, M.R., Machavaram, V.R., Mahendran, R.S., **Shotton-Gale, N.**, Wait, C.F., Paget, M.A., Hudson, M. and Fernando, G.F. (2012) do, G.F. (2012) . (2012) ns: (house CFW; (ii) concept and simulations' lateral spreading of a fibre bundle via mechanical means' *Journal of Composite Materials*, Vol 46, Issue 3, pp. 311-330.

Patent:

Fernando, G.F., Pandita, S.D., Paget, M.A. and **Shotton-Gale, N.** (2011) US Patent Number: 2011/0300301 A. and ns' *Journal of Composite Materials*, Vol 4

Conference proceedings:

Shotton-Gale, N., Pandita, S.D., Paget, M., Wait, C., Allen, J.A., Harris, D. and Fernando, G.F. (2009) ando, G.F. (2009) Wait, C., Allen, J.A., Harris, D. and Ferf CompositlCCM 17, Edinburgh, Scotland.

Shotton-Gale, N., Paget, M., Smith, C., Jameson, N., Wang, L., Malik, S., Burns, J., Biddlestone, F., Prasad, A., Harris, D., Machavaram, V., Mahendran, R. and Fernando, G.F. (2010) 'An investigation into techniques to fabricate highly aligned short-fibre prepregs' SAMPE Europe, Paris, France.

Smith, C., **Shotton-Gale, N.**, Wait, C., Paget, M., Harris, D., Machavaram, V., Wang, L., James, J., Price, R. and Fernando, G.F. (2010) 'Manufacture and evaluation of filament wound tubes from loom (weaving) waste', SAMPE Europe, Paris, France.

GLOSSARY

Acidification potential: A reduction in the pH of soil or water as a result of the transformation of air pollutants into acids.

Autoclaving: A composite manufacturing process which involves the curing of a component under vacuum and heat simultaneously.

Axial flow: Resin flow in the general direction of the parallel fibres

Curing: A process by which a resin mixture solidifies into a permanent structure.

Eutrophication potential: Also known as 'overfertilisation', is the enrichment of nutrients in aquatic or terrestrial environments which disrupt the environmental conditions of numerous ecosystems.

Exotherming: A chemical reaction or process that releases energy, usually in the form of heat.

Fibre bobbin: A spool for storing continuous reinforcing fibres.

Fibre impregnation: A process where a mixed resin system is applied to a fibre tow to form a composite component.

Fibre tow (or bundle): A collection of individual fibre filaments in parallel alignment.

Fibre volume fraction: The percentage of fibre in a composite component.

Freshwater aquatic ecotoxicity potential: The impact of toxic substances emitted to freshwater aquatic ecosystems.

Global warming potential: The impact of green-house gas emissions on the environment.

Human toxicity potential: The impacts on human health produced by toxic components emitted to the environment.

Macropore flow: Flow of resin between multiple fibre tows.

Mandrel: A forming tool which dictates the shape of a composite.

Marine aquatic ecotoxicity potential: The impact of toxic substances emitted to marine aquatic ecosystems.

Micropore flow: Flow of resin in-between the individual filaments of a fibre tow.

Ozone layer depletion potential: The ability of a set of chemicals to destroy ozone gases.

Photochemical ozone creation potential: The production of ozone gases at ground-level.

Pot-life: The length of time that a mixed resin system remains at a viscosity which will allow processing.

Resin system: A mixed mass of resin and hardener components.

Stoichiometric ratio: The desired ratio of the individual components of a resin system.

Terrestrial ecotoxicity potential: The emission of toxic chemicals into terrestrial atmospheres.

Thermoset: A polymeric resin system which forms a hardened plastic material upon curing.

Transeverse flow: Flow of resin through a tow which is perpendicular to parallel nature of the fibres.

Void content: The percentage of a composite which consists of air or gas which has been trapped inside the component.

CHAPTER 1: INTRODUCTION

1.1 Introduction to Filament Winding

In recent decades, much attention has been dedicated to the utilisation of fibre reinforced composites in various engineering sectors [1,2,3]. The desire to use these materials is based on their high stiffness-to-weight and strength-to-weight ratios. Due to their popularity in numerous applications [4,5,6], it was estimated that over 4 million tonnes of fibre-reinforced composites were produced in 2010 [7,8]. Amongst this 4 million tonnes, approximately 300,000 tonnes was fabricated via a method termed 'filament winding' [7,9].

In general, the method of filament winding can be performed with a number of processing techniques, including: (i) resin bath-based impregnation [10]; (ii) wet- and dry-tape winding [11,12,13]; (iii) electrostatic deposition [14,15]; (iv) prepreg winding [4,16]; and (v) laser-assisted impregnation [11,17,18]. The resin bath-based impregnation method is the predominant technique used in industry and generally involves the use of thermosetting resin systems [4,5,6]. In this study, the term "resin system" is used to describe an intimately mixed resin and hardener.

A schematic illustration of conventional wet-filament winding, incorporating a resin bath-based impregnation process, is shown in Figure 1. With reference to Figure 1, the reinforcing fibre tows (A) from creels or bobbins (B) are fed through a tensioning system (C) and into a resin bath (D). Inside the resin

both the fibres are generally manipulated by a resin drum-roller and are impregnated with a resin system. Here, the individual components of the resin system are mixed manually in the required stoichiometric proportions and poured into the resin bath (D). The impregnated fibres (E) are then fed through a traversing carriage (F) which deposits the fibres in a pre-determined fashion along the length of a rotating mandrel (G). Here, the winding angle of the fibres can be controlled as a function of traverse rate and rotation speed of the mandrel. For the remaining sections of the current study, wet-filament winding shall be referred to as conventional filament winding.

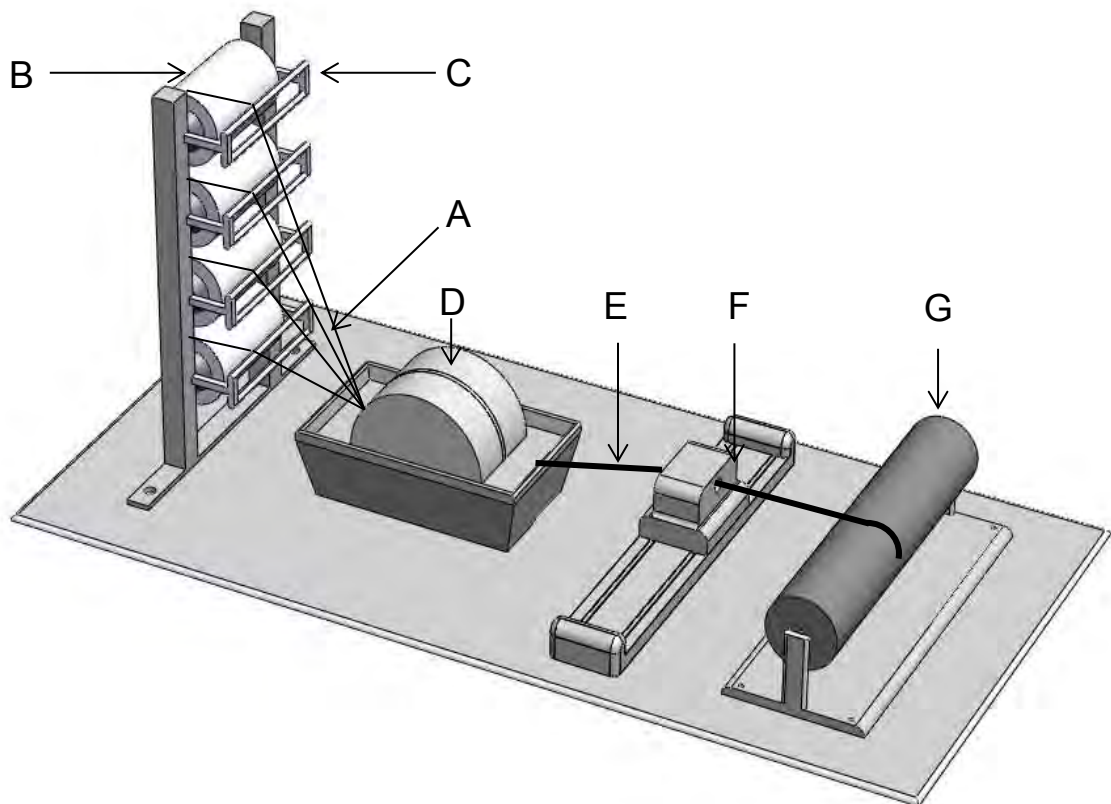


Figure 1. Schematic illustration of the conventional filament winding process.

(See text for details of highlighted components)

Once the required amounts of impregnated fibre are deposited, the assembly is transferred to an oven and cured. The curing temperature and duration is dependent on the resin system used. Details of the main components of Figure 1 are discussed below.

(A) Reinforcing fibres: The reinforcements, in the form of continuous fibres, can consist of a wide-range of materials, for example; glass, carbon, aramid or polyethylene [19,20]. The use of a particular type of reinforcing fibre is dependent on the desired specifications of the end product i.e. carbon fibres are generally used for lightweight and high-strength applications.

The presence of a 'binder' in the fibre bundles can also be an important factor. The function of the binder is to: (i) lubricate the fibres to minimize abrasion damage during production; (ii) act as a bonding agent to hold the tow filaments together; and (iii) influence the wettability or receptiveness of the resin system towards the reinforcement [21].

(B) Bobbins: The reinforcements can be supplied on bobbins where the fibres are drawn from the centre or outer-circumference. The bobbins with centre-drawn, or 'centre-pull', fibres are the most common for production processes such as filament winding.

(C) Tensioning and guiding systems: Tensioning and guiding systems are predominantly used to maintain fibre 'control' during production. By adjusting fibre tension it is possible to control the deposition accuracy of the fibres onto the rotating mandrel as well as the fibre volume fraction of the component and hence mechanical properties [4,22,23]. For example, Mertiny and Ellyin [23]

and Cohen *et al.* [24] demonstrated that variations in winding tension can produce an increase in composite loading capabilities.

(D) Resin bath: Resin baths (~ 5 litre capacity) are generally used to achieve fibre impregnation [4]. Here, the resin is normally mixed manually and deposited into the bath. In general, thermosetting resins, for example epoxy resins, are used during the conventional filament winding method [25,26,27,28].

(E) Resin-impregnated fibre bundles: Once impregnated, the reinforcing fibres have any excess resin removed by a 'doctor-blade' (incorporated into the resin bath) before they are transferred to the rotating mandrel. By using a doctor-blade it is possible to control the volume of resin that is 'picked-up' in the resin bath.

(F) Traversing carriage: The traversing carriage is used to deposit the impregnated-fibres in a pre-determined fashion onto the rotating mandrel. In general, deposition can occur in three main forms: (i) hoop; (ii) helical (angle); or (iii) polar winding [4]. In many publications, the deposition (winding) angle has been shown to be an important factor when fabricating filament wound composites [4,29,30,31,32,33]. For example, Kaynak *et al.* [34] presented hoop tensile (split-disk) strength results which showed that from choosing the appropriate winding angle, the mechanical strength of a component can be increased from ~ 10 MPa up to 850 MPa.

(G) Mandrel: Once cured (cross-linked), the mandrel is normally removed from the composite via conventional extraction systems. However, certain

applications allow/require the mandrel to be built into the final component [5]. A discussion of the various mandrel systems which have been used to date is presented in the following section.

From reviewing the above-discussion, it can be noted that there are various issues and constraints associated with conventional filament winding. The following section presents a review of these issues.

1.2 Issues and Constraints Associated with Conventional Filament Winding

There are a number of issues associated with conventional filament winding. The following section presents a detailed discussion of these points.

(i) Pot-life of the pre-mixed resin system: Mixed resin systems have a finite pot-life, after which the viscosity of the resin increases and the fibre impregnation process becomes progressively more difficult. The limited pot-life also means that there is a possibility of the resin system setting or cross-linking into a solid in the processing equipment. The cross-linked resin has to be removed prior to the resumption of production. The removal of the cross-linked resin from the processing equipment can be a tedious, time-consuming and costly operation.

Furthermore, as the ambient temperature can influence the viscosity and cross-linking rate of thermosetting resins, the limited pot-life also means that low-temperature-curable resins are not generally suitable for conventional filament winding.

(ii) Solvents: A major issue with conventional filament winding is the need for the equipment to be cleaned thoroughly with a copious volume of solvent at the end of each production run. This results in the need to recover the solvent prior to disposal of the waste resin and for adequate ventilation and personal protective equipment for the workforce. Legislation also dictates the exposure limits for the workforce with regards to specified chemicals and solvents.

(iii) Resin bath: The resin and hardener are weighed and mixed manually prior to transferral to the resin bath. During filament winding, the resin bath has to be replenished manually. Open-top resin baths can also result in significant emissions of low-molecular weight components from the resin system to the atmosphere.

(iv) Excess resin: The excess resin remaining in the bath after a filament winding operation is typically transferred to a disposable container and allowed to cross-link to a solid before disposal. Precautions have to be taken to avoid storing or cross-linking a large volume of mixed resin in a single operation as this can result in the resin exotherming. In other words, the cross-linking reaction can become auto-catalytic as it proceeds. This can result in a significant increase in the temperature of the resin system, leading to thermal degradation and emission of potentially toxic gaseous by-products. The volume of waste resin generated in the conventional filament winding process will depend on a number of factors, for example: (i) the capacity of the resin bath used; and (ii) on-site manufacturing practices i.e. over-impregnation of the reinforcing tows.

Due to these issues and constraints, a modified filament winding method termed 'clean filament winding' (CFW) was developed in this study; the following section outlines the aims and objectives.

1.3 Aims and Objectives

This study reports on the development of a modified filament winding method termed 'clean filament winding' (CFW). The aims and objectives of this study were as follows:

- i. To design, manufacture and evaluate a resin impregnation unit to enable the realisation of the CFW concept.

This philosophy involves the use of a resin dispensing unit where the resin and hardener are stored separately and pumped on-demand through a static mixer to a custom-designed resin impregnation unit. In the resin impregnation unit, the fibres are impregnated in-flight.

- ii. To manufacture and compare the mechanical and physical properties of filament wound tubes produced via a conventional resin bath and CFW methods.

Filament wound tubes were manufactured in-house and on-site and then evaluated via the following procedures: (a) image analysis; (b) resin burn-off;

(c) scanning electron microscopy (SEM); (d) hoop tensile (split-disk) strength testing; (e) inter-laminar shear strength testing; and (f) lateral compression strength testing.

iii. To assess the 'green' credentials of the CFW process using life cycle assessment (LCA) and life cycle cost (LCC) analyses.

Commercially available LCA software 'GaBi4' was used to assess the environmental impacts of the conventional and CFW processes. A simple study was also undertaken to assess the economic benefits of the CFW method in comparison to its conventional predecessor.

iv. To undertake site trials with the CFW method in an industrial environment

Site-trials were undertaken at an industrial manufacturing site (Portsmouth, UK) where the resin impregnation unit was retro-fitted onto a conventional filament winding machine to produce filament wound tubes.

v. To apply the CFW process to specified industrial applications, such as:
(a) the use of waste-fabrics for producing filament wound tubes; and (b) the overwrapping of aluminium pressure vessels to form composite over-wrapped pressure vessels (COPVs).

The CFW method was modified to allow for the processing of composite materials for specific industrial applications.

The remaining sections of this thesis are structured as follows:

(i) Chapter 2 presents a detailed review of the literature with regards to: (a) filament winding; (b) impregnation modelling; (c) fibre spreading; (d) composites recycling; and (e) life cycle assessment (LCA).

(ii) Chapter 3 outlines the experimental investigations which were carried out to develop the clean filament winding process with regards to: (a) process improvement; (b) impregnation modelling; (c) fibre spreading; (d) composites recycling; and (e) life cycle assessment (LCA).

(iii) Chapter 4 presents an in-depth analysis and discussion of the results produced from the experiments outlined in Chapter 3. Here, qualitative and quantitative analysis of the clean filament winding method with respect to its conventional predecessor was carried out.

(iv) Chapter 5 summarises: (i) the main milestones achieved throughout this research project; and (ii) the possible research projects which could be undertaken to further progress the investigations presented in the current study.

CHAPTER 2: LITERATURE REVIEW

The following section presents a literature review which aided in developing the CFW method. The structure of this review consists of the following key topics:

(i) *Filament winding*; this was carried out to assess the current status of filament winding.

(ii) *Fibre impregnation modelling*; this was completed to aid the design of a prototype resin impregnation unit.

(iii) *Fibre spreading methods*; this was undertaken to assist with the transverse impregnation of a fibre tow.

(iv) *Waste composite legislation*; this was reviewed to justify the development of a composite recycling method.

(v) *Thermoset composite recycling methods*; this review was carried-out to aid the development of a method termed 'Recycled-Clean filament winding' (R-CFW).

(vi) *Life cycle assessment (LCA) analyses with regards to composite manufacturing*; this was undertaken to assist with the development of a method to evaluate the 'green' credentials of the CFW method.

2.1 Filament Winding

Filament winding is a manufacturing process which can offer: (i) a high degree of automation [35,36,37]; (ii) relatively high processing speeds (> 50 m/min winding speed); and (iii) an ability to fabricate composites with relatively high fibre volume fractions (~ 70%). Table 1 presents an overview of the various components which can be fabricated via this method. For reference, Table 1 also presents a selection of filament winding manufacturers/research facilities.

Table 1. Overview of filament winding components and manufacturers.

Component	Manufacturer	Reference
Marine exhaust silencers	Halyard Precision Composites, UK (2011)	[38]
	Silencer Marine, Italy (2011)	[39]
	JA Chamberlain, USA (2011)	[40]
Automotive drive shafts	Crompton Technology Group Ltd, UK (2011)	[41]
	CTiHuatai Composites Co., China (2011)	[42]
	FWT Wickeltechnik, Austria (2011)	[43]
	BAC Technologies, USA (2011)	[44]
Missile launchers	Composite Solutions, USA (2011)	[45]
	Tata Advanced Materials, India (2011)	[46]
Pressure vessels	WindTec Winding Technology AS, Norway (2009)	[47]
	Luxfer Gas Cylinders, France (2011)	[48]
	Crompton Technology Group Ltd, UK (2011)	[41]

Table 1 - continued.

Pressure vessels	SA Composites, USA (2011)	[49]
	CTiHuatai Composites Co., China (2011)	[42]
	BAC Technologies, USA (2011)	[44]
	Composite Solutions, USA (2011)	[45]
Piping/tubes	QinetiQ, UK (2003)	[50]
	CK Composites, USA (2011)	[51]
	The University of Plymouth, UK (2011)	[52]
	FWT Wicheltechnik, Austria (2011)	[43]
	CPL, France (2011)	[53]
	Composite Solutions, USA (2011)	[45]
	Crompton Technology Group Ltd, UK (2011)	[41]
Medical MRI machines	Ershings Inc, USA (2009)	[54]
Lightning protection masts	CST Composites (2009)	[55]

On inspecting Table 1, it can be seen that filament wound composites are used in many sectors. Due to this popularity, much research has been conducted to develop and advance the filament winding process; the following text describes how the filament winding process has been developed over recent years.

Much attention has been directed towards the development of automated filament winding machines. In particular, the evolution of computer aided design (CAD) software packages, such as CADWIND [56], has aided in improving its industrial appeal. From incorporating such software packages it has been

possible to determine winding angles, material needs and processing programs before any winding trials are completed. The development of such automation has also made it possible to develop multi-axis filament winding machines; these can produce multiple components in a single winding trial. Figure 2 presents a filament winding method which has been developed to simultaneously wind multiple components.



Figure 2. Multi-component filament winding [57]. Here, four carbon fibre pressure vessels (A) are filament wound simultaneously.

As mentioned in Section 1.1, attempts have also been made to develop alternative filament winding impregnation processes; such developments have been reported by Palmer *et al.* [58] and DuVall *et al.* [14].

Palmer *et al.* [58] reported on the development of a filament winding process which incorporated a vacuum infusion process to achieve fibre impregnation. Here, dry fibres were wound onto a rotating mandrel before being applied with

a release film, 'bleeder' cloth and vacuum bag (the release film and bleeder cloth aided with component extraction and excess resin removal respectively). A vacuum was then applied to the deposited fibres in order to remove the air from inside the vacuum bag. Once a vacuum was produced, a resin system was allowed to flow into the reinforcement and impregnation of the fibres could be achieved.

From incorporating the method presented by Palmer *et al.* [58], it is possible to avoid many of the issues presented in Section 1.2. However, from incorporating this method such issues as vacuum bag application, fibre damage during dry-winding and processing time can somewhat negate any improvements.

Duvall *et al.* [14] proposed the use of prepreg (pre-impregnated) fibres during processing instead of on-line impregnation of dry fibres (as shown in Figure 1). From incorporating prepreg material, and removing the need to impregnate the material on-line, the authors stated that a cleaner process was produced. However, from incorporating this method the cost-of-manufacture was considerably increased; due to higher material costs.

Many researchers have also directed much effort towards the development of 'specialised' mandrel systems. Table 2 presents an overview of the mandrel systems which have been developed to date.

Table 2. Summary of mandrel systems used during filament winding.

Mandrel system	Overview	Comments	Reference
Steel cylindrical mandrel	Standard reusable mandrel system	Repeatable with relatively low costs	[1,4,5]
Cardboard mandrel	Inexpensive mandrel system	Reduce tooling costs	[5]
Wood mandrel	Inexpensive mandrel system		[5]
Water-soluble mandrel	Removable mandrel system	Address mandrel extraction issues	[5,59]
Segmented mandrel	Collapsible mandrel system		[5]
Deflate-able mandrel	Inflatable/memory mandrel system		[60,61]
Integrated mandrel	Non-removable mandrel system	Negate mandrel extraction needs	[5,62]

Many researchers have also directed attention towards quantifying the mechanical and physical properties of filament wound tubes. Table 3 presents an overview of various mechanical and physical testing procedures which have been reported to date.

Table 3. A summary of test methods used to assess filament wound composites.

Property	Aim	Reference
Fibre volume fraction	Calculate the ratio of fibre-to-resin via resin burn-off procedures	[23,63]
Void content	Determine the void content of a composite via resin burn-off procedures	[64]
Vessel pressure burst strength	Assess the structural strength of a composite vessel under internal pressure loading	[65,66,67,68,69]
	Model the internal pressure burst strength of a composite vessel	[65,69,70,71]
Hoop-tensile strength	Assess the hoop-strength of a composite tube section	[33,34,72,73]
Inter-laminar shear strength	Measure the shear-strength of multiple composite layers	[74,19]
Compressive strength	Quantify a tubes compressive strength i.e axial, lateral etc.	[75,76,77]
Biaxial loading strength	Analyse the effect of multi-axial composite loading	[78,79,80]
Fatigue strength	Measurement of a tubes long-term fatigue strength	[81,82,83]
Structural 'health'	Employ sensor networks to analyse a composites structural 'health'	[84,85]

A selection of the points presented in Table 3 are discussed in greater detail below:

Fibre volume fraction: Conventional resin burn-off or image analysis procedures can be employed to ascertain the fibre volume fraction of a filament wound composite. In general, a fibre volume fraction of ~70% is deemed appropriate; Table 4 presents a comparison of the relative fibre volume fractions which can be achieved via other composite manufacturing methods. Here, a value of ~ 70% is generally used in filament winding as this allows for an adequate amount of load bearing fibres to be incorporated into the composite with enough resin for full impregnation [23]. For example, Mertiny and Ellyin [23] showed the importance of fibre volume fraction by investigating ratios of 70.8% and 74%, as a result of increasing the winding tension from 26.7 N to 44.5 N. This change in fibre volume fraction produced significant increases in the fibre-dominated mechanical properties of filament wound composites.

Void content: Conventional resin burn-off procedures can also be employed to measure the void content of a filament wound composite. In general, it is desirable that the void content should be as low as possible as the presence of any voids can severely influence the loading capabilities of a composite [24]. For reference, void contents between 1% and 5% have been consistently reported in the literature [1,24,86].

Table 4. Comparison of fibre volume fractions produced by composite manufacturing methods.

Manufacturing process	Fibre volume fraction (%)	Comments	Reference
Filament winding	70.8	E-glass fibres with 26.7 N winding tension	[23]
	74	E-glass fibres with 44.5 N winding tension	[23]
	60	Carbon-fibre/epoxy composite	[73]
Pultrusion	69	E-glass fibre/chopped strand mat/polyester resin	[87]
	50 – 64	Impregnation investigations with V_f 's of 50, 60 and 64%.	[88]
	70	Unidirectional glass-fibre reference composite	[1]
Resin transfer moulding	50 – 60	Unidirectional glass-fibre reference composite	[1]

Binetruy *et al.* [89] have proposed that void formation can occur from the presence of two 'forms' of resin advancement during fibre impregnation. These were defined as: (i) micropore flow, where resin advancement occurs inside the fibre bundle; and (ii) macropore flow, where resin advancement

occurs in-between multiple fibre bundles. The two resin advancement mechanisms described by Binetruy *et al.* [89] are shown in Figure 3.

With reference to Figure 3, resin advancement was said to be slower during micropore flow (flow in-between the individual fibres) as opposed to macropore flow (flow in-between individual bundles). As a result, a lag time between the two flow types could develop. This differential lag between the two flow advancements is believed to be a main cause of void formation during fibre impregnation.

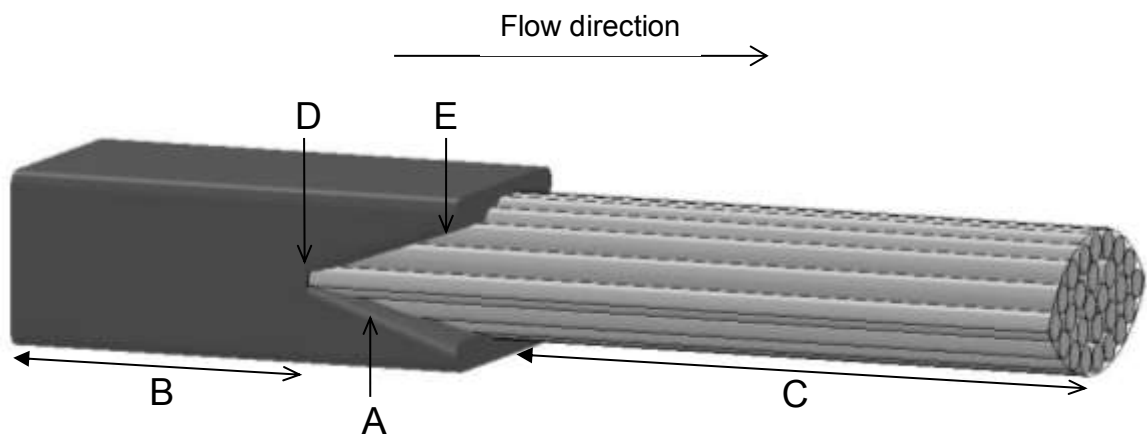


Figure 3. A cross-sectional view of meniscus shaped flow advancement: (A) meniscus shaped flow advancement; (B) fully impregnated region; (C) dry tow; (D) micropore flow front; and (E) macropore flow front [89].

If the differential lag becomes substantial then void formation, as shown in Figure 4, can occur. With reference to Figure 4, void formation was said to occur as a result of four sequential phases: (i) phase 1, a differential lag between micropore and macropore flow develops; (ii) phase 2, the inner-

edges of the lag start to come into near-contact; (iii) phase 3, the lag inner-edges come into direct contact; and (iv) phase 4, void formation.

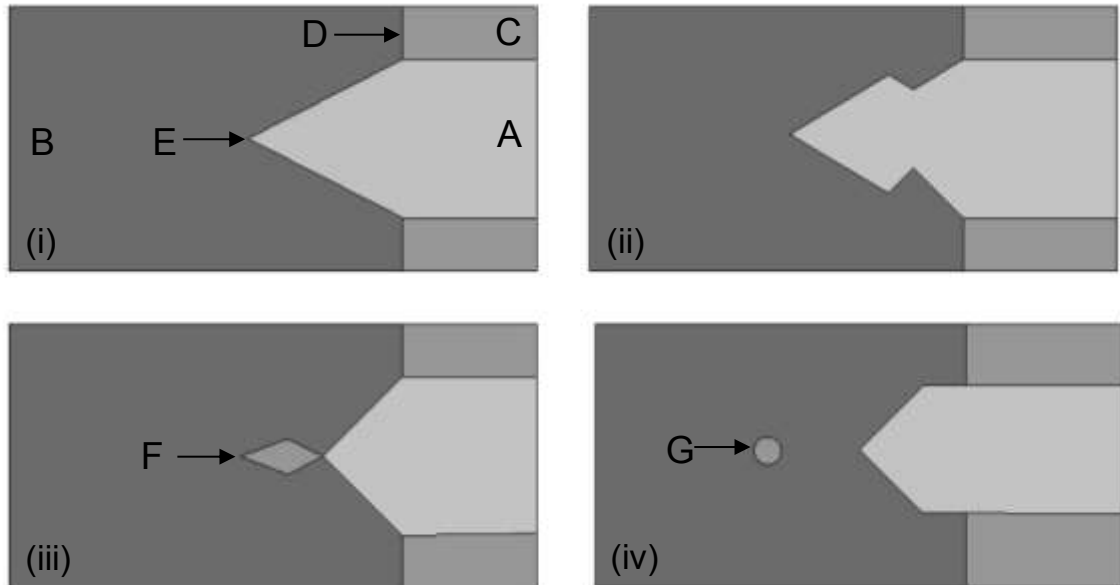


Figure 4. A diagram showing void formation caused by differential macropore and micropore flow: (A) fibre bundle; (B) advancing resin; (C) inter-tow space; (D) macropore flow; (E) micropore flow; (F) void formation; and (G) a void [89].

Hoop-tensile (split-disk) strength: Much attention has been directed towards assessing the hoop-tensile (split-disk) strength of filament wound tubes. Here, a tube is normally machined into individual rings (with nominal widths) and ‘pulled-apart’ by two internally mounted semi-circular disks (ASTM D2290, more details provided in a later section) [90]. For reference, Table 5 presents an overview of the hoop-tensile (split-disk) strength results which have been published in the literature.

Table 5. An overview of selected publications on hoop tensile strengths.

Author	Details	Hoop-tensile strength (MPa)
Buarque <i>et al.</i> (2006) [64]	Glass-fibre (continuous/short-fibre)/ Vinyl ester rings (31% fibre volume fraction)	303.6 (± 0.03)
Ha <i>et al.</i> (2005) [33]	Thick-walled glass-fibre/epoxy rings (2.5 mm width) with varied winding angles (90°, 75° and 60°)	29.14 (± 1.87) [90° fibre angle] 25.59 (± 3.44) [75° fibre angle] 24.7 (± 4.32) [60° fibre angle]
Chen <i>et al.</i> (2007) [74]	Carbon-fibre (T800)/epoxy rings (150 mm ID)	1889
Naruse <i>et al.</i> (2001) [73]	Carbon-fibre/epoxy rings (10 mm width, 80 mm ID and a thickness of 2 or 5.5 mm)	2 mm = 2080 5.5 mm = 1210
Kaynak <i>et al.</i> (2005) [34]	Glass-fibre (1200 Tex)/epoxy rings (60 mm ID) and carbon-fibre/epoxy rings (60 mm ID)	Glass = 840 Carbon = 1150
Sobrinho <i>et al.</i> (2011) [91]	Glass-fibre (675 Tex)/epoxy rings (101.6 mm ID and 35 mm width)	731

With reference to Table 5, Kaynak *et al.* [34] presented results for glass-fibre/epoxy rings (60 mm inner-diameter (ID) and 23.5 mm width) which were wound with a winding angle of $\pm 90^\circ$ during a conventional filament winding process. The manufactured components were then subjected to hoop tensile

(split-disk) strength testing and an average tensile strength of ~840 MPa was produced. Figure 5 presents an image of a composite test piece after hoop tensile (split-disk) strength testing. From analyzing Figure 5, the following conclusions were made by the presenting authors: (i) failure occurred in the gauge section i.e. in the notched section where a reduced sample width was present; and (ii) fibre/matrix debonding parallel to the fibres and loading axis was followed by fibre fracture.

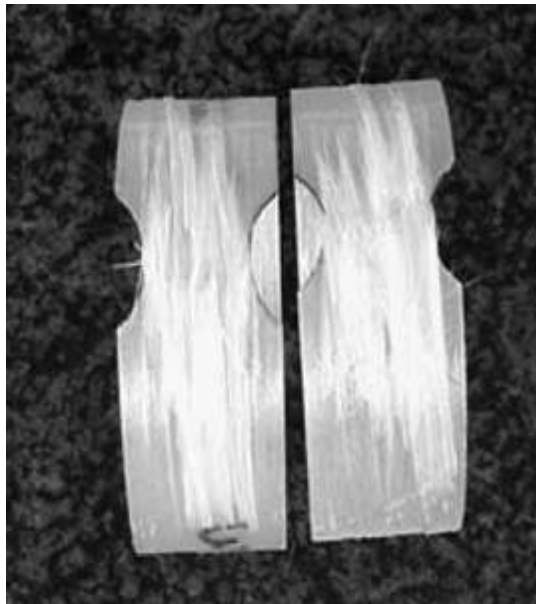


Figure 5. Image of a composite test piece after hoop tensile (split-disk) strength testing [34].

Sobrinho et al. [91] also presented hoop tensile (split-disk) strength testing results. Here, glass-fibre(675 Tex)/epoxy filament wound tubes were manufactured with a conventional method to produce samples with a wall thickness of 5.6 mm and an internal diameter of 101.6 mm. An angled winding

method of $[88^{\circ}_2/\pm 55^{\circ}_2/88^{\circ}_2]$ was employed and the final components were cut into rings with a nominal width of 35 mm and tested in the experimental set-up presented in Figure 6.

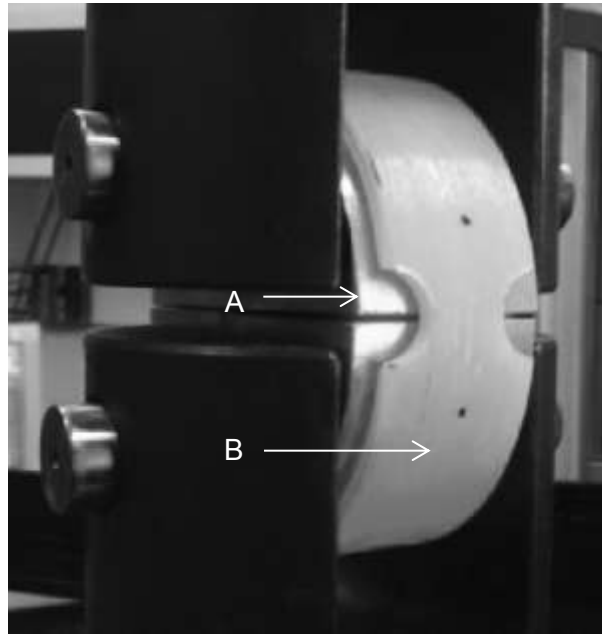


Figure 6. Image showing the hoop tensile (split-disk) testing procedure employed by Sobrinho et al. The highlighted components are: (A) central split-disks; and (B) a composite ring [89].

From employing the testing procedure shown in Figure 6, an average strength of 731 MPa was produced; an example of a failed testing sample is presented in Figure 7. With reference to Figure 7, the following conclusions were made by the presenting authors: (i) failure occurred in the gauge section; and (ii) fibre/matrix debonding parallel to the fibres and loading axis was followed by fibre fracture.



Figure 7. Image of a failed hoop tensile (split-disk) testing sample presented by Sobrinho et al [89].

Inter-laminar shear strength: Many authors have also attempted to measure the inter-laminar shear strengths of filament wound tubes. Van Paepegem *et al.* [19] and Chen *et al.* [74] employed a three-point bend testing procedure. Van Paepegem *et al.* investigated the possibility of using hoop-wound carbon-fibre filament wound tube sections for storm surge barriers. Here, the authors tested carbon-fibre/epoxy sections (20 mm width and 80 mm length), which had a maximum fibre volume fraction of 63%, and measured their inter-laminar shear strength to be 61.3 MPa [19]. In a similar vein, Chen *et al.* showed that a carbon fibre (T800)/epoxy section could offer an inter-laminar shear strength of 67 MPa [74]. Despite the different materials used i.e. carbon-fibre instead of glass-fibre, the results presented by Van Paepegem *et al.* and Chen *et al.* were deemed the most comparable to the results presented in the current study. As a result, in the remaining sections of this study the results presented by Van Paepegem *et al.* and Chen *et al.* were used as a benchmark.

2.2 Impregnation Modelling

A schematic illustration presenting an overview of the various models that were considered for the design of a resin impregnation unit is shown in Figure 8. Here, the rationale for investigating numerous impregnation models was to ensure that the impregnation unit (developed in the current study) was able to offer the minimum residence time (time the fibres are immersed in the resin) needed to inject the required volume of resin into the fibre tows to achieve full impregnation.

The interpretation of Figure 8 is as follows: the majority of the models that have been developed for predicting the permeability and time required to achieve impregnation of fibre tows are based on Darcy's equation (see Equation 1). There are four key components to this equation: (i) permeability; (ii) dimensions of the reinforcement; (iii) viscosity; and (iv) pressure.

In the following section, each component of Darcy's equation (A1-A4) is discussed sequentially before being adapted and applied to two models developed by Foley and Gillespie (B1) [94] and Gaymans and Wevers (B2) [95] respectively.

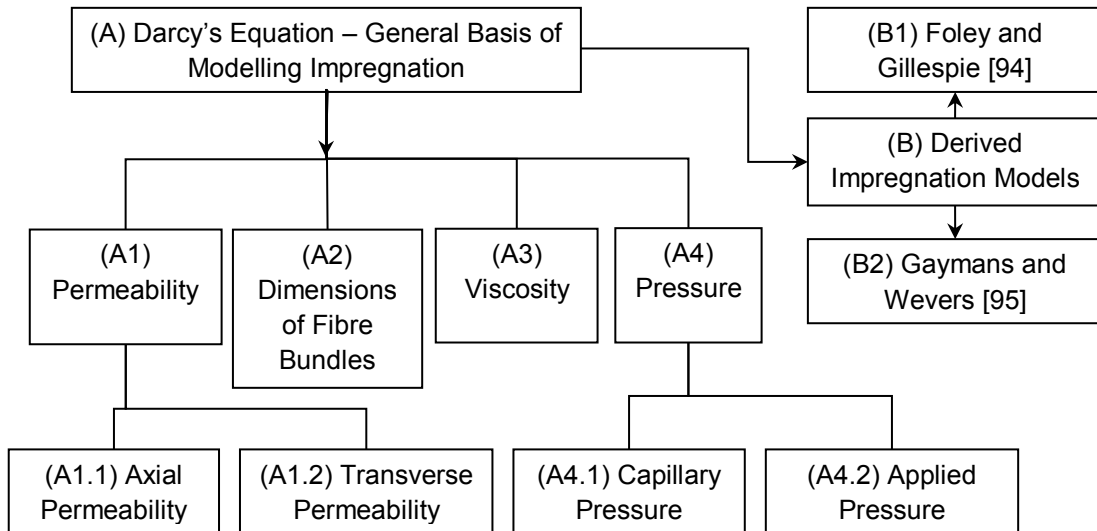


Figure 8. Schematic illustration presenting an overview of the various models that were considered for the design of the resin impregnation unit.

In general, the majority of the studies presented in this review considered the resin to be an incompressible Newtonian fluid that permeated through a porous medium (fibre array). The starting point for the majority of these models was Darcy's equation:

$$\bar{v} = \frac{K}{\eta \varepsilon} \frac{\Delta P}{L} \quad (1)$$

where \bar{v} is the superficial velocity that can be observed on a macroscopic scale, K is the permeability of the porous medium, ε is porosity, η is the viscosity of the fluid and $\Delta P/L$ is the pressure gradient over a characteristic dimension L .

In the context of developing the design basis for the resin impregnation unit, the following sections present a brief overview of selected models that considered the four components of Darcy's equation.

2.2.1 Impregnation Modelling: Permeability

(i) *Axial Permeability (A1.1)*: Gebart [96] predicted the axial permeability of a fibre bundle by calculating the frictional factor λ of axial flow along a duct that was formed in the interstitial space between a fibre bundle. The frictional factor λ was derived analytically for specified cross-sections (circular, quadratic, hexagonal, etc.) and was calculated using the following relationship:

$$\lambda = \frac{\Delta P}{L} \frac{2D_h}{\rho U^2} \quad (2)$$

where

$$\lambda = \frac{c}{\text{Re}} \quad (3)$$

In Equation 2, $\Delta P/L$ is the pressure gradient, D_h is hydraulic diameter (duct cross-sectional area divided by wetted perimeter), ρ is density of the fluid and U is the mean resin velocity over the fibre cross-section. In Equation 3, c is a dimensionless shape factor and Re is a Reynolds number. By elaborating the frictional factor, Gebart [96] derived the axial permeability, K_x , as:

$$K_x = \frac{8r_f^2 (1-V_f)^3}{c V_f^2} \quad (4)$$

where r_f is fibre radius, c is equal to 57 and 53 for quadratic and hexagonal fibre arrays respectively, and V_f is fibre volume fraction. Further models that considered axial permeability are summarised in Table 6 but are not discussed further in this study.

Table 6. Summary of selected models reported in the literature that considered axial permeability. Here, $B(V_a)$, $C(V_a)$ and $m(V_a)$ are maximum packing capacity curve fitting constants.

Authors	Axial Permeability (K_x)
Amico and Lekakou [97]	$K_x = \frac{\eta \varepsilon}{P_c} a_h \quad (5)$
Carman-Kozeny [98]	$K_x = \frac{r_f^2 (1-V_f)^3}{4k V_f^2} \quad (6)$
Cai and Berdichevsky [99]	$K_x = \frac{r_f^2}{8V_f} * \left[\ln \left(\frac{1}{V_f^2} \right) - (3-V_f)(1-V_f) \right] \quad (7)$
Berdichevsky and Cai [100]	$K_x = r_f^2 \frac{e^{(B(V_a)+C(V_a)V_f)}}{V_f^{(m(V_a))}} \quad (8)$

(ii) *Transverse Permeability (A1.2)*: Gebart [96] also investigated the resistance to transverse flow that occurred between individual fibres. It was reported that if the fibres were in intimate contact, they formed a channel with an undulating area between them. However, this variation in the cross-sectional area was assumed to be negligible. As a result, inertia effects were not considered. Furthermore, when a constant pressure differential was applied between these two regions, the pressure gradients were said to vary slowly in relation to the resin flow direction; the velocity profile V_p , was considered to be approximately parabolic at each flow position and this was calculated using Equation 9.

$$V_p = \frac{H_{(1/2)}^2}{2\eta} \frac{dP}{dx} \left(\frac{y^2}{H_{(1/2)}^2} - 1 \right) \quad (9)$$

where $H_{(1/2)}$ is the channel half-height, η is the resin viscosity, and x and y are the vertical and horizontal coordinates of the flow position respectively. By elaborating Equation 9 and taking the geometry of the fibre arrays to be quadratic or hexagonal, Gebart [96] derived equations for predicting the transverse permeability:

$$K_{y,quadratic} = \frac{16r_f^2}{9\pi\sqrt{2}} \left(\sqrt{\frac{V_A}{V_f}} - 1 \right)^{5/2} \quad (10)$$

$$K_{y,hexagonal} = \frac{16r_f^2}{9\pi\sqrt{6}} \left(\sqrt{\frac{V_A}{V_f}} - 1 \right)^{5/2} \quad (11)$$

where, V_A is the maximum packing capacity of a fibre bundle.

Table 7 presents a summary of additional models which also predict the transverse permeability of a fibre bundle.

Table 7. Selection of models which predict transverse permeability (K_y).

Authors	Transverse Permeability (K_y)
Cai and Berdichevsky [103]	$K_y = \frac{r_f^2}{8V_f} \left[\ln \frac{1}{V_f} - \frac{1-V_f^2}{1+V_f^2} \right] \quad (12)$
Bruschke and Advani [105]	$K_y = \frac{r_f^2}{3} \frac{(1-l^2)^2}{l^3} * \left(3l \frac{\arctan(\sqrt{(1+l)/(1-l)})}{\sqrt{1-l^2}} + \frac{l^2}{2} + 1 \right)^{-1} \quad (13)$
	$l^2 = \frac{4}{\pi} V_f \quad (14)$

2.2.2 Impregnation Modelling: Dimensions of Fibre Bundles

With reference to Figure 8, it was necessary to calculate the effective thickness of the fibre tows. This can be estimated using the following relationship:

$$Area = T_0 w = \frac{N\pi r_f^2}{V_f} \quad (15)$$

where T_0 is the thickness of the fibre tow, w is the width of the tow, N is the number of fibres in the tow, r_f is the fibre radius and V_f is the fibre volume

fraction. On inspecting Equation 15, it can be seen that the thickness of a fibre bundle is related to its width. Devices and techniques for spreading reinforcing fibres have been reported extensively in patent literature. A summary and review of selected patents that deal with fibre spreading is given in Section 2.3.1.

2.2.3 Impregnation Modelling: Viscosity of Resin

With reference to the development of the CFW technology, a commercially available resin system, LY3505 epoxy resin and XB3403 amine hardener, was used. The viscosity at the point of impregnation was assumed to be constant. This is a reasonable assumption as there is a relatively low dead-volume within the impregnator, which in turn means that the resin system cannot stagnate. Moreover, when the resin is injected into the fibre tow, a “fresh” batch of mixed resin system is supplied continuously.

2.2.4 Impregnation Modelling: Pressure

(i) *Capillary Pressure (A4.1)*: Ahn and Seferis [106] developed a model to calculate the capillary pressure based on the Young-Laplace relationship:

$$P_c = \frac{4\zeta \cos \theta}{D_E} \quad (16)$$

where P_c is the capillary pressure, ζ is the surface tension of the wetting fluid, Θ is the contact angle between the fluid and solid, and D_E is the equivalent

diameter of pores in a fibre bundle. Ahn and Seferis [106] employed the following relationship for evaluating D_E for an array of unidirectional fibres:

$$D_E = \frac{8r_f}{F} \frac{\varepsilon}{1-\varepsilon} \quad (17)$$

where, r_f is the fibre radius, ε is the porosity, and F is a form factor. F was said to equal two for transverse flow and four for axial flow. A simulation of this can be seen in Figure 9 where the capillary pressure was calculated using Equations 16 and 17. The fibre radius was assumed to be 8.5 micrometres, the contact angle for the uncured epoxy resin was taken as 57° and the surface tension was taken as 0.044 N/m [101]. In conclusion, it was found that the capillary pressure in the axial direction was higher than in the transverse direction.

(ii) *Applied Pressure (A4.2)*: Bates *et al.* [107] proposed that the fibre pressure (P) can also be generated through the use of cylindrical pins during the impregnation process:

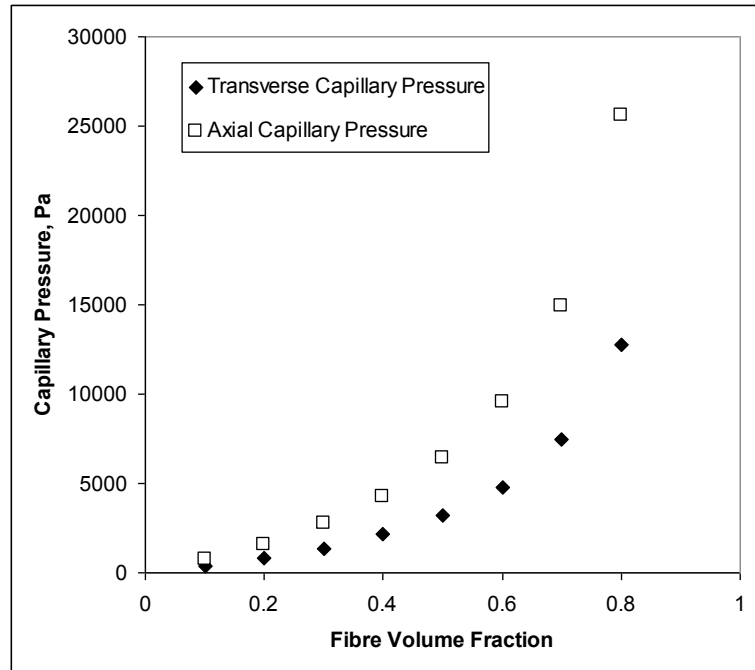


Figure 9. Capillary pressure plotted against fibre volume fraction in accordance with the model proposed by Ahn and Seferis [106].

$$P = \frac{T_e}{wC} \quad (18)$$

where T_e is the fibre tension, w is the width of the tow and C is the radius of curvature of the tow. In contrast, Chandler *et al.* [108] modeled the build-up of fibre tension during pin-based impregnation using the lubrication theory.

With reference to Figure 10, Chandler *et al.* [108] proposed four main zones to exist within the pin impregnator: (1) the entry zone, where the fibre tow approaches the pin at a pre-determined angle; (2) the impregnation zone, where the resin between the fibre and pin is forced into the fibre tow; (3) the contact zone, where sufficient resin has been applied to the fibres and where

the tension is built up as a result of Coulombic friction and viscous drag; and (4) the exit zone, where the tow leaves the pin.

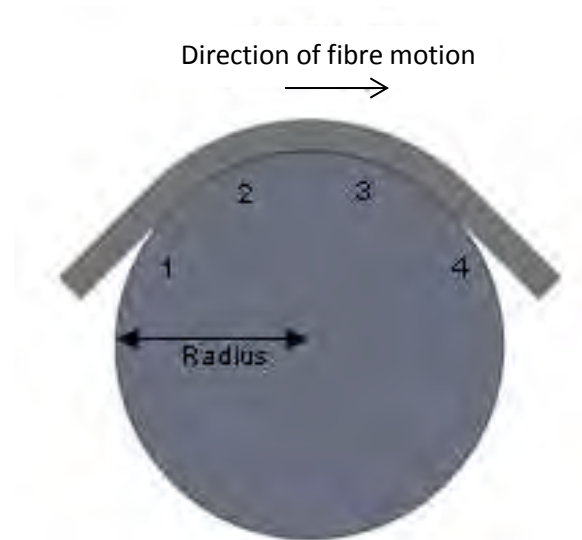


Figure 10. Regions of behaviour in pin impregnation: (1) entry; (2) impregnation; (3) contact; and (4) exit [108].

A selection of the previously-mentioned impregnation models (Equations 11, 16 and 18) were then analysed for their ability to model the impregnation process used during the clean filament winding method. The application of these models is presented in Section 3.3.1.

2.3 Fibre Spreading

The possibility of 'spreading' a fibre bundle prior to resin impregnation was considered. Here, fibre spreading is defined as the act of laterally displacing the constituent monofilaments of a fibre bundle to produce a spread tow with

a uniform fibre distribution and thickness. Figure 11 shows a schematic illustration of fibre spreading.

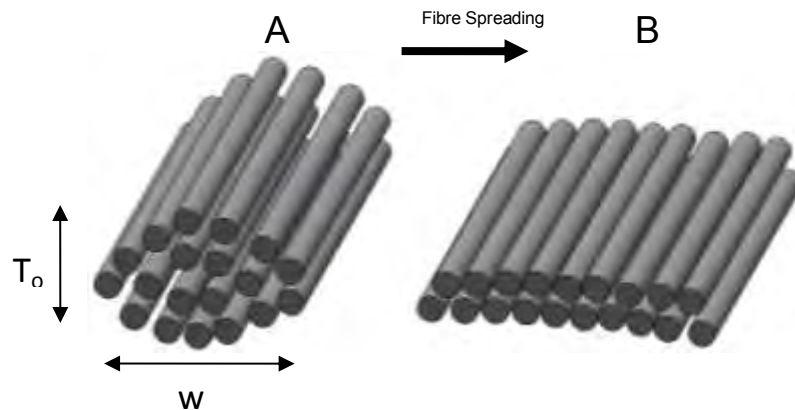


Figure 11. An illustration of fibre spreading. (A) An un-spread fibre bundle; and (B) a spread fibre bundle. Here 'w' and ' T_o ' are the fibre bundle width and thickness respectively.

On inspecting Figure 11, it can be seen that there is a concomitant decrease in the effective thickness of a fibre bundle as its width is increased. Figure 12 presents a simulation of this concomitant relationship over a range of possible bundle widths. With reference to Figure 12, it is hypothesized that any decrease in the effective thickness of a fibre bundle could enhance the transverse impregnation rate of the mixed resin system into the fibres; this issue is discussed in greater detail in Section 4.6.

Due to the concomitant relationship shown in Figure 12, and the associated reduction in transverse impregnation time, many authors have directed their attention towards the development of fibre spreading techniques. The

following section presents a review of currently published fibre spreading technologies.

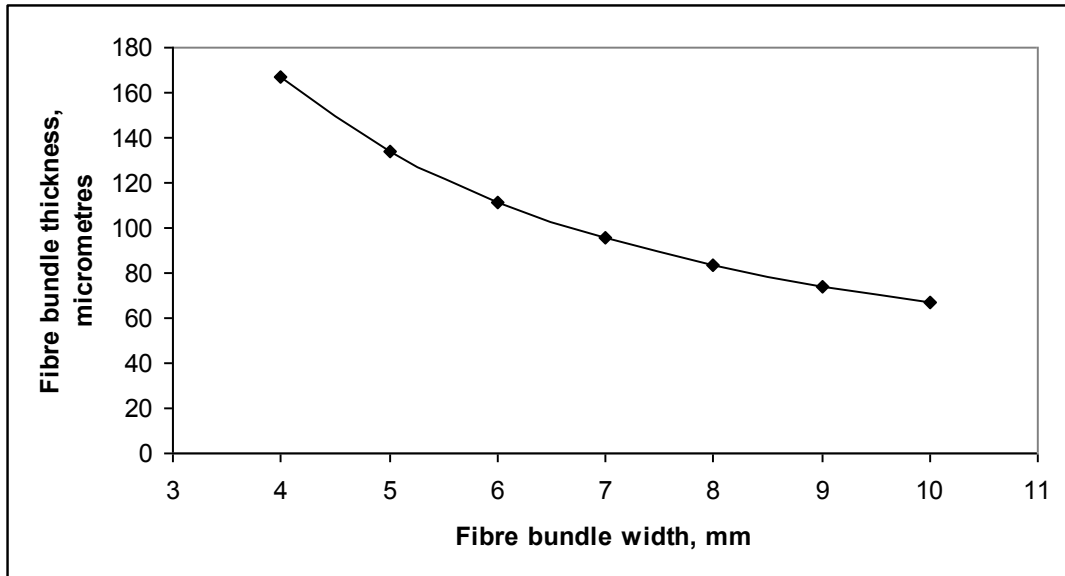


Figure 12. Simulation of the effect of fibre spreading on fibre bundle thickness.

2.3.1 Patent Review on Fibre Spreading Techniques

To date, many patented techniques have been reported to spread a fibre bundle. In general, these can be grouped into three main categories: (A) mechanical; (B) gas-based; and (C) electrostatic. A selection of these methods are presented in Table 8 and discussed in detail in the subsequent sections.

2.3.1.1 Mechanical Techniques for Fibre Spreading

Mechanical fibre spreading is normally achieved by the passing of fibre tows over a fixed pin or roller [109]; Figures 13 and 14(a and b) show schematic illustrations. Figure 13 shows a fibre passing over a cylindrical pin fixture and Figure 14(a and b) shows a schematic idealisation of mechanically-induced fibre spreading.

Table 8. Summary of selected papers and patents on fibre spreading methods.

Fibre spreading techniques	Comments	References
Mechanical	<ul style="list-style-type: none"> - Inexpensive and simple - Usable with multiple tows - Affected by sizing agents and twists - Minimal health and safety risks - Repeatable 	[110] [111] [112] [113] [114] [115] [116] [117] [118] [119] [120] [121] [122] [123] [124] [125] [126]
Gas-based	<ul style="list-style-type: none"> - Relatively expensive - Effected by multiple tows - Severely inhibited by fibre twists - Health and safety concerns with pressurised gases 	[127] [128] [129] [130] [131] [132] [133] [134] [135] [136] [137] [138]
Electrostatic	<ul style="list-style-type: none"> - Minimal fibre contact - Relatively expensive - Effected by fibre twists - Health and safety concerns 	[139] [140] [141] [142]

With reference to Figure 14, the idealised spatial location of each layer of each reinforcing fibre is indicated. When the tow is traversed over a fixture (pin or roller) the resulting tension causes two mechanisms to occur. Initially, the upper fibre layers (blue and red layers) are forced downwards into the interstitial spaces of the lower layers (green and orange layers). Secondly, the lower layers (green and orange layers) are forced to spread sideways in order to accommodate the fibres being forced downwards (blue and red layers). The overall result is the formation of a fibre tow with a reduced thickness and increased width.

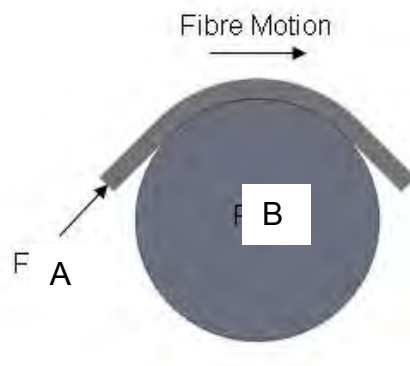


Figure 13. Schematic illustration of mechanical fibre spreading (transverse view). (A) Fibre tow; and (B) spreading pin.

With further reference to Figure 14, Peters and McLarty [143] produced a set of processing guidelines which outlined the ideal operating conditions for mechanical fibre spreading. Peters and McLarty [143] suggested the following parameters which would aid in spreading-out a fibre tow: (i) spreading fixtures should have smooth/polished surfaces; (ii) static fixtures i.e. pins, should be

used as opposed to rotating fixtures; (iii) spreading fixtures should have diameters greater than 12 mm (12 – 24 being optimal); (iv) an ‘S-wrap’ fibre path, as shown in Figure 15, consisting of two fixtures placed one above the other is preferable; and (v) multiple spreading fixtures i.e. > 1 should be used. However, from reviewing the above suggestions, concern should be taken before all of these rules are applied; if all of the suggestions are implemented then considerable fibre damage could be produced.

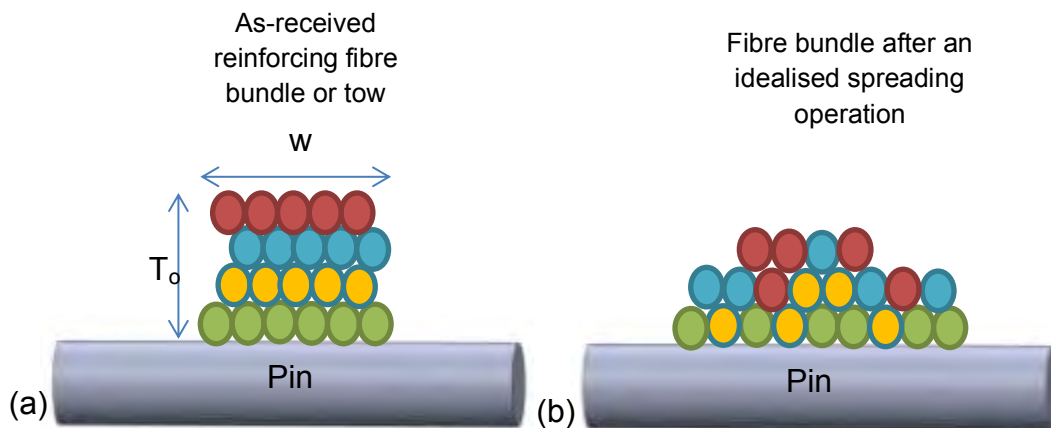


Figure 14. Schematic illustration of mechanically-induced fibre spreading (idealised view): (a) before fibre spreading; and (b) after fibre spreading.

Peters and McLarty [143] also stated that: (i) the winding speed is of little significance to fibre spreading; and (ii) the first spreading fixture should be: (a) on the horizontal and vertical centerlines of the supplying fibre bobbin; and (b) separated from the supplying fibre bobbin by at least ~ 0.5 m. The authors also recommend that the exit/entry angles of the fibres in relation to the fixtures should not exceed 20° (to the normal). It was hypothesized that exit/entry angles $> 20^\circ$ would cause significant fibre damage to occur.

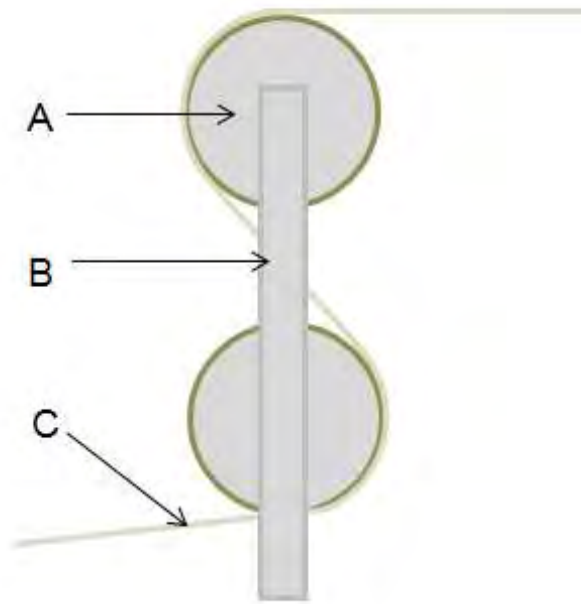


Figure 15. Schematic illustration of an 'S-wrap' fibre spreading set-up. The highlighted components are: (A) spreading fixtures; (B) supporting side plates; and (C) a fibre tow [143].

In the current study, the method presented in Figure 15 was termed 'conventional mechanical fibre spreading'. However, in addition to this method, various other mechanical spreading methods have also been developed, such as: (i) ridged-fixture mechanical spreading [110,111]; (ii) profiled-fixture mechanical spreading [112,113,114]; (iii) 'interval' mechanical spreading [112,115]; (iv) 'comb' mechanical spreading [117]; and (v) vibration-mechanical spreading [110]. A description of these alternative mechanical spreading methods is presented in Appendix A.

2.3.1.2 Gas-based Techniques for Fibre Spreading

Techniques have been developed to spread a fibre bundle via a gas-based means. Kawabe and Tomoda [137] have developed such a method, as shown in Figure 16.

With reference to Figure 16, fibre spreading was achieved by applying an air-jet to the tow. This air-jet (velocities up to 1200 m/min) then caused the fibres to separate in a region in-between two steel cylindrical pins (10 mm diameter). To promote fibre spreading, the air-jet was also heated (80–150 °C) in order to soften the sizing agent of the fibre tows. Here, the heat source was supplied from a far-infrared radiation heater. From utilising the method presented in Figure 16, the authors were able to increase the width of a carbon fibre bundle (1200 Tex) from 5 mm up to 20 mm; the authors also noted that the bundle thickness decreased from 0.15 mm to 0.04 mm.

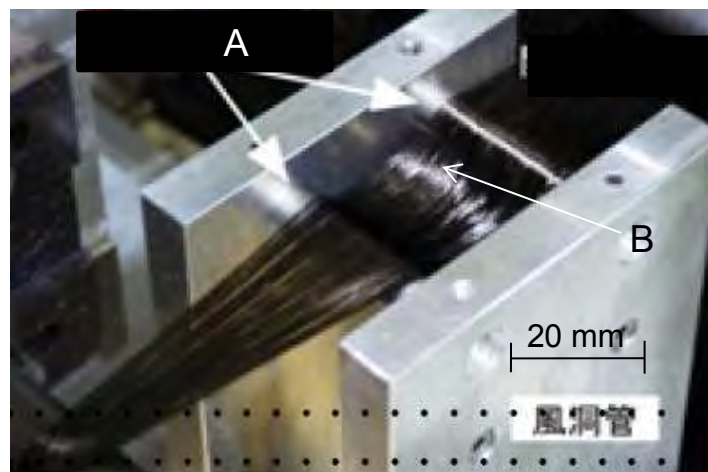


Figure 16. Schematic illustration of gas-based fibre spreading [137]. The highlighted components are: (A) spreading fixtures; and (B) spread fibres.

Conversely, Baucom *et al.* [138] devised a method that employed side air-vacuums to achieve fibre spreading. Figure 17 shows a schematic illustration of this method.

With reference to Figure 17, fibre tows (A) were fed into a spreading chamber (B) (0.25 cm height and 43.8 cm length) which had an entrance slot width (C) of 0.22 cm and an exit slot width (D) of 5.08 cm. The fibres were then directed through the chamber where they experienced a vacuum via multiple side-ports (E). These vacuum ports (up to eight on each side) aided in sequentially ‘pulling’ or spreading-out the fibre tows along the length of the chamber. The ports also increased in diameter towards the exit slot (0.2, 0.23, 0.27, 0.31, 0.35, 0.39, 0.43 and 0.47 cm) where forces of up to 0.72 Pa were produced to spread a fibre tow uniformly (5.08 cm width) at winding speeds of up to 3 m/min.

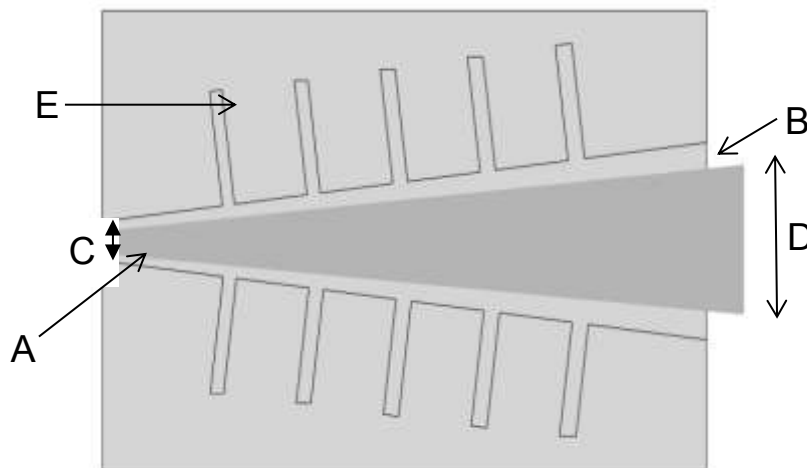


Figure 17. Schematic diagram of side-vacuum gas-based fibre spreading [138] (See text for details).

From reviewing Figures 16 and 17, it can be seen that these methods were developed to promote fibre spreading with low mechanical friction forces. The advantages of this were: (i) a reduced chance of fibre abrasion during production; and (ii) a reduced need for constant machine maintenance i.e. maintenance and replacement of smooth spreading fixtures. However, despite these advantages, gas-based fibre spreading methods also have negative aspects, such as: (i) the need to heat the fibres to relatively high temperatures; and (ii) their limited capacity in a multi-tow manufacturing process.

Due to the multiple issues which are present with each spreading method, the following section presents an overview of their comparative advantages and disadvantages.

2.3.2. Summary of Fibre Spreading Review

All of the above-discussed spreading techniques were attempting to fulfill the following criteria:

(i) Maximise fibre spreading: As previously mentioned, the lateral spreading of a fibre tow can produce reductions in its nominal thickness; these reductions can aid with the transverse impregnation of a fibre tow. However, this is not a straight-forward issue; the presence of fibre twists (produced from the unwinding of a bobbin) will inhibit the ability of a method to spread-out a fibre tow.

(ii) Maximise fibre spreading without causing fibre damage: The issue of fibre spreading is further complicated by the presence of a binder system which coats the individual filaments of a fibre tow. To enable efficient lateral separation of the individual filaments within a tow, the mechanical integrity of the binder has to be reduced without inducing secondary damage to the reinforcement. The development of a fibre spreading method must not cause any fibre damage during production; any damage will negate any improvements which the spreading method could produce.

(iii) Health and Safety: All fibre spreading processes must comply with strict health and safety legislation. The generation of air-borne particles is an issue for glass and carbon fibres respectively. Therefore, adequate measures will have to be taken to trap and extract any debris generated during all fibre spreading processes. Electrical safety issues will also need to be considered if any electrical potentials are used to induce fibre separation.

(iv) Cost-effective: A fibre spreading process must also not considerably increase the overall cost of a composite production method. Ideally, the fibre spreading method should offer: (i) low maintenance costs; (ii) low electrical consumption costs; and (iii) no dedicated man-power processing costs i.e. fully automated.

2.4 EU Directives and Waste Disposal Legislation

Thermoset composite materials can be found in many engineering sectors such as automotive, aerospace and sporting [144]. However, despite their

popularity (approximately 4 million tonnes produced in 2010 [7]) relatively little attention has been directed towards the management of end-of-life composite materials. To date, UK legislation regarding end-of-life (waste) composite materials is controlled by the Environmental Action Program 6 (EAP6 2002); entitled 'Environment 2010: Our Future, Our Choice' [145,146]. This program has four main priority areas: (i) climate change; (ii) biodiversity; (iii) environment and health; and (iv) sustainable management of resources and waste.

The EAP6 2002 action program was developed to address multiple issues within various fields, however with regards to composite materials/manufacturing, this action program was developed to: (i) aid with the reduction of waste material production; (ii) improve waste material recycling processes; and (iii) strictly control the disposal of any waste materials. In particular, the EAP6 2002 action program aided with the enforcement of multiple legislative directives and attempted to address the increasing costs associated with the disposal of waste composites [147].

The directives which were developed by the EAP6 2002 action plan were established in-tandem with voluntary agreements, taxes and subsidies; examples of such directives are:

- i. Waste Framework Directive (2008/98/EC) [148]
- ii. Landfill Directive (2003/33/EC) [149]
- iii. End-of-life Vehicle Directive (2005/673/EC) [150]

To enforce the EAP6 2002 action plan in the UK a set of Environmental

Permitting (EP) Regulations were introduced in 2007 [151]. In essence, the EP regulations acted as an 'organisational umbrella' under which over 40 items of individual legislation were pooled [152] i.e. EU directives 2008/98/EC [148], 2003/33/EC [149], 96/61/EC [153] and 2005/673/EC [150] etc. These regulations have since been updated over recent years and 'EP Regulations 2010' are currently in force.

From reviewing the highlighted directives, it can be seen that the composites industry will need to dedicate considerable attention to the development of efficient and economically viable composite recycling methods. The following section presents a review of the methods which have already been developed to recycle thermoset composite components.

2.5 Review of Thermoset Composite Recycling Methods

The following section presents a review of various methods which have been developed to recycle thermoset composite materials. In general, thermoset composite recycling methods can be categorised into four main areas, namely; (i) thermal; (ii) mechanical; (iii) chemical; and (iv) re-use. An overview of these processing methods is presented in Figure 18. With reference to Figure 18, this diagram has been adopted from the illustrations presented previously by Pickering [154] and Otheguy *et al.* [155].

2.5.1 Thermal Composite Recycling Methods [154]

Thermal recycling methods generally utilise high-temperature environments

in order to pyrolise polymeric matrices. Here, the reinforcing fibres are usually the recovered material and the matrix is normally either discarded or burned-off for energy recovery purposes. In the current review, thermal recycling processes are categorised into three main techniques: (i) fluidised bed [156,157]; (ii) combustion with energy recovery [154]; and (iii) pyrolysis [158,159,160,161]. The following text presents a review of selected methods.

Fluidised bed: Pickering *et al.* [154,162] have reported on a method whereby a fluidised bed of silica sand (particle size of 0.85 mm) was used to recover reinforcing fibres from a waste composite component. Here, the composite material (already reduced in size to ~ 25 mm by a cutting process) was fed into a sand-bed where a hot air stream (0.4 – 1 m/s) was blown through the sand at temperatures of up to 450 - 550 °C; the fibres were then transported out of the sand by the hot-air stream. From incorporating this method, Pickering *et al.* [154] stated that tensile strengths of the recycled fibres were only 50% lower than virgin fibres.

Here, the issues which need further attention are: (i) the need for pre-processing cutting procedures; (ii) the relatively high processing temperatures; and (iii) the limited form of the produced recycle i.e. the recovered material generally consists of short-fibres.

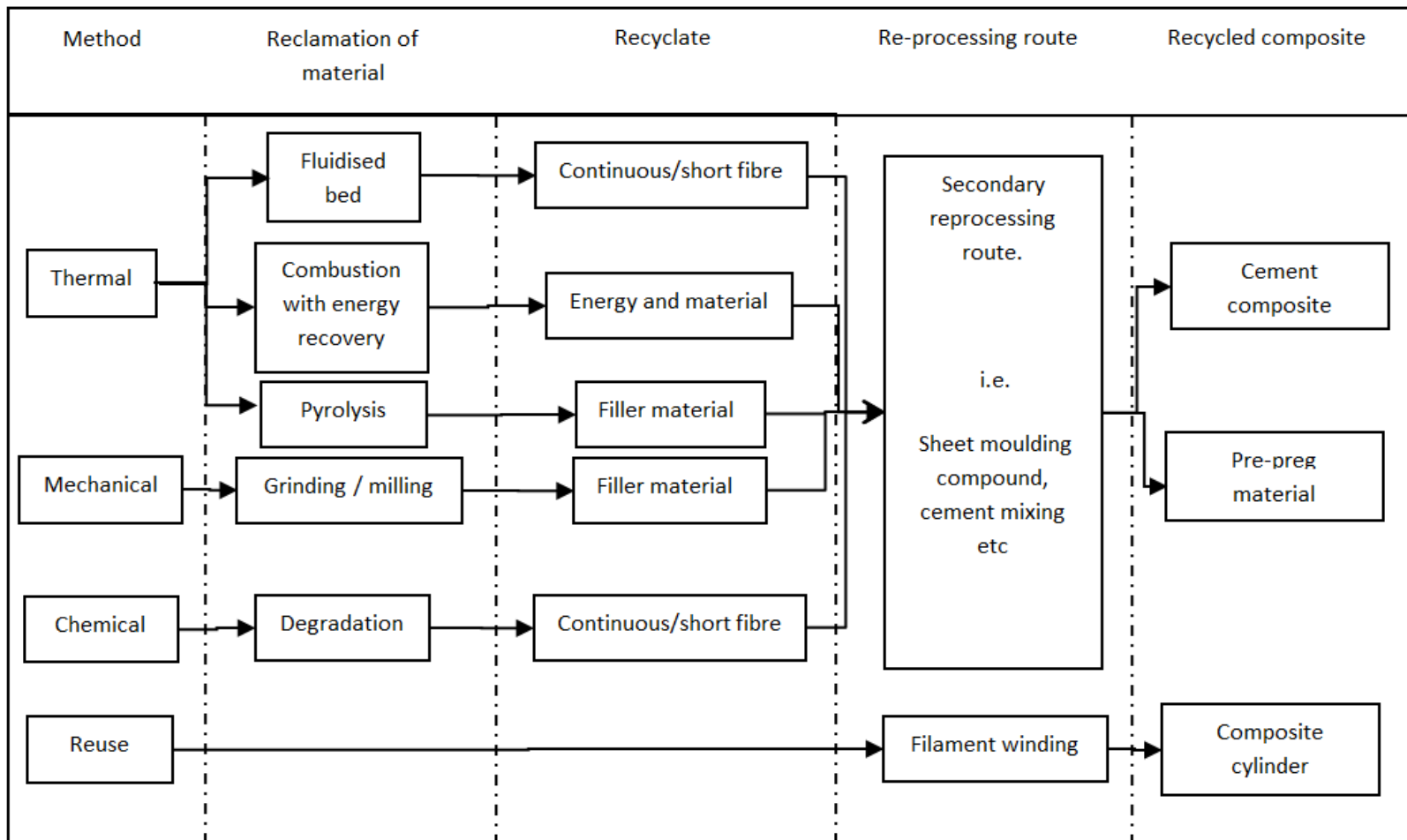


Figure 18. Overview of recycling processes; adapted from the work reported in references [154] and [155].

Pyrolysis: Cunliffe and Williams [158] have reported on a process for recycling a polyester/styrene glass-fibre composite. Here, a fixed-bed reactor was used to heat a composite at 5 °C per minute up to ~450 °C whilst being purged with nitrogen gas. This process burned-off the resin system and released the reinforcing fibres. The remaining fibres were then heat treated at 450 °C and had any remaining ash removed. From incorporating this method, Cunliffe and Williams [158] stated that they were able to produce recycled reinforcing fibres which could be substituted into virgin fibre composites (25% weight replacement). The experimental data from this study showed that the replacement of virgin fibres with recycled fibres produced a 27%, 10% and 19% reduction in the composites Charpy impact strength, flexural strength and flexural modulus respectively.

A summary of the above-mentioned thermal recycling methods is presented in Table 9. With reference to Table 9, various thermal recycling methods which were not discussed in this review are also presented for reference. From reviewing the methods presented in Table 9, it can be seen that relatively successful recovery of reinforcing fibres have been reported. However, as mentioned in various studies [154,163], the efficiency, output rates and cost-effectiveness of these methods are considerably lower than that which is necessary for economic viability. It was postulated that composite recycling methods will only become cost-effective if mass carbon-fibre recycling opportunities are available [154,163]. For example, the method presented by Pickering *et al.* would have to process 10,000 tonnes of waste glass-fibre per

year in order to be cost-effective [154]; a carbon-fibre recycling plant would only have to produce a fraction of this amount to be cost-effective.

Table 9. A summary of thermal recycling methods and references.

Thermal Recycling Method	Comments	Reference
Fluidised-bed process	Microwave heated fluidised bed during recycling	[157]
	450 – 550 °C sand bed with air-stream removal process	[154]
	Characterisation of glass-fibres from fluidised-bed recycling	[164]
	Characterisation of carbon-fibres from fluidised-bed recycling	[165]
	Glass-fibre fluidised-bed with alternative materials	[166]
	550 °C and 1 m/s pyrolysis temperature and fluidising air velocity	[167]
	Automotive application of recycled glass-fibres	[168]
Combustion with energy recovery	3000 kJ/kg recovered from resin system	[154]
Pyrolysis	450 °C fixed bed reactor purged with nitrogen	[158]
	Polyester/glass-fibre processing at ~ 500 °C	[159]
	Carbon-fibre pyrolysis in Nitrogen and Oxygen atmospheres	[160]
	Low temperature pyrolysis recycling of glass-fibre	[161]
	500 °C optimal carbon-fibre pyrolysis temperature	[169]
	Pyrolysis recycling of sheet mould compound material	[170]
	Characterisation of recycled carbon-fibres by pyrolysis	[171]
	Discussion of pyrolysis with multiple materials i.e.phenolic or epoxy resins, glass- or carbon-fibres	[172]

2.5.2 Mechanical Composite Recycling Methods [173,154]

Mechanical recycling of composite materials generally involves a chopping and/or milling process which can be used to reduce waste composites into

recycled particles [174]. Here, a crushing and/or chopping method is initially used to reduce all waste materials into parts of 50–100 mm in size [154]. The chopped/crushed components are then placed inside a hammer mill or high-speed mill where a further reduction in the size of the waste composite is achieved (~50 μm). A classifying method i.e. sieving, is normally then employed to separate the recycled particles into fractions of different size [175]. The produced components are a mixture of fibre and resin (in a powder form) which can be used as filler materials in secondary applications [176,177,178].

As mentioned in various review papers [154], it has not yet been possible for a mechanical recycling method to achieve long-term financial viability. To date, many attempts have been made to make this method a viable option [179], however none of these attempts were successful due to: (i) the lack of a strong outlet market; (ii) relatively high-production costs; and (iii) relatively low production rates.

2.5.3 Chemical Composite Recycling Methods

Chemical methods, as that proposed by Jiang *et al.* [180] and others [181-189], can also be used to recycle waste composite materials. With reference to the study presented by Jiang *et al.* [180], recycling was achieved via the use of supercritical alcohols (supercritical *n*-propanol) where degradation of the polymer matrix allowed for the reclamation of reinforcing fibres. Here, processing took place in a semi-continuous flow reactor where composite samples (~10 mm x 200 mm) were exposed to supercritical *n*-propanol whilst

the reactor reached a maximum temperature of 310 °C and pressure of 52 Bar. After a processing time of 40 minutes, the matrix was said to have been fully degraded and was washed away with the *n*-propanol. The remaining fibres could then be cleaned and dried and used in a secondary application [180]. A summary of the study presented by Jiang *et al.* [180] and other chemical recycling methods is presented in Table 10.

2.5.4 Re-use Composite Recycling Methods

In the current study, the term 're-use recycling' was defined as the direct use of a used/waste material in a manufacturing process or secondary application. This method, unlike all of the processes described above, does not involve any reclamation of any of the constituent components of the composite and therefore is relatively simple. For example, re-use recycling can be achieved from the simple reincorporation of a used vehicle front guard (bumper) into the manufacture of a new vehicle [182]. However, this method has been predominantly used with thermoplastic materials and the incorporation of thermoset materials has been severely limited.

The limited use of re-use thermoset recycling, however simple, is still relatively uncommon with composites due to [183]: (i) the possible presence of defects in the supposed end-of-life products; (ii) a lack of applicable situations; and (iii) the lack of a lucrative market which would create a great enough demand for economic viability.

Table 10. Summary of chemical recycling methods and references.

Author(s)	Comment	Reference
Jiang <i>et al.</i> (2008)	Supercritical <i>n</i> -propanol degradation	[180]
Pinhero-Hernanz <i>et al.</i> (2008)	Recycling with sub- or super-critical alcohols	[181]
Yuyan <i>et al.</i> (2009)	Resin degradation with super-critical water	[184]
Pinhero-Hernanz <i>et al.</i> (2008)	Recycling with near- or super-critical water	[185]
Bai <i>et al.</i> (2010)	Recycling carbon fibres in super-critical water	[186]
Buggy <i>et al.</i> (1995)	Resin degradation in solvents	[187]
Yoshiki <i>et al.</i> (2005)	Liquid-phase recycling	[188]
Hyde <i>et al.</i> (2006)	Carbon fibre recycling with super-critical propanol	[189]

2.6 Life Cycle Assessment (LCA)

In the current study, the 'green' credentials of the clean filament winding method were assessed by completing a LCA. The following section presents a review of: (i) the development of LCA as an assessment tool; and (ii) previously published studies on manufacturing composites.

2.6.1 Development of LCA as an Assessment Tool

LCA is the study of the potential environmental impacts of a product throughout its lifetime [190]. This takes into account: (i) raw material acquisition; (ii)

production; (iii) use; and (iv) end-of-life management options i.e. recycling, incineration, and/or disposal [191]. To undertake an LCA the following steps must be completed: (a) an inventory of relevant inputs and outputs of a production system must be compiled; (b) the potential environmental impacts associated with the aforementioned inputs and outputs must be evaluated; and (c) the results presented by the inventory analysis and impact assessment phases must be interpreted [191].

Originally, the method of LCA was developed as a result of the 'Earth Summit' held in Rio de Janeiro, Brazil, in 1992 [192]. Here, world leaders signed and 'agreed' with a legislative framework which would attempt to address issues related to climate change and biological diversity. As a result, an ISO technical committee (Committee 207) for environmental management was created in 1993. One of the main aims of this ISO committee was to standardise and develop a series of ISO 1404(x) standards which governed the development of LCA as an environmental assessment tool and management system [192,193].

A summary of the ISO 1404(x) standards is presented below:

- *ISO 14040* [194]: An overview of the practice, application and limitations of LCA to potential users.
- *ISO 14041* [195]: A guide to the preparation and development of a life cycle inventory analysis. This involves the compilation and quantification of the relevant input and outputs of a production system.
- *ISO 14042* [196]: A guide for completing the impact assessment phase of an LCA analysis.

- *ISO 14043* [197]: An outline for completing the impact interpretation phase of an LCA analysis. This should relate to the goal and scope of the analysis.

A review of LCA studies which have been developed to analyse various composite manufacturing methods is presented in the following section.

2.6.2 Review of LCA Studies

Several LCA analyses of production methods for composites have been published. For instance, many authors have analysed the effects of using natural fibres during composites manufacturing [198,199]; Table 11 presents a selected summary of such papers.

Many authors have also analysed the effects of improving vehicle fuel efficiency through the use of lightweight composite components [200,201,202]. For example, Song *et al.* [201] completed an LCA investigation into composite materials in the automotive industry. Song *et al.* [201] analysed: (i) the flow and consumption of energy during the production of glass fibre/polyester pultruded rods; and (ii) the feasibility of using composite materials in the automotive industry. The four main stages of this LCA investigation were as follows:

(i) Material production: To produce polyester resin (via a conventional chemical processing method) and glass-fibre (via a conventional drawing process) an estimated 63-78 MJ/kg and 13–32 MJ/kg of energy was consumed respectively.

Table 11. Summary of natural fibre LCA studies and references.

Natural/Synthetic Material	Aim	Reference
Hemp fibres	Replace glass-fibres for Audi A3 side panel	[203]
	Replace glass-fibres as insulation for a Ford car	[204]
Kenaf fibres	Replace wood with kenaf fibres for insulation	[205]
China reed fibres	Replace glass-fibres for fabrication of pallets	[206]
Sugarcane bagasse fibres	Implement sugarcane bagasse fibres into polypropylene composites	[207]
Rice husks	Fabricate environmentally friendly composites	[208]
Jute fibres	Replace glass-fibres for an off-road vehicle bonnet	[209]
Straw fibres	Manufacture straw/polyester composites	[210]
Curaua fibres	Replace glass-fibre for vehicle side panels	[211]

(ii) *Manufacturing*: To process the aforementioned materials into composite rods, a pultrusion process which independently consumed 3.1 MJ/kg was incorporated. Here, the consumption of energy was attributed to: (i) the curing cycle; (ii) process duration; and (iii) the degree of automation.

(iii) *Use*: The consumption of energy during the 'use' phase of a composite component was said to be dependent on many factors i.e. duration and/or maintenance. This section is the main area of improvement which Song *et al.* [201] were investigating. In particular, they were analysing the energy savings which could be accrued from using lighter composite materials instead of relatively heavy metals.

(iv) *End-of-life*: On completing its duty, an end-of-life composite component can be recycled, re-used, incinerated or landfilled. To date, the predominant option

is to landfill any waste. However, the method of landfilling is considerably wasteful and, as a result, all 'material energy' is lost. This restrictive end-of-life phase acts as a major barrier to the application of composite materials into many sectors [201].

On completing the above-mentioned phases, the authors calculated that 50.31 MJ of energy was needed for the production of a 1 kg pultruded rod. This value was then used to calculate the life-cycle energy consumption of composite pultruded rods when used as a substitution for steel in the manufacture of an automotive Truck (Isuzu N-Series). Here, the truck had an overall mass of 3600 kg, of which 643 kg (17.9% of the total truck weight) comprised steel rods.

The results of this comparison showed that the use of composite rods produced an overall life cycle energy saving of 184.2 GJ of energy; 13.6 GJ of energy during manufacture, 181 GJ during use (assumed for a travelling distance of 190,000 km over ten years) and -10.4 GJ during end-of-life. With reference to the 'use' phase, considerable energy savings were possible due to the overall reduction (429 kg) of the truck weight due to the use of lightweight composite materials. However, with reference to the 'end-of-life' phase, the energy deficit (-10.4 GJ) was attributed to the poor end-of-life options of the composite materials i.e. lack of re-use and/or recycling options.

The LCA study carried out by Song *et al.* [201] showed that the use of composite materials could be beneficial to the automotive industry. However, comparative results of this study also showed that the substitution of aluminium, instead of a composite, would result in even further energy reductions. It was

demonstrated that the limited end-of-life management options of composite materials inhibits the comparative LCA performance of composite components. A summary of this study and other studies which have completed LCA analyses of composite materials in the automotive industry are presented in Table 12.

However, in contradiction to the above studies, Marsh [212] has recently stated that it should no longer be acceptable to state that composites help the environment by simply improving the fuel efficiency of various vehicles. Marsh [212] argued that the composites industry must react to ensuing legislation and directives which will attempt to address various issues with regards to: (i) energy-intensive manufacture; (ii) emission of volatile substances; and (iii) the production of waste material that is inherently difficult to recycle. As a result, a report called '*The green guide to composites: an environmental profiling system for composite materials and products*', produced from a research project involving NetComposites, the Building Research Establishment (BRE) and the UK's Department of Trade and Industry has been reported [212]. This guide was produced in an attempt to aid composite manufacturers in choosing a processing method which fulfils their specific manufacturing needs whilst also being environmentally and socially acceptable. In this report, a rating system was used to grade various manufacturing materials and methods depending on their environmental and social impacts; the ratings ranged from A (good) to E (poor). A summary of the overall environmental ratings for the processes analysed during this study are presented in Table 13. In this table, it should be noted that these results were not produced from a complete cradle-to-grave LCA analysis; the authors stated that no 'use' or 'end-of-life' issues were able to

be included. The results in Table 13 were produced from just: (i) the material production phase; and (ii) the manufacturing phase.

With reference to Table 13, the overall environmental ratings were said to be dependent on many factors, such as: (i) fibre volume fraction of fabricated components; (ii) processing safety i.e. open or closed to the atmosphere; (iii) mixing of components i.e. addition of fillers; and (iv) the use of pre-impregnated (prepreg) materials. In general, these issues were mainly related to the production and use of man-made resin systems. Here, the resin systems were said to have a higher environmental impact than the reinforcing fibres due to: (a) their organic precursors; (b) their energy intensive production methods; and (c) their high yield of bi-products. Environmental issues were also attributed to the emission of hazardous atmospheric pollutants (HAPs) i.e. styrene, to the atmosphere during spraying and/or resin impregnation methods.

From reviewing the 'Green guide to composites' and other presented LCA studies, it can be seen that many LCA analyses of composite manufacturing methods have been carried out. However, from further analysis it can also be seen that none of these studies present an in-depth LCA analysis of filament winding and/or recycling processes with respect to energy, resin, raw material and solvent consumption. To date, only two studies have attempted to solve some of these issues; these studies were presented by Vieira *et al.* [57] and Lee *et al.* [160] respectively.

Table 12. Summary of selected papers that have discussed the LCA of materials in the automotive industry.

Author (Year of Publish)	Aim	Reference
Kasai <i>et al.</i> (1999)	Replacement of steel propeller shaft	[200]
Song <i>et al.</i> (2009)	Replacement of steel body part	[201]
Keoleian and Kar (2003)	Analyse the manufacturing method for a composite engine manifold	[202]
Zah <i>et al.</i> (2007)	Use of natural fibres as body-panels	[211]
Suzuki <i>et al.</i> (2005)	Replacement of steel chassis	[213]
Wotzel <i>et al.</i> (1999)	Use natural fibres for body panel	[203]
Tonn <i>et al.</i> (2003)	Analyse the use of composite materials in main-stream vehicles	[214]
Pickering (2000)	Use recycled fibres for vehicle headlamps	[154]

Table 13. Overall ratings from 'The green guide to Composites' [212]. Here, the ratings range from A (good) to E (poor).

Process	Materials	Overall environmental rating
Autoclaving	Glass-fibre/Epoxy prepreg	B
Compression moulding	Sheet moulded compound (SMC)	C
Hand lay-up	Chopped strand-mat (CSM) / Polyester	E
Resin-transfer moulding (RTM)	Woven glass/polyester	C

Firstly, Vieira *et al.* [57] attempted to complete an LCA analysis of a filament winding method for the production of steel/glass-fibre thermoplastic composite overwrapped pressure vessels (COPV). However, the LCA results presented by

Vieira *et al.* [57] were not comprehensive and did not allow for a detailed analysis of the filament winding process. Furthermore, the recycling process used by Vieira *et al.* [57] was not for thermoset composite materials.

Secondly, Lee *et al.* [160] undertook an LCA of two thermoset composite recycling methods: (i) chemical recycling (with nitric acid); and (ii) thermal recycling (pyrolysis in oxygen). In summary, Lee *et al.* [160] concluded that the chemical recycling method had a lower environmental impact (in comparison to the thermal recycling method) due to its reduced consumption of electrical energy (heating energy) during processing; chemical recycling at 80 – 110 °C and thermal recycling at ~ 500 °C.

The results presented by Lee *et al.* [160] aided in providing the most fore-front analysis of any thermoset composite recycling methods. However, from reviewing this study and the aforementioned LCA analyses, it can be concluded that there is little published literature which presents an in-depth LCA analysis of filament winding and/or recycling processes with respect to energy, resin, raw material and solvent consumption. As a result, the current study was produced to evaluate and compare the LCA results of the following filament winding and recycling processes; (i) conventional filament winding; (ii) clean filament winding (CFW); and (iii) recycled-clean filament winding (R-CFW).

2.7 Conclusion of the Literature Review

From carrying out the literature review, the following conclusions were made:

- (i) The method of filament winding was shown to be able to manufacture a wide range of composite components; for example, pressure vessels and drive shafts. On manufacturing these components, issues such as fibre volume fraction, void content and winding tension were highlighted as critical parameters.
- (ii) The method of impregnation used during filament winding can be modelled by various equations; the majority of which are derived from an equation termed Darcy's Law. Derivations of Darcy's Law were identified and highlighted as possible methods to model the impregnation process of filament winding.
- (iii) Fibre spreading was highlighted as a critical component during filament winding. Here, fibre spreading was thought to be an important parameter during fibre impregnation and can be achieved via such methods as mechanical, gas-based and electrostatic methods.
- (iv) Many composite recycling methods were identified, for example thermal, mechanical, chemical and re-use. However, the considerable issues associated with these methods were highlighted, including processing speeds and volumes. As a result, it was concluded that no long-term recycling success has been achieved to-date but in the near future, due to ensuing legislation, considerable advancements will have to be made.

- (v) Life cycle assessment (LCA) was identified as a quantitative method which can be used to assess the environmental impact of a composites manufacturing process. However, from reviewing the literature it was concluded that very little research has been presented with regards to filament winding and composites recycling.

CHAPTER 3: EXPERIMENTAL

The following section presents details of the experimental procedures which were carried out during this thesis. In general, the following section presents details of: (i) materials and equipment; (ii) the development of resin impregnation and fibre spreading units; (iii) filament winding trials; and (iv) composite evaluation procedures.

3.1 Materials and Equipment

3.1.1 Reinforcing Fibres

Three types of reinforcing fibres were used in the current study: (i) continuous E-glass fibres (EC15 1200 Tex); (ii) waste slitting fibres; and (iii) direct-loom waste (DLW) fibres. Here, the E-glass fibres were used as-received and were supplied by PPG Industries (UK). The waste slittings and direct-loom waste were waste glass-fibre materials and were produced from an industrial glass-fibre weaving process. The following section presents a detailed description of these materials. For clarification, the waste-fibre materials were used to investigate the development of a composites recycling method, termed Recycled-Clean filament winding. A greater discussion of this point is presented in a later section.

(i) As-received E-glass fibres: The E-glass fibres (1200 Tex) were supplied on conventional bobbins, as shown in Figure 19, where the fibres were drawn from the outer circumference during filament winding. Table 14 outlines some general physical properties of the E-glass fibres used in this study.

Table 14. Properties of E-glass fibres (EC15 1200 Tex) [21].

Property	Units	Value
Fibre radius	μm	8.5
Number of fibres	-	2000
Tow width	mm	4
Tow thickness	μm	160 – 170

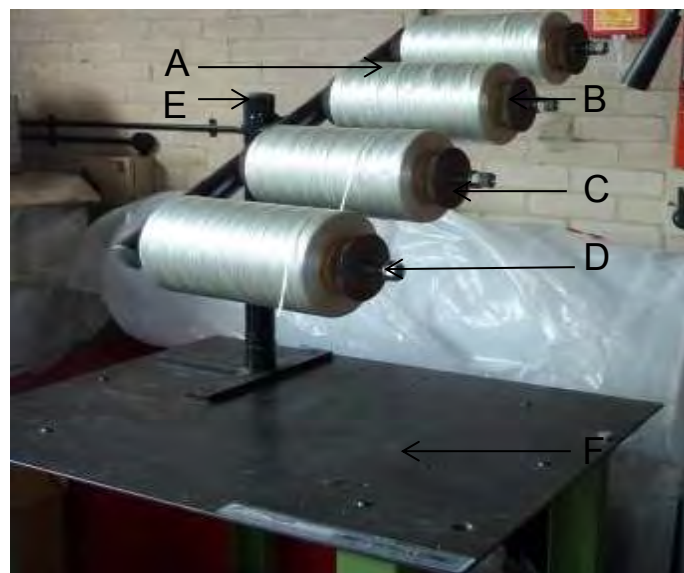


Figure 19. Photograph of the as-received E-glass fibres on conventional bobbins. The scale is represented by a 30 cm ruler that is located on the supporting table and the highlighted components are: (A) glass-fibre bobbins; (B) mounting arms; (C) holding-cones; (D) springs; (E) adjustable stand; and (F) supporting table.

With reference to Figure 19, the bobbins (A) were loaded onto individual mounting-arms (B) with holding-cones (C) which were held in place by mounted springs (D). Here, the cones allowed the bobbins to rotate in their holding

position whilst the springs were used to control the relative tension of the fibres during winding.

To control winding tension, the springs could be tightened or loosened depending on the winding tension desired. Throughout this study, winding tension was measured with conventional fish-scales; the method with which these scales were used is presented in a later section.

The mounting-arms (B) were also engineered so that the bobbins could be staggered, as shown in Figure 19, in order to minimise the relative angles used during production.

(ii) Waste slittings: The waste slittings used in this study were waste glass-fibre fabric off-cuts from an industrial weaving process. Here, the idea of incorporating this material (and the direct-loom waste) into the current study was to aid with the development of a method which could be used to recycle waste composite materials (instead of deposition into landfill; as is currently employed). These fibres consisted of a woven material which had been heat-cleaned, silane-finished and coated with a proprietary resin sealant. The material had an average width of 15 mm with approximately 5 mm of the weft fibres protruding from the edge of the fabric. Figure 20 shows the relative dimensions of the warp and weft fibres of the waste slittings.

These waste fibres are normally deposited into a waste disposal bin and transported to a landfill site for disposal. However, for the purposes of this project, the waste slittings were removed manually from this waste disposal bin and were wound onto conventional fibre bobbins.

Figure 21 shows a photograph of a fibre bobbin with waste slittings. For reference, approximately 1920 kg of waste slittings is landfilled per annum by the manufacturer.

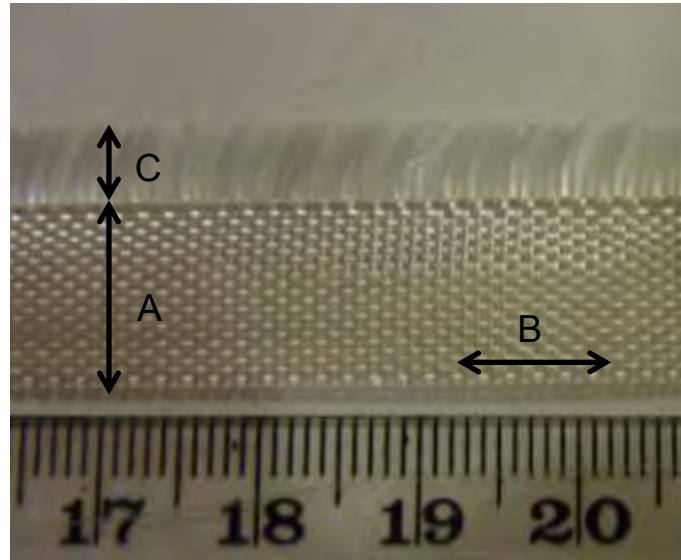


Figure 20. Photograph of the waste slittings showing the relative dimensions of the warp and weft fibres. The highlighted components are: (A) weft fibres; (B) warp fibres; and (C) protruding weft fibres.

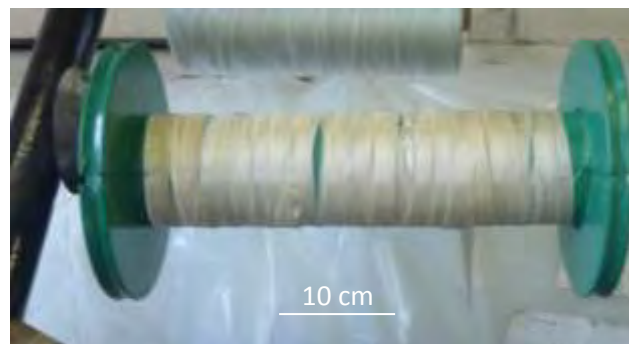


Figure 21. Photograph of a fibre bobbin with waste slittings.

(iii) *Direct-loom waste*: As with the waste slittings, the direct-loom waste fibres were glass-fibre fabric off-cuts from an industrial weaving process. In particular,

the off-cuts consisted of a woven material which had an average width of 60 mm where the weft fibres were secured in position by 5 rows of stitched cotton threads (warp fibres). It should be noted that the direct-loom waste material had not undergone the same heat cleaning and/or silane treatment procedures that the waste slittings had experienced. Figure 22 shows the relative dimensions of the warp and weft fibres of the direct-loom waste.

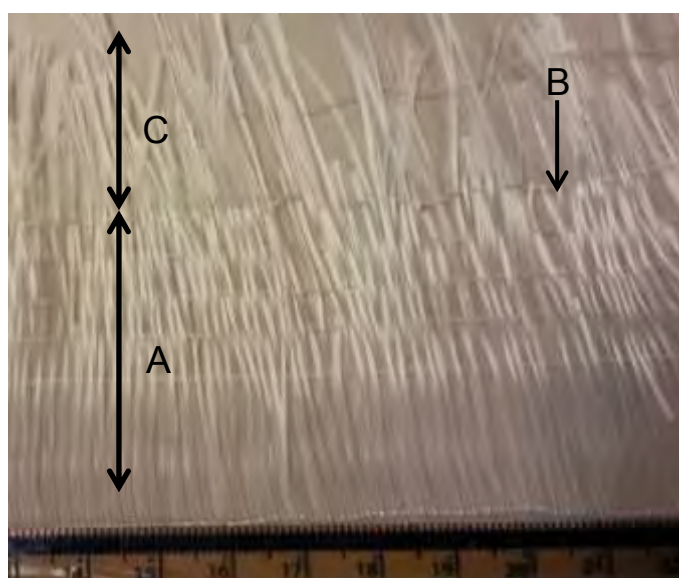


Figure 22. Photograph of direct-loom waste fibres showing the relative dimensions of the warp and weft fibres. The highlighted components are: (A) weft fibres; (B) warp fibres (cotton threads); and (C) unsecured weft fibres.

As with the waste slittings, these waste fibres are normally placed into a waste disposal bin and transported to a landfill site for disposal. However, for the purposes of this project, the direct-loom waste was removed manually from this waste disposal bin and wound onto conventional bobbins. Figure 23 shows a

photograph of a bobbin with wound-on direct-loom waste. For reference, approximately 48,000 kg of direct-loom waste is landfilled per annum by the manufacturer.



Figure 23. Photograph of a bobbin with direct-loom waste.

3.1.2 Resin and Hardener

The previously described reinforcing fibres were processed with an epoxy/amine resin system (LY3505/XB3403) as supplied by Huntsman Advanced Materials. The viscosity of the mixed resin and hardener was 0.3 – 0.4 Pa.s at 23 °C.

3.1.3 Manufacturing Equipment

3.1.3.1 Clean Filament Winding (CFW)

A method termed 'clean filament winding' was developed during the current study to address the aforementioned issues associated with conventional wet-filament winding [215,216]. This modified method was then used to manufacture filament wound tubes using two independent filament winding machines at: (i) the University of Birmingham (in-house manufacture); and (ii) a conventional filament winding plant [38] (on-site manufacture).

(i) In-house Clean Filament Winding: A schematic illustration of the CFW method is shown in Figure 24. With reference to Figure 24, (A) represents the reinforcing fibres mounted on outer-circumference drawn bobbins. The fibre tows are then fed through a tensioning and fibre-guide system (B) which controls the trajectory of the tows. The tows are then directed to a fibre spreading station (C), which consists of rollers and/or pins, where the fibre tows are spread out. This effectively reduces the thickness with a concomitant increase in the width of the tows. The spread fibres are then directed to a resin impregnation unit (D) which is connected to a static mixer (E) and a resin dispensing unit (F). Item (G) represents the traverse-carriage (supported and powered by a conventional filament winding machine) that oscillates across the length of the mandrel (H). The relative speeds of the traverse-carriage and the mandrel dictate the angle at which the fibres are laid down on the mandrel.

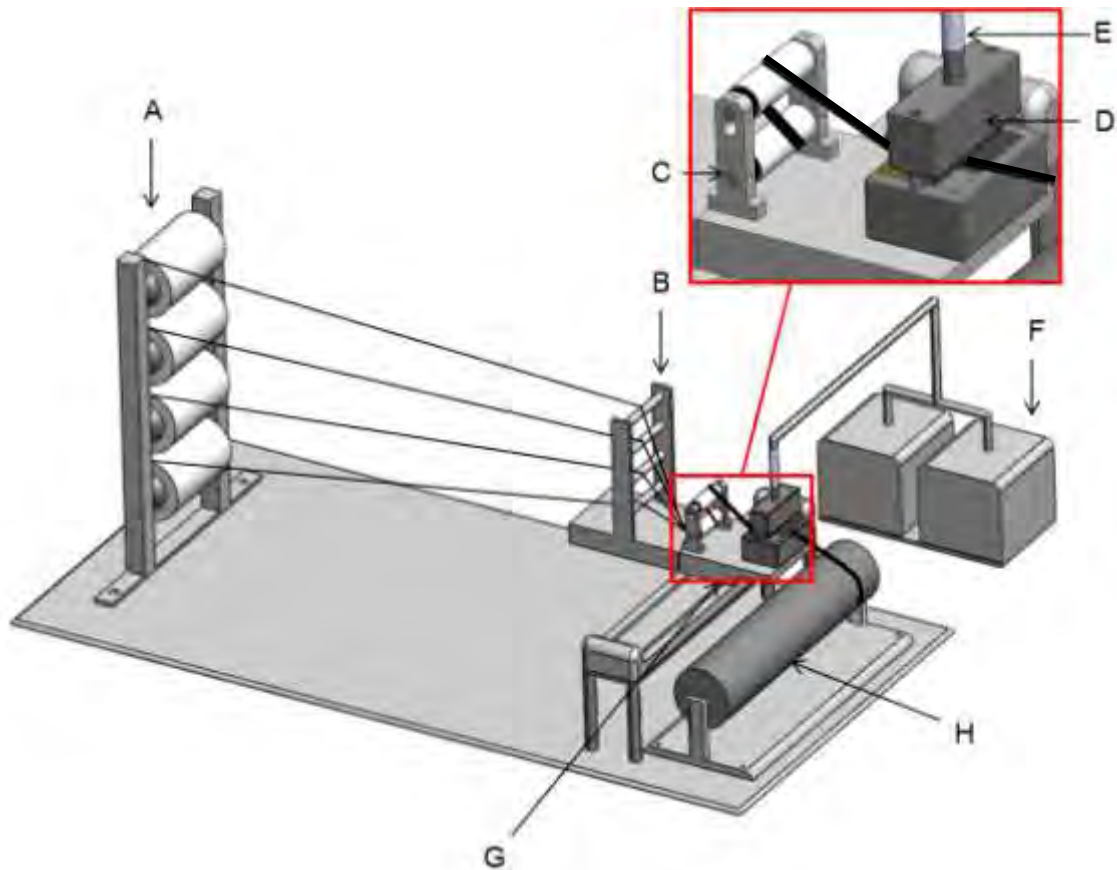


Figure 24. Schematic illustration of the clean filament winding process (see text for details).

With further reference to Figure 24, the following section presents a detailed description of the highlighted components:

[A] Reinforcing fibres: The reinforcements, in the form of continuous fibres, are drawn from the outer-circumference of four bobbins.

[B] Fibre-guide pulleys: The pulleys are pivoted and they perform two functions. Firstly, they control the trajectory of the fibres before they are spread out and impregnated. Secondly, they aid in breaking up the binder present on the fibres.

[C] Fibre spreading station: A key component of the CFW method was a fibre spreading station. Here, the filaments within each bundle were spread-out by mechanical manipulation before they entered the resin impregnation unit. A detailed description of the fibre spreading station used during this study is presented in Section 3.4.

[D] Resin impregnation unit: Unlike conventional wet-filament winding, where a resin bath is used to impregnate the fibres, in the CFW process a custom-designed resin impregnation unit was used. A detailed description of the resin impregnation unit used during this study is presented in Section 3.3.

[E] Static mixer [217]: In the CFW process, the resin and hardener are “mixed” intimately via a conventional Kenics™ static-mixer. Figure 25 presents a photograph of the type of static mixers used during this study. In the CFW process, the static mixer was connected to the resin dispensing unit via a simple manifold connection. The opposite end of the static mixer was connected directly to a resin impregnation unit [D].

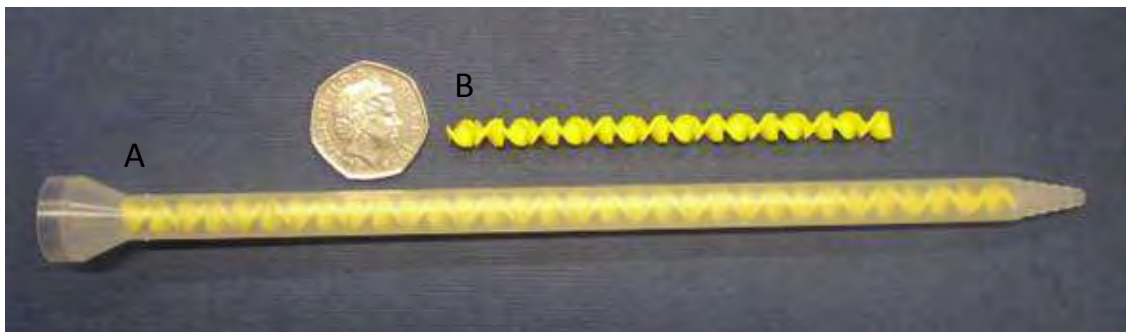


Figure 25. Photograph of: (A) a static mixer; and (B) a static mixing element.

[F] Resin dispensing system: The resin and hardener are contained in separate reservoirs and pumped on-demand via precision gear-pumps to a conventional static mixer. The deployment of the gear-pumps enabled the throughput and stoichiometry of the resin and hardener to be controlled accurately.

The resin dispenser used in this study (shown in Figure 26) was developed and supplied by Dalling Automation Ltd. It consisted of two individual precision gear pumps (Figure 26 (D)) capable of handling liquids in the viscosity range of 20 - 10,000 mPa.s and a throughput range of 10 and 110 g.min⁻¹. The stoichiometric ratio of the two components (epoxy resin and amine hardener) was controlled by the throughput of the individual pumps; 0.6 and 0.3 ml per revolution respectively.

[G] *Traversing carriage*: As shown in Figure 24, the traversing carriage provides an ideal platform to retrofit the resin impregnation unit. Here, the traversing carriage was supported and powered by a filament winding machine which consisted of a custom-modified lathe (Coil Winding Technology, UK). From placing the resin impregnation unit on the traversing carriage, it was possible to minimise any waste-resin dripping onto the floor.

[H] *Mandrel*: In Figure 24, a steel mandrel with a length, outer-diameter and wall thickness of 400 mm, 100 mm and 10 mm, respectively, was used to deposit the impregnated fibres. This mandrel was also connected to a feedback control system which enabled the throughput of the dispensing pumps to be controlled in proportion to the rotation rate of the mandrel.

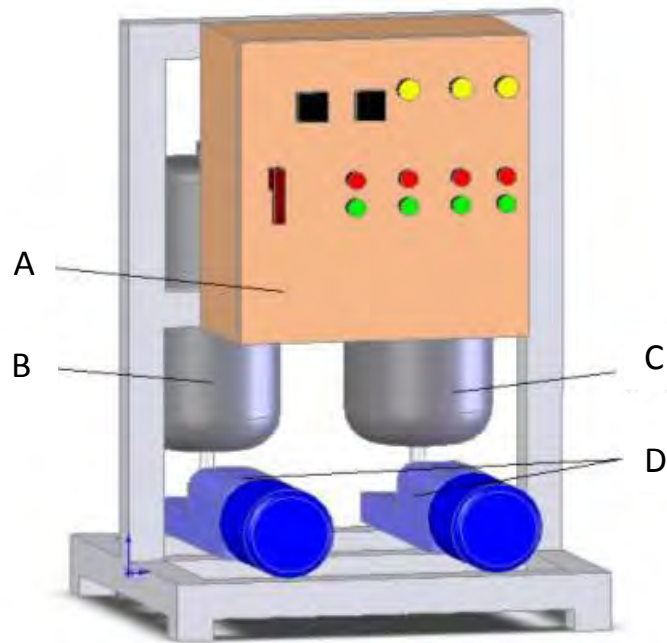


Figure 26. Schematic illustration of the clean filament winding resin delivery system. The labeled items are: (A) feedback control unit; (B) resin reservoir; (C) hardener reservoir; and (D) gear pumps.

Once the required number of impregnated fibre tows were deposited on the mandrel, the assembly was transferred to an air-circulating oven (Figure 27a) for curing at 70 °C for six hours. A mandrel extraction unit was then used to remove the filament wound tubes after processing in the oven (Figure 27b). With reference to Figure 27(b), extraction was carried out by placing the filament wound composite (A), still in assembly with the mandrel (B), onto the mandrel extraction frame (C). An aluminium end-plate was then inserted into one end of the mandrel and a ram (D) was pumped manually to 'push' the mandrel out from the tube inner cavity and through an aperture (E) at the opposite end of the mandrel extraction frame.

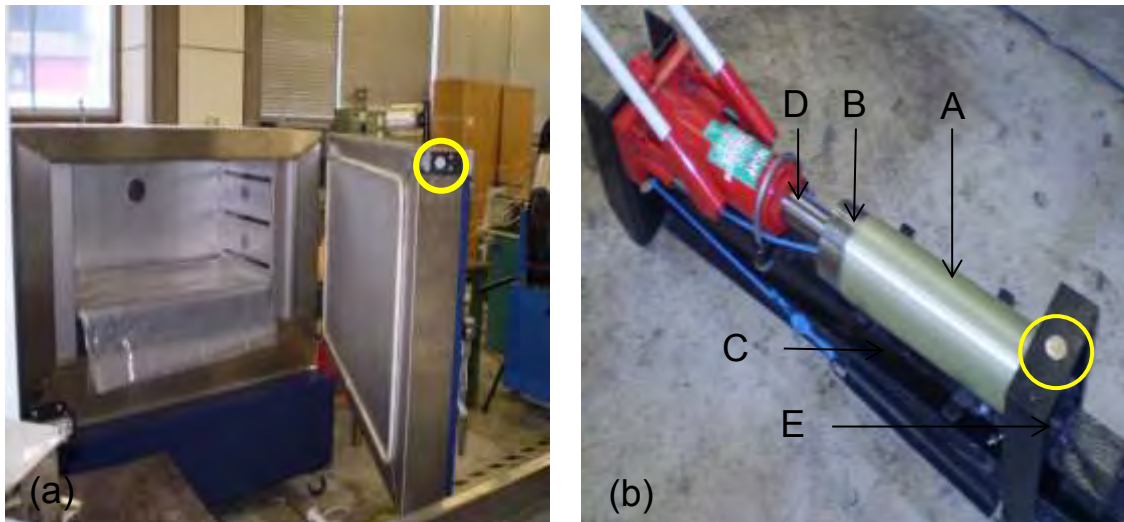


Figure 27. Photographs of: (a) the air circulating oven; and (b) the mandrel extraction system used during the in-house CFW trials. The highlighted components of (b) are presented in the above text.

(ii) *On-site Clean Filament Winding:* The CFW method was also used to manufacture filament wound tubes during an industrial site trial in Portsmouth, UK. Here, the CFW method was retro-fitted onto a conventional 2-axis filament winding machine. Figures 28 and 29 show images of the conventional 2-axis filament winding machine and the retro-fitted CFW equipment respectively. With reference to Figure 29, it can be noted that the retro-fitting of the CFW method was achieved through the use of a ‘simple’ adapter plate. The adapter plate was clamped onto the conventional filament winder and the CFW equipment was bolted directly onto the adapter plate. This adapter plate allowed for a simple and inexpensive connection of the CFW equipment onto the conventional winder and did not require any modification of the winder itself.

In all, the following equipment was transported to Portsmouth and used during the site trials: (i) the resin dispenser; (ii) static mixers; (iii) the resin impregnation unit; (iv) an adapter plate; (v) a creel stand and bobbins (1200 Tex E-glass fibres); (vi) a fibre spreading station; and (vii) a fibre guiding system.



Figure 28. Photograph of the conventional 2-axis filament winding machine used during the industrial site trials in Portsmouth, UK. The scale is indicated by the 3 m mandrel mounted on the machine.

Once the required number of impregnated fibres were deposited on the mandrel, the assemblies were transferred to an air-circulating oven and processed at 70 °C for 6 hours. A mandrel extraction unit was then used to remove the filament wound tubes after processing in the oven. Figure 30(a and b) shows images of the oven and mandrel extraction unit used during the site trials.

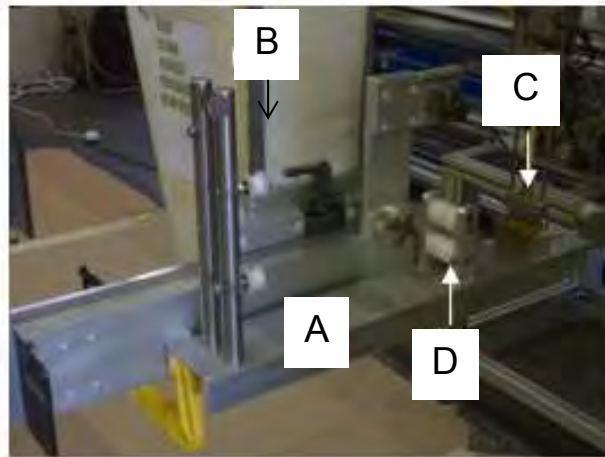


Figure 29. Photograph of the retrofitted CFW equipment onto the conventional 2-axis filament winding machine. The highlighted components are: (A) the adapter plate; (B) the traversing carriage; (C) the resin impregnation unit; and (D) the fibre spreading station.

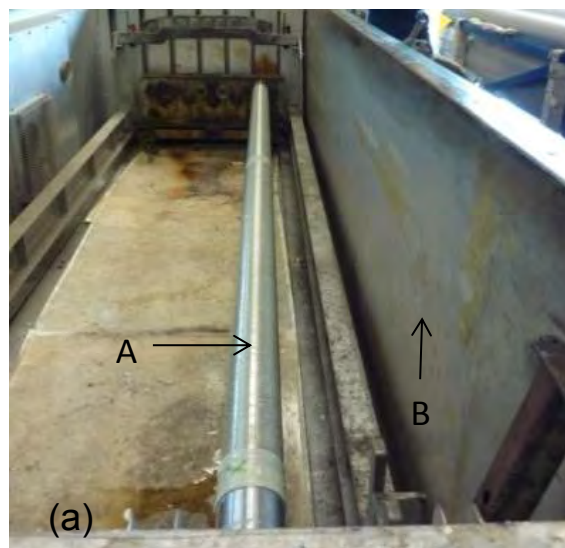


Figure 30(a). Photograph of industrial oven used in sie trial. The scale is indicated by the 3 m mandrel mounted in the oven and the highlighted components are: (A) filament wound tube; and (B) oven.



Figure 30(b). Photograph of the mandrel extraction unit used during site trials.

3.1.3.2 Conventional Filament Winding

Conventional filament wound tubes were also manufactured during this study; these tubes provided reference data which allowed for a comparison between the CFW and conventional filament winding methods.

Conventional filament winding trials were undertaken with the same set-up as that described in Figure 1. Here, reinforcing fibres were fed under a 100 mm diameter nylon roller which directed the fibres into a conventional 5 litre resin bath (width and length of 600 mm). The fibres were then fed over a 300 mm diameter resin impregnation drum which applied the manually mixed resin onto the reinforcing fibres. Once impregnated, the fibres were hauled-off from the impregnation drum, via an exit roller, and directed towards a rotating mandrel which was mounted on the filament winding machine presented in Figure 28. Figure 31 shows the resin-bath impregnation system used during the conventional filament winding trials.

Once the required amount of impregnated fibres were deposited onto the rotating mandrel, the mandrel extraction system and oven shown in Figure 30(a and b) were employed respectively.

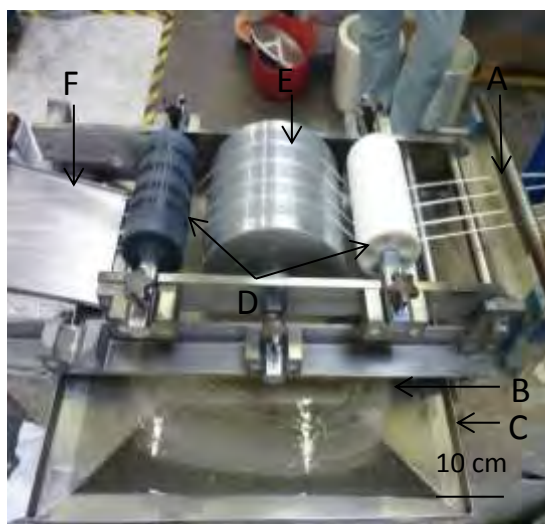


Figure 31. Photograph of the conventional filament winding resin bath. The highlighted components of are: (A) dry fibres; (B) deposited mixed resin; (C) the resin bath; (D) nylon feed rollers; (E) the drum-based impregnation unit; and (F) impregnated fibres.

3.1.4 Analysis Equipment

The following section presents a brief overview of the analysis equipment which was also used during the current study. It should be noted that this section is merely a summary and a detailed description of each piece of analysis equipment is provided in the highlighted sections.

(i) *Leitz DMRX image analysis microscope*; this microscope was employed to analyse the microstructure of filament wound tubes. Further details of this item and procedure associated with its use are presented in Section 3.6.1.

(ii) *JEOL 6060 scanning electron microscope*; this microscope was incorporated to acquire magnified images of the waste-fibre materials and aid in fractography analyses. Here, samples were mounted on conventional scanning electron microscopy (SEM) stubs and were viewed.

(iii) *Zwick-1484 mechanical test machine*; this testing machine (described in greater detail in Section 3.6.3) offered a 100 kN loading capacity and was utilised to complete hoop-tensile (split-disk) testing.

(iv) *Instron-5566 mechanical test machine*; this 10 kN capacity machine was employed to complete the inter-laminar shear and lateral compression testing presented in Sections 3.6.4 and 3.6.5 respectively (greater detail provided in the highlighted sections).

(v) *TQC hydrostatic testing machine*; this external testing facility was situated in Nottingham, UK and was used to complete pressure burst testing of composite overwrapped pressure vessels (equipment described in-detail in Section 3.6.6).

(vi) *Muffle-furnace*; to complete resin burn-off procedures (described in greater detail in Section 3.6.2) a muffle-furnace was employed.

3.2 Calibration of the Resin Dispensing Unit

The following calibration experiments were undertaken before any filament winding trials were completed. This calibration ensured that accurate and consistent resin dispensing rates were achieved.

The resin dispensing unit was assessed for its ability to: (i) independently dispense epoxy resin (LY3505); (ii) independently dispense amine hardener

(XB3403); and (iii) dispense a mixed epoxy resin system (LY3505/XB3403) in the required stoichiometric ratio.

To undertake the first two phases of this calibration, the volume of the dispensed liquid (LY3505 resin or XB3403 hardener) was measured by setting the relevant pump to 4.5 cm³/min (5 rpm), 9 cm³/min (10 rpm), 13.5 cm³/min (15 rpm) and 18 cm³/min (20 rpm). (Note: for independent dispensing, only one pump was turned-on and allowed to dispense). The epoxy or amine was then pumped for two minutes, prior to its collection in a glass beaker for thirty seconds, and the mass of the dispensed liquid was determined by using a four-digit analytical balance. The measured masses were then compared to pre-calculated theoretical values for five calibration measurements across five static mixers.

To carry out the final calibration phase, the throughput of the resin dispensing unit at 11.25 cm³/min (12.5 rpm) (normal dispensing rate for a mixed resin system) was assessed. Here, a similar methodology to that presented above was employed; this ensured that mixed resin was also dispensed at the required rate.

3.3 Development of a Clean Filament Winding Resin Impregnation Unit

A schematic illustration of the prototype resin impregnation unit which was developed during this study is presented in Figure 32. With reference to Figure 32, a cross-sectional schematic illustration of the fibre 'path' through the resin impregnation unit is shown in the expanded view and the key components are described as:

(i) *A primary spreading pin (A)*: a single pin (15 mm diameter) was used to induce further spreading of the fibre tows. The reader is reminded that rollers were also used to induce fibre spreading ahead of the resin impregnation unit.

(ii) *A miniature resin reservoir (B)*: this was a rectangular excavation (12 ml capacity) and it served as a miniature reservoir for the mixed resin system.

(iii) *A resin supply channel for the injector pin and resin bath (C)*: the static mixer was directly attached to the resin supply channel.

(iv) *A resin injector housing (D)*: the resin injector housing was adjustable to enable the fibre tows to be plunged to the desired depth within the miniature resin reservoir.

(v) *A resin injector pin (E)*: this was a pin with a 2 mm slot at the bottom to enable the mixed resin to be injected into the fibre tows. The depth to which the resin injector housing was plunged into the mixed resin system dictated the contact-length and the overall trajectory of the fibre tows.

(vi) *A resin impregnation roller (F)*: this was a cylindrical pin (30 mm diameter) which was placed inside the miniature resin bath (B) to aid with impregnation. This pin caused a resin 'wedge' action to occur between the fibre tow and resin and, as a result, a 'squeezing' action of the resin into the fibre tows was produced.

(vii) *An exit pin (G)*: this pin (15 mm diameter) served as a doctor-blade but it also acted to control the contact-length of the fibre tow with the resin injector pin (E).

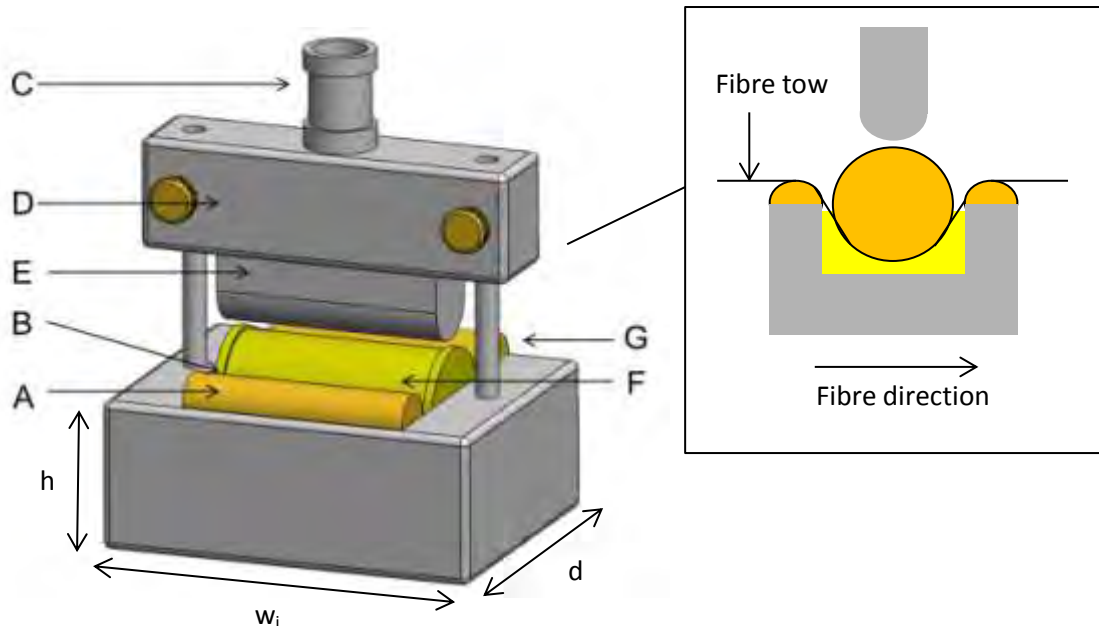


Figure 32. Schematic illustration of the resin impregnation unit. Here, ' w_i ' is the injector width (100 mm), ' d ' is the injector base depth (80 mm) and ' h ' is the injector base height (40 mm). (See text for further details).

3.3.1 Application of Impregnation Modelling

With reference to Section 2.2, two models proposed by Foley and Gillespie [94] (Equation 19) and Gaymans and Wevers [95] (Equation 21) were identified as the most-appropriate to model the overall CFW impregnation process. To apply these equations, the values for the transverse permeability, fibre dimensions, resin viscosity and impregnation pressure were calculated as follows:

Transverse permeability: the transverse permeability was predicted by applying Gebart's model [96] (Equation 11), where the architecture of the fibre bundle was assumed to be hexagonal and the maximum packing capacity was taken as 0.9.

Fibre dimensions: the ‘fibre volume fraction’ and bundle width were defined as 72% and 7 mm respectively. The fibre volume fraction and bundle width were calculated from initial image analysis and fibre spreading investigations.

Resin viscosity: as mentioned previously, the resin system used during this study had a viscosity in the range of 0.3 – 0.4 Pa.s at 23 °C.

Impregnation pressure; capillary pressure and pressure generated by the fibre traversing over a pin. With reference to the CFW technique, the capillary and fibre pressure values were calculated using Equations 16 and 18 respectively. Here, the contact time between the pin and the fibre bundles was calculated using a curvature length of 15 mm and a winding rate of 10 m/minute. The contact time was calculated to be 0.09 seconds and the fibre tension was 10 N.

Once the above-mentioned variables were defined they were then applied to the models proposed by Foley and Gillespie [94] (Equation 19) and Gaymans and Wevers [95] (Equation 21).

With reference to the model proposed by Foley and Gillespie [94], the shape of the fibre bundle was assumed to be circular. However, in the CFW technique, the shape of the fibre bundle at the point of resin injection was a rectangular ribbon; the original equation proposed by Foley and Gillespie [94] was modified accordingly. Furthermore, the impregnation process was assumed to take place over an arbitrary change in the infiltration thickness $T_i = T_1 = c_1 T_0$ to $T_2 = c_2 T_0$, where T_i is the infiltration thickness and T_1 and T_2 are arbitrary steps of infiltration thickness. The infiltration time, t_i , was reformulated as:

$$t_i = \eta(1 - V_f) T_0^2 \left[\frac{c_1^2 \left(\ln \left(\frac{1}{c_1} \right)^2 + 1 \right) - c_2^2 \left(\ln \left(\frac{1}{c_2} \right)^2 + 1 \right)}{4K_y(\Delta P)} \right] \quad (19)$$

Where t_i is infiltration time, η is the viscosity, V_f is the fibre volume fraction, T_0 is the initial thickness of fibre tow, c_1 and c_2 are constants, K_y is the transverse permeability and ΔP is the pressure differential. From Equation 19, the degree of impregnation, D_I , was calculated as:

$$D_I \% = \left[\frac{T_i}{T_0} \right] * 100 \quad (20)$$

The second model that was considered during this study was proposed by Gaymans and Wevers [95]. Here, the degree of impregnation, D_I , was defined as:

$$D_I = \frac{T_i}{T_0} = \sqrt{\frac{2K\Delta P t_i}{\eta \varepsilon T_0^2}} \quad (21)$$

where K is the permeability, η is the viscosity of the liquid, T_i is the infiltration thickness, T_0 is the thickness of the fibre tow, ε is the fibre tow porosity, and ΔP is the pressure differential. Equation 21 can be rearranged in terms of infiltration time, t_i :

$$t_i = (D_I)^2 \frac{\eta \varepsilon T_0^2}{2K\Delta P} \quad (22)$$

The results of the Foley and Gillespie [94] and Gaymans and Wevers [95] simulations are presented in Section 4.5.1. These results were used as a theoretical basis for the optimal residence time needed for the resin impregnation unit presented in the previous section.

3.4 Fibre Spreading During Clean Filament Winding

As mentioned in Section 3.1.3.1, a key feature of the CFW process was also the induced spreading of the fibre tows prior to impregnation. With reference to Section 2.3, fibre-spreading effectively reduces the “thickness” of the fibre tows and facilitates a faster and more efficient transverse impregnation. A schematic illustration of the mechanical fibre spreading station used during this study is shown in Figure 33.

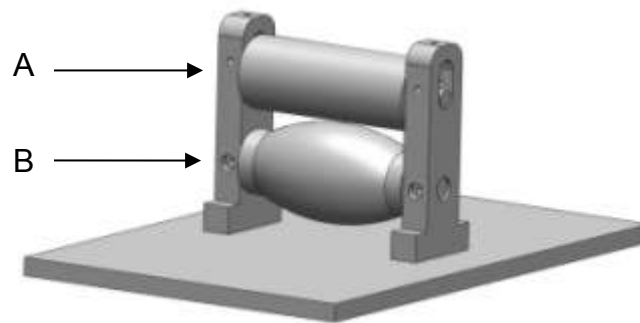


Figure 33. Mechanical fibre spreading station. The highlighted components are: (A) a 35 mm diameter acetyl cylindrical roller (Direct Plastics, UK); and (B) a 50 mm diameter (diameter at middle of pin) acetyl convex roller (Direct Plastics, UK).

With reference to Figure 33, the fibres were fed under the convex roller (mounted on bearings (RS Components, UK) to allow free rotation) and then fed through an ‘S-shape’ route to pass in between the two rollers and over the final cylindrical roller. The fibres were spread through this route and then transported into the resin injector.

The “Taguchi method” [218] was then used to assess the relevance of the following parameters to aid fibre spreading: (i) contact length between the fibre tows and the fixtures of the fibre spreading station; (ii) winding speed; (iii) fixture configuration (pin or roller); and (iv) the number of fibre spreading fixtures. These input factors are summarised in Table 15 where two levels have been specified per parameter corresponding to a minimum (Level 1) and maximum (Level 2). For example, the filament winding speeds at Levels 1 and 2 were set at 2.5 m/min (minimum) and 10 m/min (maximum) respectively.

As four input factors with two level variations were investigated, a 2^4 Taguchi matrix (known as L_{16}) was used for this study. This matrix produced a set of 16 experiments which allowed for an analysis of each input factor for the two level variations. Table 16 shows the Taguchi matrix used during this study. The important columns of Table 16 are A, B, D and H, these columns defined the level settings for the four factors of each experiment. For example, the conditions of experiment 1 are: 2.5 cm contact length (Level 1, shown in column A); 2.5 m/min winding speed (Level 1, shown in column B); roller fixture (Level 1, shown in column D); and 1 pin (Level 1, shown in column H). The other remaining columns of Table 16 i.e. C, E, F, G, I and J, were interactions of the four investigated parameters; these interaction columns were not addressed during this study and only the direct results of columns A, B, D and H were evaluated and discussed. Each experiment was repeated five times and an average degree of fibre spreading for the experiments was taken. The resin impregnation unit and fibre spreading station, shown in Figures 32 and 33 respectively, were used in this study. The degree of fibre spreading was

recorded by using a charge-coupled device camera and fibre tension was also measured by using a 0–50 N fish-scale mounted in-between the resin impregnation unit and the rotating mandrel. The results of the Taguchi analysis outlined in this section are presented in Section 4.6.

Table 15. Input factors for the L₁₆ Taguchi analysis.

	Factors	Level 1	Level 2
A	Contact Length (cm)	2.5	10
B	Winding Speed (m/min)	2.5	10
D	Fixture Configuration	Roller	Pin
H	Number of Fixtures	1	2
	Interactions		
C	Contact Length vs Winding Speed	-	-
E	Contact Length vs Fixture Configuration	-	-
F	Winding Speed vs Fixture Configuration	-	-
G	Contact Length vs Number of Pins	-	-
I	Winding Speed vs Number of Pins	-	-
J	Fixture Configuration vs Number of Pins	-	-

Table 16. L₁₆ Taguchi array.

	A	B	C	D	E	F	G	H	I	J
1	1	1	1	1	1	1	1	1	1	1
2	1	1	1	1	1	1	1	2	2	2
3	1	1	1	2	2	2	2	1	1	1
4	1	1	1	2	2	2	2	2	2	2
5	1	2	2	1	1	2	2	1	1	2
6	1	2	2	1	1	2	2	2	2	1
7	1	2	2	2	2	1	1	1	1	2
8	1	2	2	2	2	1	1	2	2	1
9	2	1	2	1	2	1	2	1	2	1
10	2	1	2	1	2	1	2	2	1	2
11	2	1	2	2	1	2	1	1	2	1
12	2	1	2	2	1	2	1	2	1	2
13	2	2	1	1	2	2	1	1	2	2
14	2	2	1	1	2	2	1	2	1	1
15	2	2	1	2	1	1	2	1	2	2
16	2	2	1	2	1	1	2	2	1	1

3.5 Filament Winding Trials

Filament wound tubes were manufactured using two filament winding machines and three filament winding methods. In all, five winding conditions were utilised: (i) in-house CFW; (ii) on-site CFW; (iii) on-site conventional filament winding; (iv) in-house R-CFW; and (v) on-site R-CFW. The difficulties associated with comparing filament wound tubes manufactured using two different machines are duly acknowledged, however this was necessary in order to fulfil the aims of

this study highlighted in Section 1.3. Details of the five winding conditions are presented in the following sections.

3.5.1 In-house Clean Filament Winding

In the first instance, in-house CFW trials were carried out on a custom-modified lathe (Coil Winding Technology, UK). Here, a winding speed of 10 m/minute, with a pitch (traverse distance per mandrel revolution) of 4 mm and a dispensing rate of 11.25 cm³/min (12.5 rpm) were used to deposit the impregnated glass-fibres onto a 100 mm outer-diameter steel mandrel. Note; all mandrels used during this study were pre-coated with a release agent (Wurtz, PAT/607 PCM) to aid with extraction after winding. Once the required number of impregnated fibre tows were laid on the mandrel, the assembly was transferred to an air-circulating oven (shown in Figure 27) and processed at 70 °C for 6 hours. A mandrel extraction unit (also shown in Figure 27) was then used to remove the filament wound tubes after processing in the oven.

The method outlined in this section was used to manufacture six 4-layered hoop-wound glass-fibre tubes with a wall thickness of ~ 2 mm. The methods used to evaluate the properties of the tubes fabricated during this study are described in greater detail in Section 3.6.

3.5.2 On-site Clean Filament Winding

The CFW method was also used to manufacture filament wound tubes during an industrial site trial in Portsmouth, UK.

The retro-fitted CFW equipment was used to fabricate two 1.5 m glass-fibre filament wound tubes. The first tube was fabricated by winding the impregnated glass-fibres at 7 m/min onto a 106 mm outer-diameter steel mandrel. The winding speed (7 m/min) and mandrel diameter (106 mm) were used as these were the most comparable to the winding conditions used during the in-house winding trials.

The second tube was fabricated by winding the impregnated fibres at 21 m/min (maximum winding speed of machine) onto a 106 mm outer-diameter steel mandrel. During manufacture, the 7 m/min tube was fabricated with a resin throughput rate of 13.5 cm³/min (15 rpm) and the 21 m/min tube was fabricated with the resin dispenser's maximum resin throughput rate of 18 cm³/min (20 rpm). Once the required numbers of impregnated fibre tows were laid on the mandrel, the assemblies were transferred to an air-circulating oven and processed at 70 °C for 6 hours.

3.5.3 Conventional Filament Winding

Conventional filament winding trials were completed with the manufacture of a 1.5 m glass-fibre tube which was also fabricated during the site trials at Portsmouth, UK. During these trials, a winding rate of 21 m/min was used to deposit the impregnated fibres onto a 106 mm outer-diameter steel mandrel. The resin-bath (60 cm width and 60 cm length) was filled with 5 L of mixed resin and, as shown in Figure 31, incorporated a drum-based impregnation system. Once the required number of impregnated fibre tows were laid on the mandrel,

the assembly was subjected to the same curing and extraction methods as outlined in Section 3.5.2.

3.5.4 In-house Recycled-Clean Filament Winding

The CFW method was also developed to manufacture recycled glass-fibre thermoset composites. This method, termed Recycled-Clean filament winding (R-CFW), was developed to incorporate the loom-waste materials (waste slittings and direct-loom waste) which were produced from an industrial weaving process (mentioned in Section 3.1.1). These waste-fibres were used as a fibre feed-stock instead of virgin glass-fibres.

With reference to the manufacture of waste slitting tubes, a winding speed of 5 m/min, with a pitch of 7 mm, was used to deposit the required number of resin-impregnated fibres onto the rotating mandrel (100 mm OD). Here a resin delivery rate of 13.5 cm³/min (15 rpm) was used. With reference to the manufacture of direct-loom waste tubes, a winding speed of 2.5 m/min, with a pitch of 15 mm was used. Here resin was injected into the waste fibres at a rate of 13.5 cm³/min (15 rpm). With regards to the relatively slow winding speeds of 2.5 and 5 m/min, these speeds were used in order to minimise any damage of the relatively delicate waste fibres during processing. Once wound, each waste fibre tube was also processed with the same curing and extraction processes as shown in Section 3.5.1.

The method outlined in this section was used to manufacture six waste slitting and six direct-loom waste hoop-wound tubes. These tubes were then assessed

for their physical and mechanical properties via the methods outlined in later sections.

3.5.5 On-site Recycled-Clean Filament Winding

The R-CFW method was also used during the previously described industrial site trial in Portsmouth, UK (site trial detailed in Section 3.5.2). The R-CFW method was used to manufacture waste-fibre filament wound tubes using the waste slittings material. The use of the waste slittings, as opposed to the direct-loom waste, was based on the preliminary testing data provided by the waste-fibre tubes which were manufactured in Section 3.5.4. This preliminary data showed that the waste slittings were able to offer considerably higher mechanical properties than the direct-loom waste; detailed results are presented in a later section. The higher mechanical properties of the waste slittings, along with its relatively 'easier' handling and processing capabilities (faster winding speeds etc), made it an obvious choice for use during the site trial.

During the site trial, two waste-fibre tubes were manufactured: (i) a hoop-wound waste slittings tube; and (ii) an angle-wound ($\pm 48^\circ$) waste slittings tube. Here both tubes were fabricated with a winding rate of 7 m/min and a resin dispensing rate of 13.5 cm³/min (15 rpm). The impregnated fibres were then deposited onto a 169 mm outer-diameter steel mandrel; the justification for using a 169 mm outer-diameter steel mandrel is explained in detail in Section 4.3.

At this point, it should be noted that both waste-fibre tubes were fabricated with the same retro-fitted equipment (resin injector, resin dispenser etc) as described in Section 3.5.2; the only equipment change involved the use of a custom-made bobbin, shown in Figure 34, to supply the waste slittings to the injector during processing.

Once the required number of impregnated fibre tows were laid on the mandrel (16 layers), the assembly experienced the same curing and extraction methods as outlined in Section 3.5.2.



Figure 34. Photograph of the custom-made bobbins used during the industrial site-trials. The scale is indicated by a UK 50-pence piece.

3.5.6 Manufacture of Composite Overwrapped Pressure Vessels (COPVs)

The versatility of CFW method was demonstrated further by manufacturing composite overwrapped pressure vessels (COPVs). Here, COPV liners were used to characterise the pressure burst strength of the CFW method as a

procedure to test un-lined filament wound tubes was deemed inaccurate and non-repeatable. A photograph of the COPV liners which were used during this study is presented in Figure 35. With reference to Figure 35, the liners had a 2 litre capacity, an average weight of 1.52 – 1.58 kg and were fabricated from a 7060 aluminium alloy.



Figure 35. Photograph of aluminium liners used to manufacture composite overwrapped pressure vessels (COPV's).

The aluminium liners used during this study had a minimum burst strength of 295 bar. However, when coupled with layers of T700 HW carbon-fibre, this minimum strength value was raised to 578 bar; during this study, a similar minimum burst value was also incorporated as a base-line reference for all CFW COPVs, despite the use of glass-fibre material and not high-strength carbon.

In-house manufacture of COPVs: During this study, six glass-fibre COPVs were manufactured with the use of the CFW method presented in Figure 24. However, due to the shape and configuration of the aluminium liners, a set of customised end-fittings needed to be included; Figure 36 shows photographs of the customised end-fittings. Figure 36 also shows an image of a COPV (with the custom-made end-fittings) mounted on the modified lathe in the correct position.

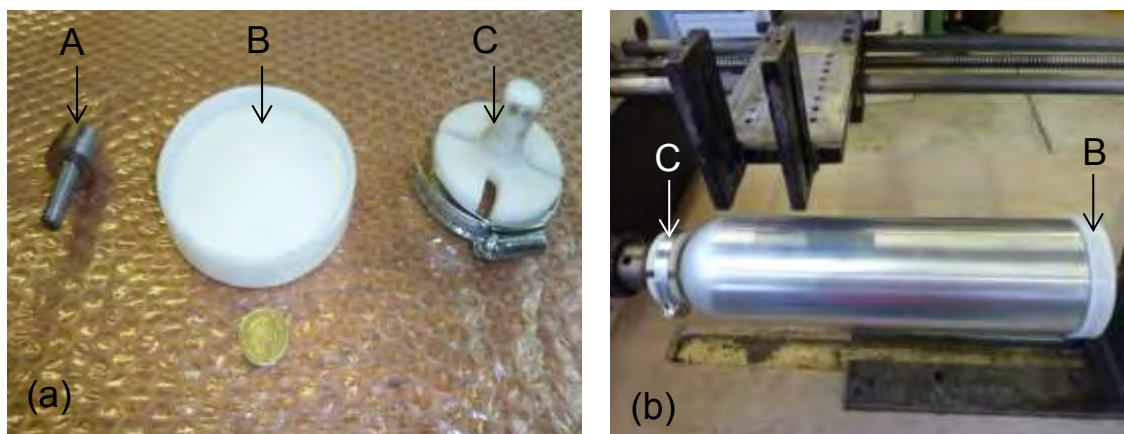


Figure 36. Photographs of: (a) custom-made end-fittings; and (b) an aluminium liner held in-place on the in-house filament winding machine (customised lathe). The highlighted components are: (A) liner nozzle fitting; (B) acetyl base mount; and (C) liner mount. Here, a scale is indicated by a UK £1 coin in Figure 36(a).

With reference to Figure 36(b), the liners were cleaned with acetone prior to winding; this was done to de-grease the surface of the liner. The COPVs were then fabricated with a winding speed of 7 m/min and a resin dispensing rate of 11.25 cm³/min (12.5 rpm). Once the required number of impregnated fibre tows were laid on the mandrel, the assembly was transferred to an air-circulating

oven and processed at 70 °C for 6 hours. This method was repeated to fabricate six 4-layered glass-fibre COPVs.

3.6 Evaluation Methods

The following testing procedures were conducted to evaluate the filament wound tubes manufactured in Section 3.5. Here, all tubes (apart from the two tubes wound in Section 3.5.5; which will be assessed during a further site-trial) were assessed via the following procedures.

3.6.1 Image Analysis

Test specimens (20 mm x 20 mm) were cut using a diamond-coated wheel and mounted using an epoxy adhesive (EpoSet resin and hardener, Epofix). The end-face of the mounted samples were then polished using conventional metallographic procedures. A Leitz DMRX microscope and image analysis suite were used to obtain multiple images at random locations per specimen.

3.6.2 Resin Burn-off: Fibre Volume Fraction and Void Content

The fibre volume fraction and void content of filament wound tubes were evaluated in accordance with ASTM standard D2584 [219] and D2734 [220] respectively. Test specimens (20 mm x 20 mm) were cut from the filament wound tubes using a diamond-coated cutting wheel and their mass was recorded using a five-digit analytical balance. The “burn-off” tests were carried out in a muffle-furnace at 575 °C for 10 hours.

3.6.3 Hoop Tensile (Split Disk) Strength

The procedures stipulated in ASTM D2290 [221] were used to obtain the hoop-tensile strengths of the filament wound tubes manufactured during this study. Rings of 20 mm width were cut from the filament wound tubes and notches of 3.2 mm radius were introduced. A photograph of the test fixture is shown in Figure 37. These tests were carried out at room temperature on a Zwick-1484 mechanical test machine using a cross-head displacement rate of 2 mm/min.

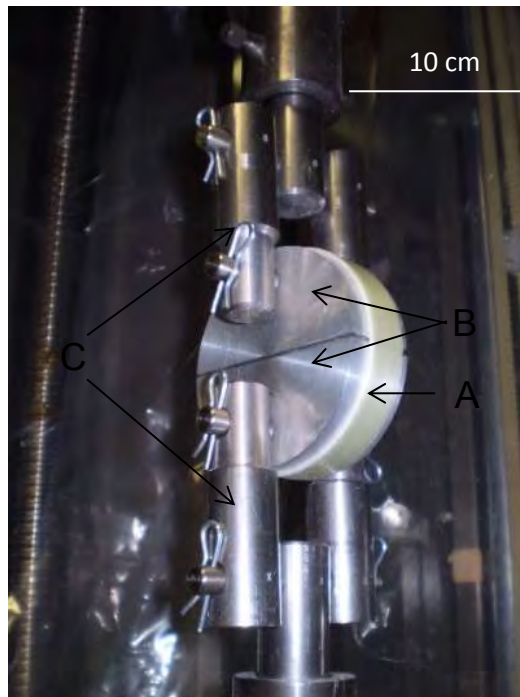


Figure 37. Photograph of the hoop-tensile test fixture. The highlighted components are: (A) a 20 mm wide composite ring; (B) two centrally mounted semi-circular disks; and (C) two metallic jigs connected to the testing machine.

3.6.4 Inter-laminar Shear Strength

The procedures outlined in ASTM D2344 [222] were used to obtain the inter-laminar shear strengths of the filament wound tubes manufactured during this study. Tube sections (arcs) with widths which were at least double the sample thickness and had a length of 32 mm (minimum required for the testing fixture) were cut from the filament wound tubes. A photograph of the test fixture is shown in Figure 38. These tests were carried out at room temperature on an Instron-5566 mechanical test machine using a cross-head displacement rate of 1 mm/min.

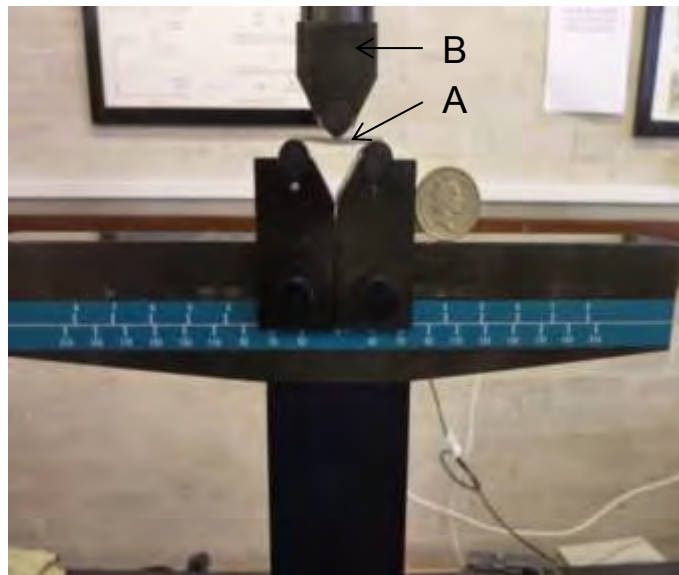


Figure 38. Photograph of the inter-laminar shear test fixture. The scale is indicated by a UK £1 coin and the highlighted components are: (A) a composite test piece; and (B) the testing fixture.

3.6.5 Lateral Compression Strength

The procedures outlined by Gupta and Abbas [223] were used to obtain lateral compression strengths of the tubes manufactured during this study. Here, rings of 15 mm widths were cut from the filament wound tubes and the test fixture shown in Figure 39 was incorporated. These tests were carried out at room temperature on an Instron-5566 mechanical test machine using a cross-head displacement rate of 2 mm/min. Once tested, an identical method as that presented in Section 3.6.3 was incorporated to determine the lateral compression strength.

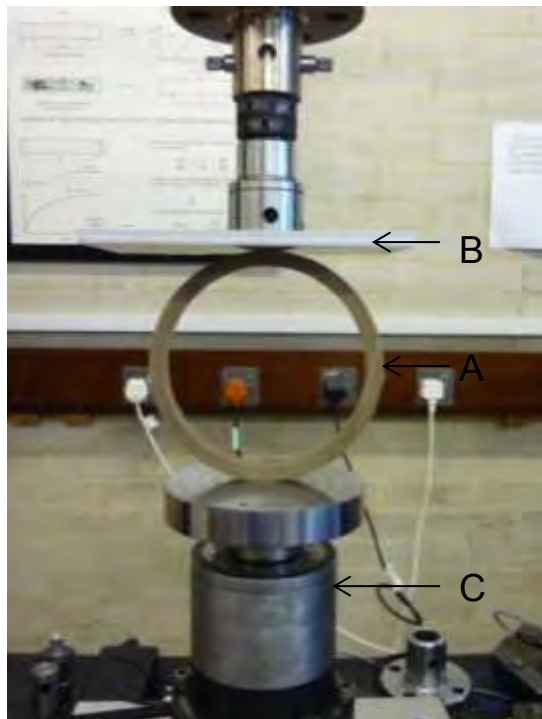


Figure 39. Photograph of the lateral compression test fixture with a cardboard tube ring in-situ. The highlighted components are: (A) a test piece; (B) flat testing platen; and (C) the testing machine.

3.6.6 Pressure Burst Strength of COPV's

A procedure to assess the pressure burst strength of COPVs was also used during this study. Figure 40 presents a schematic illustration of the testing procedure. With reference to Figure 40, the COPV (A) was mounted with a steel end-nozzle (B) which sealed the COPV and connected it with a high-pressure hydrostatic water pump (C). The fixture was then transferred into an underground water chamber (D) where it was filled with water to create a pressure loading rate of ~150 - 200 bar per minute. Figure 41(a and b) shows photographs of the highlighted components of Figure 40.

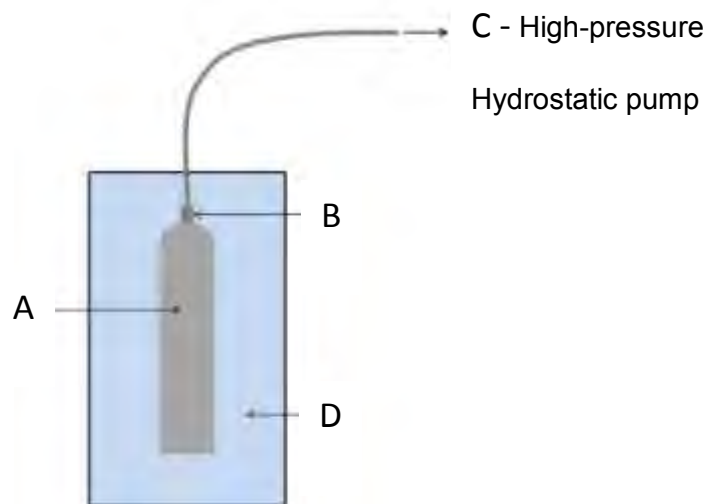


Figure 40. Schematic illustration of the COPV pressure burst test method. The highlighted components are: (A) a COPV; (B) an end-nozzle; (C) the high-pressure hydrostatic pump; and (D) an underground water chamber.

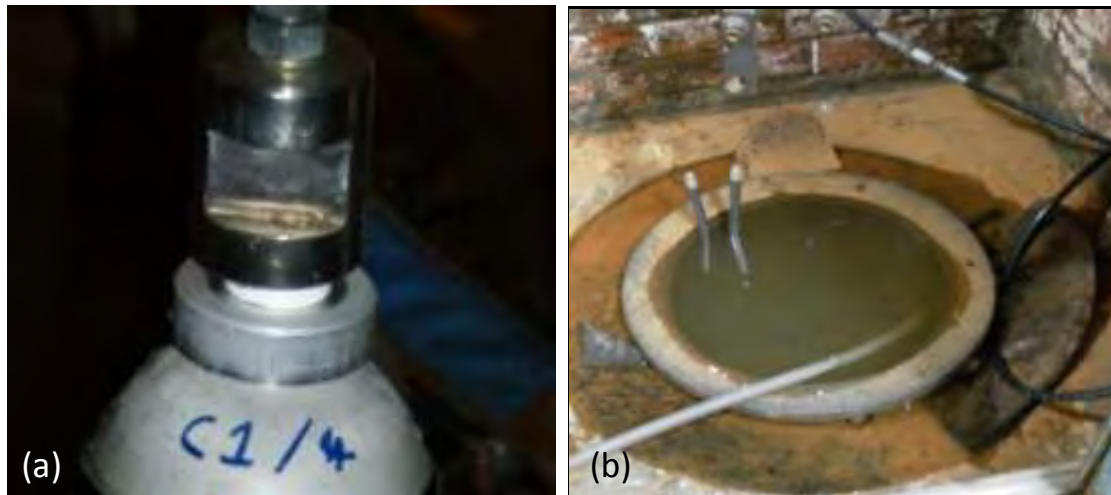


Figure 41. Photographs of: (a) a steel end-nozzle mounted on a COPV; and (b) the underground water chamber.

3.6.7 Life Cycle Assessment (LCA)

With reference to Section 2.6 and ISO 14040, the following section describes an LCA investigation into four laboratory-based winding conditions. This investigation was completed to assess the 'clean' credentials of the CFW and R-CFW methods.

A comparison of the potential environmental impacts of the following winding conditions was completed during this study: (i) conventional filament winding; (ii) CFW; (iii) R-CFW (waste slittings); and (iv) R-CFW (direct-loom waste). However, it should be noted that during this study the conventional winding LCA data was taken from the on-site trials and modified accordingly to be representative of in-house laboratory-based conventional filament winding.

In order to assess and compare the above-mentioned winding conditions a detailed definition of their respective inputs and outputs was needed; Table 17

presents the relevant input and output data for the different winding methods. With reference to Table 17, the stated values refer to the production of tubes with a wall thickness of ~2 mm and a length of 30 cm. Each method was used to simulate the production of 10 tubes respectively.

Table 17. LCA input and output data for the production of 10 tubes.

Winding Method	Epoxy Resin (kg)	E-glass Fibres (kg)	Recycled Fibres (kg)	Acetone (kg)	Power (MJ)	Resin-coated Equipment (No of Pieces)
Conventional	1	3.5	0	5	375.3	5
CFW	0.605	3.5	0	0.1	395.3	3
R-CFW with WS	0.385	0	1	0.1	395.3	3
R-CFW with DLW	2.265	0	2.2	0.1	395.3	3

With reference to Table 17, it was assumed that each production method used a filament winding machine with a 5 kWh AC motor which took two hours to complete the required winding. As a result, 10 kWh or 36 MJ of electricity was assumed to be consumed. Each method was also simulated with the use of the same furnace to cross-link (cure) the respective tubes; here the furnace was assumed to be heated by 6 heating elements which individually consumed 2.3 kWh. The furnace was also equipped with an air circulating motor which consumed 0.7 kWh. As a result, for each method the simulated curing cycle consumed 94 kWh or 339.3 MJ. Furthermore, from analysing Table 17 it can be

noted that the CFW technologies consumed 20 MJ more energy than their conventional predecessor; this was attributed to the use of the resin dispensing unit.

The consumption of epoxy resin during each production method was a function of many factors, such as: (i) impregnation method i.e. resin bath or resin impregnation unit; (ii) winding speed; and (iii) resin dispensing rate. An in depth analysis of these factors is presented in the following results and discussion section.

From analysing Table 17, it can also be noted that the consumption of reinforcing E-glass fibres during the R-CFW methods was defined as zero. As a result, the potential environmental impact from using the recycled reinforcing fibres was also set as zero. This was deemed adequate as the recycled fibres used during the R-CFW method were 100% recycled i.e. if they were not used during this study then 100% of the fibres would have been deposited into a landfill.

The 'acetone' and 'resin coated equipment' factors of Table 17 could also be noted as interconnected factors. Here any decreases in acetone consumption produced from the CFW and R-CFW methods were attributed to the reduction of resin coated surfaces during manufacture.

The input and output data presented in Table 17 was then applied to a filament winding LCA template; this template was developed during this study and is presented in the following section.

With regards to the LCA template, this was used as a generic platform for all winding conditions and the relevant input and output data was then entered into this template for each independent winding method. It should also be noted that the LCA template was restricted to just the assessment of the production of filament wound tubes i.e. the system boundary confined the LCA to just the production phase and was not able to take all life-cycle phases into account i.e. material extraction or use phase.

3.6.7.1 Filament Winding LCA Template

An overview of the LCA template developed during this study is presented in Figure 42. With reference to Figure 42, the LCA template was developed with the use of a commercially available LCA software package (GaBi 4) and consisted of three levels; (i) a Level-3 plan (Input transportation); (ii) a Level-2 plan (Production); and (iii) a Top-level plan (Overview). As demonstrated in Figure 42, the LCA template was produced from independently completing each consecutive level; this produced an overall filament winding template which could be appropriately modified according to the input and output data presented in Table 17.

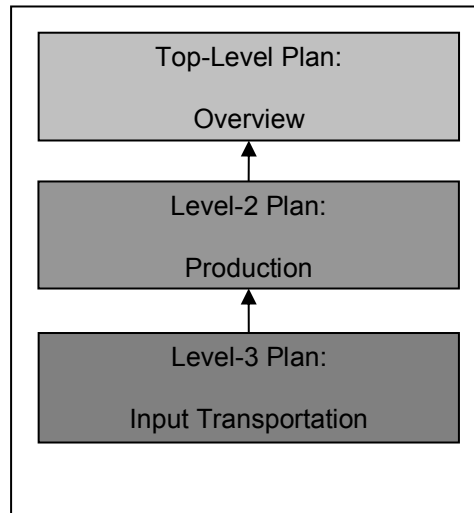


Figure 42. Schematic illustration of the LCA template developed during this study.

The Level-3 plan was generated to assess the potential environmental impacts of transporting the raw materials to the production site. This consisted of transporting the epoxy resin, acetone and reinforcing fibres with the use of a standard transport vehicle (Solo truck powered by diesel fuel). The transportation of the raw materials was said to occur over a set distance of 100 miles. The Level-3 plan (Input transportation) for the transportation of epoxy resin is presented in Figure 43. Similar plans for the transportation of acetone and reinforcing fibres were also simulated.

The Level-3 plans for the transportation of epoxy resin, acetone and reinforcing fibres were then used as input data for two Level-2 plans, namely: (i) a filament winding Level-2 plan; and (ii) a cleaning operation Level-2 plan. The two Level-2 plans are presented in Figures 44 and 45 respectively.

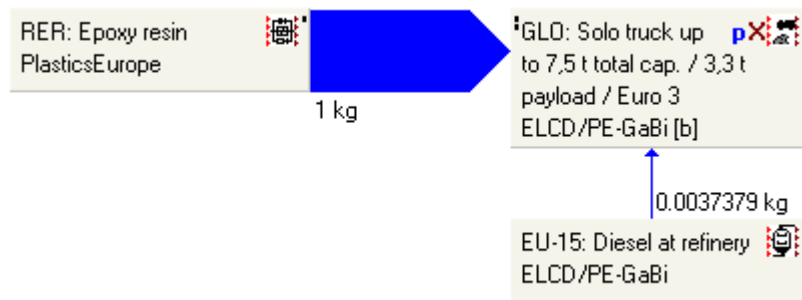


Figure 43. LCA Level-3 plan: Input transportation.

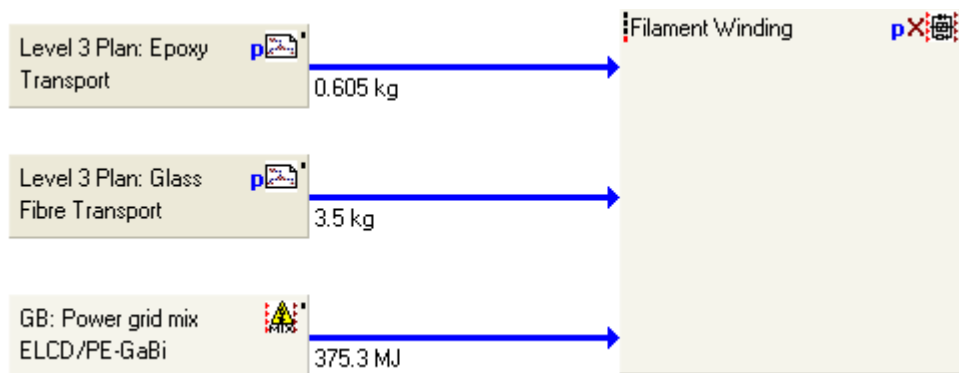


Figure 44. LCA Level-2 plan: Filament winding.

With reference to Figure 44, the filament winding Level-2 plan consisted of three inputs, namely: (i) epoxy resin; (ii) reinforcing fibre; and (iii) power. Here, the power was assumed to be provided from the local power grid mix; this supplied energy for the filament winding machine and the oven.



Figure 45. LCA Level-2 plan: Cleaning operation.

With reference to Figure 45, the cleaning operation Level-2 plan consisted of post-production cleaning of any resin coated equipment. In general, the cleaning process mainly consisted of cleaning the resin impregnation unit, the resin bath or components of the filament winding machine.

The two Level-2 plans presented in Figures 44 and 45 were then combined to produce an overall filament winding LCA template; this is shown in Figure 46.

The filament winding LCA template shown in Figure 46 was then appropriately modified with the relevant input and output data presented in Table 17. As a result, a direct comparison of the four winding conditions could be carried out.

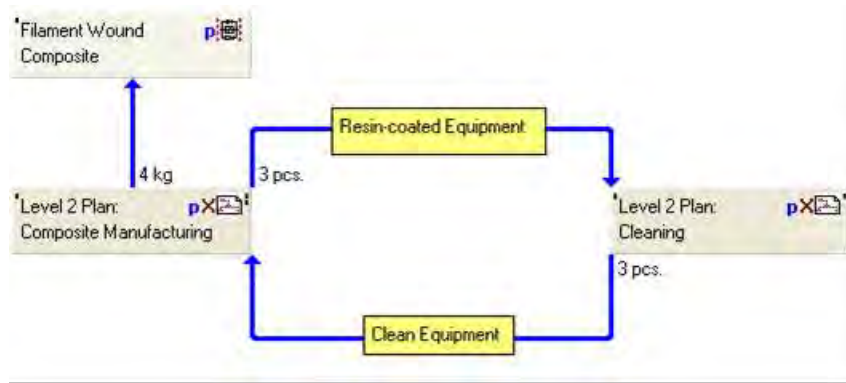


Figure 46. LCA Top-level plan: Filament winding.

3.6.8 Life Cycle Cost (LCC)

A life cycle cost (LCC) investigation into the above-mentioned winding conditions was also completed. This investigation was completed to assess the relative economic credentials of the CFW and R-CFW methods in comparison to their conventional predecessor. This investigation was highly important as no commercial success will occur for any ‘environmentally friendly’ filament winding processes which cannot compete economically with the already established conventional processes.

3.6.8.1 Life Cycle Cost of Filament Winding Methods

To assess and compare the previously-mentioned filament winding conditions, a detailed definition of their respective economic inputs and outputs was needed. Table 18 presents the relevant economic input and output data for the different filament winding methods. With reference to Table 18, the stated

values refer to the in-house production of tubes with a wall thickness of ~ 2 mm and a length of 30 cm. Each method was used to simulate the production of 10 tubes respectively.

Table 18. LCC input and output data for the production of 10 tubes.

Winding Method	Epoxy Resin (£)	E-glass Fibres (£)	Recycled Fibres (£)	Acetone (£)	Power (£)	Man-Power (£)
Conventional	15	4.2	0	11.15	9.38	40
CFW	9.07	4.2	0	0.22	9.88	25
R-CFW with WS	5.77	0	2	0.22	9.88	25
R-CFW with DLW	33.97	0	4.4	0.22	9.88	25

With further reference to Table 18, the presented costs were calculated in accordance with the data (volumes of material) presented in Table 17 and the following cost-of-acquisition data based on representative UK cost values:

Epoxy resin: the resin system (LY3505/XB3403) which was used during all winding conditions was commercially available for £15/kg. The resin was supplied by Huntsman Advance Materials, UK.

E-glass fibres: the E-glass fibres (1200 Tex) were commercially available for £1.2/kg. The fibres were supplied by PPG Industries, UK.

Recycled fibres: the two types of waste fibre (waste slittings and direct-loom waste) were both available for approximately £2/kg (PD-Interglas, UK).

However, it was proposed that if large-scale volumes could be used then the price of the waste-fibres could be waived i.e. reduced to zero; this was based on the savings the supplying company would make on reduced storage and disposal costs.

Acetone: the Acetone solvent which was used for post-production cleaning was commercially available for £2.23/kg.

Power: the power which was consumed during all winding conditions was supplied by the power grid-mix at a cost of approximately £0.09/kWh.

Man-power: during all winding trials a minimum of one machine operator was needed. Here a constant hourly-rate of £10 per operator was used to account for the man-power needed for each trial.

From knowing the above-mentioned data it was then possible to calculate and compare LCC data for each manufacturing process. The results of this analysis are presented in Section 4.8.7.

CHAPTER 4: RESULTS AND DISCUSSION

4.1 Materials

4.1.1 Reinforcing Fibres

Three types of reinforcing fibres were used during the current study: (i) as-received E-glass fibres; (ii) waste slittings; and (iii) direct-loom waste. The following section presents a discussion of the main observations related to their use.

(i) As-received E-glass fibres: The CFW experiments were carried out using: (i) minimal tension; and (ii) a fibre spreading station. Typical micrographs of polished filament wound tube cross-sections are presented in Figures 47 – 50. From analysing these micrographs the following observations and conclusions were made:

(a) the conventional, in-house and on-site CFW methods all produced samples with comparable microstructures. In particular, the micrographs show similar fibre volume fractions (approximately 70%) and no visible void contents; quantitative clarification of these values is presented in Section 4.8.1.

(b) all glass-fibre micrographs show circular fibre cross-sections, as a result, it can be concluded that the fibres were all deposited in the same load-bearing direction.

(c) due to the above observations, it was concluded that Figures 47 – 50 subjectively confirmed that the modified filament winding methods (in-house

and on-site CFW) were able to manufacture glass-fibre filament wound tubes of identical 'quality' to the conventional method.

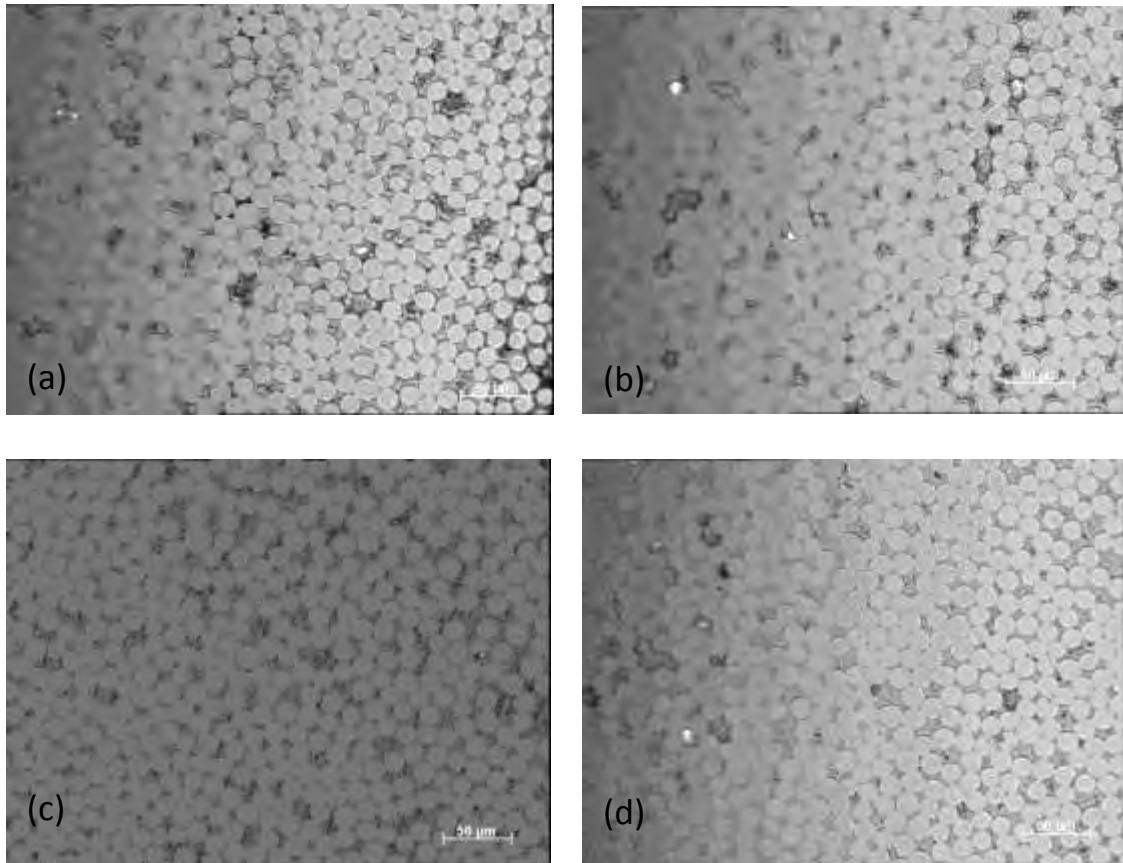


Figure 47. Image analysis micrographs of in-house CFW tube sections.

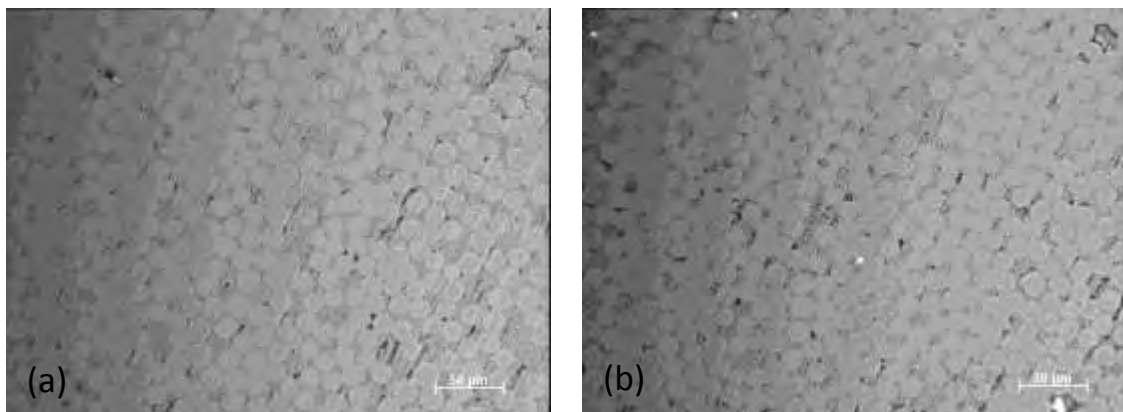


Figure 48. Image analysis micrographs of conventional filament wound tube sections.

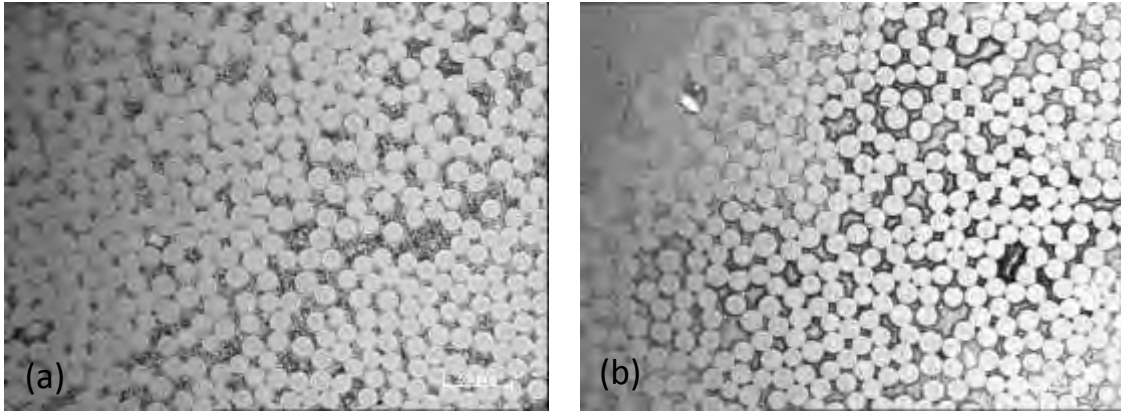


Figure 49. Image analysis micrographs of on-site CFW tube sections (7 m/min).

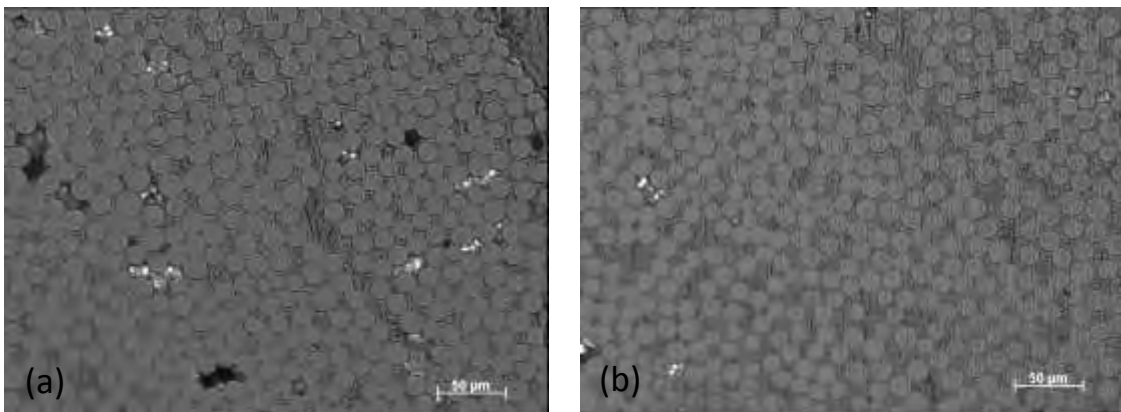


Figure 50. Image analysis micrographs of on-site CFW tube sections (21 m/min).

(ii) *Waste-slittings*: Waste slittings were used to manufacture waste-fibre composite tubes; the following figures (Figures 51 - 54) present micrographs and magnified SEM images.

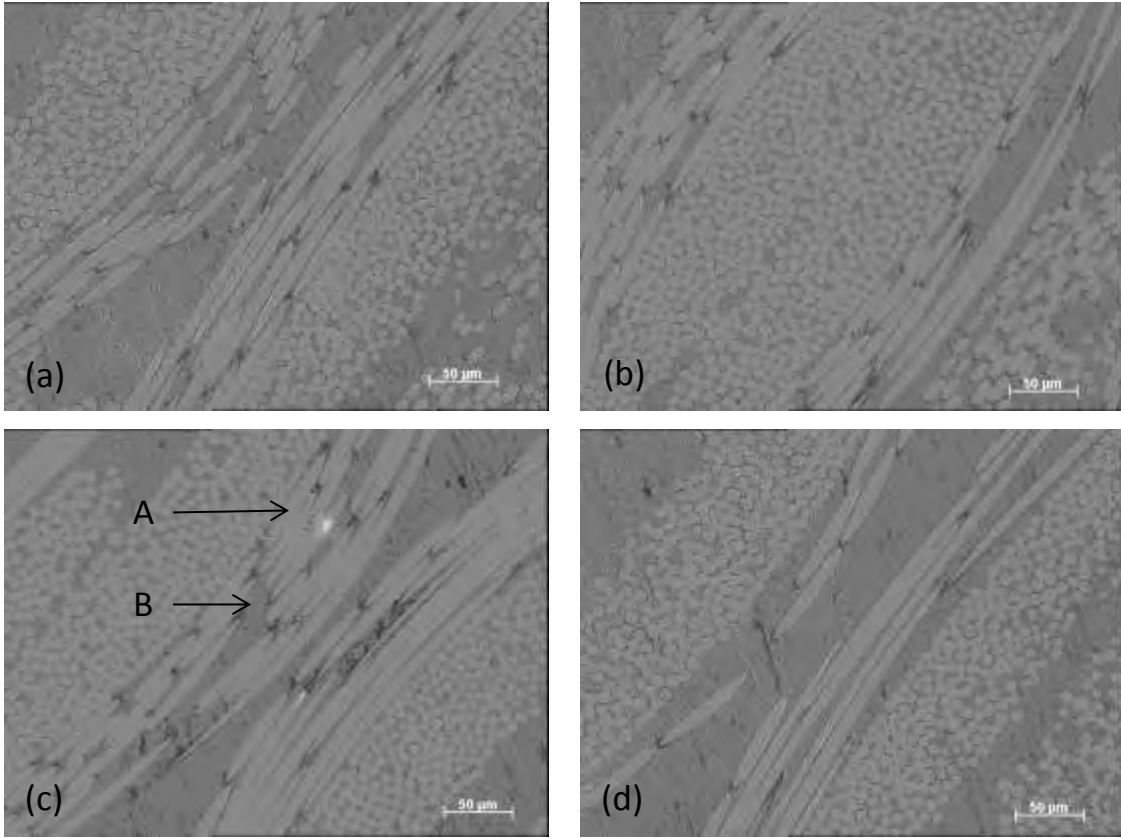


Figure 51. Image analysis micrographs of in-house R-CFW (waste slittings) tube sections. The highlighted components are: (A) reinforcing fibres; and (B) resin.

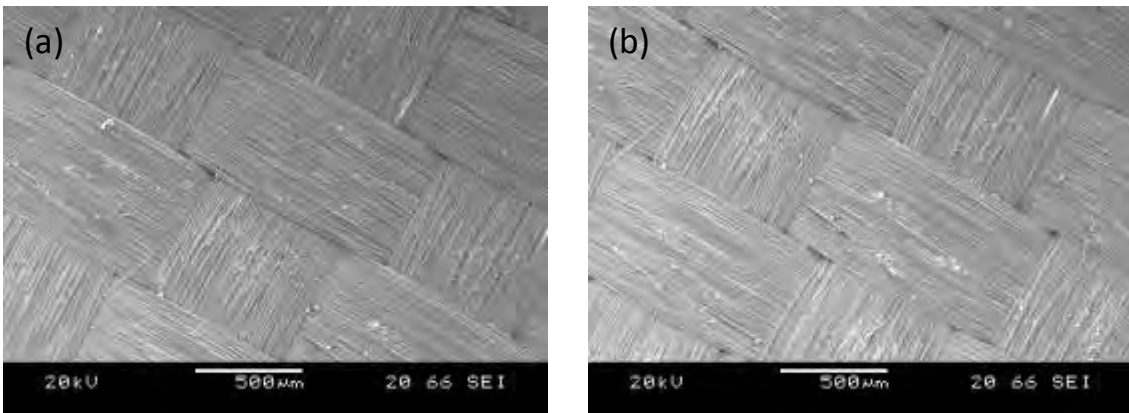


Figure 52. SEM micrographs of the waste slittings (x50 magnification)

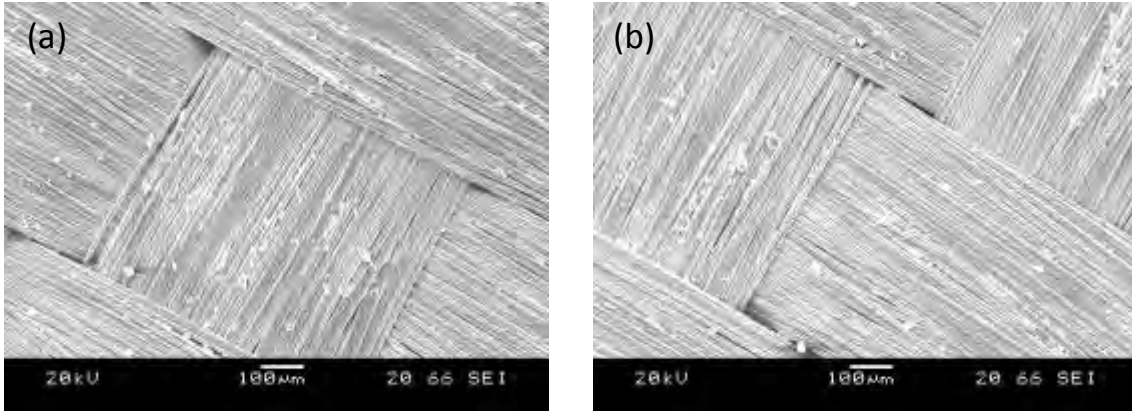


Figure 53. SEM micrographs of the waste slittings (x100 magnification)

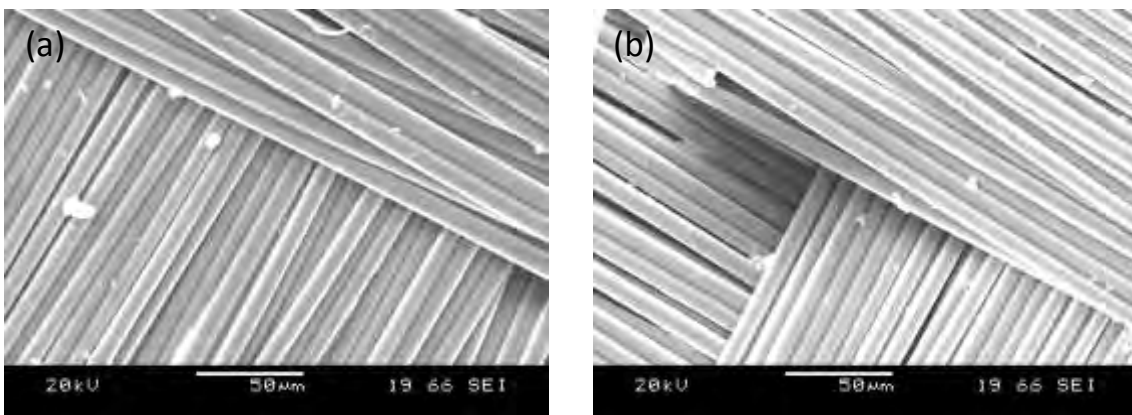


Figure 54. SEM micrographs of the waste slittings (x500 magnification)

From analysing Figures 51 - 54, the following observations were made:

- (i) the material consisted of a plain-weave fabric structure.
- (ii) the waste slittings were not able to offer fibre volume fractions which were comparable to that presented by the previous glass-fibre samples. In particular, from analysing Figure 51 it can be seen that the volume fraction of the resin is relatively high; quantitative clarification of this point shall be discussed in a later section.

(iii) a lower level of fibre alignment control in the R-CFW method was also confirmed. This was achieved by visually comparing the fibre cross-sections of the waste slittings in comparison to the glass-fibre samples presented in Figures 47 – 50. Here, it was possible to identify many waste-fibres which had elliptical cross-sections; therefore confirming that these fibres were not aligned in the same load-bearing direction.

(iv) it was also noted during manufacture that considerable fibre quality issues were present with many of the fibre tows. Figure 55 shows evidence of the varying quality of the waste slittings.

With reference to Figure 55, the observed fibre misalignment was attributed to the storage and cutting methods which were used to separate the waste slittings from its original bulk-woven material. Here, the cutting method was directed to the production of a 'clean' cut for the woven material (bulk and primary material); as a result, the less-important waste material (waste slittings) was occasionally susceptible to quality variations.

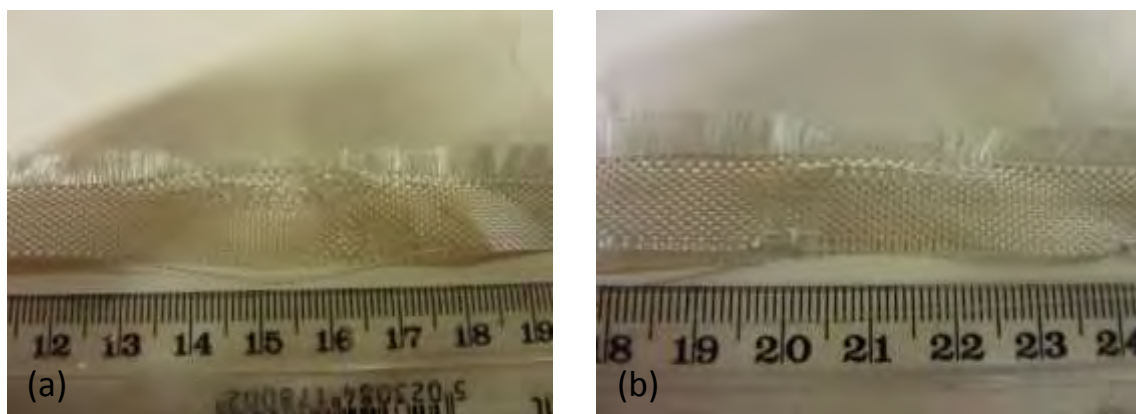


Figure 55. Photographs of varying quality waste slittings.

Despite the quality variations presented in Figure 55, the waste slittings were relatively straight-forward to process; a detailed discussion of the processing needs for this material is presented in Section 4.7.4. In brief, the waste-fibres were substituted-in as a fibre feed-stock and the only changes which had to be made to the CFW process were: (i) a reduced winding speed (10 m/min down to 5 m/min); (ii) an increased pitch (4 mm to 7 mm); (iii) a faster resin delivery rate (13.5 cm³/min); and (iv) the tow had to be flipped (folded-over) after each layer. A tow fold-over procedure was incorporated to ensure that all protruding fibres were not on the leading fibre edge and that they were directly wound-over after each mandrel rotation.

(iii) Direct-loom waste: As with the waste slittings, the direct-loom waste fibres were also used to manufacture waste-fibre composite tubes. The following figures (Figures 56 - 59) present micrographs and magnified SEM images.

From analysing Figures 56 - 59, it was observed that the material consisted of a semi-woven material which produced composite samples with relatively low fibre volume fractions and fibre alignment. Due to the considerable amount of fibre disarray which was present, the direct-loom waste fibres were very delicate and regularly deformed. Figure 60 shows evidence of the quality issues related to the direct-loom waste fibres.

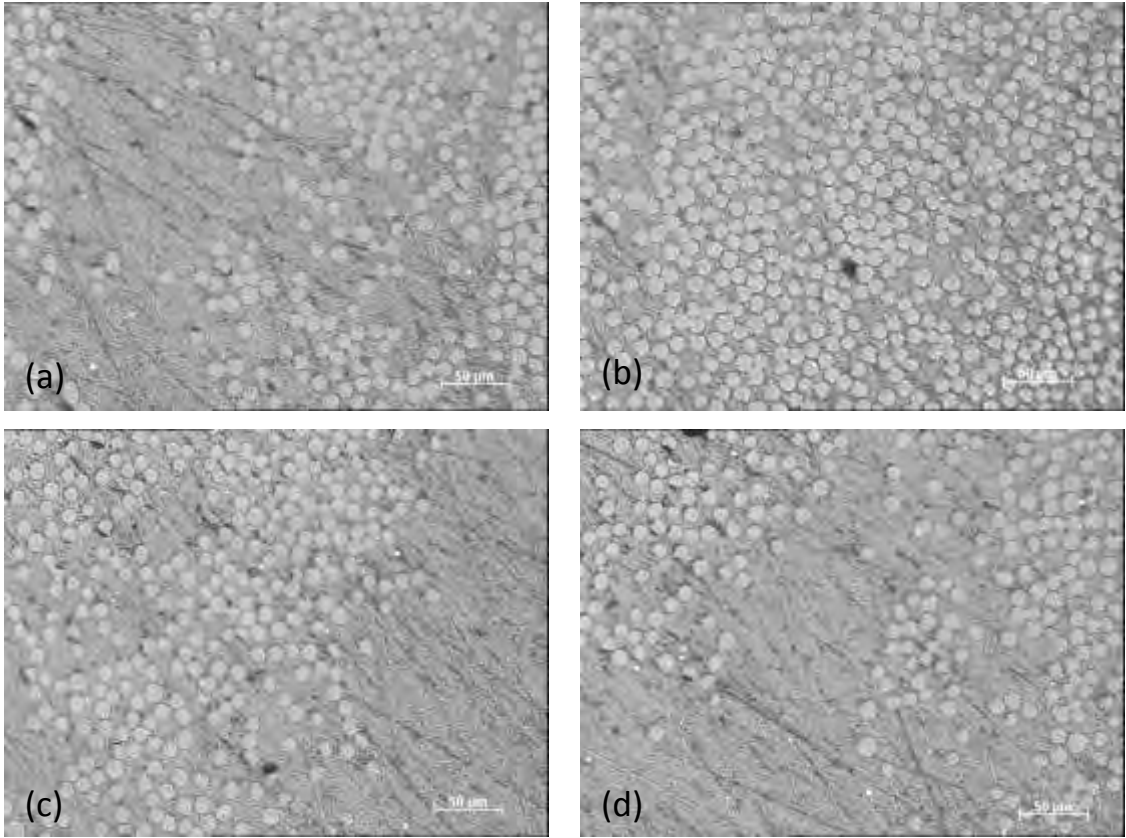


Figure 56. Image analysis micrographs of R-CFW (direct-loom waste) tube sections.

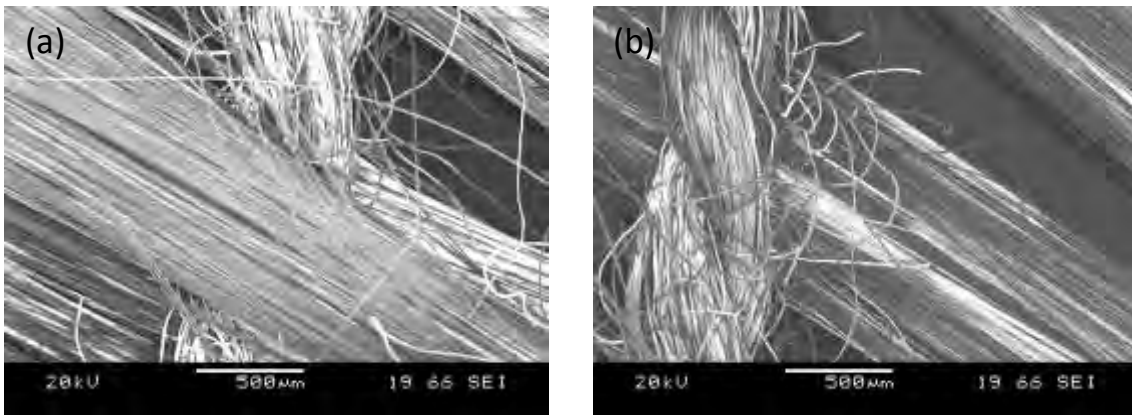


Figure 57. SEM micrographs of the direct-loom waste (x50 magnification)

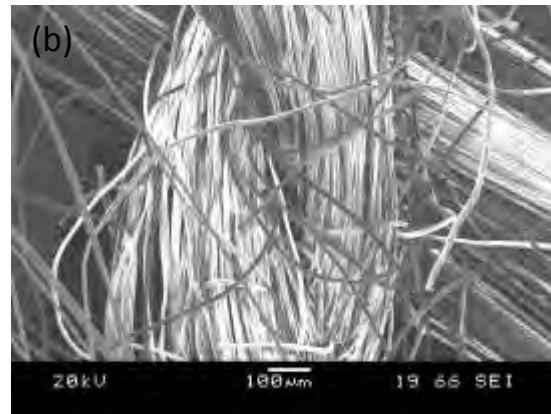
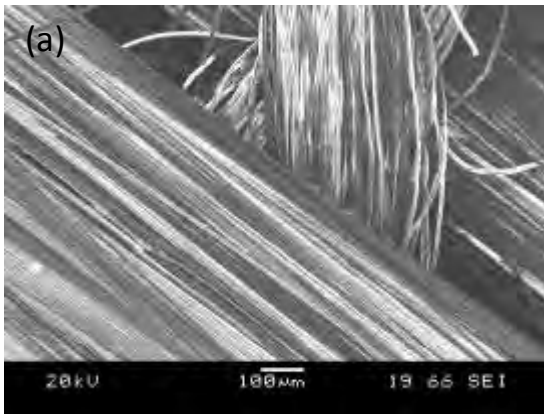


Figure 58. SEM micrographs of the direct-loom waste (x100 magnification)

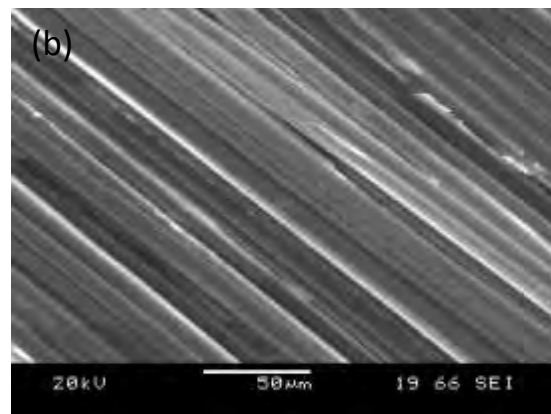
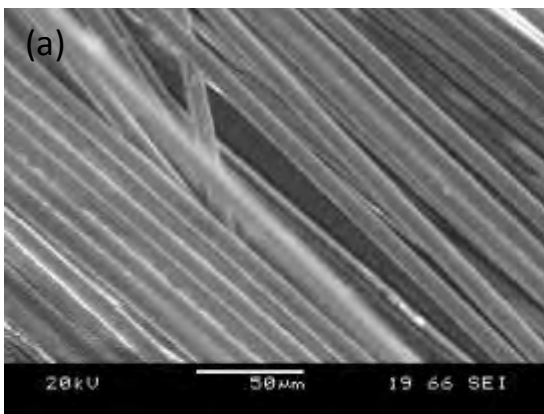


Figure 59. SEM micrographs of the direct-loom waste (x500 magnification)

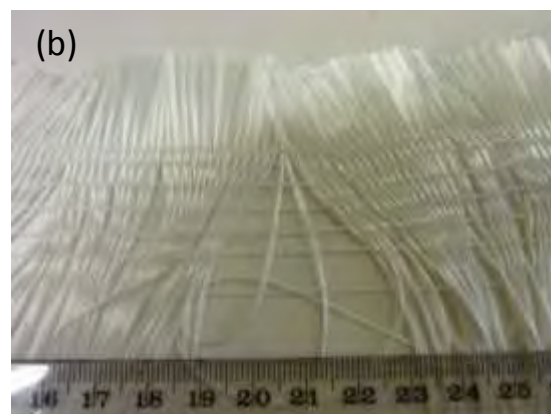


Figure 60. Photographs of varying quality direct-loom waste fibres.

As with the waste-slittings, the quality issues regarding the direct-loom waste fibres were mainly attributed to the storage and cutting methods which were used to separate the waste-fibres from their original bulk woven material. However, due to the delicate nature of the direct-loom waste, it seems improbable that any separation method would be able to produce the direct-loom waste fibres without any degree of non-uniformity.

Due to the delicate nature of these fibres, the method to process them had to be modified accordingly; a detailed discussion of the processing needs for this material is presented in Section 4.7.4. In brief, the following changes had to be made to the CFW process: (i) the winding speed was reduced from 10 m/min down to 2.5 m/min; (ii) the winding pitch was increased from 4 mm to 15 mm; (iii) the resin delivery rate was increased from 11.25 cm³/min (12.5 rpm) to 13.5 cm³/min (15 rpm); (iv) all fixtures i.e. guides, rollers, pins etc. were removed to decrease the fibre tension; (v) the fibres had to be 'flipped' (folded-over) after each layer to ensure that the protruding fibres were not on the leading edge (this ensured a greater level of fibre deposition control); and (vi) the fibres had to be manually consolidated into the previously deposited layers, with the use of a painting brush, to minimise any fibre disarray.

4.1.2 Resin and Hardener

In the current study, all trials were undertaken using the same epoxy resin system (LY3505/XB3403). The aim of this study was to develop a process which uses this resin system in the most efficient and environmentally friendly manner possible for the production of filament wound tubes.

4.2 Clean Filament Winding

To fulfill the first aim of this report, a step-change in the manufacturing process for wet-filament winding was designed, developed and demonstrated. The CFW concept was conceived by analysing the perceived problems with conventional wet-filament winding. Solutions were then proposed and evaluated under laboratory and industrial conditions. The key components of the CFW technique are discussed below:

(i) Resin dispensing unit: The resin containment and delivery system (described in Section 3.1.3.1) was developed to address the problems highlighted in Section 1.2 with regards to manually mixing the resin and hardener components. The primary advantage here was that the resin impregnation unit did not need to be replenished manually. The containment of the two components in enclosed reservoirs also avoided the issues associated with: (i) the limited pot-life of the mixed resin system; and (ii) emissions, for example, from open-top resin baths.

Section 4.4 demonstrates the ability of the resin dispensing unit to deliver a mixed resin system in the required ratio and volume.

(ii) *Static mixer*: The static-mixers, described in Section 3.1.3.1, were also used to address the problems highlighted in Section 1.2 with regards to manually mixing the resin and hardener components. Here, the static mixers consisted of a series of helical elements which were fixed within a tubular housing. These consecutive elements opposed each other and were welded together such that the adjacent edges were perpendicular. As a consequence, the fluid was split every time it exited one element and entered another. This process continued along the length of the static mixer, where with the appropriate selection of the number of helical elements in the static mixer, a good homogenisation of the resin system could be attained [224].

(iii) *Resin impregnation unit*: The resin impregnation unit, described in Section 3.3, was also developed to address the issues highlighted in Section 1.2. In particular, the resin impregnation unit resulted in a significant reduction in the volume of waste resin produced. This reduction could be attributed to the lower volume of the resin impregnation unit (approximately $1.2 \times 10^{-5} \text{ m}^3$) in comparison to the 5-litre resin bath used in the conventional filament winding technique. Moreover, the volume of solvent required to clean the resin impregnation unit was significantly lower than that needed for the resin bath. The effective free-surface areas (areas which could come into contact with resin) for a 5-litre resin bath with a rotating drum (for resin pick-up) and the current resin impregnation unit were approximately 0.448 m^2 and 0.005 m^2 respectively. As a consequence of this reduced volume, the emissions to the atmosphere were also significantly reduced in the CFW process.

During the CFW process, the resin impregnation unit was also located directly above the rotating mandrel. This was important as it essentially eliminated the probability of resin drips from the impregnated fibre bundles.

Section 4.5 presents a further in-depth analysis of the resin impregnation unit developed during this study.

(iv) Fibre spreading station: As mentioned previously, a key component of the CFW method was its ability to spread-out a fibre tow during processing. This effectively increased the width of the tow and concomitantly reduced its nominal thickness. The reduction in the thickness of the tow was necessary to enhance the through thickness impregnation rate of the fibres by the mixed resin system. Section 4.6 presents an in-depth analysis of the fibre spreading method which was used during this study.

4.3 Recycled-Clean Filament Winding (R-CFW)

The CFW method was also adapted to enable the manufacture of filament wound tubes using waste glass-fibre fabrics (waste slittings and direct-loom waste). This method (R-CFW) was developed to incorporate waste materials (waste slittings and direct-loom waste) which were produced from an industrial weaving process. The rationale for developing this method was based on the legislative procedures, presented in Section 2.4, which are attempting to reduce the environmental impact of the composites industry. One of the aims of the current study was to develop a 'closed-loop' recycling method which could be used to manufacture waste-fibre thermoset composite tubes.

During this study, 'closed-loop' recycling was defined as 'the reuse of waste materials back into the processes which produced them'. As an example, during this study waste-fibre filament wound tubes were fabricated as storage units for the glass-fibre fabrics from which the waste-fibres were produced. This closed-loop recycling method was then able to address multiple issues which were experienced by the glass-fibre fabric manufacturer, such as: (i) waste-fibre disposal costs; (ii) waste-fibre disposal restrictions; and (iii) reductions in cardboard tube usage and expenditure.

With reference to the above-mentioned third point, the waste-fibre tubes manufactured during this study were produced as substitutes for cardboard tubes; cardboard being the predominant material used for the storage of glass-fibre fabrics during the weaving process. Figure 61 shows the cardboard tubes in-use as glass-fibre fabric storage units. The replacement of cardboard tubes was ideal as there were many issues related to their usage, such as: (i) high cost; and (ii) short life-span. Here, it was estimated that the cardboard tubes only had a life-span of approximately three 'cycles' (number of uses) before they were either damaged or deformed. Figure 62 shows photographs of typically deformed cardboard tubes.

Due to their short life-span, it was reported that approximately 1800 cardboard tubes were used by this company per annum with a resulting purchasing cost of ~£5,500. In addition to this purchasing cost, it was also estimated that approximately £12,500 was expended (per annum) for the storage and disposal of these tubes. In other words, the glass-fibre fabric manufacturer was outlaying ~£18,000 per annum for the use of cardboard tubes.

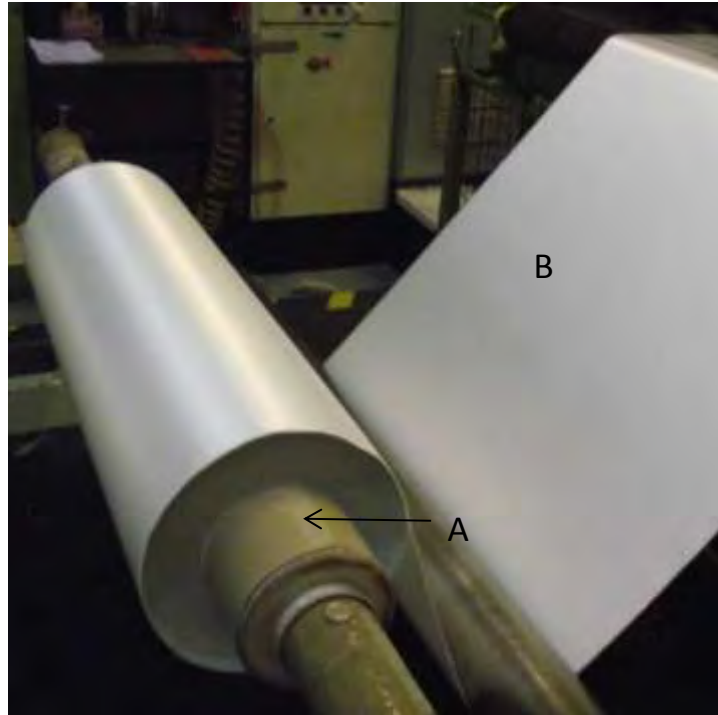


Figure 61. Cardboard tube in-use. The highlighted components are: (A) a cardboard tube; and (B) glass-fibre fabric.

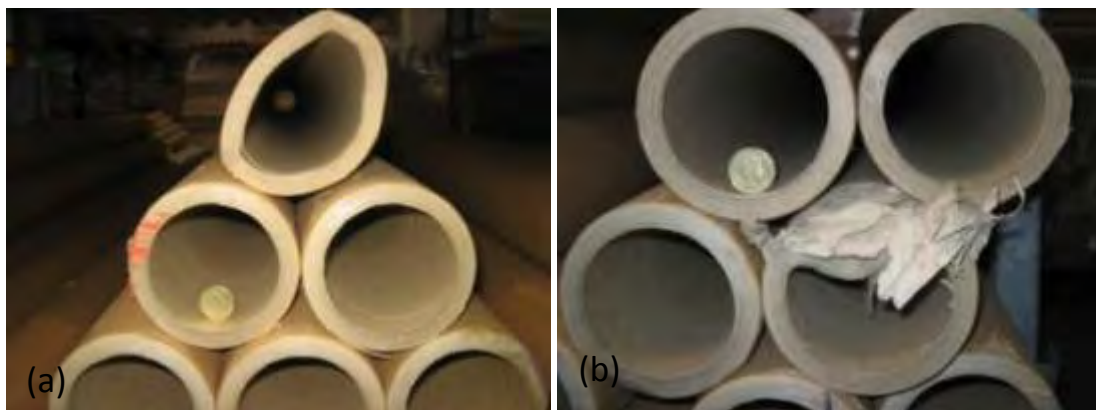


Figure 62. Photographs of end-of-life deformed cardboard tubes with: (a) lateral compressive deformation; and (b) edge-damage due to moisture ingress. A scale is provided by a UK £1 and 50p coin respectively.

Due to the above-mentioned costs, there was a clear incentive to manufacture waste-fibre tubes which could replace cardboard tubes and hence reduce processing costs. To replace the cardboard tubes, the waste-fibre tubes had to offer: (i) an economically-viable long life-span; (ii) relatively high mechanical properties, in particular lateral compression strength (as this will be the main loading direction when in-use); and (iii) a smooth outer surface (smooth surface required so no glass-fibre fabric damage could occur). Sections 4.7.4 and 4.7.5 of this study discuss the ability of the R-CFW method to fabricate waste-fibre composite tubes in-line with the above specification.

4.4 Calibration of the Resin Dispensing Unit

As mentioned in Section 3.2, the resin dispensing unit, which was a key component of the CFW process, was calibrated before any winding trials were undertaken. A summary of the results from this calibration study are presented in Table 19. With reference to Table 19: (i) the densities of the epoxy resin (LY3505) and amine hardener (XB3403) were measured to be 1.2 g/cm^{-3} and 1 g/cm^{-3} respectively; and (ii) a 95% confidence interval for each measurement was presented. Here, the confidence intervals aided in statistically analysing the accuracy of the resin dispensing unit.

The calibration results presented in Table 19 were compared to their theoretically 'predicted' volumes in Figures 63 - 65. Here, the 'predicted' volumes were the theoretical values which should have been dispensed if the geared pumps were working appropriately.

From analysing Figures 63 - 65, it can be seen that there were no significant differences between the three measured datasets and their respective 'predicted' values. However, it can be seen that there was a slight decrease in accuracy as the dispensing rates were increased. To support this observation, it can be seen that the 'predicted' volumes for the 4.5 cm³/min (5 rpm), 9 cm³/min (10 rpm) and 11.25 cm³/min (12.5 rpm) experiments fell well within the respective 95% confidence intervals produced from the 'measured' volumes. Conversely, it can be seen that the predicted volumes of the 13.5 cm³/min (15 rpm) and 18 cm³/min (20 rpm) experiments did not fall within the respective 95% confidence intervals. As a result, it can only be stated that the resin dispensing unit was able to dispense the required volume of resin, with a confidence level of 95%, at rates up to 11.25 cm³/min (12.5 rpm).

The slight accuracy deviations presented for the 13.5 cm³/min (15 rpm) and 18 cm³/min (20 rpm) dispensing rates were attributed to: (i) the possible presence of 'gear slippage' at the higher dispensing rates; and (ii) slight manual measurement errors which were amplified at the higher dispensing rates. As a result, all trials were completed with a maximum dispensing rate of 11.25 cm³/min (12.5 rpm) wherever possible.

Table 19. Dispensed volumes of the epoxy resin, amine hardener and mixed epoxy resin (LY3505/XB3403).

Material		Average measured volumes per minute (cm ³ /minute)				
		Gear pump rate: 4.5 cm ³ /min (5 rpm)	Gear pump rate: 9 cm ³ /min (10 rpm)	Gear pump rate: 11.25 cm ³ /min (12.5 rpm)	Gear pump rate: 13.5 cm ³ /min (15 rpm)	Gear pump rate: 18 cm ³ /min (20 rpm)
LY3505	Measured volume	3.0 (± 0.05)	5.98 (± 0.11)	-	8.86 (± 0.13)	11.86 (± 0.1)
	95% confidence interval	2.99 – 3.02	5.93 – 6.02	-	8.81 – 8.91	11.82 – 11.90
	Predicted volume	3	6	-	9	12
XB3403	Measured volume	1.51 (± 0.06)	2.97 (± 0.08)	-	4.37 (± 0.17)	5.84 (± 0.08)
	95% confidence interval	1.48 – 1.53	2.94 – 3	-	4.30 – 4.44	5.81 – 5.88
	Predicted volume	1.5	3	-	4.5	6
LY3505/ XB3403	Measured volume	-	-	11.29 (± 0.99)	-	-
	95% confidence interval	-	-	11.25 – 11.32	-	-
	Predicted volume	-	-	11.25	-	-

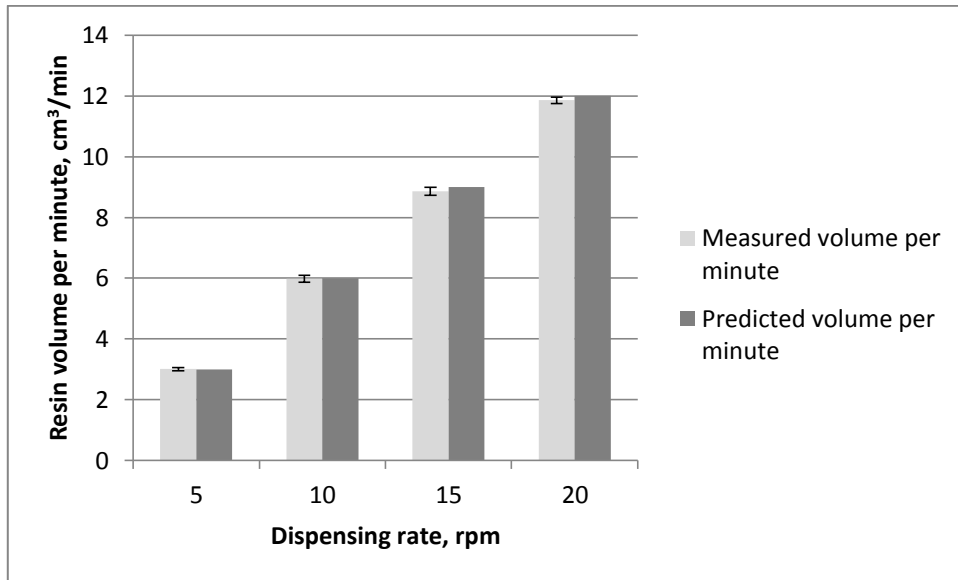


Figure 63. Comparison of measured and “predicted” volumes of the epoxy resin (LY3505) at four dispensing rates.

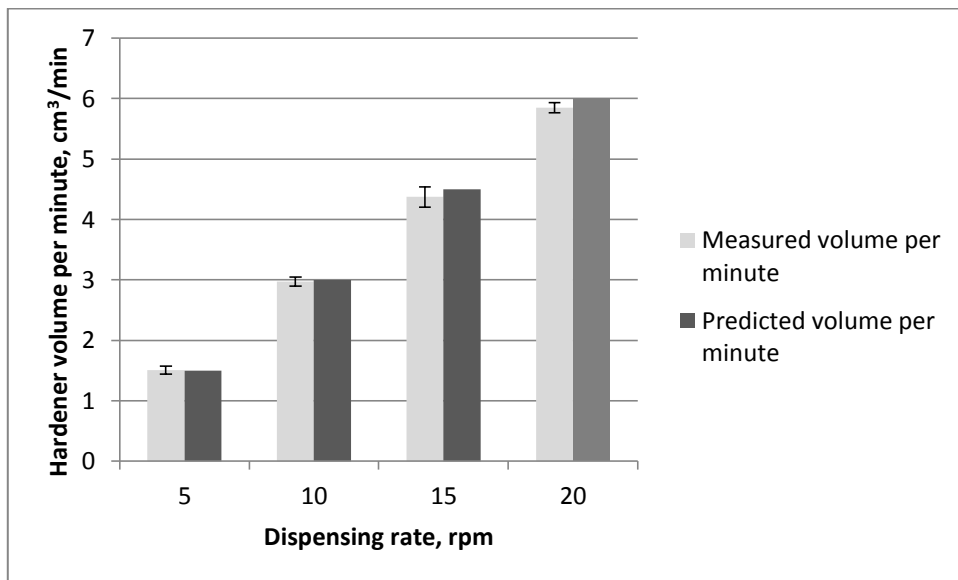


Figure 64. Comparison of measured and “predicted” volumes of the amine hardener (XB3403) at four dispensing rates.

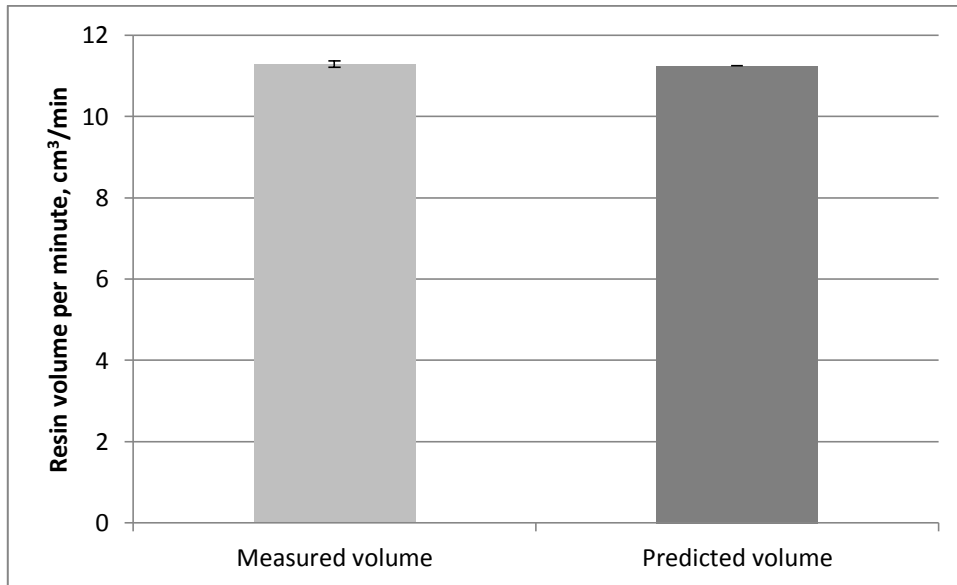


Figure 65. Comparison of measured and “predicted” volumes of the epoxy/amine resin system (LY3505/XB3403) at 11.25 cm³/min (12.5 rpm).

4.5 Development of a Clean Filament Winding Resin Impregnation Unit

The resin impregnation unit, presented in Figure 32, was an integral component of the CFW process. The evolution of the design for this resin impregnation unit was based on the following requirements:

(a) A facility to spread the fibres prior to impregnation: The rationale for this is given in Section 4.6, where the effect of the tow “thickness” on the impregnation time is discussed. The hypothesis here was that any decrease in the effective thickness of the tows would result in accelerating the through-thickness impregnation of the tows.

(b) A facility to inject the mixed resin on the top and the bottom of the tows: The requirement here was to combine the mode-of-operation of a resin bath and a

resin injection system within the resin impregnation unit. In other words, in the case of the resin bath, the resin system on the drum is squeezed into the tows; in the resin injection method, the mixed resin is injected under low-pressure into the tows. The desired outcome was to enhance the through-thickness impregnation rate.

(c) Minimising the volume of the resin impregnation unit: The rationale here was that a reduction in the volume of the resin impregnation unit would mean that the volume of solvent required to clean the equipment at the end of a production run would be significantly lower. In the case of conventional resin baths, the “dead-volume” was significantly large and hence the volume of solvent required to clean the equipment was also high.

Another reason for minimising the volume of the resin impregnation unit was to reduce its overall mass. This was desirable as it would make it easier for the resin impregnation unit to be mounted onto a traversing carriage of a filament winding machine; this meant that it would be relatively simple to retrofit the resin impregnation unit onto any existing commercial filament winding machines.

(d) Locating the resin impregnation unit near the mandrel: In the conventional wet-filament winding process, the resin bath is generally located at a distance from the mandrel and there is a high probability of the resin system dripping from the impregnated tows before they are wound onto the rotating mandrel. In the CFW process, the resin impregnation unit was placed in close proximity to the mandrel. As a result, the possibility of the resin dripping onto the floor does not arise.

(e) *A modular design for the resin impregnation unit:* This was deemed desirable to enable relatively simple assembly/disassembly and flexibility in accommodating different fibre types and number of tows.

The resin impregnation unit used during this study was shown to satisfy the above criteria and hence aim one of Section 1.3. Furthermore, this impregnation unit also successfully allowed for an extensive and robust set of filament winding trials to be carried out in a user-friendly manner on two filament winding machines.

4.5.1 Application of Impregnation Modelling

The impregnation modelling variables presented in Section 3.3.1 were calculated and applied to the models proposed by Foley and Gillespie [94] and Gaymans and Wevers [95]. By applying these models using the appropriate values, it was possible to calculate the impregnation time (and hence minimum residence time) for the resin impregnation unit.

With reference to the model proposed by Foley and Gillespie [94], Equation 19 was used to predict the impregnation time for the CFW process. Here, each fibre tow was assumed to consist of 2000 filaments with a 1200 Tex and a width of 7 mm. The impregnation time (Equation 19) and the degree of impregnation (Equation 20) were calculated and are presented in Figure 66.

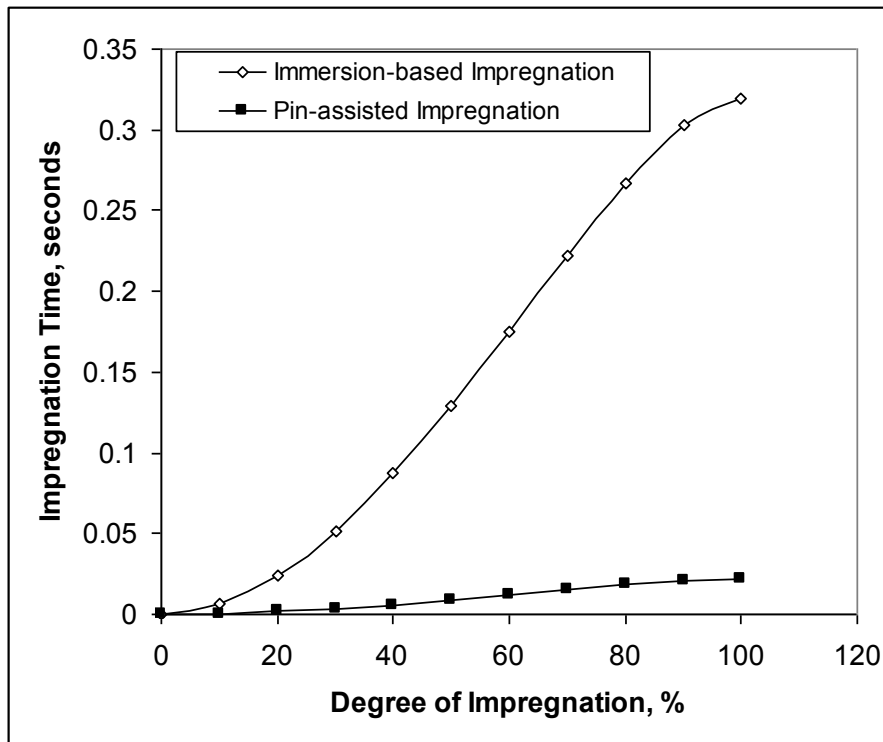


Figure 66. Simulation of the model proposed by Foley and Gillespie [94].

From analysing Figure 66, it was apparent that full impregnation of the fibre tow could be achieved after 0.022 seconds for pin-assisted impregnation. This impregnation time was approximately 15 times faster than just immersion alone.

With reference to the model proposed by Gaymans and Wevers [95], Equation 22 was used to predict the impregnation time for the CFW process. A simulation of Equation 22 is presented in Figure 67.

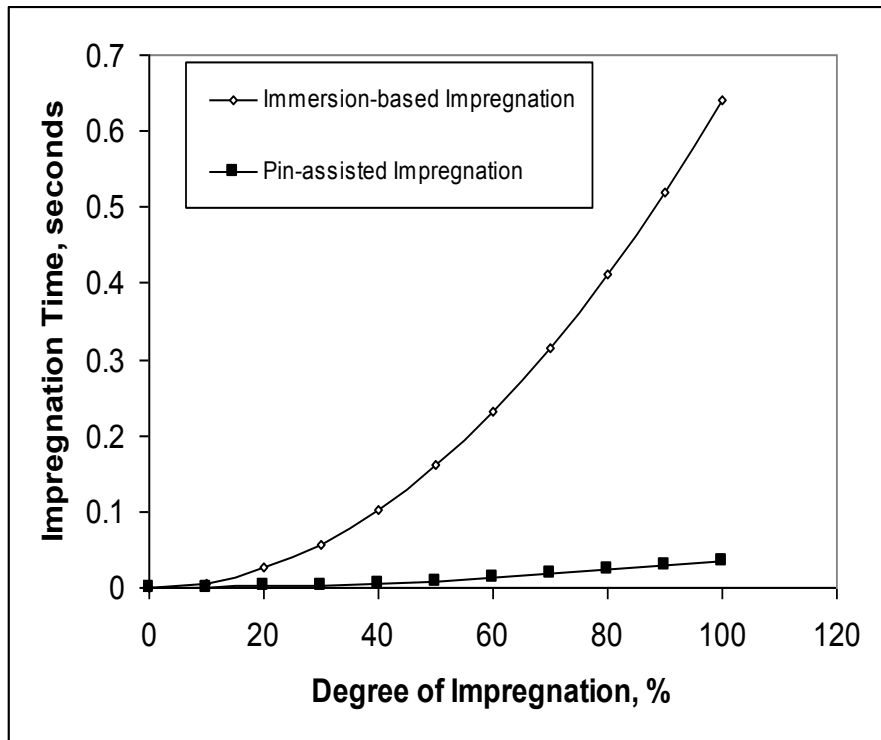


Figure 67. Simulation of the model proposed by Gaymans and Wevers [95].

On inspecting Figure 67, it can be seen that the model proposed by Gaymans and Wevers [95] also predicted that full impregnation would be achieved at a faster rate via pin-assisted impregnation. Here, the model predicted that complete impregnation could be achieved after 0.036 seconds; this impregnation time was approximately 18 times faster than just immersion alone. On comparing the two models proposed by Foley and Gillespie [94] and Gaymans and Wevers [95], it can be seen that a minimum residence time required to achieve full impregnation (with a safety factor taken into account) can be estimated to be 1 second. Table 20 presents a comparative summary of the results from the two models.

Table 20. Summary results of impregnation modelling.

Impregnation model	Time to achieve 100% impregnation: immersion (seconds)	Time to achieve 100% impregnation: pin-assisted (seconds)
Foley and Gillespie [94]	0.32	0.022
Gaymans and Wevers [95]	0.65	0.036

4.6 Fibre Spreading during Clean Filament Winding

Table 21 shows the average spreading values (Levels 1 and 2) determined by the Taguchi analysis described previously. Attention is drawn to the main experimental set-ups i.e. experiments A, B, D and H.

Table 21. Calculation of the average spreading values from the L₁₆ Taguchi analysis.

	A	B	C	D	E	F	G	H	I	J
Level 1	4.7	5.1	5	4.4	5	5.1	5	4.3	5.2	4.8
Level 2	5.2	4.9	4.9	5.6	5	4.9	5	5.7	4.7	4.5

The average fibre spreading values presented in Table 21 were then subjected to an analysis of variance (ANOVA). This involved a comparison of the average spreading values of the Level 1 and Level 2 settings of each parameter from

each of the 16 experiments. The P-value results of the ANOVA are presented in Table 22. Here a P-value lower than 0.05 was taken as having an influence on fibre spreading with a 95% confidence level.

Table 22 shows that the average fibre spreading values of factors D and H produced P-values of 0.02 and 0.01 respectively. As these P-values were lower than the 95% statistically significant value of 0.05, they were deemed to have a significant influence on fibre spreading. These factors were the 'fixture configuration' and 'number of fixtures' respectively. Figure 68 shows the average spreading results in a response plot. From analyzing Figure 68, it can clearly be seen that optimum fibre spreading could be achieved from increasing the number of fixtures and by using static fixtures. These results were attributed to an increase in frictional fibre forces which produced an increase in fibre tension; here tension was measured to vary between 10 – 20 N where the higher tension levels produced higher degrees of fibre spreading.

A typical example of the degree of fibre spreading obtained during the Taguchi analysis is shown in Figure 69. From achieving this degree of fibre spreading the concomitant increase in the tow width and decrease in thickness, as hypothesized in Section 2.3, was produced. The effect of this thickness reduction on the impregnation time of a fibre bundle is demonstrated in Figure 70.

Table 22. ANOVA analysis with a confidence level of 95%.

Factor	P-Value	Influence on Fibre Spreading
A	0.2	No Influence
B	0.59	No Influence
C	0.7	No Influence
D	0.02	Influenced
E	0.95	No Influence
F	0.57	No Influence
G	0.83	No Influence
H	0.01	Influenced
I	0.31	No Influence
J	0.4	No Influence

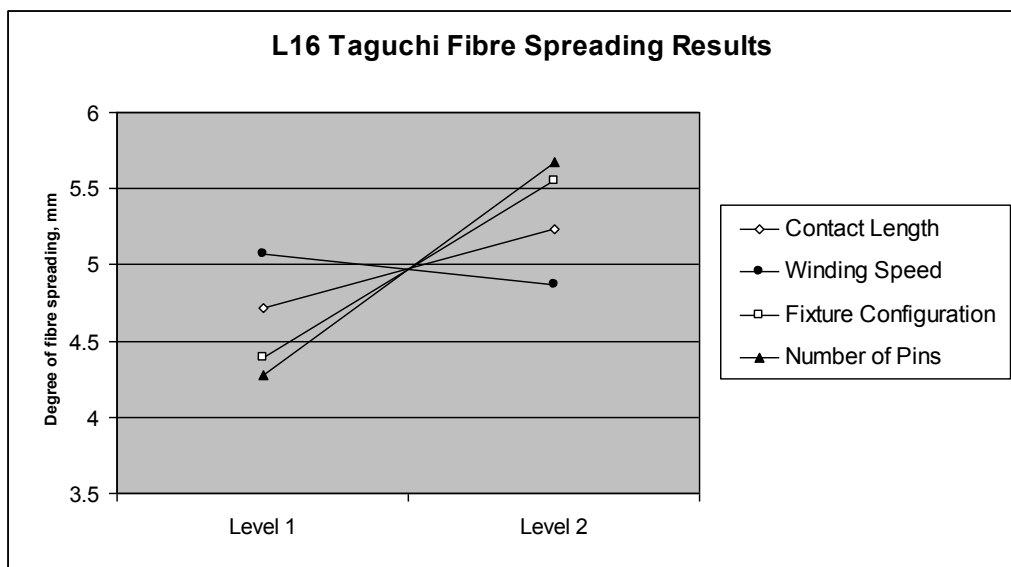


Figure 68. A response plot showing the influence of Level 1 and Level 2 variations of the four input parameters.

With reference to Figure 70, this is a simulation of the impregnation model presented in Equation 19. However, here the equation was completed for fibre tows with varying bundle widths (4 – 10 mm widths, corresponding to 67 – 167 μm thicknesses).

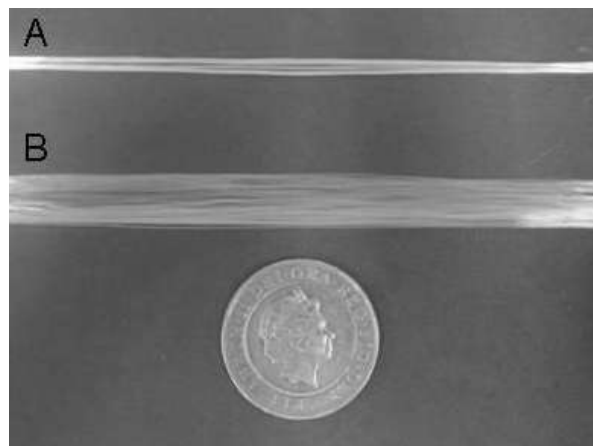


Figure 69. Photograph showing: (A) an as-received E-glass fibre tow; and (B) a fibre tow after fibre spreading. The scale indicated is a UK £2 coin.

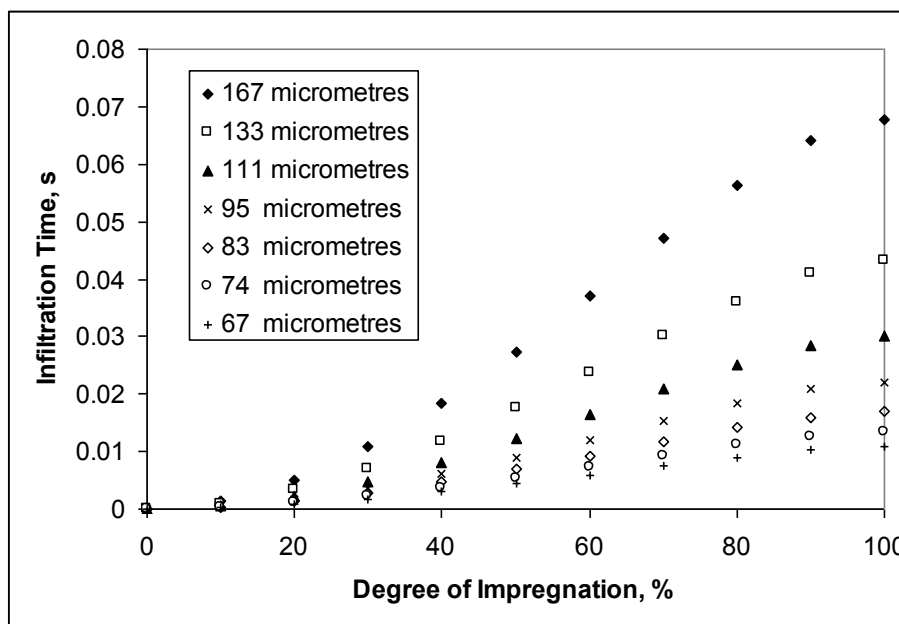


Figure 70. A graph showing the effect of fibre tow thickness variations on the transverse impregnation rates [94].

From analysing Figure 70, it can be seen that a reduction in bundle thickness can reduce the theoretical transverse impregnation time of a fibre tow; 0.07 seconds for a 4 mm tow width and 0.012 seconds for a 10 mm tow width. As a result, the discussion presented in Section 2.3 and the methodology presented in Section 3.4 were justified and the application of a fibre spreading method into the CFW method did improve the theoretical transverse impregnation rate of a fibre tow.

Despite the improvements which can be produced from fibre spreading, it should be noted that a balance must be maintained between the number of fixtures and the resultant increase in fibre tension; any dramatic increases in fibre tension may result in increased fibre damage. Due to this issue, the CFW process was only operated with a fibre spread bundle width of 7 mm and a winding tension of 10 – 15 N. This was not the maximum bundle width or fibre tension level possible (max spread width and fibre tension level of ~ 12 mm and ~ 35 N respectively) however this was deemed sufficient for efficient impregnation without causing severe fibre damage.

4.7 Filament Winding Trials

4.7.1 In-house Clean Filament Winding

CFW trials were completed in an attempt to solve the issues presented in Section 1.2. Figure 71 shows the CFW method in-use and the following text discusses the main observations and conclusions reached during and after

these trials. For reference, Figure 71 also shows a filament wound tube which was fabricated during these trials.

Resin containment, mixing and delivery: During the in-house CFW trials, the static mixers and resin dispensing unit (Figures 25 and 26 respectively) were able to dispense the required volume of mixed resin in an automated manner. This did not involve any manual mixing or deposition of the resin system and also eradicated any issues associated with the resin curing (cross-linking) on the equipment during production.

Resin impregnation unit: During these trials, the resin impregnation unit was able to provide many processing improvements, such as:

(i) *No need for manual replenishment;* the resin impregnation unit was continually replenished with 'fresh' resin from the automated resin dispensing unit.

(ii) *Reduced size;* the relatively small capacity of the resin impregnation unit was able to reduce: (a) the amount of post-production waste resin; (b) the volume of solvent needed for post-production cleaning; and (c) the time needed for post-production cleaning. With reference to the post-production cleaning time, the CFW equipment was able to be thoroughly cleaned in approximately 5 – 10 minutes; this was a considerable advantage, as with the conventional process this phase could take up to one hour.

(iii) *Positioning over the mandrel:* due to the relatively small size of the resin impregnation unit it was also possible to place the unit directly above the

rotating mandrel. From placing the mandrel in this position it was possible to minimise any waste-resin drips from the impregnated fibres onto the shop floor.

Fibre spreading station: The fibre spreading station, presented in Figure 33, was also able to achieve an 'appropriate level' of fibre spreading during these trials. Here, an 'appropriate level' was deemed to be approximately 7 mm with a winding tension of 10 – 15 N. As a result, a relatively low-tension winding method was produced where the noted 10 – 15 N winding tension was considerably less than the 26.7 and 44.5 N levels presented as reference data in the literature review section of the current study.

4.7.2 On-site Clean Filament Winding

The CFW technology was also demonstrated on-site at a company involved in filament winding (Portsmouth, UK). From completing these trials the fourth aim outlined in Section 1.3 was satisfied. Here, in order to retrofit the resin impregnation unit onto the commercial filament winding machine, a simple rectangular adaptor plate was connected to the traverse-arm of the machine. The resin impregnation unit was mounted on to this adaptor plate. The resin-feed from the dispensing unit was connected to the resin impregnation unit via a pair of flexible plastic pipes and the winding speed and angle were identical to those used by the company for commercial production of filament wound components.

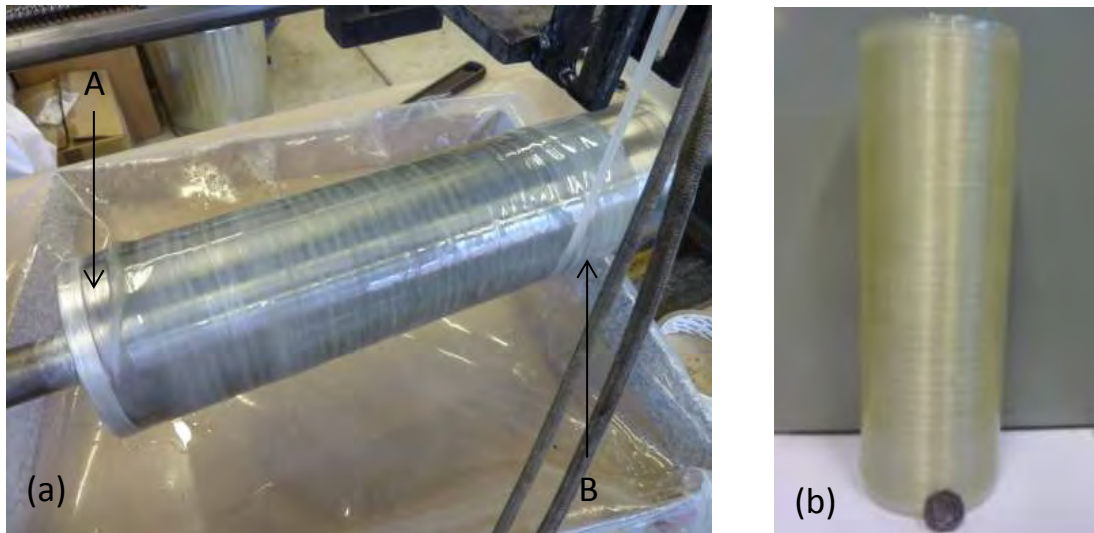


Figure 71. Photographs of: (a) a filament wound tube in production via the in-house CFW method; and (b) an example CFW tube. The highlighted components are: (A) a 100 mm OD mandrel; and (B) impregnated tows.

The key observations and conclusions reached during and after the site trial were as follows:

- (i) The retrofitting procedure was relatively straightforward and involved the construction of an adaptor plate that was bolted onto the arm of the traverse-carriage on the commercial filament winding machine.
- (ii) The retrofitting of the resin impregnation unit onto the commercial filament winding machine did not interfere or affect the normal usage of the machine or commercial manufacturing practices; the same winding speeds and angles were used when the resin impregnation unit was introduced.

(iii) Since the resin impregnation unit was located in close proximity to the mandrel, it was not possible for the resin from the impregnated tows to drip onto the workshop floor.

(iv) The feedback control between the resin dispensing unit and the filament winding machine was not used in the site trial. However, once the winding speed was set, it was relatively straightforward to adjust the throughput of the resin dispensing unit to maintain the required volume in the resin impregnation unit.

(v) The three major advantages of the CFW process over its conventional predecessor were as follows: (a) the volume of mixed resin retained in the resin impregnation unit was vastly reduced in comparison to that retained in the 5-litre resin bath; (b) the volume of solvent required to clean the resin impregnation unit was a fraction of that required to clean the resin bath; and (c) the time required to clean the resin impregnation unit at the end of each production run was approximately 5 - 10 minutes, compared to 55 – 60 minutes required to clean the resin bath. Photographs of the on-site trials are presented in Figure 72.

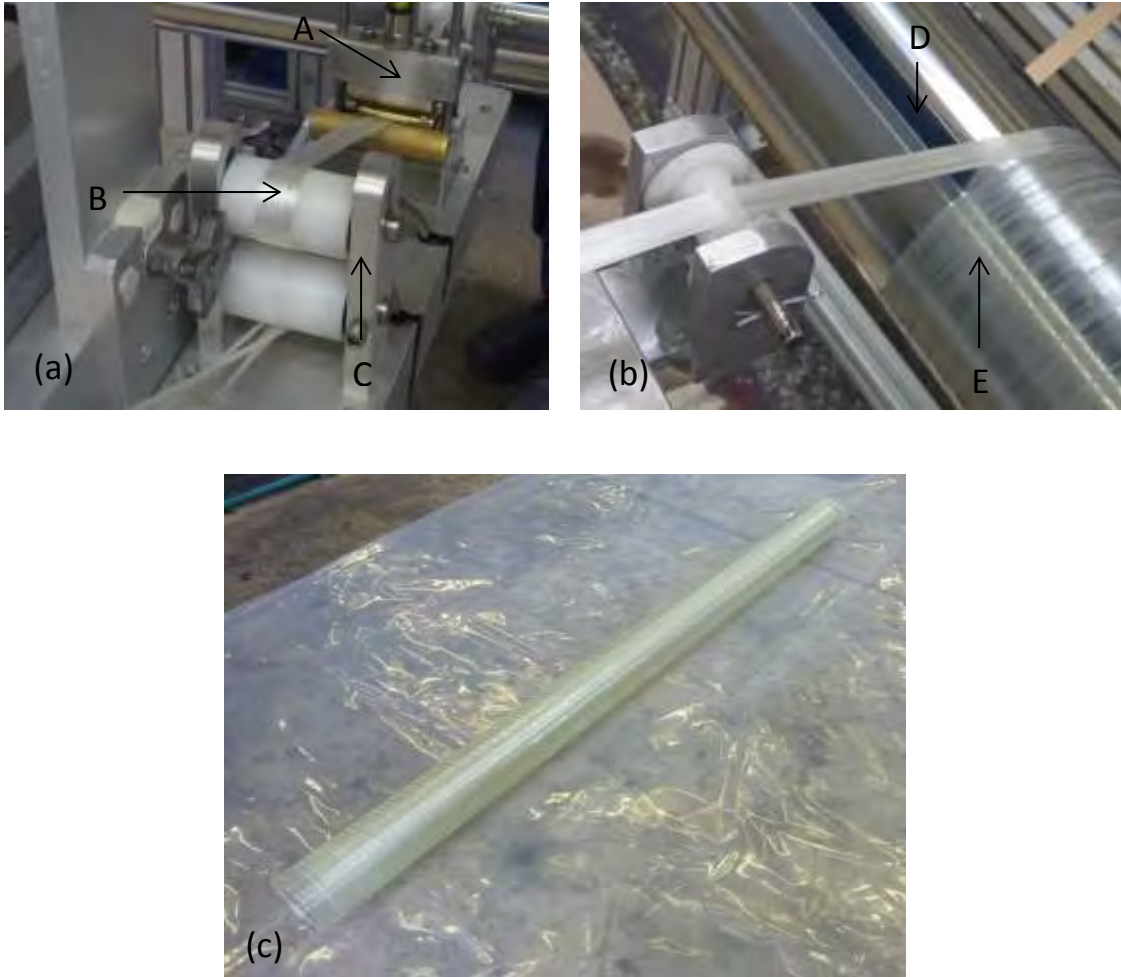


Figure 72. Photographs of: (a) the spreading station and resin impregnation unit in-use during the on-site trials; (b) impregnated fibre tows being applied to a rotating mandrel (106 mm diameter); and (c) a 1.5 m CFW tube manufactured on-site. The highlighted components are: (A) the resin impregnation unit; (B) glass-fibres; (C) fibre spreading station; (D) 106 mm OD mandrel; and (E) impregnated fibres.

4.7.3 Conventional Filament Winding

Conventional filament winding trials were also completed during the current study. These trials were completed to provide important reference data to which the CFW method could be compared. Photographs of the conventional filament winding trials are presented in Figure 73.

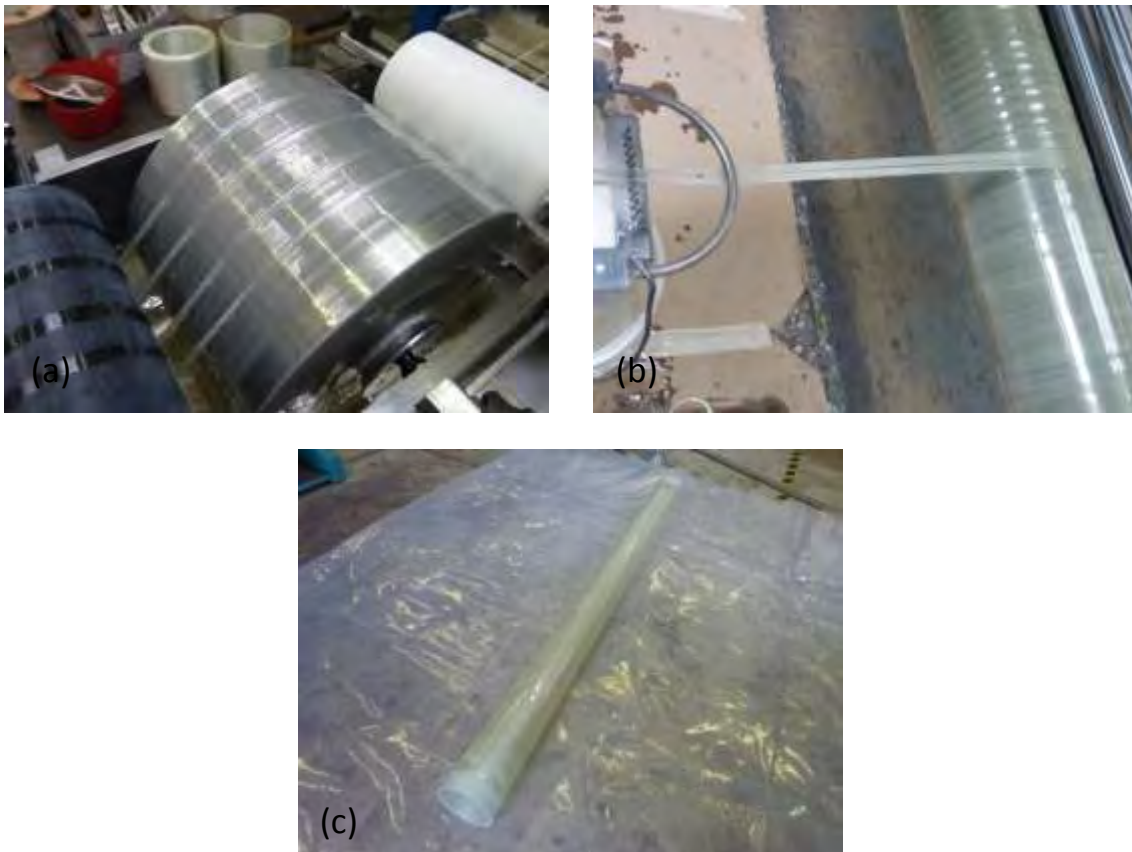


Figure 73. Photographs of: (a) the resin-bath used during conventional filament winding; (b) the impregnated fibres being wound on to the rotating mandrel; and (c) a 1.5 m filament wound tube manufactured using a conventional resin bath.

The key observations and conclusions reached during and after the conventional filament winding trials were as follows:

(i) It was observed that significant resin 'aeration' occurred inside the resin bath during the trials. This aeration of the resin system (shown in Figure 74) was attributed to the rotating motion of the impregnation drum where it was believed that the resin was made to move-around inside the resin bath and hence entrap air from the atmosphere; the resultant effect was termed 'resin frothing'.

(ii) A higher level of fibre tension was also noted during these trials. Here, fibre tension was caused by the multiple contact points of the tows with various pieces of equipment, such as: (a) the fibre tensioning system; (b) the impregnation drum inside the resin bath; (c) the multiple rollers used to steer the fibres through the resin bath; (d) the multiple fixtures used to guide the fibres out of the resin-bath and into the traversing carriage; and (e) the traversing carriage. Due to the significant friction caused by these fixtures it was postulated that the fibre tension was at least double that experienced during the CFW trials; ~ 30 N. Unfortunately, the tension of the fibres was not able to be quantitatively defined during the conventional trials and only a qualitative estimate, at the time of winding, can be used to support this point.

In comparison to the reference data presented in Section 2.1, where two winding tension levels of 26.7 N and 44.5 N were described, the estimated 30 N winding tension during the conventional winding trials was deemed appropriate.

(iii) A considerable amount of waste resin dripping onto pieces of equipment and the workshop floor was also noted during these trials. Figure 74(b and c) show evidence of this resin dripping. From analysing Figure 74(c) it can be seen that a plastic container was needed to catch the dripping resin.

(iv) A significant volume of waste resin (> 3 L) was retained in the resin bath after production. This resin was removed from the bath and discarded into a waste container for curing. Once cured, the waste resin was deposited into a bin and taken to landfill.

(v) Once emptied (retained waste resin removed) the resin bath and all of its ancillary equipment i.e. rollers, were thoroughly cleaned with a solvent (Acetone). This cleaning process consumed approximately 5 kg of solvent and took ~ 1 hour. Here, the main consumption of solvent occurred during the resin-bath cleaning phase. This was due to the large free-surface areas (areas which could come into contact with mixed resin) which required considerable amounts of solvent to be used to ensure no remaining resin would harden inside the resin bath.



Figure 74. Photographs highlighting the issues associated with conventional filament winding, in particular: (a) the resin bath with obvious air ‘bubbles’ present in the resin; (b) resin dripping onto the conventional guiding equipment; and (c) ‘waste pots’ catching excess resin drips. The highlighted components are: (A) a resin drum; (B) resin bath; (C) resin ‘bubbles’; (D) resin drips; (E) impregnated fibres; (F) traversing arm; (G) plastic container catching resin drips; and (H) protective flooring.

4.7.4 In-house Recycled-Clean Filament Winding

As described in Section 3.5.4, the R-CFW method was used to manufacture waste-fibre composite tubes (Figure 75). From completing these trials aim 5(a),

regarding the application of the CFW method into industrial applications, was fulfilled.

The justification for using these waste materials (waste slittings and direct-loom waste) was presented in Section 4.3 and the following section summarises the key aspects of the R-CFW method.

(i) Both types of waste-fibre (waste slittings and direct-loom waste) were able to be used as fibre feed-stock; the waste-fibres (on bobbins) were used in the same manner as that shown in Figure 24.

(ii) The waste-slittings were able to be processed in an identical manner to the glass-fibre trials presented in Section 4.7.1. The only changes of note were: (a) a slower winding speed; (b) a larger pitch; (c) a faster resin delivery rate; and (d) the tows had to be flipped (folded) at the end of each layer. These minor changes were mainly implemented to ensure that sufficient impregnation of the waste slittings could be achieved. Impregnation assurance was desired here as initial trials showed that the presence of a resin sealant seemed to hinder the impregnation process.

(iii) The waste slittings were far more 'suitable' for processing than the direct-loom waste fibres. Here, the direct-loom waste fibres were able to be manufactured into waste-fibre composite tubes, but the following changes had to be made:

(a) A slower winding speed (2.5 m/min) was used; this aided in maintaining the fibres in their original form and minimised fibre disarray/damage.

(b) A larger pitch (15 mm) was used; this was needed to allow for the width of the direct-loom waste.

(c) All fixtures (points of contact) i.e. rollers, guides or pulleys, were removed; this assisted with reducing the fibre tension and decreased the level of fibre disarray/damage.

(d) The fibres were flipped (folded) manually after every layer; this ensured: (i) that protruding fibres were not on the lead-edge; and (ii) the protruding fibres were immediately over-wound after one full mandrel rotation.

(e) A manual consolidation procedure was also needed to minimise any fibre disarray which invariably occurred during processing. Here, a brush was used to 'flatten down' the impregnated waste fibres as they were wound on to the rotating mandrel. This procedure was incorporated to help produce a tube with more consistent fibre alignment and outer-diameter dimensions. This was obviously not ideal and this served as the main issue during processing.

(iv) The waste slitting tubes were able to satisfy one of the criteria specified in Section 4.3. From viewing Figure 75, it can be seen that the R-CFW process was able to produce waste slitting tubes with a smooth outer-diameter. To confirm this point, Table 23 shows the relatively consistent wall thickness dimensions which were present in the waste slittings tubes. Here, the waste slittings were shown to be able to produce a tube with an average wall thickness of 3.31 mm (± 0.1). From satisfying this criterion, the waste slitting tubes were then used during the on-site R-CFW trials.

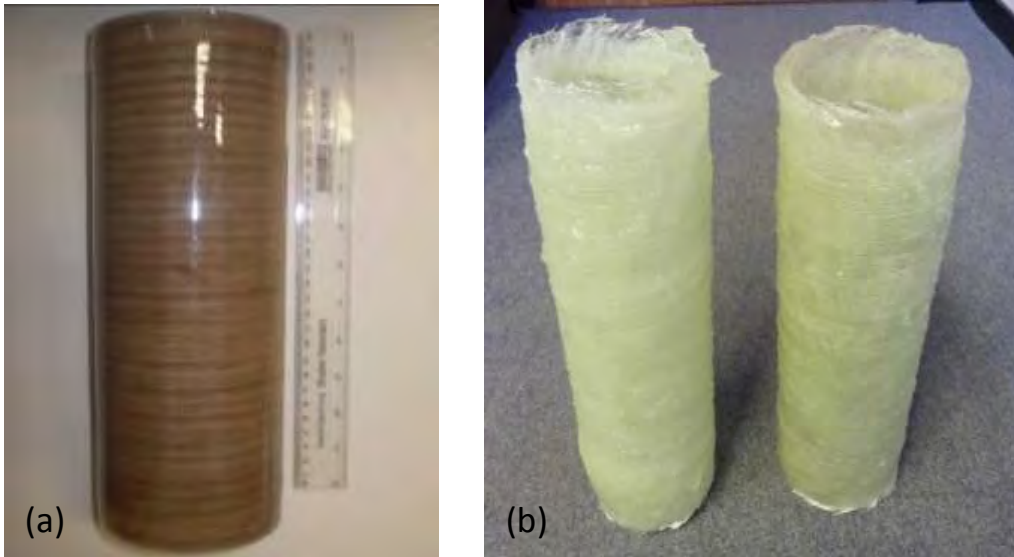


Figure 75. Photographs of: (a) a 100 mm inner-diameter waste slittings tube manufactured by the in-house R-CFW method; and (b) two 100 mm inner-diameter direct-loom waste tubes manufactured by the in-house R-CFW method.

Table 23. Waste slittings wall thickness data.

Number of measurements	1	2	3	4	5	6	7	8	Average
Wall thickness (mm)	3.22	3.27	3.45	3.42	3.23	3.42	3.22	3.25	3.31 (±0.1)

4.7.5 On-site Recycled-Clean Filament Winding

As described in Section 3.5.5, the R-CFW method was also used to manufacture composite tubes using the waste slittings during an industrial site trial. The justification for producing these tubes was discussed in Section 4.3. Photographs of the on-site R-CFW trials, during and after production, are presented in Figures 76 - 79.

With reference to Figure 76(a and b), images of the waste slittings during hoop-winding are presented. Figure 76a shows the first layer of fibres being deposited onto the rotating mandrel and Figure 76b shows the second layer. From analysing both figures it can be seen that adequate fibre coverage was present and no gaps in-between the tows was present.

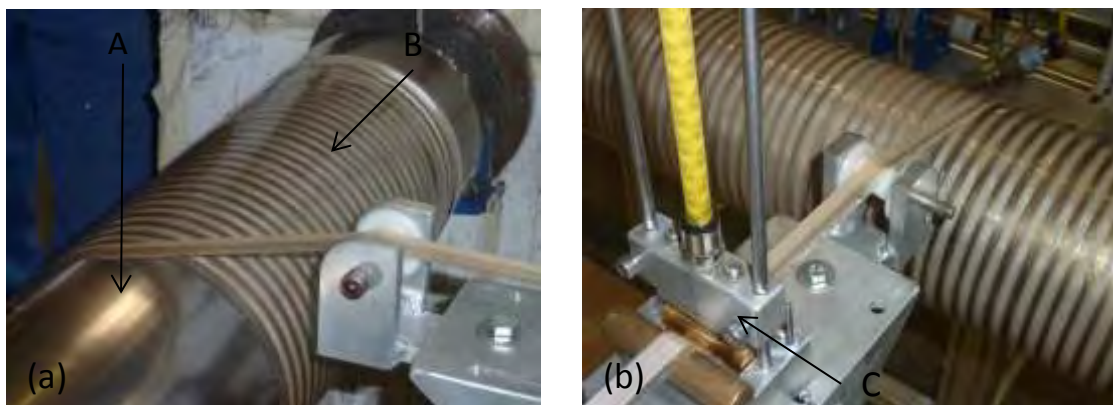


Figure 76. Photographs of the hoop-wound waste slittings tube during on-site production. The highlighted components are: (A) 106 mm OD mandrel; (B) impregnated waste slittings; and (C) resin impregnation unit.

Figure 77 presents images of the hoop-wound waste-slittings after curing, from analysing these images it can be seen that a smooth tube surface was present with a consistent outer-diameter. Furthermore, Figures 78 and 79 present similar images of the angle-wound winding trials.

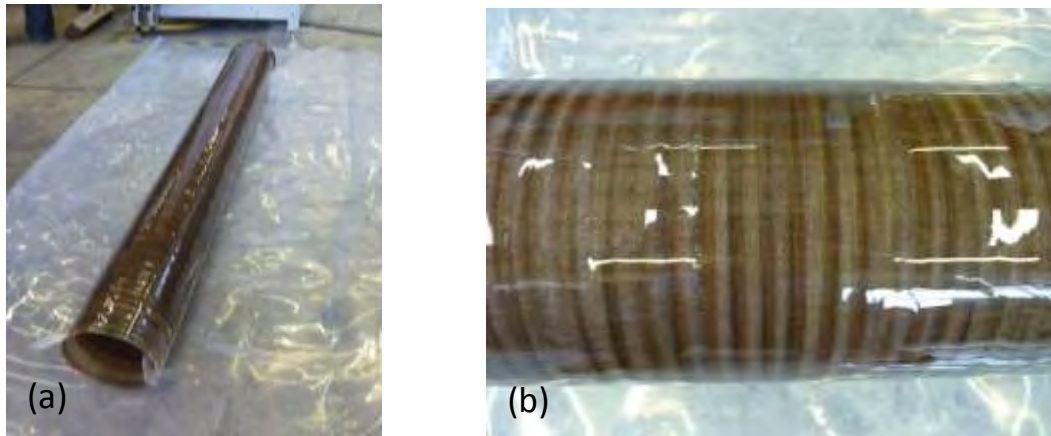


Figure 77. Photographs of the hoop-wound waste slittings tube.

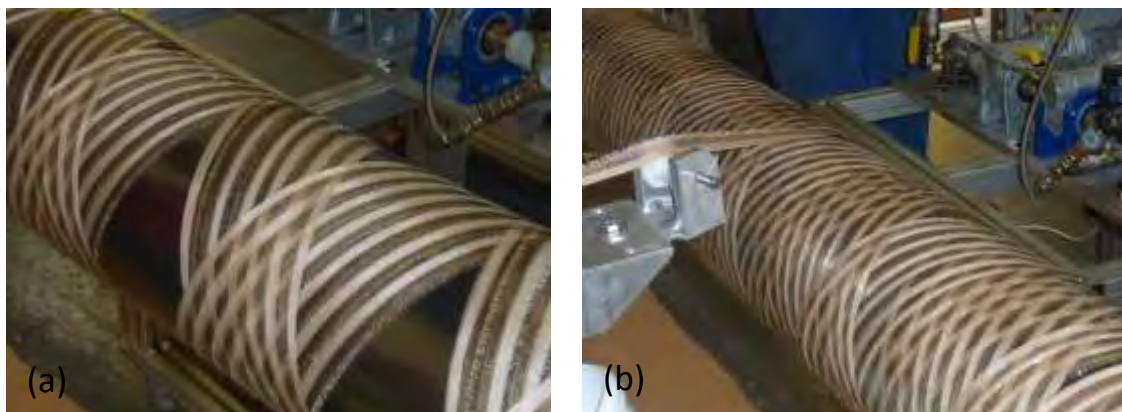


Figure 78. Photographs of the angle-wound waste slittings tube during on-site production.

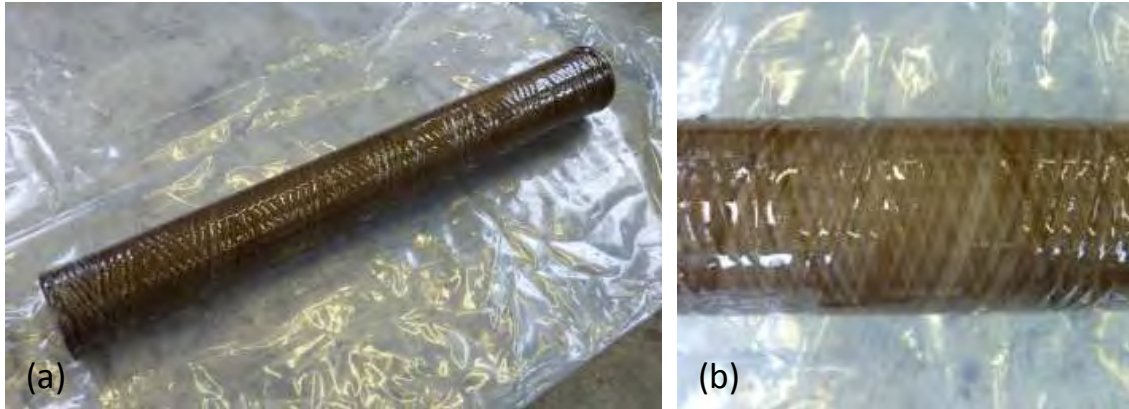


Figure 79. Photographs of the angle-wound waste slittings tube.

The following text summarises the key aspects of the on-site R-CFW trials.

(i) The waste slittings were able to be used with an identical manufacturing process i.e. winding speed, winding angle etc. to that presented in Section 4.7.2. The only difference occurred when the tow had to be flipped (folded-over) after each layer to ensure the protruding fibres were not on the leading edge.

(ii) The retrofitting procedure of the R-CFW method was also relatively straightforward. This involved the use of the same method as described in Section 4.7.2 where the only difference was the fibre feed-stock.

(iii) The retrofitted recycling method was also able to be cleaned in a relatively short time period (5 – 10 minutes).

(iv) Once placed in the oven for curing, the waste fibre tubes were slightly over-impregnated with an additional resin layer to ensure a smooth outer-diameter was present. This was particularly necessary with the angle-wound tube as the chosen winding pattern did not successfully over-wind the protruding edges of

the waste slittings. Table 24 and Figure 80 show evidence of the relatively smooth and consistent outer-diameters of the hoop-wound and angle-wound tubes. In particular, Table 24 shows that the hoop-wound and angle-wound tubes had wall thickness dimensions which did not vary much more than the in-house waste fibre tubes; 3.91 mm (± 0.19) and 3.13 mm (± 0.21) respectively. Here, the variations in wall thickness dimensions between the two on-site tubes were attributed to the different winding angles.

The tubes manufactured during this section were then used as cardboard tube replacements during an industrial site trial. Details of this site trial are presented in Section 4.8.8.

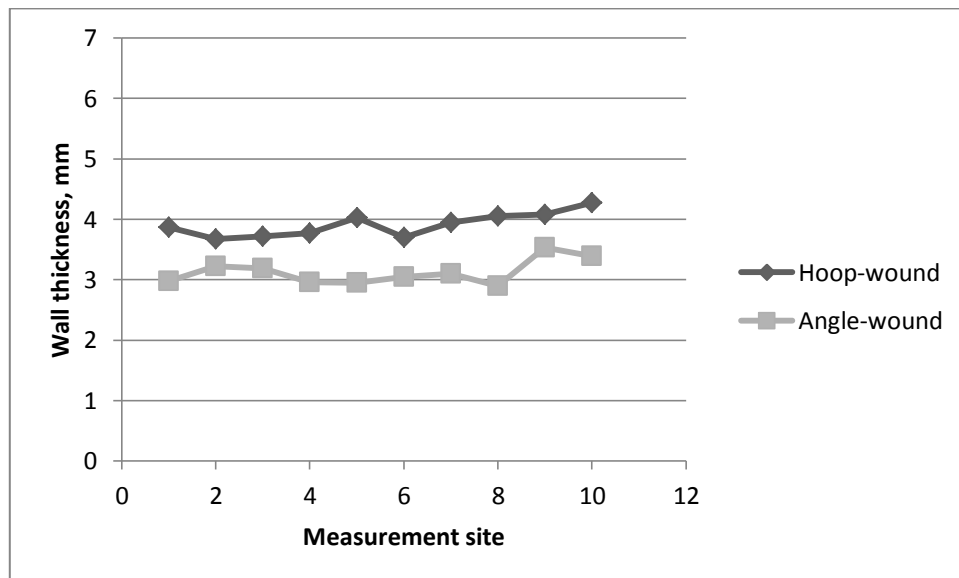


Figure 80. Comparison of hoop-wound and angle-wound wall thickness dimensions of on-site R-CFW tubes.

Table 24. Relative wall thickness dimensions of the on-site waste-fibre filament wound tubes.

Number of measurement sites	Hoop-wound wall thickness (mm)	Angle-wound wall thickness (mm)
1	3.87	2.98
2	3.67	3.22
3	3.72	3.19
4	3.77	2.96
5	4.03	2.95
6	3.7	3.05
7	3.95	3.1
8	4.05	2.9
9	4.08	3.53
10	4.27	3.39
Average	3.91	3.13
Standard deviation	0.19	0.21

4.7.6 Manufacture of Composite Overwrapped Pressure Vessels (COPVs)

The final trials completed during this study were undertaken to manufacture the six glass-fibre COPVs presented in Figure 81. From completing these trials aim 5(b), with regards to the manufacture of CFW COPVs, was fulfilled. The

following section describes the main observations and conclusions reached during and after these trials.

(i) The custom-made end-fittings (Figure 36) allowed for a simple and effective method of mounting the COPVs onto the filament winding machine. Throughout these trials there were no issues with COPV 'slippage' (between the COPV and the filament winding machine) whilst the fibres were applied during winding.

(ii) The COPVs (and end-fittings) did not interfere or affect the normal usage of the CFW equipment i.e. the same winding angles and equipment were used. The only change of note was the reduced winding speed (7 m/min); a slower winding speed was used to further ensure the initial layer of fibres was impregnated and there were no dry fibres at the composite/liner interface.

(iii) Much care had to be taken to ensure the fibres were not applied to the COPV near the curved (convex) neck region. If the fibres were placed too close to this region then they had a tendency to 'slide' out of alignment and the alignment of the tows was lost.

(iv) No attempts were made to apply a bonding agent to the composite/liner interface; the interface region was only de-greased (with acetone) prior to winding.



Figure 81. Photograph of the COPVs manufactured with the in-house CFW method. Here, the highlighted scale is a UK £1 coin.

4.8 Evaluation Methods

To fulfil the second aim presented in Section 1.3, with regards to the comparison of the mechanical and physical properties of the tubes manufactured during this study, the following text presents and compares the physical and mechanical properties of filament wound tubes produced by the winding procedures outlined in Section 3.5.

4.8.1 Resin Burn-off: Fibre Volume Fraction and Void Content

Appreciating the fact that filament wound tubes were produced on two different filament winding machines, a summary of the fibre volume fraction and void contents are presented in Table 25. For reference, density data for each method is also presented along with the comparative reference values which have been discussed earlier in the literature review section.

Fibre volume fraction: The fibre volume fraction results presented in Table 25 are summarised in Figure 82. From analysing Figure 82, it can be seen that the in-house CFW method was able to manufacture filament wound tubes with a fibre volume fraction of ~ 70%. This also justifies the estimated fibre volume fraction value (72%) which was used to complete the modeling simulations presented in Sections 4.5.1 and 4.6. The consistency of these tubes was also confirmed by the relatively small standard deviation of the average fibre volume fraction; ~ 2.5%.

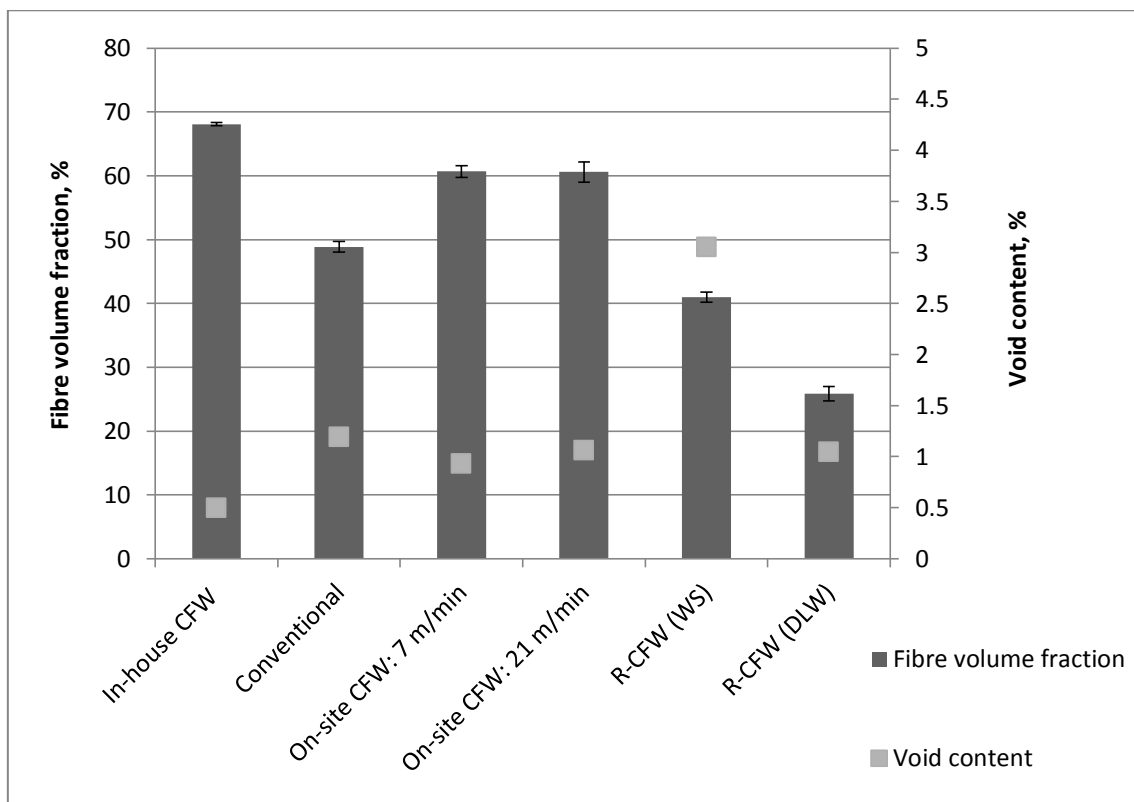


Figure 82. Fibre volume fraction and void content results.

In comparison, it can be seen that the conventional filament winding method was only able to produce a fibre volume fraction of ~ 50%. It was not expected

that this value would be so low (20% lower than the CFW tubes), however from inspecting the tubes it was hypothesized that this occurrence could be attributed to: (i) the lack of a fibre spreading method; and (ii) over-impregnation of the unspread tows to achieve an efficient level of impregnation. With reference to this second point, the over-impregnation of the fibres tows resulted in a resin film (up to 400 μm thickness) to be formed on the outer circumference of the filament wound tube. Figure 83 presents evidence of the formation of a resin film on the outer surface of the conventional filament wound tube as also experienced in other studies [23]. Here, it was believed that this resin film was the main reason for the relatively low fibre volume fraction results. Without a resin film it was estimated that a similar fibre volume fraction as that measured in the in-house and on-site CFW tubes, for example $\sim 65\%$, would be produced; this hypothesis is in agreement with the qualitative image analysis micrographs presented earlier.

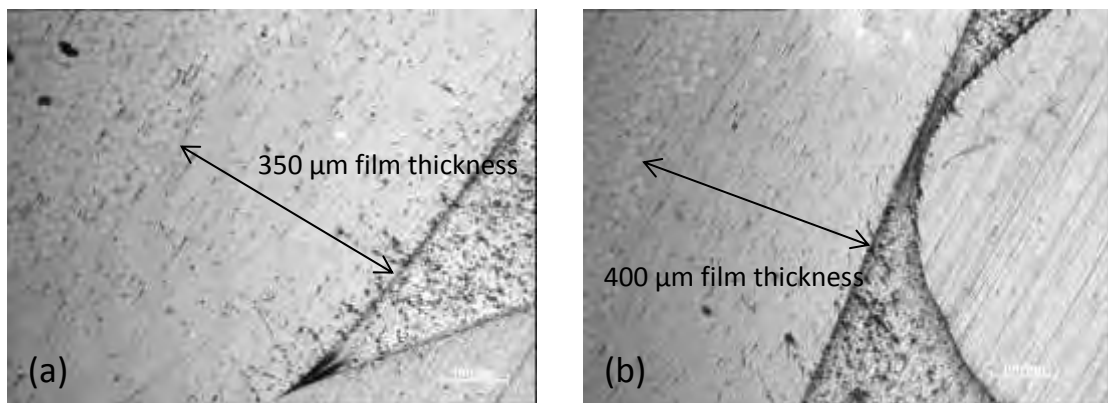


Figure 83. Conventional filament wound tube sections with an outer surface resin film present.

With further reference to Figure 82, it can be seen that the CFW method also had the capacity to be used on-site to manufacture filament wound tubes with comparable fibre volume fractions. Here, both tubes had similar fibre volume fractions of 60.7% and 60.59%; resulting in a difference of just 0.11%. The reduction in fibre volume fraction of these tubes, in comparison to the standard 70%, was not anticipated. However, on reflection this was believed to have occurred as a result of the different winding conditions (i.e. winding speed, winding angle, tension etc.) which were present on-site.

It can also be seen that the in-house R-CFW method was able to manufacture filament wound tubes with relatively consistent fibre contents. Here, the average fibre volume fraction of the waste slittings and DLW tubes (six of each) were 40.12% and 26.01% respectively. The consistency of these tubes was confirmed by the relatively small standard deviation of these results; 2.77% and 1.47%. Despite this methods ability to produce relatively consistent fibre volume fractions, it can obviously be seen that these values are considerably lower than that produced by the as-received glass-fibre tubes. This lower fibre volume fraction was attributed to the need to over-impregnate the waste-fibres during production; this was to ensure a smooth outer finish and, in the case of the DLW fibres, to ensure fibre control during deposition.

Table 25. Fibre volume fraction and void content results.

Method	Density (g/cm ⁻³)	Fibre volume fraction (%)	Void content (%)
In-house CFW	2.108 (±0.04)	68.10 (±2.57)	0.496 (±0.04)
Conventional	1.82 (±0.03)	48.86 (±2.51)	1.19 (±0.52)
On-site CFW (7 m/min)	1.99 (±0.026)	60.7 (±1.46)	0.93 (±0.63)
On-site CFW (21 m/min)	1.99 (±0.018)	60.59 (±0.94)	1.06 (±0.59)
R-CFW (waste slittings)	1.69 (±0.004)	40.12 (±2.77)	3.05 (±0.93)
R-CFW (direct-loom waste)	1.51 (±0.004)	26.01 (±1.47)	1.04 (±0.11)
V _f Ref: Mertiny and Ellyin (26.7 N winding tension) [23]	-	70.8	-
V _f Ref: Mertiny and Ellyin (44.5 N winding tension) [23]	-	74	-
Void Ref: Cohen <i>et al.</i> [24]	-	-	2
Void Ref: Gabrys <i>et al.</i> [86]	-	-	1
Void Ref: Miracle <i>et al.</i> [1]	-	-	5

Void content: With regards to the void content results presented in Figure 82, it can be seen that the CFW method was also able to produce filament wound tubes with consistently low void contents. Here, the average void content was 0.49 % with a standard deviation of just 0.18%. These void contents can also be put into perspective when compared to the reference values (1 to 5%) which were also presented in Table 25.

With further reference to Figure 82, it can be seen that the CFW method also had the capacity to be used on-site to manufacture tubes with relatively low void contents. Here, both on-site CFW tubes had similar void contents of 0.93% and 1.06%; this resulted in a variation of just 0.13%.

The ability of the CFW method to produce high fibre volume fractions and low void contents was attributed to:

- (i) The use of a resin dispensing unit to deliver the exact amount of resin to the fibres at any one time. From using this method there was no over-impregnation of the fibre tows and a 'fresh' batch of mixed resin was constantly supplied; as opposed to a pre-deposited batch of mixed resin which may have been in the bath for up to 1 hour.
- (ii) The incorporation of a static mixer to intimately mix the two components of the resin system. From incorporating this method it was possible to ensure that the resin system supplied was homogenous.

(iii) The use of a resin impregnation unit to impregnate the fibre tows. Here, top and bottom impregnation was used to ensure that efficient impregnation of the entire tow was achieved.

(iv) The inclusion of two fibre spreading mechanisms (spreading station and resin impregnation unit) to reduce the thickness of the tows. The reduction in tow thickness aided in improving its through thickness permeability.

(v) The relatively low level of fibre tension was present throughout the trials. This minimised tow damage whilst still allowing a certain degree of tow porosity to be present; the presence of tow porosity aided with efficient impregnation.

Finally, from reviewing Figure 82, it can also be seen that the R-CFW method achieved varying levels of success in manufacturing filament wound tubes with consistently low void contents. Here, the aforementioned presence of a resin sealant on the waste slittings inhibited the impregnation process; producing a void content of ~ 3%. Conversely, the low void contents produced with the direct-loom waste were attributed to the use of an over-impregnation and 'brushing' procedure. It was acknowledged that these void contents were considerably low; however these were not achieved in a consistent and repeatable manner. The issue of achieving efficient impregnation of the direct-loom waste in a repeatable, simple and effective manner was identified as a significant area for future research.

4.8.2 Hoop Tensile (Split-Disk) Strength

A summary of the hoop tensile (split-disk) strength results are presented in Table 26. With reference to the following section, results were presented with regards to: (i) failure load (N); (ii) hoop-tensile (split-disk) strength; and (iii) normalised hoop tensile (split-disk) strength. For reference, example hoop tensile (split-disk) testing load/displacement curves are presented in the appendix.

Here, normalised results were presented in an attempt to account for the differing fibre volume fractions which were presented in Section 4.8.1. All normalised results were calculated with regards to a 69% fibre volume fraction. However, it should be noted that: (i) due to the discussion presented in Section 4.1.1 and 4.8.1 all conventional filament wound tube sections were normalised from a fibre volume fraction of 65% (and not the ~ 50% which was presented in Table 25). This was deemed appropriate as the image analysis results presented in Section 4.1.1 confirmed that the measured fibre volume fraction results of the conventionally wound sections may have been affected by the presence of a resin film. (ii) The waste-fibre results were not normalised, this was due to the relative misalignment of many of these fibres which meant that they were not in the load bearing direction and therefore any normalised results would be inaccurate.

It should also be noted that in the following section the failure load data was only provided for reference and the main discussion was based on the normalised hoop tensile (split-disk) strength results.

The results presented in Table 26 are summarised in Figure 84. With reference to Figure 84, and comparing it to the data presented in Section 2.1, it can be seen that the in-house CFW method was able to produce relatively high normalised hoop (split-disk) tensile strengths. In particular, the in-house CFW method produced an average strength which: (i) was within 10% of that reported by Kaynak *et al.* [34]; and (ii) offered a 95% confidence interval (705.82 – 844.34 MPa) which encapsulated the normalised hoop tensile strength produced by the conventional filament winding method (842.63 MPa).

This production of glass-fibre tubes with comparative normalised hoop tensile strengths was also achieved in a consistent and repeatable manner. To prove this point, it can be seen that a relatively small standard deviation was produced (65.99 MPa); this equated to a variation of just 8.5% for the six CFW tubes.

Figure 84 also presents the normalised hoop tensile strengths of the on-site CFW method. Here, relatively high strengths of 902.71 MPa (± 46.82 MPa) and 983.17 MPa (± 36.51 MPa) were produced by the 7 m/min and 21 m/min winding trials respectively. To put these values in perspective, the 21 m/min winding method was able to produce a normalised hoop tensile strength value which was 15% higher than that presented by the conventional filament winding method. The presence of the high hoop-tensile (split-disk) strengths produced by the CFW methods was attributed to the combination of a low void content, fibre spreading and the relatively low fibre tension.

Finally, with reference to Figure 84, it can be seen that the waste slittings were able to produce a considerably higher hoop tensile (split-disk) strengths than

the direct-loom waste; 172.85 MPa (± 20.47) and 32.04 MPa (± 5.86 MPa) respectively. In addition to this higher average strength, the waste slittings also created a more consistent set of tubes which only produced a standard deviation of 31.72 MPa; this equated to a percentage variation of just 10% in comparison to the 20% variation produced by the direct-loom waste (± 17.00 MPa). The higher and more consistent results produced by the waste slittings were attributed to: (i) the lower degrees of fibre quality variation; and (ii) the more consistent deposition of aligned fibres. With reference to the second point, it can be seen that the waste slittings had an equal percentage of fibres in the warp and weft directions i.e. 50% of the fibres were aligned in the load bearing direction. However, from analysing Figure 22, it can be seen that only a small amount of the direct-loom waste fibres were present in the load bearing direction (estimated that 80% of the DLW fibres were oriented in a non-load bearing direction). Due to this misalignment, it was deemed unlikely that the direct-loom waste fibres would ever be able to provide hoop tensile (split-disk) strengths which were comparable to that of the waste slittings. This conclusion aided in confirming that the waste slittings used during the on-site CFW trials was the correct material; the use of the stronger material would increase the chances of manufacturing a waste-fibre tube which could be used as a replacement for cardboard tubes.

Due to the 50% misalignment of the waste slittings, these fibres were however not able to produce hoop tensile (split-disk) strengths which were comparable to that produced by the unidirectional (and undamaged) glass-fibres.

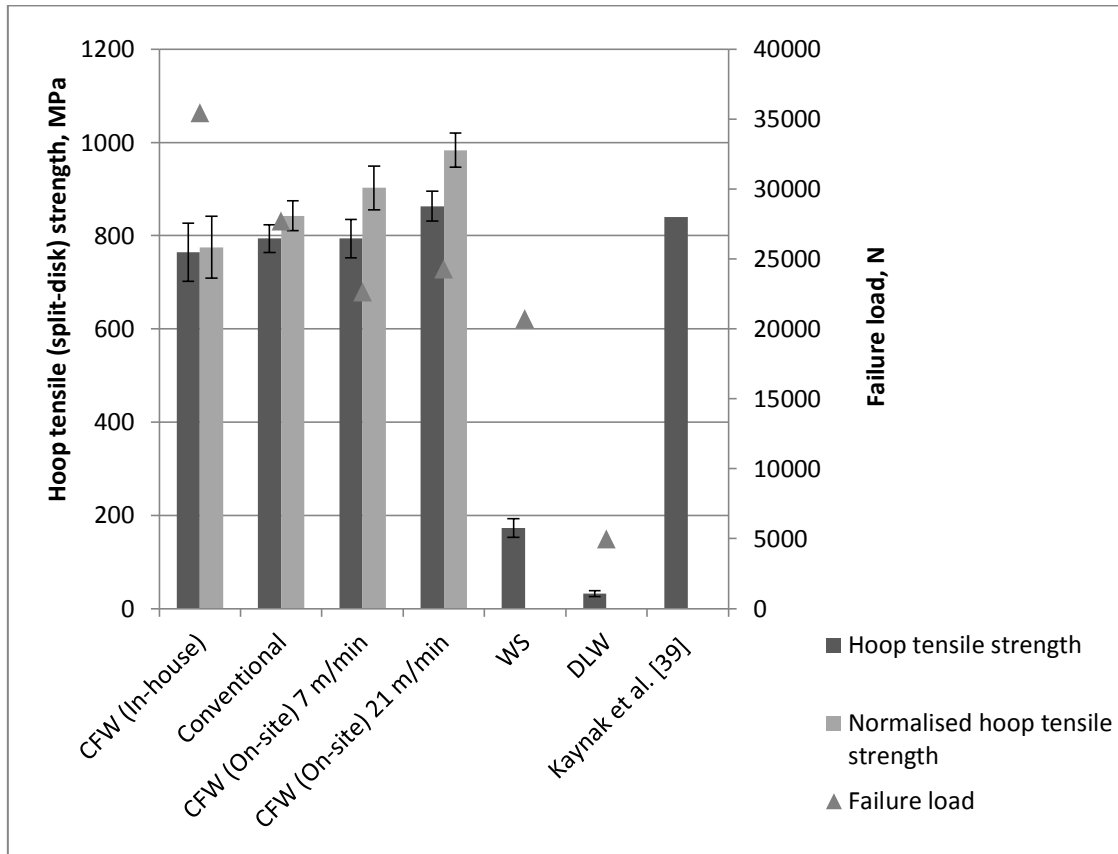


Figure 84. Summary of hoop tensile (split-disk) strength results.

In addition to the numerical analyses presented above, attempts were also made to assess the fractography of the failed hoop tensile (split-disk) samples. Fractography analyses were completed by either image or SEM analysis; Figures 85 – 88 present images of typically failed samples. From analysing these samples the following observations and conclusions were made:

- (i) All samples failed at the desired location of failure i.e. at the notched sections, with identical characteristics as described by Kaynak *et al.* [34] and Sobrinho *et al.* [91], for example: (a) complete fibre breakage; (b) fibre

delamination; and (c) fibre 'pull-out'. These three failure mechanisms are highlighted in Figure 85.

(ii) Each sample failed with complete separation at the site of failure i.e. no intact fibres remained across the site of failure.

(iii) The CFW method was able to produce samples with similar failure mechanisms in comparison to its conventional predecessor; this further confirmed that this method can fabricate filament wound tubes with comparable mechanical properties.

(iv) With reference to Figures 87 and 88, it can be seen that the modes of failure for the waste-fibre materials were relatively comparable to that presented in Figures 85 and 86. This was confirmed by the SEM images which were also presented in Figures 87 and 88; from examining these figures it can be seen that failure also occurred as a result of fibre fracture and fibre 'pull-out'.

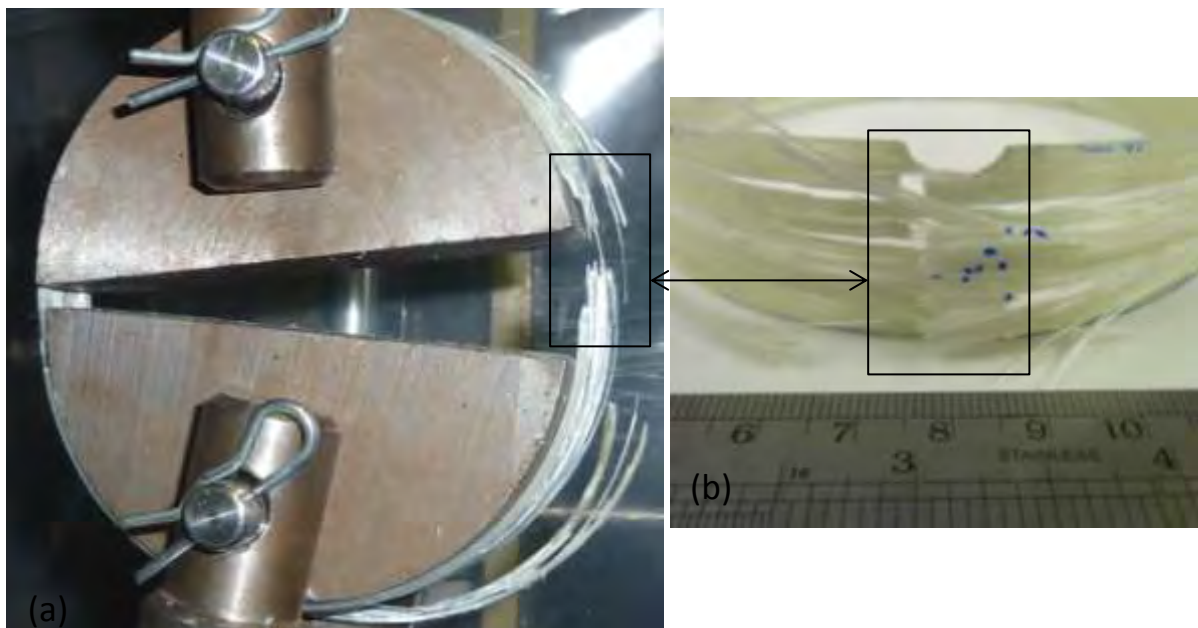


Figure 85. Photographs of hoop tensile (split-disk) failed samples manufactured by the in-house CFW process.

Table 26. Hoop tensile (split-disk) strength results.

Method	Failure load (N)	Hoop tensile (split disk) strength (MPa)	Normalised hoop tensile (split-disk) strength (MPa)	95% confidence interval (Normalised strength) (MPa)
In-house CFW	35459.8 (±2222)	764.29 (±43.96)	775.08 (±65.99)	705.82 – 844.34
Conventional	27730.1 (±1438)	793.78 (±29.9)	842.63 (±31.74)	809.31 – 875.94
On-site CFW (7 m/min)	22644 (±1887)	794.13 (±41.19)	902.71 (±46.82)	853.57 – 951.86
On-site CFW (21 m/min)	24267.6 (±643)	863.33 (±32.06)	983.17 (±36.51)	944.84 – 1021.49
R-CFW (waste slittings)	20723.5 (±1302)	172.85 (±20.47)	-	-
R-CFW (direct-loom waste)	4961.7 (±1078)	32.04 (±5.86)	-	-
Kaynak reference [34]	-	840	-	-

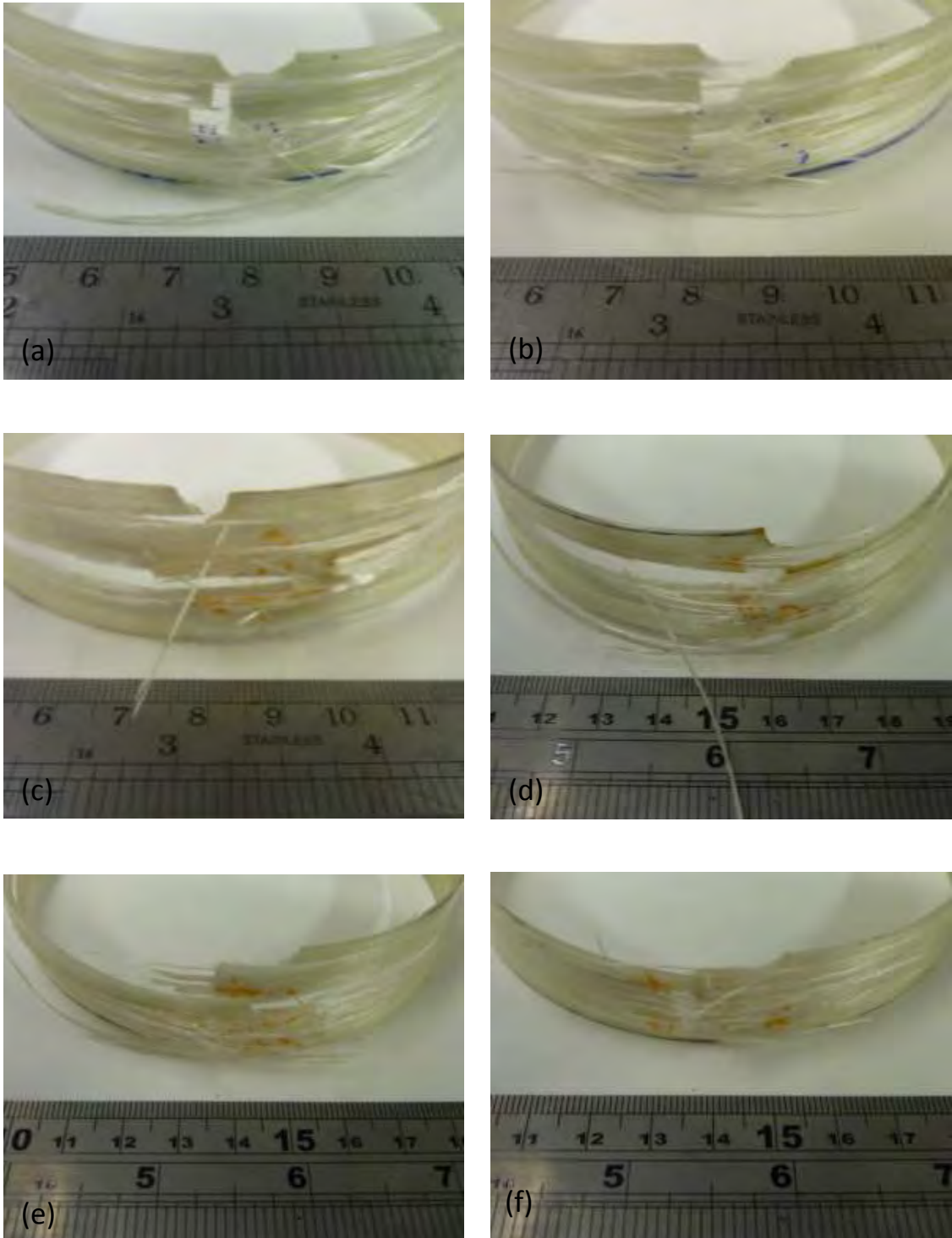


Figure 86. Photographs of hoop tensile (split-disk) failed samples. (a and b) conventional filament winding; (c and d) on-site CFW (7 m/min); and (e and f) on-site CFW (21 m/min).

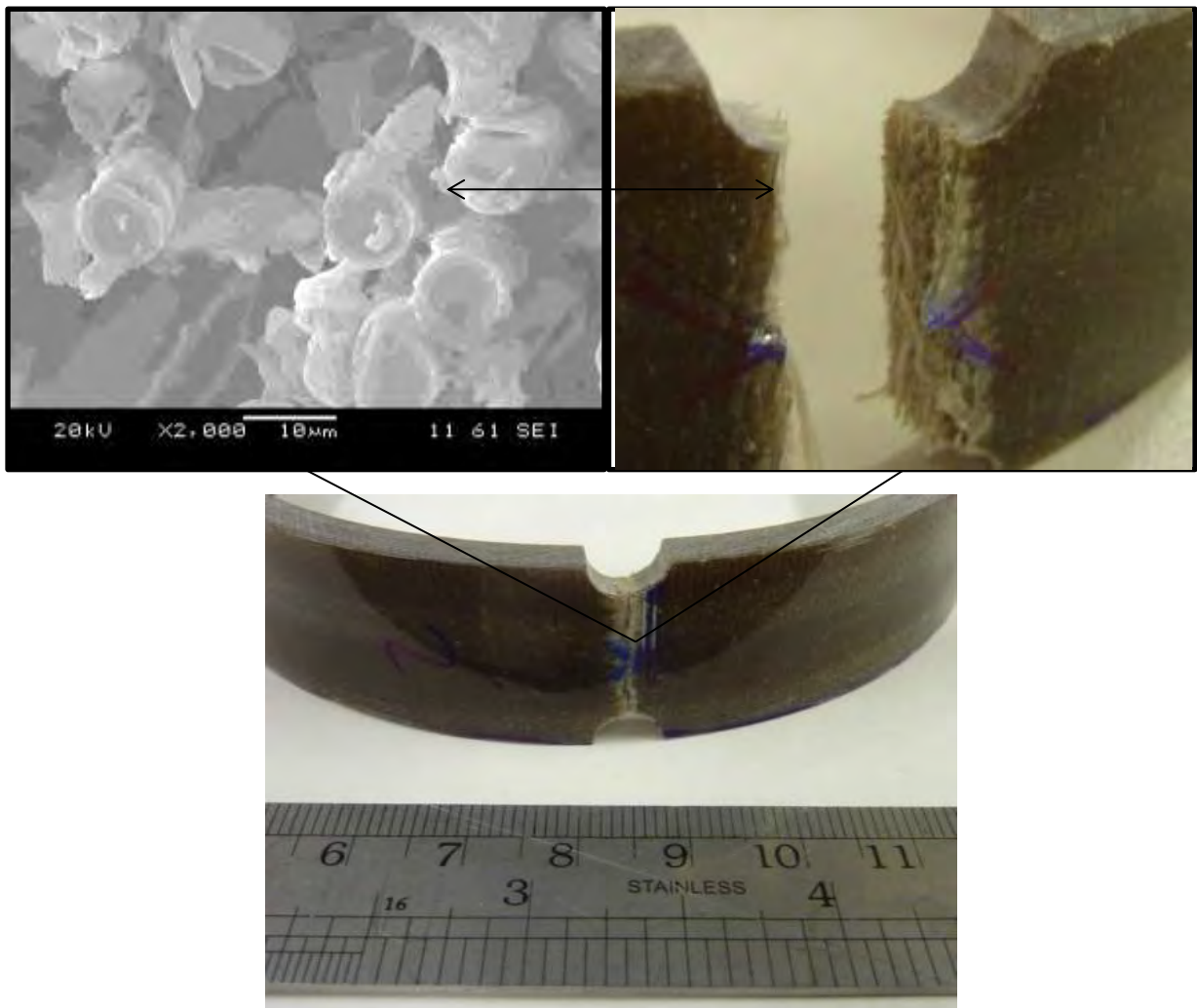


Figure 87. Photographs and SEM image of a failed waste slittings hoop tensile (split-disk) test sample.

4.8.3 Inter-laminar Shear Strength

Inter-laminar shear strength results are presented in Table 27 and summarised in Figure 89. With reference to Figure 89, no normalised results were presented as in the previous section; this was due to the fact that this property was not primarily dictated by just fibre loading but also the bonding strength between the

resin and the fibres. For reference, typical inter-laminar shear testing load/displacement curves are presented in the appendix.

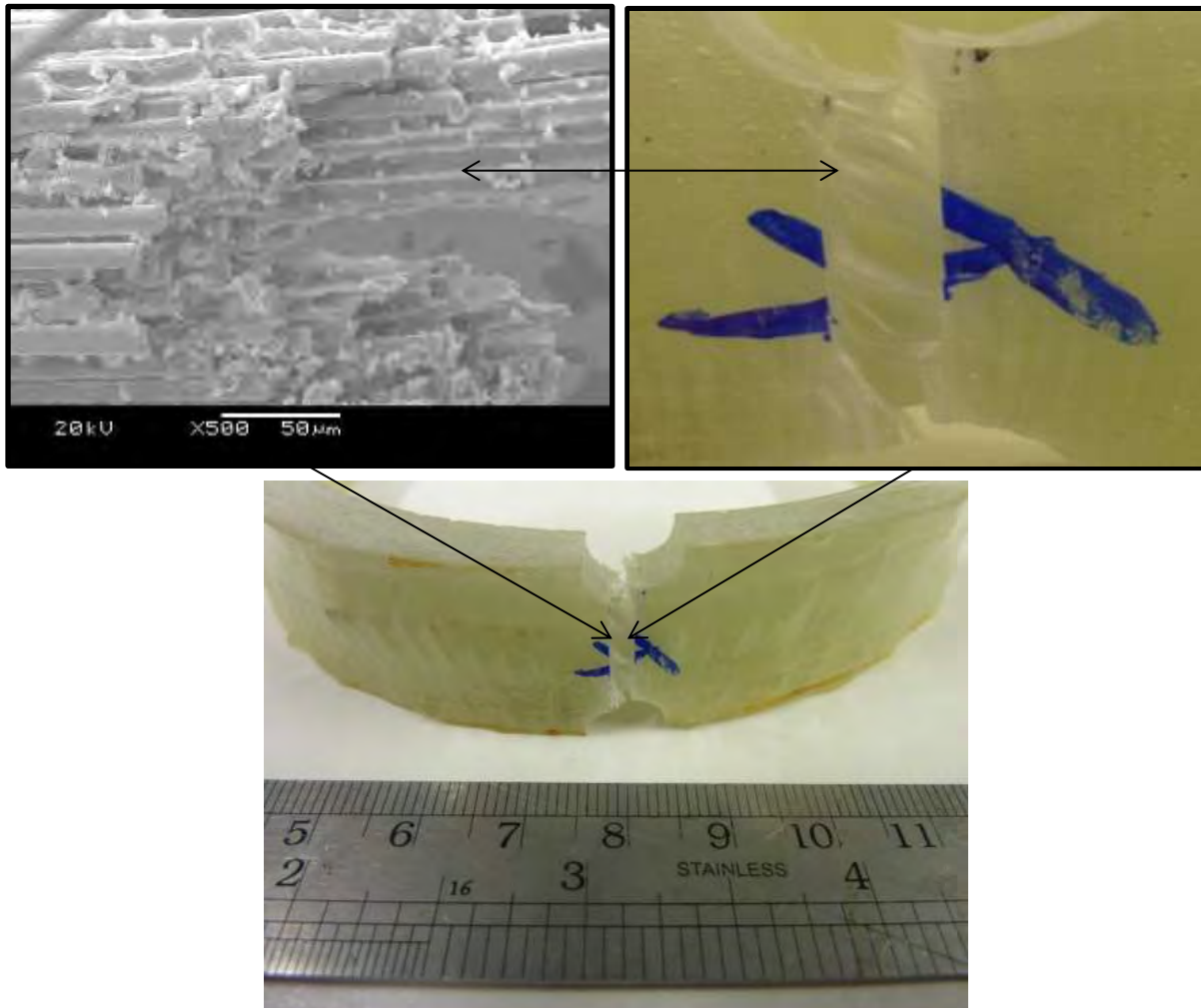


Figure 88. Photographs and typical SEM image of a failed direct-loom waste hoop tensile (split-disk) test sample.

With regards to Figure 89, it can be noted that the in-house CFW method was able to produce a relatively high inter-laminar shear strength (33.81 MPa) with a relatively small scatter (standard deviation) of 1.63 MPa which was comparable

to that presented as reference data in Section 2.1. Here a reference value for a carbon-fibre sample was defined as ~ 60 MPa, however owing to the considerable strength differences between glass- and carbon-fibre, it was concluded that the presented 33.81 MPa inter-laminar shear strength was acceptable. For reference, a typical load/displacement curve of an in-house CFW tube is presented in Appendix B.

To further reinforce the above point, it can also be noted that the CFW method was able to produce an inter-laminar shear strength which was higher than the upper limit of the 95% confidence interval (26.72 to 31.86 MPa) offered by the conventional method. These results were attributed to the use of: (i) the resin impregnation unit; and (ii) the fibre spreading station. It was postulated that both of these facilities aided in achieving efficient tow impregnation (<1% void content); this then produced a high degree of bonding between the multiple glass-fibre layers.

Figure 89 also presents the inter-laminar shear strength results of the on-site CFW method. Here, relatively high strengths of 26.11 MPa (± 2.25) and 24.14 MPa (± 2.51) were produced for the 7 m/min and the 21 m/min winding speeds respectively. These results confirmed that the CFW method was able to offer comparable inter-laminar shear strengths both on-site and in-house.

Table 27. Inter-laminar shear strength results.

Method	Failure load (N)	Inter-laminar shear strength (MPa)	95% confidence interval (MPa)
In-house CFW	733.4 (±36)	33.81 (±1.63)	32.09 - 35.53
Conventional	498.2 (±38.8)	29.29 (±2.45)	26.72 – 31.86
On-site CFW (7 m/min)	384.1 (±30.68)	26.11 (±2.25)	23.75 – 28.48
On-site CFW (21 m/min)	344.8 (±41.73)	24.14 (±2.51)	21.51 – 26.77
R-CFW (waste slittings)	1590.2 (±253.62)	28.19 (±3.3)	24.74 – 31.64
R-CFW (direct-loom waste)	693.9 (±236.11)	6.84 (±1.51)	5.25 – 8.42
Reference: Van Paepegem <i>et al.</i> [19]	-	61.3*	-
Reference: Chen <i>et al.</i> [74]	-	67*	-

* Carbon-fibre reference samples

With further reference to Figure 89, it can also be noted that the waste slittings were able to produce a considerably higher inter-laminar shear strength than the direct-loom waste; 28.19 MPa (± 3.3) and 6.84 MPa (± 1.51) respectively. This equated to an approximately four times higher strength produced by the waste slittings. In addition to this higher average strength, the waste slittings also produced a more consistent set of tubes with a standard deviation of 3.3 MPa; this equated to a percentage variation of 11% in comparison to the $\sim 20\%$ variation produced by the direct-loom waste; ± 1.51 MPa. As in Section 4.8.3, the higher and more consistent results produced by the waste slittings were attributed to: (i) a more consistent level of fibre deposition; and (ii) less fibre quality issues.

Finally, unlike that discussed in Section 4.8.3, despite the relative misalignment of the reinforcing fibres, the waste slittings were able to offer considerable inter-laminar shear strengths. Here, the waste slittings were able to offer inter-laminar shear strengths which were $\sim 8\%$ higher than that produced by the conventional filament winding method. The presence of such an inter-laminar shear strength was not completely understood. At the point of writing, this occurrence was attributed to the considerable sample thickness and possible bonding of the resin through the 'broken-down' resin sealant. Here, it was postulated that the resin sealant may have created a small interface region which essentially allowed the resin to 'grip' to the waste slittings and hence create a considerable bond between multiple layers. This theory was not able to be proved during this study and could be a point for future study.

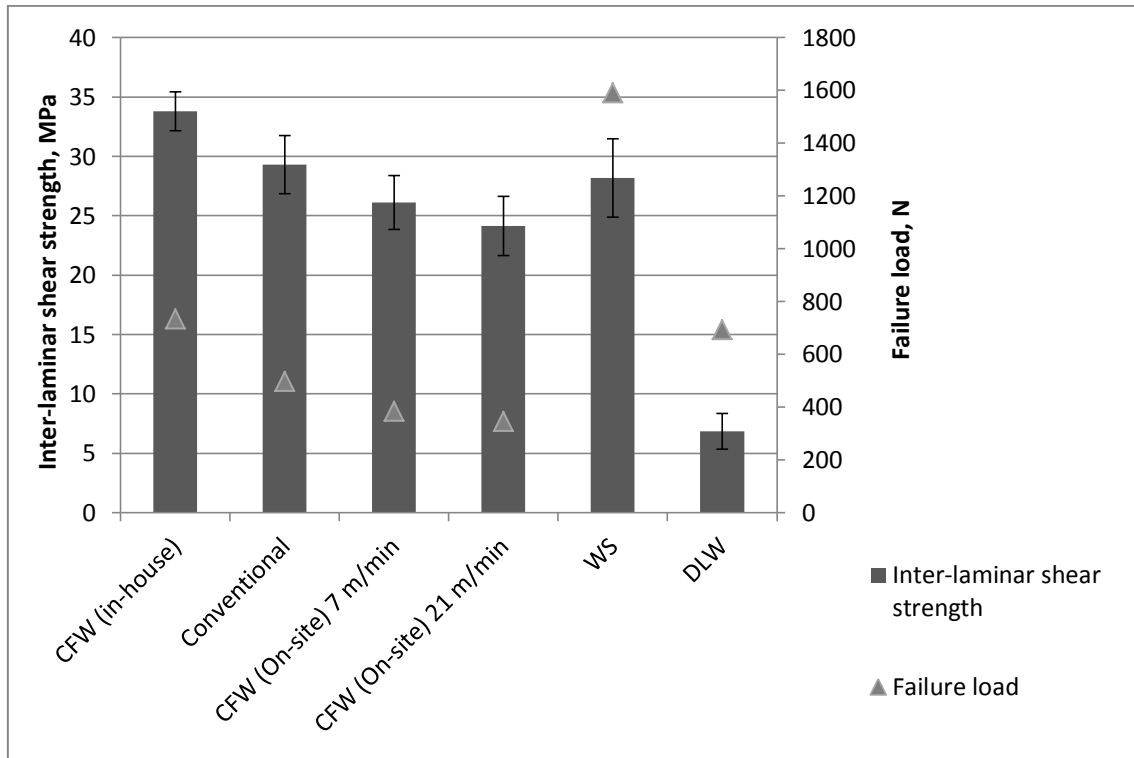


Figure 89. Summary of inter-laminar shear strength results.

As in Section 4.8.3, all tested samples were subjected to fractography analysis. Figures 90 - 92 present images of typically failed inter-laminar shear strength samples; from analysing these samples the following observations and conclusions were made:

- (i) Failure of the samples occurred as a result of delamination and fibre breakage. Highlighted sections of fibre delamination and breakage are presented in Figures 90 and 91.
- (ii) No other failure mechanisms i.e. fibre 'pull-out', were visibly evident.
- (iii) Identical failure mechanisms were present in the test specimens produced using the in-house CFW, on-site CFW and conventional filament winding methods.

(iv) The non-uniform nature of the DLW samples can be seen in Figure 92. Here, it can be noticed that sample failure did not occur in a straight line in the loading direction (as in Figures 90 and 91) and in fact many of the fibres were loaded and failed in $\pm 0^\circ$, $\pm 45^\circ$ and $\pm 90^\circ$ orientations.

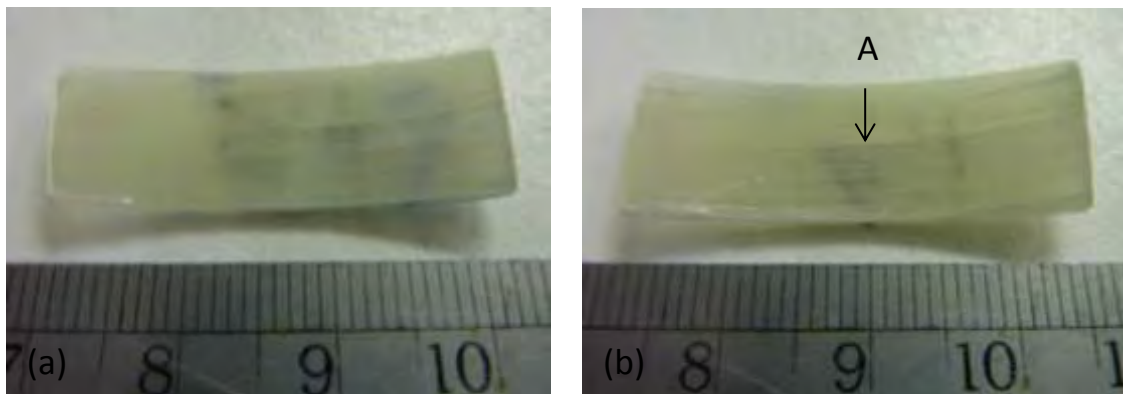


Figure 90. Photographs of inter-laminar shear failed samples; in-house CFW samples. The highlighted section (A) are areas of delamination.

4.8.4 Lateral Compression Strength

Table 28 and Figure 93 present a summary of the lateral compression strength results. Here, it should be noted that lateral compression strength results for the cardboard tubes discussed in Section 4.3 were presented and typical load/displacement curves are presented in the appendix.

From studying Figure 93, it can be noted that the in-house CFW method was able to produce considerably high lateral compression strengths. Here, the average strength was 18.49 MPa and the scatter (standard deviation) was just 0.84 MPa; this small scatter equated to a variation of just approximately 5%. For

reference, an example load/displacement curve of an in-house CFW tube after lateral compression testing is presented in Appendix B. To put these results into perspective, the conventional filament winding method was only able to produce a lateral compression strength of 12.97 MPa (± 0.66).

To further support the ability of the CFW method to produce relatively high compression strength results, the on-site CFW method also presented comparable results of 11.76 MPa (± 0.82) for the 7 m/min tube and 12.87 MPa (± 0.87) for the 21 m/min tube. In particular, the 21 m/min tube was able to offer a strength which fell within the 95% confidence interval offered by the conventional method (12.28 – 13.67).

From comparing the above results, it can be seen that the CFW method was able to successfully manufacture filament wound tubes which can offer comparable and/or superior mechanical (lateral compression) properties to that produced by its conventional predecessor.

As in Section 4.8.2, the relatively high mechanical properties produced by the CFW method were attributed to the use of the resin impregnation unit, resin delivery system and fibre spreading station. It was thought that the combination of these facilities aided in achieving efficient tow impregnation (<1% void content); this then went on to produce the considerably high properties which were documented.

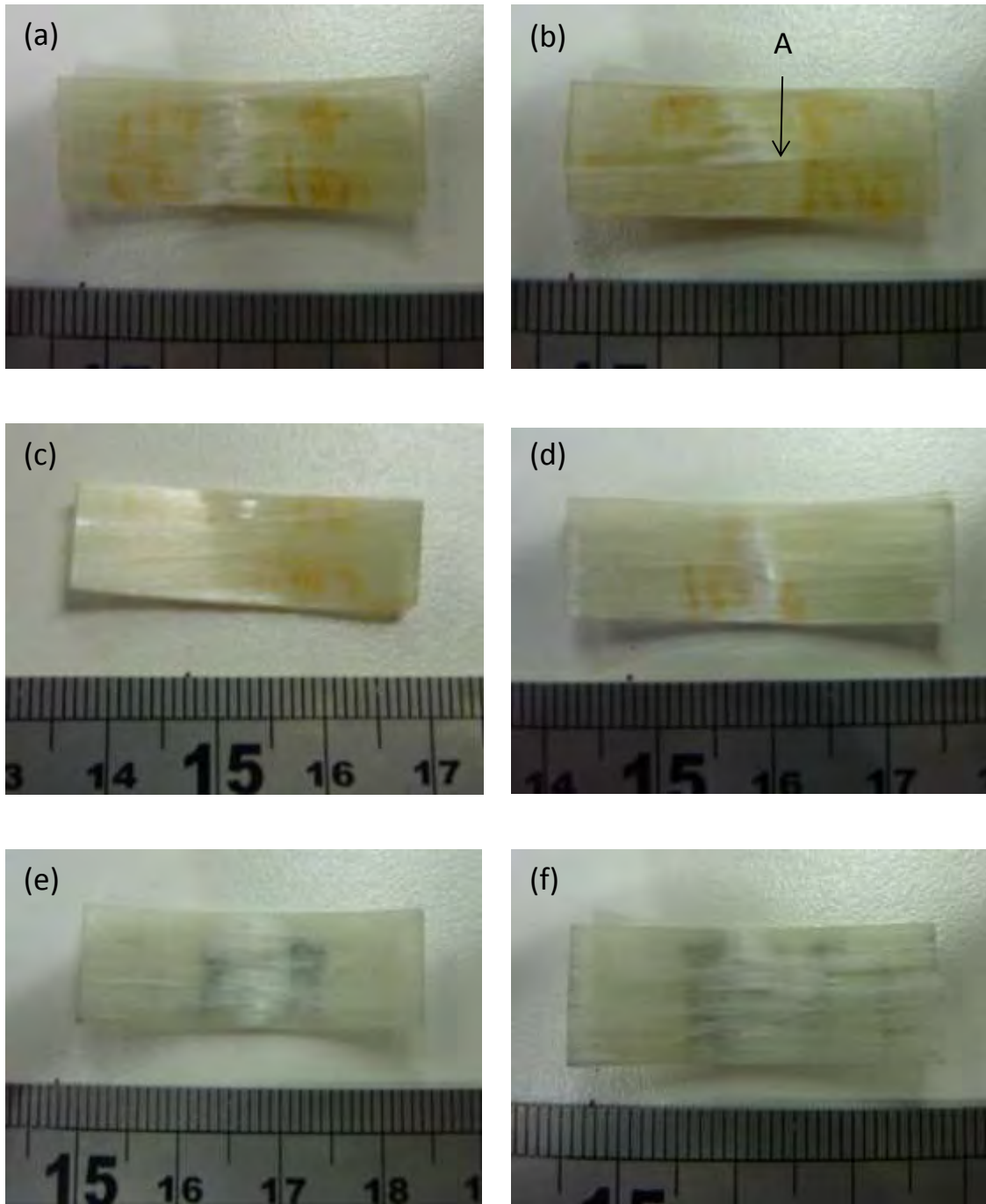


Figure 91. Photographs of inter-laminar shear failed samples. (a and b) conventional filament winding; (c and d) on-site CFW (7 m/min); and (e and f) on-site CFW (21 m/min). The highlighted sections (A) are areas of delamination.

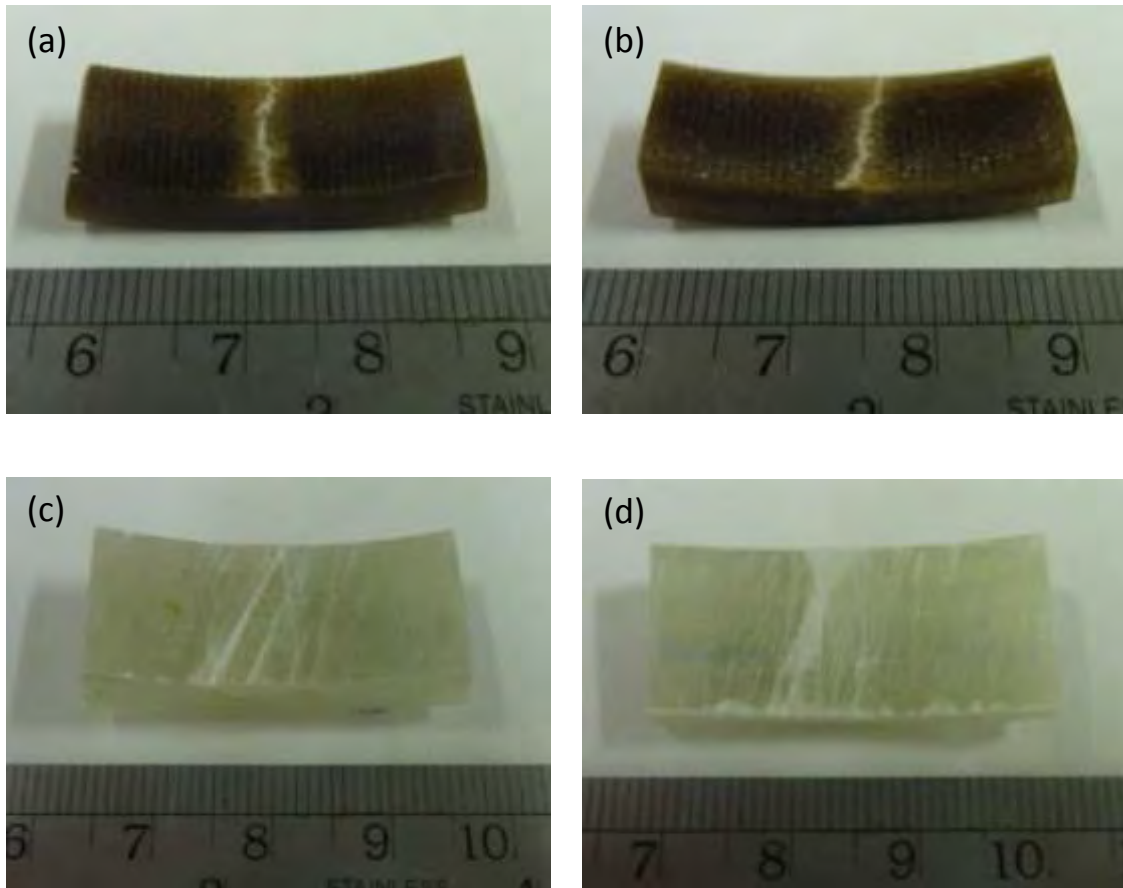


Figure 92. Photographs of inter-laminar shear failed samples; (a and b) R-CFW (waste slittings) samples; and (c and d) R-CFW (direct-loom waste) samples.

In a similar fashion to that discussed in multiple sections above, the waste slittings were also able to produce considerably higher mechanical properties than the direct-loom waste; 7.07 MPa (± 0.59) and 2.14 MPa (± 0.27) respectively. This equated to an approximately three times higher strength produced by the waste slittings. As in Sections 4.8.2 and 4.8.3, the higher and more consistent results produced by the waste slittings were attributed to: (i) a more consistent level of fibre deposition; and (ii) fewer fibre quality variations.

Finally, in addition to the above comparisons, the waste slitting tubes were also shown to offer considerably higher strengths than the cardboard tubes which were also presented in Figure 93. Here, it can be seen that the waste slitting tubes were able to offer lateral compression strengths which were approximately seventeen times stronger than the comparative cardboard tubes. The considerably higher mechanical properties provided by the waste slittings over the cardboard tubes aided in satisfying the criteria outlined in Section 4.3. Figures 94 - 96 present typical images of fractured lateral compression samples. From analysing these figures, the following fractography observations and conclusions were made:

(i) Sample failure occurred as a result of fibre delamination. Highlighted sections of fibre delamination are presented in multiple figures below.

(ii) No other failure mechanisms i.e. fibre 'pull-out' or breakage, were visibly evident.

(iii) Fibre failure occurred at the extreme edges i.e. east and west edges, of the sample. Figure 97 presents clarification of the observed sites of failure.

(iv) From reviewing Figures 94 - 96, it was concluded that identical failure mechanisms were present. This similarity confirmed that the CFW and R-CFW methods were able to produce filament wound tubes which could offer comparable lateral compression loading characteristics.

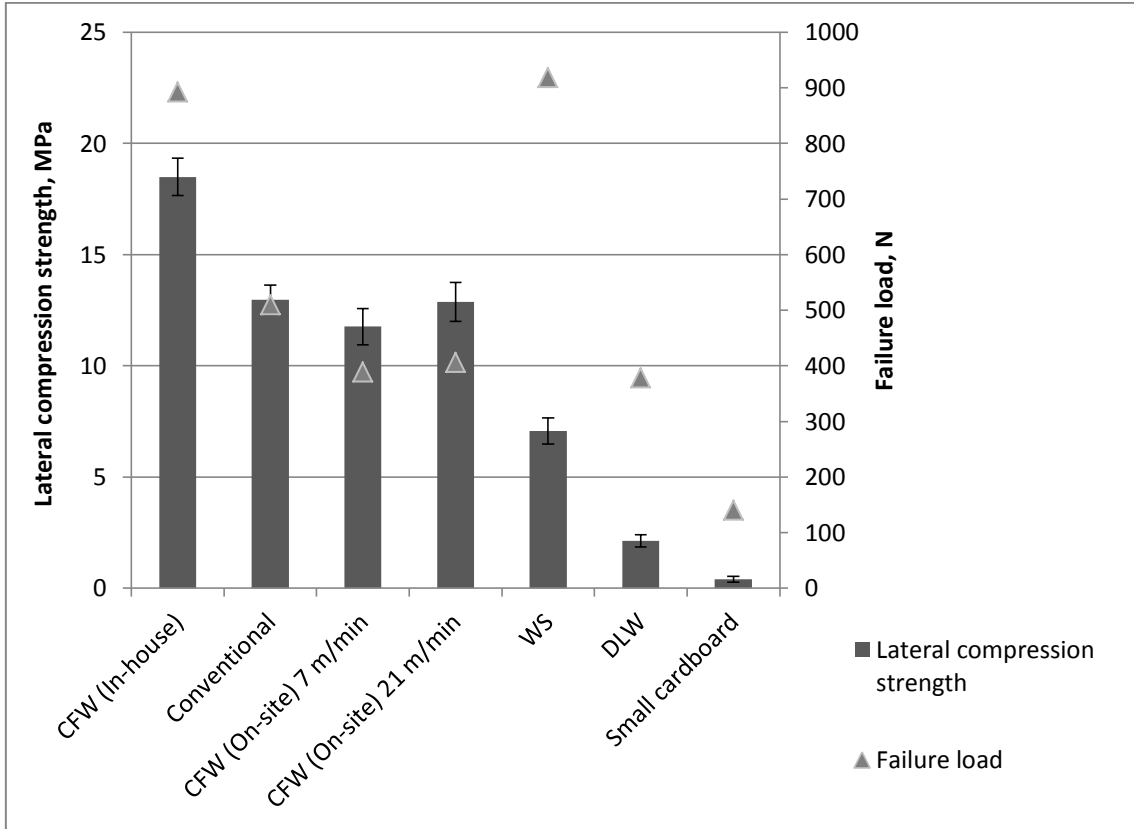


Figure 93. Summary of lateral compression strength results.

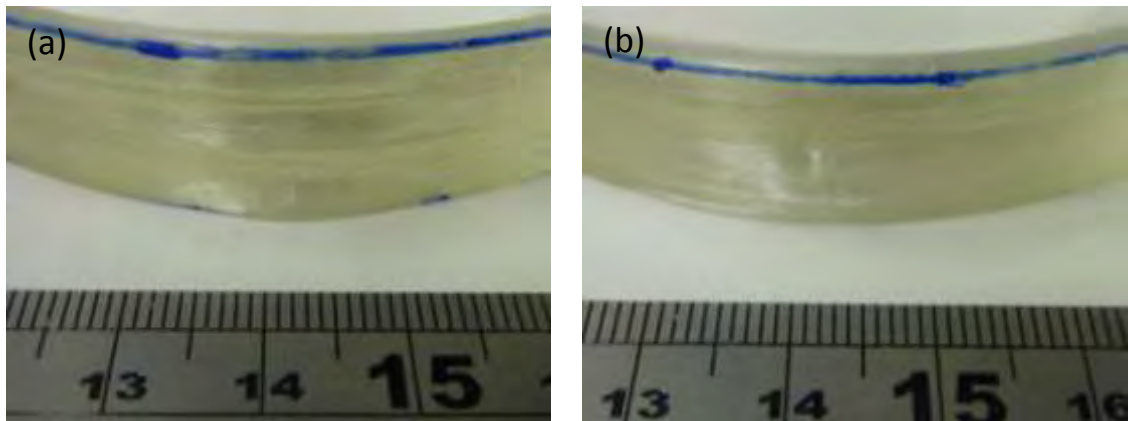


Figure 94. Photographs of failed lateral compression samples; in-house CFW.

Table 28. Lateral compression strength results.

Method	Failure load (N)	Lateral compression strength (MPa)	95% confidence interval (MPa)
In-house CFW	892.7 (±37.97)	18.49 (±0.84)	17.61 – 19.38
Conventional	510 (±14.64)	12.97 (±0.66)	12.28 – 13.67
On-site CFW (7 m/min)	389 (±21.71)	11.76 (±0.82)	10.90 – 12.62
On-site CFW (21 m/min)	406 (±17.63)	12.87 (±0.87)	11.95 – 13.79
R-CFW (waste slittings)	918.1 (±137.79)	7.07 (±0.59)	6.44 – 7.69
R-CFW (direct-loom waste)	377.9 (±88.75)	2.14 (±0.27)	1.83 – 2.42
Cardboard tube	140.79 (±48.24)	0.41 (±0.13)	-

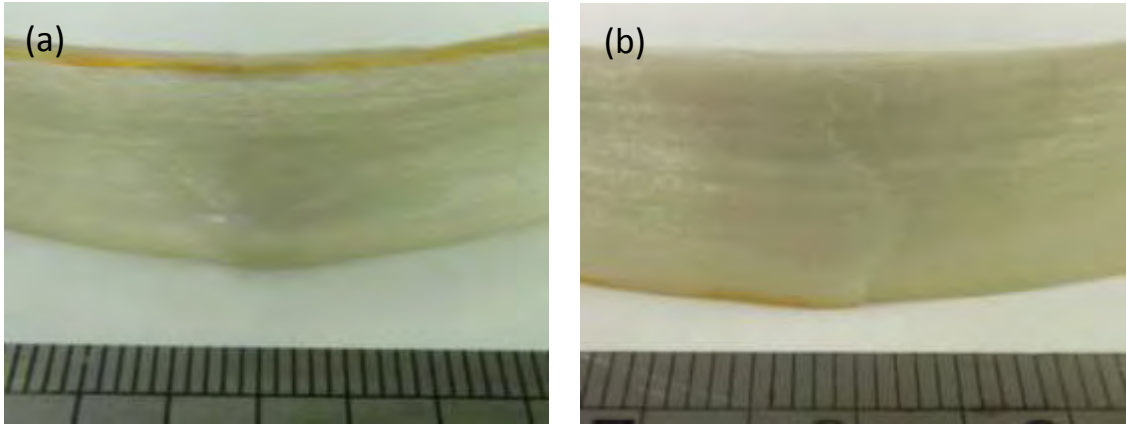


Figure 95(a). Photographs of failed lateral compression samples: conventional filament winding.

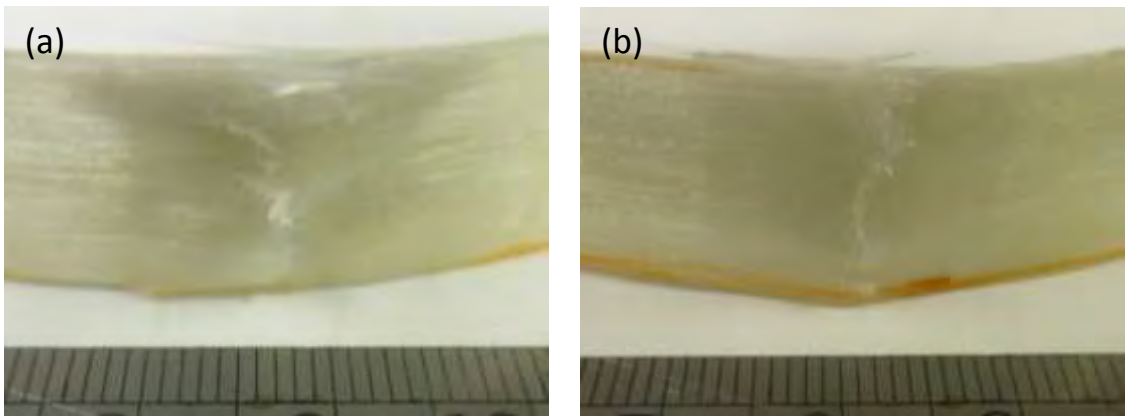


Figure 95(b). Photographs of failed lateral compression samples: on-site CFW (7 m/min).

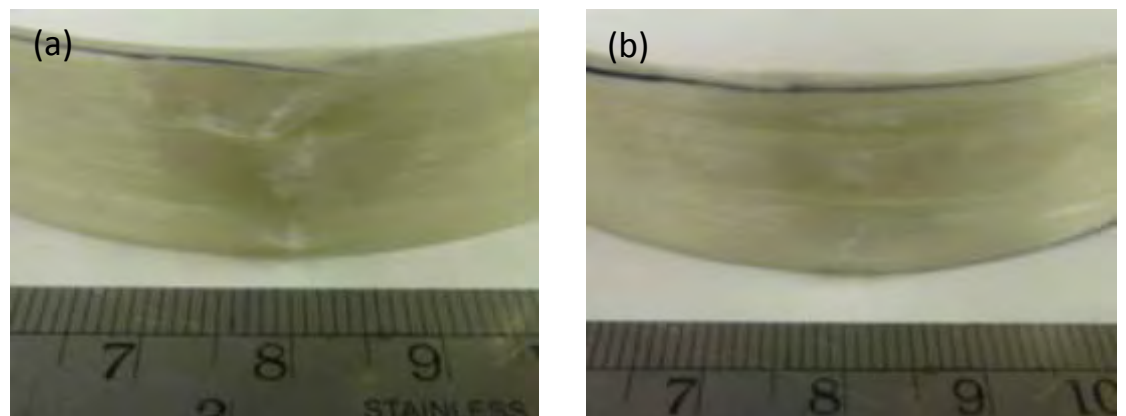


Figure 95(c). Photographs of lateral compression failed samples: on-site CFW (21 m/min).

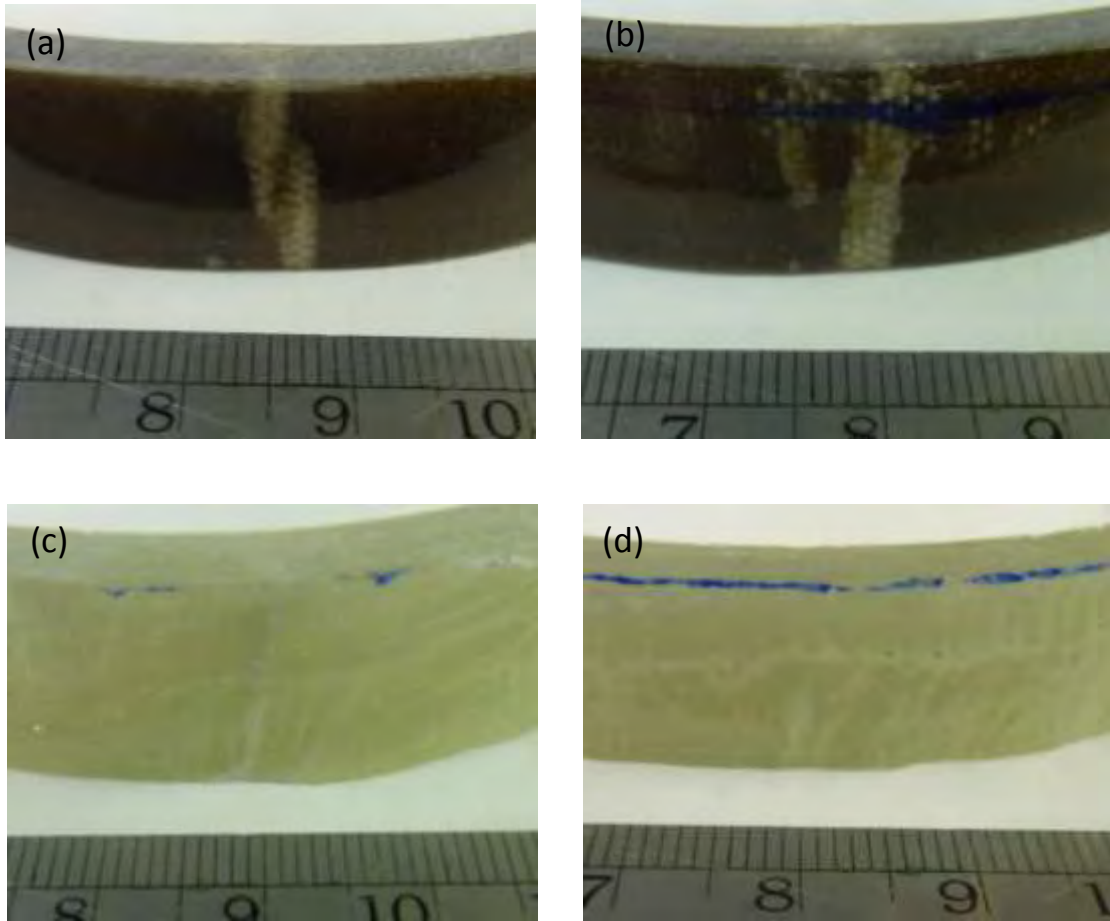


Figure 96. Photographs of lateral compression failed samples; (a and b) R-CFW (waste slittings) samples; and (c and d) R-CFW (direct-loom waste) samples.

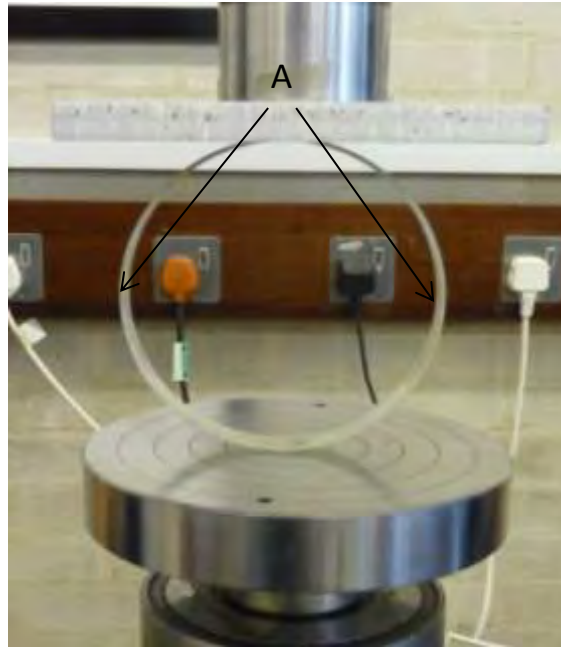


Figure 97. Photograph of the lateral compression test fixture. The highlighted components (A) confirm the site-of-failure.

4.8.5 Pressure Burst Strength of Composite Overwrapped Pressure Vessels (COPV's)

Table 29 presents the pressure burst strength results of the COPVs manufactured by the CFW method. With reference to Table 29, it can be seen that the CFW method was able to repeatedly manufacture COPVs with consistently high pressure burst strengths. Here, the minimum failure load was 702 bar, the maximum was 728 bar and the average was 714 bar (± 9.37). Figure 98 presents a summary of these results. However, for clarity it should be noted that the 578 bar reference figure was only a minimal threshold value and in-fact carbon-fibre COPV failure would normally occur at ~ 1000 bar. The presence of such high pressure burst strengths was attributed to the use of the CFW methods resin impregnation unit and fibre spreading stations. It was

believed that these facilities aided in producing a set of COPVs which offered similar low void contents as presented in Table 29. Due to this result, it was concluded that the CFW method was able to manufacture COPVs with appropriately high mechanical properties and the aim of this study, highlighted in Section 1.3, with regards to the manufacture of clean filament wound COPVs was achieved successfully.

Figure 99 also presents images of typically failed COPVs. Here, it can be seen that complete catastrophic failure was achieved. It can also be noted that the samples were separated into two components. This would normally be undesirable, however for the purposes of this study, this was deemed acceptable as the initial investigation was to evaluate the ability of the CFW method to achieve the stipulated strength targets. Now this has been proven, attempts to address health and safety guidelines can be endeavoured in future studies.

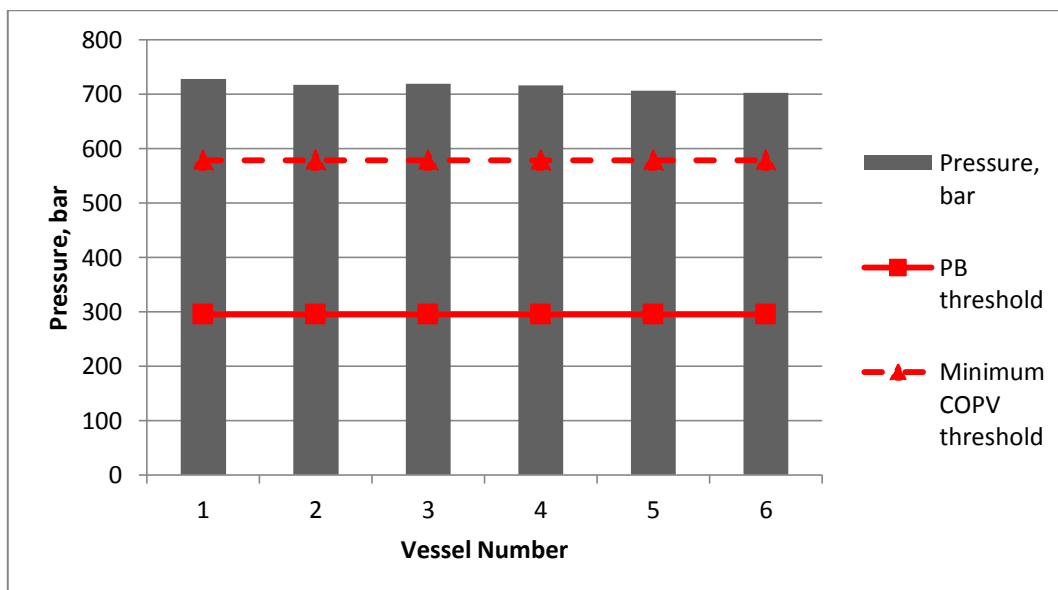


Figure 98. Pressure burst strengths of overwrapped COPVs.

Table 29. Summary of COPV pressure burst strength results.

Number of COPV	Failure load (Bar)	Comments
1	728	- Failure in COPV mid-section - COPV fragmentation at failure - Fibre/liner separation
2	717	- Failure in COPV mid-section - COPV fragmentation at failure
3	719	- Failure in COPV top-section - COPV fragmentation at failure
4	716	- Failure in COPV mid-section - COPV fragmentation at failure - Fibre/liner separation
5	706	- Failure in COPV bottom-section - COPV fragmentation at failure
6	702	- Failure in COPV mid-section - COPV fragmentation at failure - Fibre/liner separation
Average	714 (±9.37)	



Figure 99. Photographs of burst COPV's.

4.8.6 Life Cycle Assessment (LCA)

To satisfy the third aim of the current report with regards to assessing the 'green' credentials of the CFW method, the following section presents the results of the LCA analysis presented in Section 3.6.7.

Table 30 shows the LCA results of the four winding conditions which were investigated during this study. This table shows the raw environmental impact data with regards to: acidification potential, eutrophication potential, freshwater aquatic ecotoxicity potential, global warming potential, human toxicity potential, marine aquatic ecotoxicity potential, ozone layer depletion potential, photochemical Ozone creation potential and terrestrial ecotoxicity potential. For reference, the glossary section of the current study presents a set of definitions

for the aforementioned LCA measurement parameters. Each potential impact was measured against an equivalent emission i.e. acidification potential was measured in kilograms of SO₂ equivalent emitted. During this study, no 'weighting' methods were used and only raw data was presented. Furthermore, to aid with the comparison of the three winding methods, the percentage change of each environmental impact potential in comparison to the conventional filament winding impact potential was also shown in Table 30. The percentage change of each impact potential was shown in brackets beneath the raw data for each category.

From reviewing Table 30 it can be seen that the CFW method had a lower environmental impact than the conventional filament winding method. Figure 100 shows a radar plot of these environmental impact reductions; in this figure, 100% represents the impact potential of conventional filament winding. With reference to Figure 100, the CFW method was able to produce a 9% reduction in global warming potential, a 3% reduction in human toxicity potential and a 25% reduction in eutrophication potential. However, it can be noted that the CFW method actually had a higher Ozone layer depletion potential; this was attributed to the increased power consumption of the CFW method with its use of a resin dispensing machine. Taking this into account, the CFW method was able to produce an overall environmental impact reduction of 11%; this confirmed the 'clean' credentials of the modified filament winding technique.

The reduced environmental impact of the CFW method was attributed to: (i) the reduced consumption of solvent for post-production cleaning; and (ii) the reduced production of waste resin. The removal of the resin bath and

subsequent replacement with a resin impregnation unit was believed to be the main reason for these improvements.

Table 30. Potential environmental impact data

LCA Parameter	Winding Method			
	Conventional	CFW	R-CFW: WS	R-CFW: DLW
Acidification potential (kg SO ₂ – Equivalent)	0.52	0.48 (-8%)	0.41 (-21%)	0.45 (-13%)
Eutrophication potential (kg Phosphate – Equivalent)	0.04	0.03 (-25%)	0.02 (-50%)	0.03 (-25%)
Freshwater aquatic ecotoxicity potential (kg DCB – Equivalent)	0.13	0.12 (-7%)	0.11 (-15%)	0.12 (-7%)
Global warming potential (kg CO ₂ – Equivalent)	114.91	104.36 (-9%)	76.51 (-33%)	91.79 (-20%)
Human toxicity potential (kg DCB – Equivalent)	5.50	5.34 (-3%)	5.11 (-7%)	5.26 (-4%)
Marine aquatic ecotoxicity potential (kg DCB – Equivalent)	4457.76	4113.4 (-7%)	3698.2 (-17%)	4271.3 (-4%)
Ozone layer depletion potential (kg R11 – Equivalent)	1.08E-05	1.13E-05 (+4%)	1.07E-05 (-1%)	1.07E-05 (-1%)
Photochemical Ozone creation potential (kg Ethene – Equivalent)	0.05	0.04 (-20%)	0.02 (-60%)	0.03 (-40%)
Terrestrial ecotoxicity potential (kg DCB – Equivalent)	0.083	0.065 (-21%)	0.057 (-0%)	0.077 (-0%)
Average percentage Reduction (%) (compared to conventional filament winding)	-	-11	-26	-13

With further reference to Figure 100, it is believed that additional reductions could be achieved if the consumption of power could be significantly reduced. It is understood that the consumption of electrical power is the main cause for the remaining environmental impact potentials. As a result, it is hypothesised that if a fast curing epoxy resin system is used during the CFW method then a potential reduction of up to 50% could be achieved.

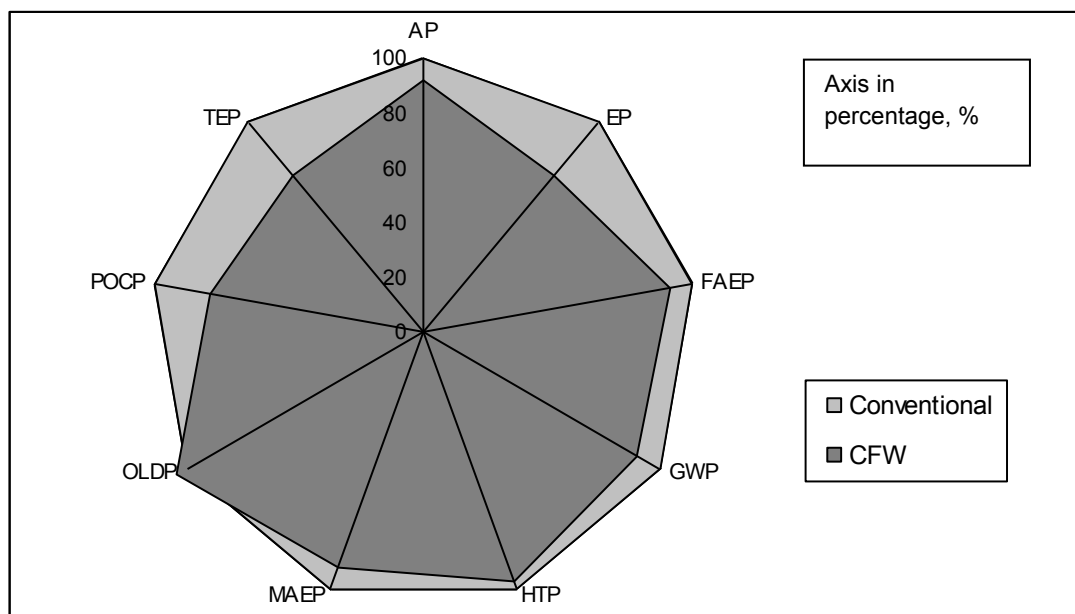


Figure 100. Radar plot comparing the environmental impact potentials of conventional and CFW. Here the axis headings represent: acidification potential (AP); eutrophication potential (EP); freshwater aquatic ecotoxicity potential (FAEP); global warming potential (GWP); human toxicity potential (HTP); marine aquatic ecotoxicity potential (MAEP); Ozone layer depletion potential (OLDP); photochemical Ozone creation potential (POCP); and terrestrial ecotoxicity potential (TOP).

The results in Table 30 also show that the R-CFW method was able to extend the CFW environmental reductions presented in Figure 100. In comparison to conventional filament winding, the R-CFW method with waste slittings was able to produce a 33%, 7% and 50% reduction in global warming potential, human toxicity potential and eutrophication potential respectively (shown in Figure 101). As a result, the R-CFW method with waste slittings was able to produce an overall reduction of 26%. Furthermore, in comparison to CFW the waste slittings were able to produce a 27%, 33% and 50% reduction in global warming potential, eutrophication potential and photochemical ozone creation potential respectively. As a result, an overall reduction of 17% could be produced; this confirmed that the use of recycled reinforcing fibres did reduce the environmental impact of the CFW technology.

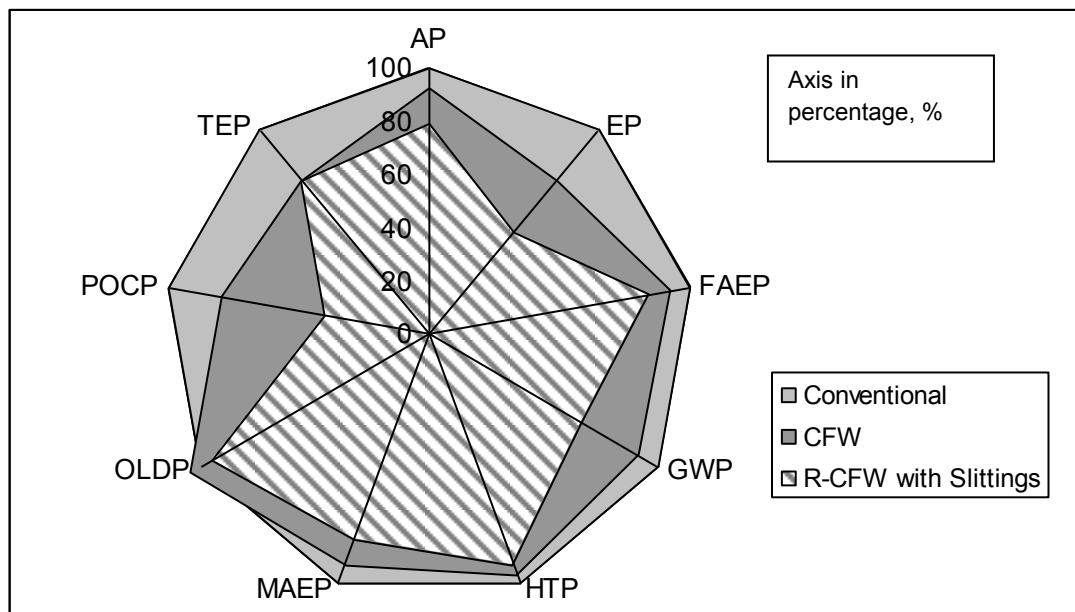


Figure 101. Radar plot comparing the environmental impact potentials of conventional, CFW and R-CFW (waste slittings). The axis headings in this figure are identical to those defined in Figure 100.

The R-CFW method with the use of DLW was also able to accrue environmental savings in comparison to conventional filament winding. Figure 102 shows a radar plot of these environmental impact reductions. In comparison to conventional filament winding the DLW was able to produce an overall impact reduction of 13%. However, the DLW was only able to produce a 2% reduction in comparison to CFW. This relatively small reduction was attributed to the use of a relatively large amount of epoxy resin during production; this occurred as a result of the relatively large volumes of resin which were needed to impregnate and control this fibre type. This consumption of resin partially negated any improvements that the recycled fibres could offer.

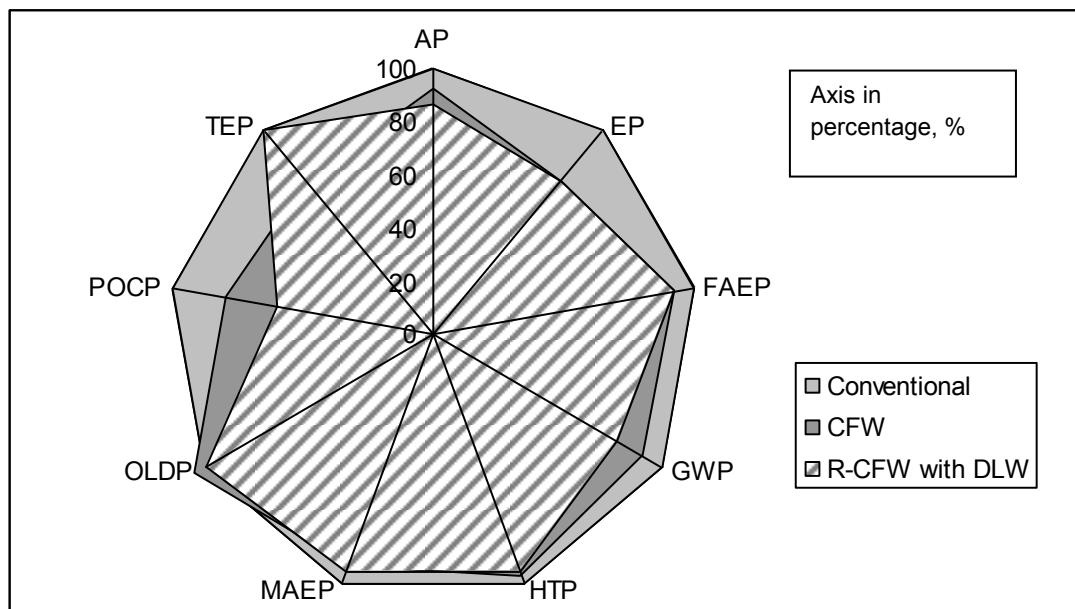


Figure 102. Radar plot comparing the environmental impact potentials of conventional, CFW and R-CFW (DLW). The axis headings in this figure are identical to those defined in Figure 100.

Figure 103 shows the overall impact reductions of the CFW and R-CFW methods in comparison to conventional filament winding. As in Figures 100 - 102, 100% represents the impact potential of conventional filament winding. In conclusion, it can clearly be seen that the CFW and R-CFW methods have a lower environmental impact potential than the conventional filament winding method. The results of this study confirm the 'clean' credentials of the modified filament winding method presented in this study.

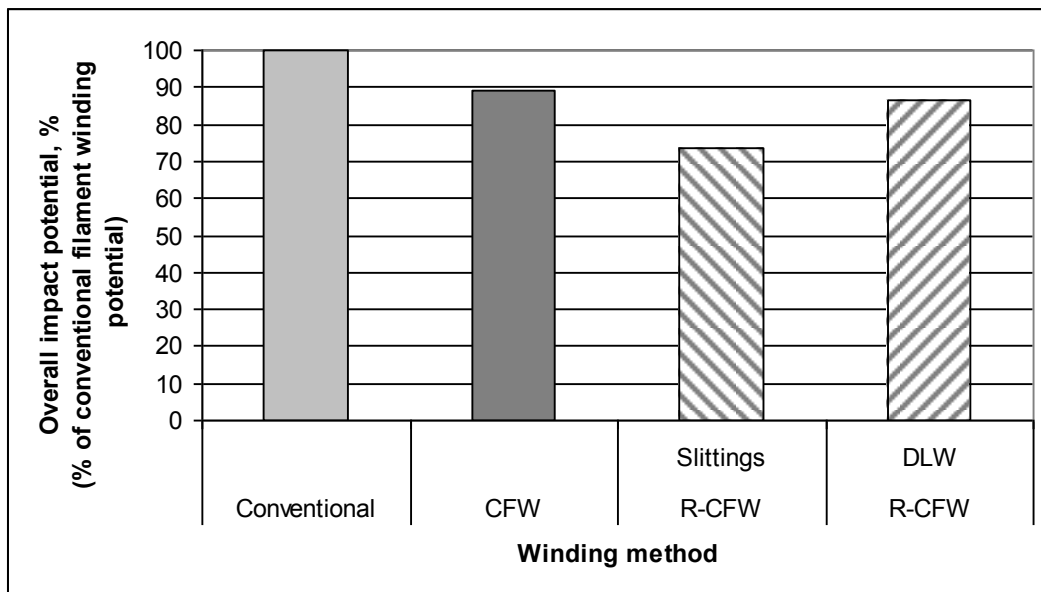


Figure 103. Overall environmental impact reductions achieved by the CFW and R-CFW methods in comparison to conventional filament winding.

4.8.7 Life Cycle Cost (LCC)

A summary of the life cycle cost (LCC) results are presented in Tables 31 and 32. With reference to the following section, results were presented with regards to: (i) an LCC simulation of four in-house filament winding conditions; and (ii) an

LCC assessment of the on-site R-CFW method. With regards to the second point, from undertaking this assessment it was possible to decide if the waste slittings were able to satisfy the economic criteria set-out in Section 4.3.

Firstly, Table 31 presents the results of the in-house filament winding LCC simulations; these results are also graphically shown in Figure 104. The simulated winding conditions presented here were: (i) CFW; (ii) conventional filament winding; (iii) R-CFW (waste slittings); and (iv) R-CFW (direct-loom waste). With reference to Figure 104, the yearly cost simulations were for the production of 5 tubes per day over the course of one working year.

From analysing Figure 104, it can be seen that the CFW method was far cheaper than its conventional predecessor. In particular, the modified method was £31.38 (39%) cheaper per tube; this resulted in an overall reduction in manufacturing costs of >£30,000 per year (39% decrease). These substantial cost savings were attributed to: (a) the reduction in waste resin production; (b) the decrease in solvent consumption; and (c) the reduction in post-production cleaning time.

Table 31 also presents the LCC results of the R-CFW method. From analysing this data, it can be noted that the waste slittings were able to accrue even further savings than the CFW method. Here, the waste slittings were able to produce a tube for £41.08; this resulted in an overall yearly reduction of ~£8,700 and ~£45,000 per year in comparison to the modified and conventional methods respectively. These reductions were attributed to the use of cheaper waste-fibres and relatively small amounts of resin.

However, from further analysing Table 31, it can be noted that such savings were not able to be produced by the direct-loom waste. The direct-loom waste was only able to produce small savings in comparison to conventional filament winding (~£10 per tube). Here, the relatively expensive production costs were produced from the considerable consumption of resin during processing; the need to over-impregnate these waste-fibres essentially negated any savings which could be produced by the CFW method.

Table 31. Life cycle cost output data for the manufacture of a 3 meter filament wound tube via: (i) in-house CFW; (ii) conventional filament winding; and (iii) in-house R-CFW.

LCC parameter	Winding method			
	CFW	Conventional	R-CFW (WS)	R-CFW (DLW)
Cost (£/3 m tube)	48.38	79.73	41.08	69.52
Overall cost (£/year)	95,679	58,056	49,296	83,424

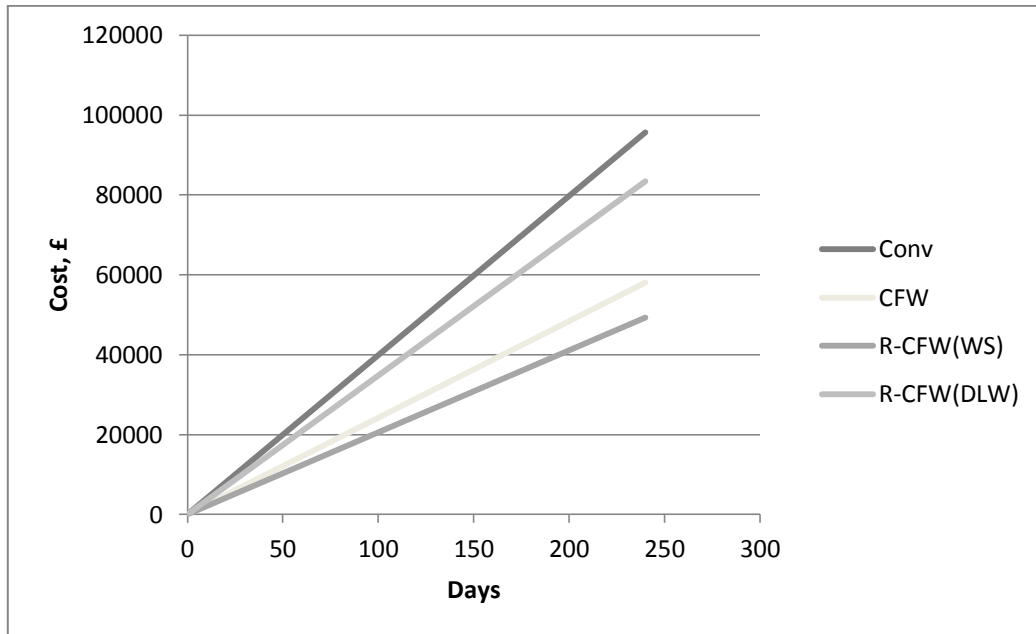


Figure 104. Life cycle cost output data.

Table 32 presents the on-site R-CFW LCC results. From analysing Table 32, it can be seen that three R-CFW conditions were presented; expensive, intermediate and cheap. These three conditions were presented to investigate the possible cost savings which could be accrued if certain winding conditions were implemented i.e. cheaper resin systems (Polyester resin, £2.6/kg) and from applying 'economy of scale' procedures.

In Table 32, the 'expensive' condition was a simulation of the method presented in Section 3.5.5; data was taken from this winding condition wherever possible, however some data was simulated from the in-house winding conditions. The other winding conditions (intermediate and cheap) were then presented as alternative simulations of this 'expensive' condition.

From analysing Table 32, it can be seen that the three winding simulations were able to produce a filament wound tube for an overall cost of £65.35, £37.98 and £17.20 respectively. Here, it can be seen that considerable cost savings could be produced if the waste slittings tubes were to be manufactured with the cheapest possible materials and with an 'economy to scale' manufacturing process. However, from comparing these values to that presented in Table 33, it can be seen that all of these simulation values were considerably higher than the average cost of a cardboard tube (£3.24). As a result, for the waste slittings tubes to be a viable option they would need to have a life-span which was considerably higher than that produced by the cardboard tubes. Figures 105 – 107 present simulations of the needed life-spans for each scenario. With reference to Figures 105 – 107, these simulations were based on: (i) the even consumption of storage and disposal costs across one working year; (ii) three tubes had to be in-use at all times; and (iii) the storage and disposal costs would be far cheaper for the waste slittings in comparison to the cardboard tubes; this was justified by the considerable reduction in volume of the waste-fibre tubes i.e. ~ 1800 cardboard tubes and < 100 waste fibre tubes

With reference to Figure 105, it can be seen that the 'expensive' waste-fibre tubes would need to achieve a minimum life-span of 30 cycles before they would become cost effective. However, if these tubes were able to last 50 or 100 cycles then an overall saving of approximately £6,000 or £12,000 could be achieved respectively.

Further economic reductions were found to be produced in Figures 106 and 107. From analysing these figures, it can be seen that the needed life cycle

could be reduced down to a minimum of 8 cycles before cost effectiveness was achieved.

From reviewing the considerable cost savings which could be produced by the waste-fibre tubes, it was concluded that the criteria set-out in Section 4.3 was completely satisfied (i.e. the waste fibre tubes produced a smooth outer-circumference finish, offered relatively high mechanical properties and were cost effective). As a result of this criteria satisfaction, it was decided that the waste-fibre tubes manufactured during the on-site CFW trials would be evaluated in an industrial site-trial. From completing this site-trial the waste-fibre tubes would: (i) complete the closed-loop re-use recycling concept proposed in Section 4.3; and (ii) be evaluated for their capacity to replace cardboard tubes as glass-fibre storage units. The following section describes the site-trial which was completed during this study.

Table 32. Simulated life cycle cost output data for On-site R-CFW (WS) with three winding conditions: (i) 'expensive'; (ii) 'intermediate'; and (iii) 'cheap'.

LCC parameter	Winding method		
	R-CFW (WS): 'expensive'	R-CFW (WS): 'intermediate'	R-CFW (WS): 'cheap'
Epoxy resin (£)	25.2	5.376	/
Polyester resin (£)	/	/	3.36
Waste-fibre (£)	5.04	2.52	0
Acetone (£)	0.22	0.2	0.15
Power (£)	9.882	9.882	7.686
Man-power (£)	25	20	10
Overall (£ / tube)	65.35	37.98	17.20

Table 33. LCC output data for cardboard tubes.

Tube parameter	Value
Cost per tube (£)	3.24
Number of tubes used per annum	~ 1800
Tube 'life-cycle' (number of cycles)	3 – 4
Storage costs per annum (£)	10,000
Disposal costs per annum (£)	2,661
Overall costs per annum (£)	~ 18,000

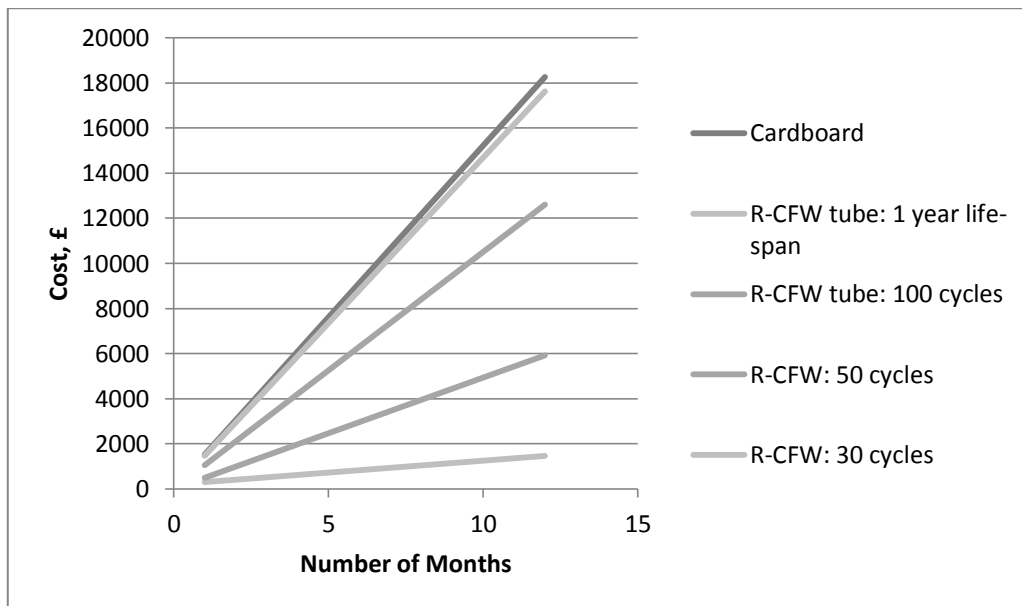


Figure 105. Life cycle cost simulations for R-CFW (WS): 'expensive'.

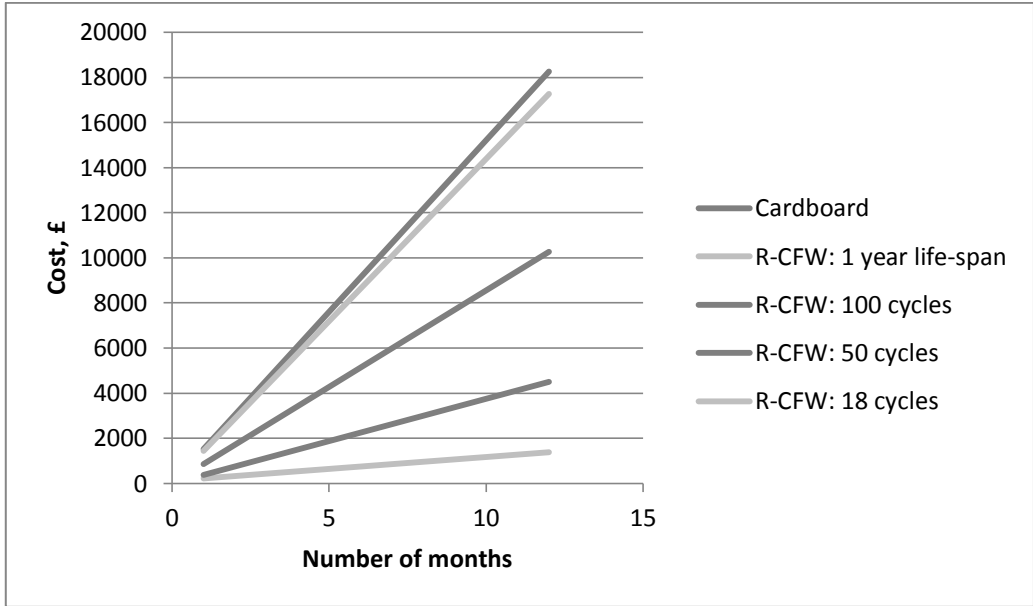


Figure 106. Life cycle cost simulations for R-CFW (WS): 'intermediate'.

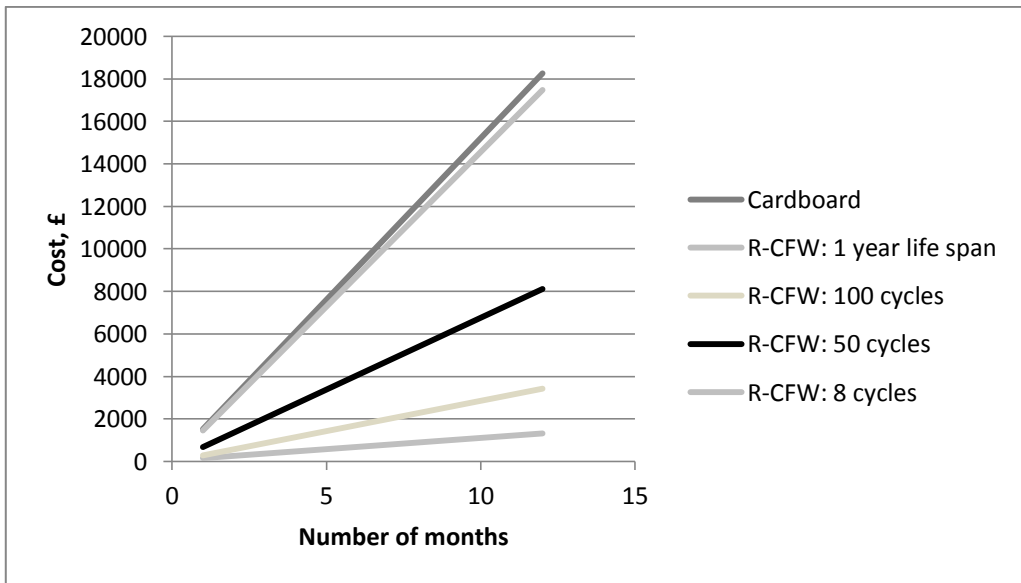


Figure 107. Life cycle cost simulations for R-CFW (WS): 'cheap'.

4.8.8 Site Trial of Waste-fibre Tubes

As mentioned in Section 4.8.7, a site-trial was undertaken to assess the ability of waste-fibre tubes manufactured during the on-site R-CFW trials to be used as direct replacements for cardboard tubes. From completing this trial: (i) a closed-loop recycling method was completed; and (ii) the issues presented in Section 2.4, with regards to composite recycling, were addressed.

To date, the waste-fibre tubes have been used during 20 life cycles and the following observations and conclusions were made:

(i) The waste-fibre tubes were considerably lighter than the cardboard tubes; 2 kg lighter. This reduction in weight made them easier to handle for the site-trial operators.

(ii) The angle-wound tube had to be polished to ensure the outer-diameter was as smooth as the hoop-wound tube. This was needed as the chosen winding angle did not completely cover the protruding waste slitting fibres.

(iii) The waste-fibre tubes had to be fitted with custom-made end fittings. This was completed as the waste-fibre tubes had a slightly larger inner-diameter than the commonly-used cardboard tubes. This discrepancy could not be avoided as this was the nearest possible mandrel size and the manufacture of a mandrel with a desired diameter would have been too costly for the current project.

(iv) Initial trials have shown that the waste-fibre tubes could be successfully moved by both manual and automated means i.e. by hand and by fork-lift.

In conclusion, the waste-fibre tubes are currently not cost-effective, however the tubes only need to complete ten more cycles to become cost-effective. It is anticipated that this threshold will be considerably surpassed and the tubes will become cost effective in the very near future.

CHAPTER 5: CONCLUSIONS

(a) *Clean filament winding*: A step-change in the manufacturing process for wet-filament winding was designed, developed and demonstrated. The clean filament winding concept was conceived by analysing the perceived problems with conventional filament winding. Solutions were then proposed and evaluated under laboratory and industrial (on-site) conditions. In summary, the clean filament winding process consisted of the following components: (i) a resin dispensing unit, which stored the resin and hardener components in separate reservoirs. The two components were then pumped on-demand using precision gear pumps. (ii) A conventional static mixer was used to intimately mix the resin and hardener. (iii) A custom-designed resin impregnation unit, which was developed on the basis of a detailed impregnation modelling study, was used to achieve efficient impregnation of the reinforcing fibre tows instead of a resin bath. (iv) A fibre spreading station, which was developed by reviewing previously patented fibre spreading technologies, that was used to mechanically spread the fibre tows prior to resin impregnation. This component was incorporated to further improve the possible transverse impregnation rate of the fibre tows.

The clean filament winding technique was used to facilitate a significant reduction in the generation of waste resin. Furthermore, the site trial verified that the volume of solvent required to clean the resin impregnation unit was a fraction of that required for conventional filament winding. The emission of

solvents and low molecular weight components to the atmosphere was also reduced significantly with clean filament winding.

(b) Recycled-Clean filament winding: The clean filament winding technique was also shown to have the capacity to be modified to manufacture composite components from waste glass-fibre materials. Here, two waste materials, termed waste slittings and direct-loom waste, were used as fibre feed-stocks and were manufactured with a comparable method to that used to manufacture glass-fibre composites. From developing this method, a relatively simple and cheap re-use recycling method was produced.

(c) Comparison of physical and mechanical properties: The properties of filament wound tubes manufactured in the current study demonstrated that the clean filament winding method was able to offer comparable or superior fibre volume fractions and void contents as that produced by the conventionally filament wound tubes. In particular, the modified method was able to offer considerably low void contents; lower than 1%.

The hoop tensile (split disk), inter-laminar shear and lateral compression strengths were also similar, or superior, for the glass-fibre tubes manufactured using the modified and conventional filament winding techniques. The comparable, or superior, properties provided by the modified techniques were mainly attributed to the efficient impregnation method and hence low void contents of the produced composites.

It was also shown that the waste-fibre composite components were generally not able to offer comparable properties to that presented by the as-received glass-fibre tubes. However, it was shown that the waste slittings offered

considerably superior properties as opposed to the direct loom waste. These superior properties were attributed to the higher percentage of the waste slitting reinforcing fibres being present in the load-bearing direction.

(d) Clean filament wound COPVs: The CFW method was also developed to manufacture COPVs and from analysing the pressure burst strength results presented in Section 4.8.5, it can be seen that the modified wet-filament winding method was able to manufacture glass-fibre COPVs which offered comparatively high mechanical properties.

(e) Life cycle assessment (LCA) and Life cycle cost (LCC) analysis: Due to the results presented in Section 4.8.6 and 4.8.7, it was shown that the modified filament winding methods were able to significantly improve the economic and environmental impacts of filament wound components. Here, any economic or environmental improvements were attributed to the reduced production of waste resin and consumption of solvents for cleaning purposes and time required for post-production cleaning.

Due to the above conclusions, it was shown that the CFW and R-CFW methods can be favourable alternative options for the manufacture of filament wound composite components. Furthermore, the concepts applied in this study can be adapted and incorporated into other manufacturing methods such as pultrusion.

5.1 Recommendations for Future Research

In addition to the research presented in the current document, many areas for future investigation have been identified. Firstly, attempts to apply the clean filament winding method to different reinforcing fibre materials i.e. central-pull fibres, carbon fibres or natural fibres. Here, it seems that an obvious progression of the clean filament winding method would be to incorporate many of the materials that are commonly used in the filament winding industry. This would open the method up to wider use in many different applications.

Another obvious progression for the CFW method would be to incorporate different resin systems which could further enhance the economic and environmental validity of the modified method. Here, fast-curing resin systems could now be used, owing to the fact that the resin is constantly supplied to the resin impregnation unit, and there is a reduced possibility of the resin curing and hardening on the filament winding equipment. From initial investigations, it is hypothesised that the incorporation of a fast-curing resin system could produce a 50% reduction in the environmental impact of the clean filament winding method.

Finally, other areas of future research could include: (i) attempts to achieve efficient impregnation of the direct-loom waste fibres, where the large volume of waste material currently produced, could provide a valid long-term recycling method. (ii) An investigation into hybrid composite manufacture, where the fibre spreading station could be used to achieve efficient hybridisation of multiple reinforcing fibre materials. (iii) On-line impregnation of short-fibre hybrid filament

wound tubes; and (iv) the application of the 'clean' methodology into other manufacturing methods i.e. pultrusion.

CHAPTER 6: APPENDIX

6.1 Appendix A: Alternative Mechanical Fibre Spreading Methods

Ridged-fixture Mechanical Spreading [110,111]

In contrast to the recommended use of smooth fixtures by Peters and McLarty [143], many authors have also developed fibre spreading methods which incorporated the use of fixtures with non-uniform surfaces [110,111]. For example, Akase *et al.* [110] suggested the use of a freely rotating roller with a plurality of ridges extending in the axial direction. Figure A1 presents a schematic illustration of a ridged fibre-spreading fixture.



Figure A1. Schematic illustration of a ridged fibre spreading pin [110].

Profiled-fixture Mechanical Spreading [112,113,114]

Many authors have also incorporated the use of profiled fixtures during mechanical fibre spreading [112,113,114]. Figure A2 presents a schematic illustration of a profiled fixture which was used by Nakagawa *et al.* [112]. In

general, as shown in Figure A2, most authors have adopted the use of profiled fixtures with convex, as opposed to concave, profiles.

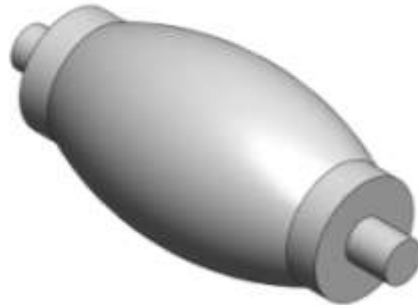


Figure A2. Schematic illustration of a profiled (convex) fixture [112].

With reference to Figure A2, the convex fixture could be described as ‘having a “bulging” thick-centre profile which tapered towards the ends of the fixture’. This bulging profile was incorporated to promote fibre spreading by allowing the edges of the bundle to ‘slip’ along the pin and allow the centre of the fibre bundle to spread.

Interval Mechanical Spreading [112,115]

Interval mechanical spreading was defined during this study as ‘a method to spread a fibre tow which incorporated a non-consistent or intermittent mechanical spreading process’. This method could be characterized by: (a) the use of multiple fixtures which rotated around an independent axis; (b) intermittent contact of the spreading fixtures with the fibre bundles; and (c) relatively short fibre/fixture contact lengths. An example of an interval mechanical spreading method is presented in Figure A3 (a and b).

With reference to Figure A3 (a and b), the method incorporated four convex rollers, made of aluminium or titanium, which had a thick central radius curvature of 30 - 100 mm. These pins were then placed on the circumference of a circular disk and rotated so that the fibre bundles came into intermittent contact. The fibres (with a winding speed and contact angle of 1 – 3 m/min and $\sim 45^\circ$ respectively) were spread-out at each contact point and were transferred from pin-to-pin in order to maintain the spread width.

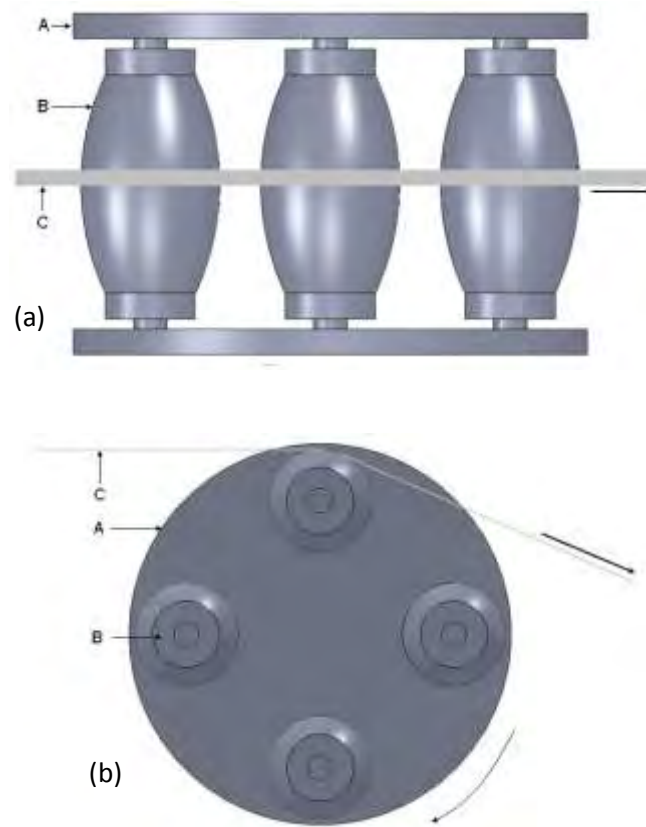


Figure A3. Schematic illustration of the interval mechanical spreading method developed by Nakagawa *et al.* [112]; (a) above-view; and (b) side view. The highlighted components are: (A) supporting side plates; (B) convex spreading fixtures; and (C) a fibre bundle. Here the fibre- and disk-rotation motion is indicated by the arrows on the right-hand side of the figure.

Comb Mechanical Spreading [117]

Mechanical fibre spreading can also be achieved with the use of a spreading 'guide' or 'comb' [117,118]. For example, guide spreading, as shown in Figure A4, can involve the use of a grooved fixture that separates and spreads the individual fibres of a bundle.

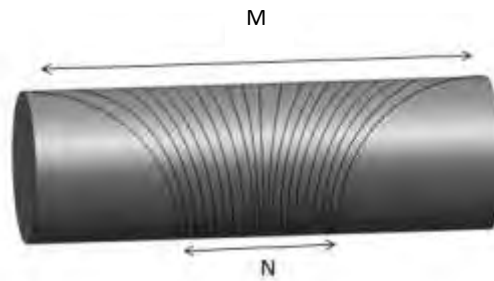


Figure A4. Schematic diagram of guide spreading.

With reference to Figure A4, the comb achieved fibre spreading through the use of non-parallel grooves which were of a diverging fashion. Here, the fibre tow entered the comb at its narrowest section (N) and exited at the widest section (M). As the tow travelled from (N) to (M) the individual fibres were separated by the diverging grooves and a spread tow was produced.

Vibration-mechanical Spreading [110]

Much attention has also been directed towards the development of a vibration-mechanical spreading method. This method involves the use of ultrasonically vibrating spreading fixtures (vibrating in the axial direction) to spread-out a fibre tow [126]. An example of such a method is schematically shown in Figure A5.

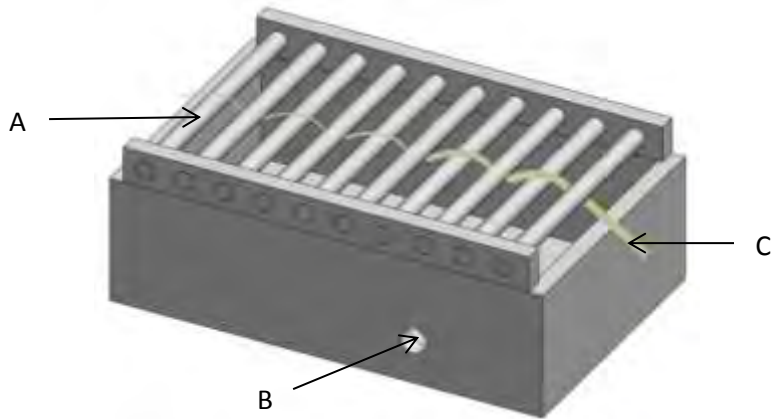


Figure A5. Schematic diagram of a vibration-mechanical fibre spreading method. The highlighted components are: (A) spreading fixtures; (B) a speaker system; and (C) a spread fibre tow.

With reference to Figure A5, fibre spreading was achieved by using acoustic energy from a vibrating device i.e. speaker system, to form a vibrating gaseous medium. Fibre spreading was then achieved through the combined action of axial fixture vibration and gaseous movement. For reference, the method shown in Figure A5 was used to spread a fibre tow (Hercules AS4 carbon-fibres with a 5 mm width) up to ~ 9 cm at a recommended sound level of 80 - 130 dB with a preferred frequency of 32 - 39 Hz [126].

6.2 Appendix B: Mechanical Testing Load/Displacement Curves

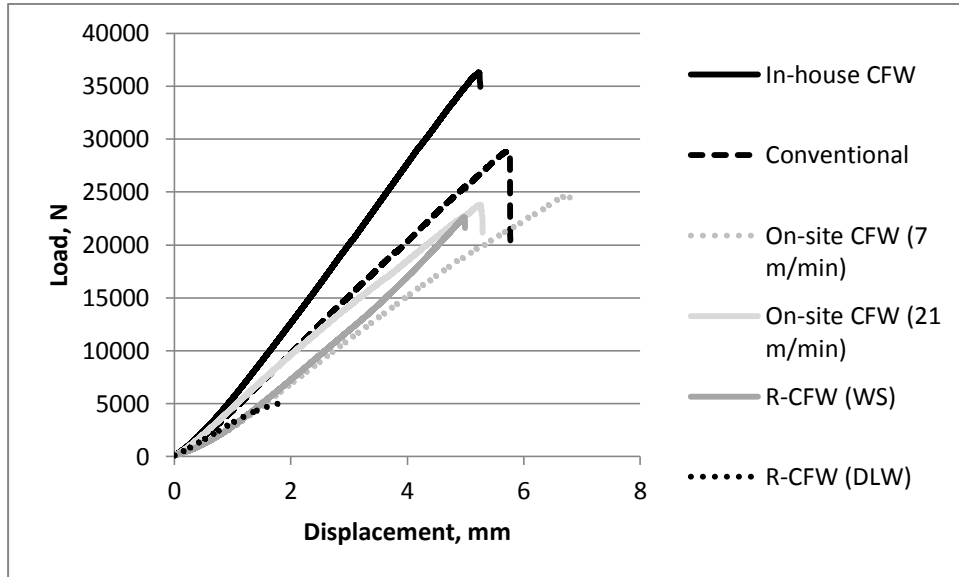


Figure B1. Typical load-displacement curves of filament wound tube sections under hoop tensile (split-disk) loading.

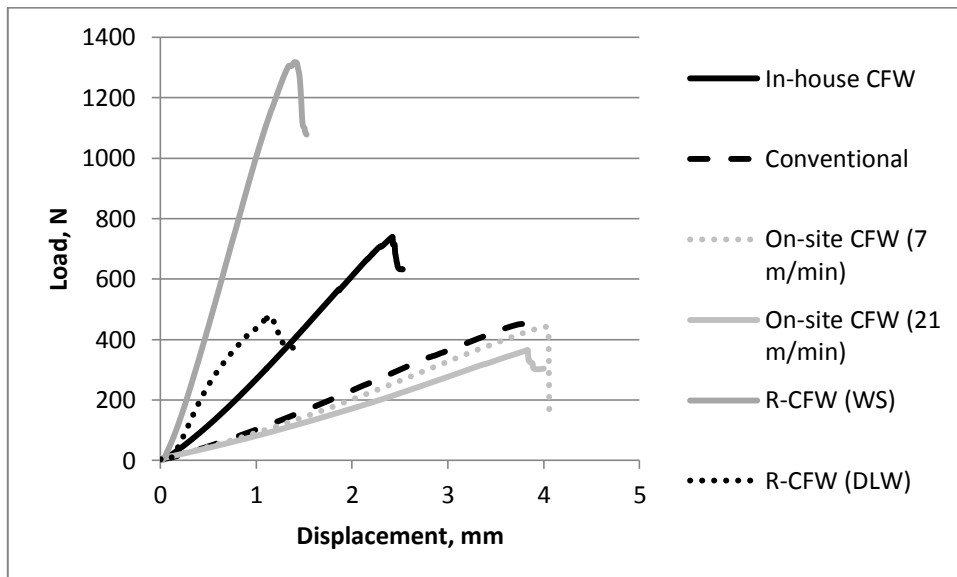


Figure B2. Typical load-displacement curves of filament wound tube sections under inter-laminar shear loading.

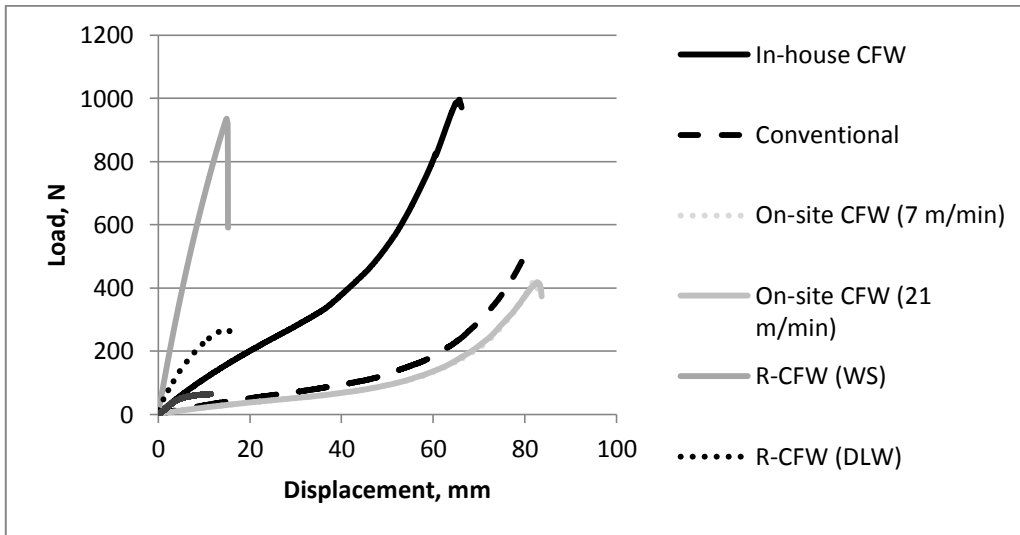


Figure B3. Typical load-displacement curves of filament wound tube sections under lateral compression.

CHAPTER 7: LIST OF DEFINITIONS AND/OR

ABBREVIATIONS

A	: Pin radius
a_h	: Gradient of velocity (\bar{v}) against distance (L)
ANOVA	: Analysis of variance
BRE	: Building research establishment
$B(V_A)$: Curve-fitting constant as a function of maximum packing capacity
C	: Radius of curvature of the roving
c	: Dimensionless shape factor
CAD	: Computer aided design
CFW	: Clean filament winding
COPV	: Composite overwrapped pressure vessel
CSM	: Chopped strand mat
$C(V_A)$: Curve-fitting constant as a function of maximum packing capacity
c_1, c_2	: Constants
d	: Injector depth
D_E	: Equivalent diameter of pores in a fibre bundle
D_h	: Hydraulic diameter
D_i	: Degree of impregnation
DLW	: Direct loom waste
EAP	: Environmental action program
F	: Form factor
h	: Injector height

HAP	: Hazardous atmospheric pollutants
$H_{(1/2)}$: Channel half-height
H_0	: Resin/film thickness at the beginning of the impregnation region
H_1	: Resin/film thickness at the end of the impregnation region
ID	: Inner-diameter
k	: Kozeny constant
K	: Permeability of the porous medium
K_x	: Axial permeability
K_y	: Transverse permeability
$K_{y.quadratic}$: Transverse permeability assuming a quadratic fibre architecture
$K_{y.hexagonal}$: Transverse permeability assuming a hexagonal fibre architecture
LCA	: Life cycle assessment
LCC	: Life cycle cost
L_1	: Impregnation length
L_{16}	: Taguchi array
$m(V_A)$: Curve-fitting constant as a function of maximum packing capacity
N	: Number of individual filaments in a fibre tow
OD	: Outer diameter
P	: Pressure generated by a fibre traversing over a pin
P_c	: Capillary pressure
R-CFW	: Recycled-Clean filament winding
Re	: Reynolds number
r_f	: Fibre radius
rpm	: Revolutions per minute

SEM	: Scanning electron microscopy
SMC	: Sheet moulded compound
T_e	: Fibre tension
T_{e0}	: Initial fibre tension
T_{e1}	: Tension per width in the impregnation region
t_i	: Infiltration time
T_i	: Infiltration thickness
T_o	: Fibre tow thickness
T_1, T_2	: Arbitrary steps of infiltration thickness
U	: Mean resin velocity over the fibre cross-section
V	: Velocity of fibre movement
V_A	: Maximum packing capacity
V_f	: Fibre volume fraction
V_p	: Velocity profile
\bar{v}	: Superficial velocity
w	: Fibre tow width
w_i	: Injector width
WS	: Waste slittings
x	: Horizontal coordinate
y	: Vertical coordinate
Z	: Cross-sectional area of the fibre tow
ε	: Porosity
η	: Viscosity of the resin
ΔP	: Pressure differential

- $\Delta P/L$: Pressure gradient over a characteristic dimension, L
- λ : Frictional factor
- ρ : Resin density
- ψ : Lateral distance between two cylindrical spreading bars
- ζ : Surface tension of the resin
- θ : Contact angle between the resin and fibre

CHAPTER 8: REFERENCES

1. Miracle, D. and Donaldson, L. (2001) *ASM Handbook, 21*, ASM International.
2. Biron, M. (2003) *Thermosets and Composites*, Elsevier Science and Technology Books.
3. AVK, (2010) 'Sustainability of fibre-reinforced plastics; An assessment based on selected examples of application' *AVK Federation of Reinforced Plastics*.
4. Abdalla, F., Mutasher, S., Khalid, S., Sapuan, S., Hamouda, A., Sahari, B. and Hamdan, M. (2005) 'Design and fabrication of low cost filament winding machine' *Journal of Materials and Design*.
5. Peters, S.T. and McLarty, L. (2001) 'Filament Winding' *ASM Handbook, 21*, ASM International.
6. Bechtold, G. and Ye, L. (2003) 'Influence of fibre distribution on the transverse flow permeability in fibre bundles' *Journal of Composites Science and Technology*, Vol 63, pp. 2069-2079.
7. Reynolds, N. and Pharaoh, M. (2010) 'An introduction to composites recycling' *Management, Recycling and Reuse of Waste Composites*, Woodhead Publishing in Materials, Chapter 1, pp. 3-19.
8. Witten, E. and Schuster, A. (2010) 'Composites market report; Market developments, challenges and chances' *AVK Federation of Reinforced Plastics*.
9. Composites Europe 2009 Newsletter, (2009) *Reinforced Plastics*, November/December.

-
10. Green, J.E. (2001) 'Overview of Filament Winding' *SAMPE Journal*, Vol 37, pp. 7-11.
 11. Funck, R. and Neitzel, M. (1995) 'Improved thermoplastic tape winding using laser or direct-flame heating' *Journal of Composite Manufacturing*, Vol 6, pp. 3-4.
 12. Toso, Y.M.P., Ermanni, P. and Poulikakos, D. (2004) 'Thermal phenomena in fiber-reinforced thermoplastic tape winding process: computational simulations and experimental validations' *Journal of Composite Materials*, Vol 38, pp. 107-135.
 13. Kim, J., Moon, T.J. and Howell, J.R. (2003) 'Transient thermal modelling of in-situ curing during tape winding of composite cylinders' *Journal of Heat Transfer*, Vol 125, pp. 137 -146.
 14. Duvall, M., Ramani, K., Bays, M. and Caillat, F. (1996) 'In-situ composite manufacture using an electrostatic powder spray process and filament winding' *Journal of Polymers and Polymer Composites*, Vol 4, pp. 325-334.
 15. Ramani, K., Wooland, D.D. and Duvall, M.S. (1995) 'An electrostatic powder spray process for manufacturing thermoplastic composites' *Journal of Polymer Composites*, Vol 16, pp. 459-469.
 16. DuVall, F.W. (2001), 'Comparisons of wet filament winding versus prepreg filament winding for type II and type IV CNG cylinders', *SAMPE Journal*, Vol 37, No 1, pp. 38-42.

-
17. Pistor, C.M., Yardiminci, M.A. and Gucery, S.I. (1999) 'On line consolidation of thermoplastic composites using laser scanning' *Journal of Composites: Part A*, Vol 30, pp. 1149-1157.
 18. Agarwal, V., McCullough, R.L. and Schultz, J.M. (1996) 'The thermoplastic laser assisted consolidation process: mechanical and microstructure characterization' *Journal of Thermoplastic Composite Materials*, Vol 9, pp. 365-380.
 19. Van Paepegem, W., Van Schepdael, L., Degrieck, J., Samyn, P., De Baets, P., Suister, E. and Leendertz, J.S. (2005) 'Fast characterisation of carbon/epoxy rings for use in ball-joints of the maeslant storm surge barrier' *Journal of Composite Structures*.
 20. Otstavnov, A.A., Pavlov, L.D., Sladkov, A.V., Ustyugov, V.A., Braslavskii, V.A., Loenko, V.A. and Yantsev, V.M. (2006) 'Determining the annual rigidity of wound, hollow-walled polyethylene pipes of up to 2m diameter' *International Polymer Science and Technology*, Vol 33, No 5.
 21. PPG Industries (UK) Ltd, Fibre Glass Division, Wigan, Lancashire, WN2 4XZ.
 22. Kugler, D. and Moon, T.J. (2002) 'Effects of mandrel material and tow tension on defects and compressive strength of hoop-wound, on-line consolidated, composite rings' *Journal of Composites: Part A*, Vol 33A, pp. 861-876.
 23. Mertiny, P. and Ellyin, F. (2002) 'Influence of the filament winding tension on physical and mechanical properties of reinforced composites' *Journal of Composites: Part A*, Vol 33, pp. 1615-1622.

-
24. Cohen, D. and Lowe, K.A. (1991) 'The influence of epoxy matrix properties on delivered fibre strength in filament wound composite pressure vessels' *Journal of Reinforced Plastics and Composites*, Vol 10, pp. 112-131.
 25. Samanci, A., Avci, A., Tarakcioglu, N. and Sahin, O.S. (2008) 'Fatigue crack growth of filament wound GRP pipes with a surface crack under cyclic internal pressure' *Journal of Materials Science*, Vol 43, pp. 5569-5573.
 26. Kharat, D.K. and Kumar, S. (2008) 'Quality ascertaining procedures for composite barrel' Business Office, Paper 15.
 27. Masmoudi, R., Mohamed, H. and Metiche, S. (2008) 'Finite element modelling for deflection and bending responses of GFRP poles' *Journal of Reinforced Plastics and Composites*, Vol 27, pp. 639-658.
 28. Helmi, K., Fam, A. and Mufti, A. (2008) 'Fatigue life assessment and static testing of structural GFRP tubes based on coupon tests' *Journal of Composites for Construction*, Vol 12, pp. 212-223.
 29. Mertiny, P., Ellyin, F. and Hothan, A. (2004) 'An experimental investigation on the effect of multi-stage filament winding on the strength of tubular composite structures' *Journal of Composites Science and Technology*, Vol 64, pp. 1-9.
 30. Natsuki, T., Takayanagi, H., Tsuda, H. and Kemmochi, K. (2003) 'Prediction of bending strength for filament-wound composite pipes' *Journal of Reinforced Plastics and Composites*, Vol 22, pp. 695-710.

-
31. Haftchenari, H., Al-Salehi, F.A.R., Al-Hassani, S.T.S. and Hinton, M.J. (2002) 'Effect of temperature on the tensile strength and failure modes of angle ply aramid fibre (KRP) tubes under hoop loading' *Journal of Applied Composite Materials*, Vol 9, pp. 99-115.
 32. Xia, M., Kemmochi, K. and Takayanagi, H. (2001) 'Analysis of filament-wound fiber-reinforced sandwich pipe under combined internal pressure and thermomechanical loading' *Journal of Composite Structures*, Vol 51, pp. 273-283.
 33. Ha, S.K. and Jeong, J.Y. (2005) 'Effects of winding angles on through-thickness properties and residual strains of thick filament wound composite rings' *Journal of Composites Science and Technology*, Vol 65, pp. 27-35.
 34. Kaynak, C., Erdiller, E.S., Parnas, L. and Senel, F. (2005) 'Use of split-disk tests for the process parameters of filament wound epoxy composite tubes' *Journal of Polymer Testing*, Vol 24, pp. 648-655.
 35. Carrino, L., Polini, W. and Sorrentino, L. (2003) 'Modular structure of a new feed-deposition head for a robotised filament winding cell' *Journal of Composites Science and Technology*, Vol 63, pp. 2255-2263.
 36. Polini, W. and Sorrentino, L. (2005) 'Influence of winding speed and winding trajectory on tension in robotised filament winding of full section parts' *Journal of Composites Science and Technology*, Vol 65, pp. 1574-1581.
 37. Scholliers, J. and Van Brussel, H. (1994) 'Computer-integrated filament winding: Computer-integrated design, robotic filament winding and

-
- robotic quality control' *Journal of Composites Manufacturing*, Vol 5, No 1, pp. 15-23.
38. Halyard Precision Composites, Limberline Spur, Portsmouth, PO3 5HJ, UK.
 39. Silencer marine, Via Trieste, 1/C – 31057, Silea Treviso, Italy.
 40. J.A. Chamberlain, Longwood, Florida, USA.
 41. Crompton Technology Group Ltd, Thorpe Park, Banbury, Oxfordshire, OX16 4SU, UK.
 42. Tianjin, CTiHuatai Composites Co. Ltd, Leo Creative Industry Precinct, Xiqing District, China.
 43. FWT Wickeltechnik, Werner von Siemens, Str. 7, Neunkirchen, Austria.
 44. BAC Technologies Ltd, West Liberty, Ohio, USA.
 45. Structural Composite Solutions Ltd, Bothwell, Scotland, G71 8BS, UK.
 46. Tata Advanced Materials, Jigani, India.
 47. WindTec Winding Technology AS, Hareid, Norway.
 48. Luxfer Gas Cylinders, Gerzat, France.
 49. S.A. Composites, Loveland, Colorado, CO 80537, USA
 50. Qinetiq, Cody Technology Park, Ively Road, Farnborough, Hampshire, GU14 OLX, UK.
 51. C.K. Composites Inc, 361 Bridgeport Street, Mount Pleasant, Pennsylvania, USA.
 52. Plymouth University, Advanced Composites Manufacturing Centre, Plymouth, UK.
 53. C.P.L, 168 Z.A. des aubrieres, Cedex, France.

-
54. Erschings Inc, USA.
 55. CST composites, Caringbah, Australia.
 56. Laval, C. (2006) 'CADWIND 2006 – 20 years of filament winding experience' *Reinforced Plastics*, Vol 50, pp. 34-37.
 57. Vieira, P., Tenreiro, A. and Oliveira, T. (2009) 'The increase of sustainability in cylinder manufacture' *Journal of Clean Technology and Environmental Policy*, original paper.
 58. Palmer, R.J., Bonnar, G.R. and Moore, W.E. (1990), *US patent* 4,942,013.
 59. Vaidyanthan, R., Campbell, J., Lopez, R., Halloran, J., Yarlagadda, S. and Gillespie, J.W. (2005) 'Water soluble tooling materials for filament winding and VARTM' *SAMPE '05: New Horizons for Materials and Processing Technologies*, Paper 34.
 60. Everhart, M.C., Harris, D.L., Nickerson, D.M. and Hreha, R.D. (2006) 'High-temperature reusable shape memory polymer mandrels' *SAMPE '06: Creating New Opportunities for the World Economy*, Vol 51, Paper 245.
 61. Koury, A. (2005) 'Composite tooling reusable mandrel', *SAMPE Journal*, Vol 41, pp. 36-39.
 62. Bunsell, A.R. (2006) 'Composite pressure vessels supply an answer to transport problems' *Reinforced Plastics*, Vol 50, pp. 38-41.
 63. Abdalla, F.H., Megat, M.H., Sapuan, M.S. and Sahari, B.B. (2008) 'Determination of volume fraction values of filament wound glass and

-
- carbon fiber reinforced composites' *ARPJ Journal of Engineering and Applied Sciences*, Vol 3, pp. 7-11.
64. Buarque, E.N. and d'Almeida, J.R.M. (2006) 'The effect of cylindrical defects on the tensile strength of fibre/vinyl-ester matrix reinforced composite pipes' *Journal of Composite Structures*, Vol 79, Issue 2, pp. 270-279.
65. Kim, C.U., Kang, J.H., Hong, C.S. and Kim, C.G. (2005) 'Optimal design of filament wound structures under internal pressure based on the semi-geodesic path algorithm' *Journal of Composite Structures*, Vol 67, pp. 443-452.
66. Wakayama, S., Kobayashi, S., Imai, T. and Matsumoto, T. (2006) 'Evaluation of burst strength of FW-FRP composite pipes after impact using pitch-based low-modulus carbon fiber' *Journal of Composites: Part A*, Vol 37, pp. 2002-2010.
67. Hocine, A., Chapelle, D., Boubakar, M.I., Benamar, A. and Bezazi, A. (2009) 'Experimental and analytical investigation of the cylindrical part of a metallic vessel reinforced by filament winding while submitted to internal pressure' *International Journal of Pressure Vessels and Piping*, Vol 86, pp. 649-655.
68. Huang, Y.K., Frings, P.H. and Hennes, E. (2002) 'Exploding pressure vessel test on zylon/epoxy composite' *Journal of Composites: Part B*, Vol 33, pp. 117-123.

-
69. Hwang, T.K., Hong, C.S. and Kim, C.G. (2003) 'Probabilistic deformation and strength prediction for a filament wound pressure vessel' *Journal of Composites: Part B*, Vol 34, pp. 481-497.
 70. Chapelle, D. and Perreux, D. (2006) 'Optimal design of a Type 3 hydrogen vessel: Part I – Analytical modelling of the cylindrical section' *International Journal of Hydrogen Energy*, Vol 31, pp. 627-638.
 71. Parnas, L. and Katirci, N. (2002), 'Design of fibre-reinforced composite pressure vessels under various loading conditions' *Journal of Composite Structures*, Vol 58, pp. 83-95.
 72. Jones, I.A., Middleton, V. and Owen, M.J. (1996) 'Roller-assisted variant of the split disc test for filament-wound composites' *Journal of Composites: Part A*, Vol 27A, pp. 287-294.
 73. Naruse, T., Hattori, T., Miura, H. and Takahashi, K. (2001) 'Evaluation of thermal degradation of unidirectional CFRP rings' *Journal of Composite Structures*, Vol 52, pp. 533-538.
 74. Chen, W., Yu, Y., Li, P., Wang, C., Zhou, T. and Yang, X. (2007) 'Effect of new epoxy matrix for T800 carbon fibre/epoxy filament wound composites' *Journal of Composites Science and Technology*, Vol 67, pp. 2261-2270.
 75. Hernandez-Moreno, H., Douchin, B., Collombet, F., Choqueuse, D. and Davies, P. (2008) 'Influence of winding pattern on the mechanical behaviour of filament wound composite cylinders under external pressures' *Journal of Composites Science and Technology*, Vol 68, pp. 1015-1024.

-
76. Mistry, J. (1992) 'Theoretical investigation into the effect of the winding angle of the fibres on the strength of filament wound GRP pipes subjected to combined external pressure and axial loading' *Journal of Composite Structures*, Vol 20, pp. 83-90.
77. Moon, C.J., Kim, I.H., Choi, B.H., Kweon, J.H. and Choi, J.H. (2010) 'Buckling of filament-wound composite cylinders subjected to hydrostatic pressure for underwater vehicle applications' *Journal of Composite Structures*, Vol 92, pp. 2241-2251.
78. Carroll, M., Ellyin, F., Kujawski, D. and Chiu, A.S. (1995) 'The rate-dependent behaviour of $\pm 55^\circ$ filament-wound glass-fibre/epoxy tubes under biaxial loading' *Journal of Composites Science and Technology*, Vol 55, pp. 391-403.
79. Ellyin, F., Carroll, M., Kujawski, D. and Chiu, A.S. (1997) 'The behaviour of multidirectional filament wound fiberglass/epoxy tubulars under biaxial loading' *Journal of Composites: Part A*, Vol 28A, pp. 781-790.
80. Kaddour, A.S., Hinton, M.J. and Soden, P.D. (2003) 'Behaviour of $\pm 45^\circ$ glass/epoxy filament wound composite tubes under quasi-static equal biaxial tension – Compression loading: Experimental results' *Journal of Composites: Part B*, Vol 34, pp. 689-704.
81. Liao, W.C., Liu, H.K. and Tseng, L. (2004) 'Effect of fatigue stress amplitude on the 500 cycle residual strength of non-adhesive filament wound concrete composites under compression' *Journal of Composites Science and Technology*, Vol 64, pp. 2547-2556.

-
82. Tarakcioglu, N., Akdemir, A. and Avci, A. (2001) 'Strength of filament wound GRP pipes with surface crack' *Journal of Composites: Part B*, Vol 32, pp. 131-138.
 83. Gemi, L., Tarakcioglu, N., Akdemir, A. and Sahin, O.S. (2009) 'Progressive fatigue failure behaviour of glass/epoxy (± 75)₂ filament-wound pipes under pure internal pressure' *Journal of Materials and Design*, Vol 30, pp. 4293-4298.
 84. Lee, D.H., Kim, S.K., Lee, W.I., Ha, S.K. and Tsai, S.W. (2006) 'Smart cure of thick composite filament wound structures to minimise the development of residual stresses' *Journal of Composites: Part A*, Vol 37, pp. 530-537.
 85. Qing, X.P., Beard, S.J., Kumar, A., Ooi, T.K. and Change, F.K. (2007) 'Built-in sensor network for structural health monitoring of composite structure' *Journal of Intelligent Material Systems and Structures*, Vol 18, pp. 39-49.
 86. Gabrys, C.W. and Bakis, C.E. (1997) 'Design and manufacturing of filament wound elastomeric matrix composite flywheels' *Journal of Reinforced Plastics and Composites*, Vol 16, pp. 488-502.
 87. Correia, J.R., Branco, F.R. and Ferreira, J.G. (2009) 'The effect of different passive fire protection systems on the fire reaction properties of GFRP pultruded profiles for civil construction' Accepted manuscript for *Journal of Composites: Part A*.
 88. Gadam, S.U.K., Roux, J.A., McCarty, T.A. and Vaughan, J.G. (2000) 'The impact of pultrusion processing parameters on resin pressure rise

-
- inside a tapered cylindrical die for glass-fibre/epoxy composites' *Journal of Composites Science and Technology*, Vol 60, pp. 945-958.
89. Binetruy, C., Hilaire, B. and Pabiot, J. (1998) 'Tow impregnation model and void formation mechanisms during RTM' *Journal of Composite Materials*, Vol 32, pp. 223-245.
90. Erdiller, E.S. (2004) 'Experimental investigation for mechanical properties of filament wound composite tubes' Master of Science in Mechanical Engineering Thesis, Middle East Technical University, Turkey.
91. Sobrinho, L.L, Colado, V.M.A. and Bastian, F.L. (2011) 'Development and characterisation of composite materials for production of composite risers by filament winding' *Journal of Materials Research*, Vol 14(3), pp. 287-298.
94. Foley, M.E. and Gillespie, J.W. (2005) 'Modelling the effect of fibre diameter and fibre bundle count on tow impregnation during liquid moulding processes' *Journal of Composite Materials*, Vol 39, No 12, pp. 1045-1065.
95. Gaymans, R.J. and Wevers, E. (1998) 'Impregnation of a glass fibre roving with a polypropylene melt in a pin assisted process' *Journal of Composites: Part A*, Vol 29, pp. 663-670.
96. Gebart, B.R. (1992) 'Permeability of Unidirectional Reinforcements for RTM' *Journal of Composite Materials*, Vol 26, No 8, pp. 1100-1133.
97. Amico, S.C. and Lekakou, C. (2002) 'Axial impregnation of a fiber bundle Part 1: capillary experiments' *Journal of Polymer Composites*, Vol 12, Issue 2, pp. 249-263.

-
98. Carman, P.C. (1937) 'Fluid flow through granular beds' *Transactions of the Institution of Chemical Engineers*, Vol 15, pp. 150-156.
99. Cai, Z. and Berdichevsky, A.L. (1993) 'An improved self-consistent method for estimating the permeability of a fibre assembly, *Journal of Polymer Composites*, Vol 14, Issue 4, pp. 314-323.
100. Berdichevsky, A.L. and Cai, Z. (1993) 'Preform permeability prediction by self consistent method and finite element simulation' *Journal of Polymer Composites*, Vol 14, Issue 2, pp. 132-143.
105. Brusckke, M.V. and Advani, S.G. (1993) 'Flow of generalised Newtonian fluids across a periodic array of cylinders' *Journal of Rheology*, Vol 37, Issue 3, pp. 479-498.
106. Ahn, K.J. and Seferis, J.C. (1991) 'Simultaneous measurements of permeability and capillary pressure of thermosetting matrices in woven fabric reinforcements' *Journal of Polymer Composites*, Vol 12, No 3, pp. 146-152.
107. Bates, P.J. and Charrier J.M. (1999) 'Effect of process parameters on melt impregnation of glass roving' *Journal of Thermoplastic Composite Materials*, Vol 12, pp. 276-294.
108. Chandler, H.W., Devlin, B.J. and Gibson, A.G. (1992) 'A model for the continuous impregnation of fibre tows in resin baths with pins' *Journal of Plastics, Rubber, and Composites Processing and Application*, Vol 18, Issue 4, pp. 215-220.

-
109. Ames, T., Kenley, R.L., Powers, E.J., West, W., Wydand, W.T. and Lomax, B.R. (2007) 'Method and apparatus for making an absorbent composite' US Patent: 7,181,817.
 110. Akase, D., Matsumae, H., Hanano, T. and Sekido, T. (2000) 'Method and apparatus for opening reinforcing fibre bundle and method of manufacturing prepreg', US Patent: 6,094,791.
 111. Tanaka, K., Ohtani, H., Matsumae, H., Tsuji, S. and Akase, D. (2004) 'Production device and method for opened fibre bundle and prepreg production method' US Patent: 6,743,392.
 112. Nakagawa, N. and Ohsora, Y. (1992) 'Fibre separator for producing fibre reinforced metallic or resin body', US Patent: 5,101,542.
 113. Guirman, J.M., Lecerf, B. and Memphis A. (2005) 'Method and device for producing a textile web by spreading tows' US Patent: 6,836,939.
 114. Marissen, R., Van Der Drift, L.T. and Sterk, J. (2000) 'Technology for impregnation of fibre bundles with a molten thermoplastic polymer' *Journal of Composites Science and Technology*, Vol 60, pp. 2029-2034.
 115. Lifke, J.L., Busselle, I.D., Finley, D.J. and Gordon, B.W. (2000) 'Method and apparatus for spreading fibre bundles' US Patent: 5,310,582.
 116. Pryor, J.W. (1985) 'Method and apparatus for conveying filter tow', US Patent: 4,537,583.
 117. Van den Hoven, G. (1981) 'Widening-narrowing guide for textile filament bundle' US Patent: 4,301,579.
 118. Kiss, P.A., Deaton, J.M., Parsons, M.S. and Coffey, D. (2002) 'Apparatus and method for splitting a tow of fibres', US Patent: 6,385,828.

-
119. Blackburn, R.M. (1979) 'Fibre opening apparatus for an open-end spinning machine' US Patent: 4,169,348.
 120. Krueger, R.G. (2001) 'Apparatus and method for spreading fibrous tows into linear arrays of generally uniform density and products made thereby' US Patent: 6,311,377.
 121. Belvin, H.L., Cano, R.J., Johnston, N.J. and Marchello, J.M. (2002) 'Process of making boron-fibre reinforced composite tape', US Patent: 6,500,370.
 122. Neuert, R. and Huber, B. (1993) 'Process and apparatus for guiding a tow' US Patent: 5,214,828.
 123. Yamaguchi, M., Yamaguchi, S. and Ohokubo, T. (1978) 'Tow opening apparatus' US Patent: 4,120,079.
 124. Yawaza, M., Kurihara, K., Tani, H. and Matsumoto, M. (1976) 'Method for producing laterally spread reticular web of split fibers' US Patent: 3,953,909.
 125. Vyakarnam, M.N. and Drzal, L.T. (1994) 'Apparatus and high speed method for coating elongated fibers' *US Patent*: 5,310,582.
 126. Iyer, S. and Drzal, L.T. (1991) 'Method and system for spreading a tow of fibres' US Patent 5,042,122.
 127. Chen, J.C. and Chao, C.G. (2001) 'Numerical and experimental study of internal flow field for a carbon fibre tow pneumatic spreader', *Journal of Metallurgical and Materials Transactions B*, Vol 32B, pp. 329-339.

-
128. Sihn, S., Kim, R.Y., Kawabe, K. and Tsai, S.W. (2006) 'Experimental studies of thin-ply laminated composites' *Journal of Composites Science and Technology*, Vol 67, pp. 996-1008.
 129. Chung, T.S., Furst, H., Gurion, Z., McMahon, P.E., Orwoll, R.D. and Palangio, D. (1986) 'Process for preparing tapes from thermoplastic polymers and carbon fibres' US Patent: 4,588,538.
 130. McMahon, P.E., Chung, T.S. and Ying, L. (1989) 'Process for preparing composite articles from composite fibre blends' US Patent: 4,871,491.
 131. Newell, J.A. and Puzianowski, A.A. (1999) 'Development of a pneumatic spreading system for Kevlar-based SiC-precursor carbon fibre tows, *Journal of High Performance Polymer*, Vol 11, pp. 197-203.
 132. Daniels, C.G. (1974) 'Pneumatic spreading of filaments', US Patent: 3,795,944.
 133. Klett, J.W. and Edie, D.D. (1995) 'Flexible towpreg for the fabrication of high thermal conductivity carbon/carbon composites' *Journal of Carbon*, Vol 33, No 10, pp. 1485-1503.
 134. Street, R.L. (1991) 'Process and apparatus for blowing continuous filament tow' US Patent: 5,060,351.
 135. Holliday, R.C. (1994) 'Process of preparing engineered fiber blend' *US Patent*: 5,355,567.
 136. Hall, J.N. (1972) 'Apparatus for spreading a graphite fibre tow into a ribbon of graphite filaments' US Patent: 3,704,485.

-
137. Kawabe, K. and Tomoda, S. (2006) 'Method of producing a spread multi-filament bundle and an apparatus used in the same' US Patent: 0137156 A1.
 138. Baucom, R., Snoha, J.J. and Marchello, J.M. (1991) 'Process for application of powder particles to filamentary materials' US Patent: 5,057,338.
 139. Niina, G., Sasaki, Y. and Takahashi, M. (1967) 'Process for spreading of dividing textile materials' US Patent: 3,358,436.
 140. Peritt, J.M., Everett, R. and Edelstein, A. (1993) 'Electrostatic fiber spreader including a corona discharge device', US Patent: 5,200,620.
 141. Stenberg, E.M. (1976) 'Method and apparatus for charging a bundle of filaments' US Patent: 3,967,118.
 142. Nestler, J., Vettermann, F. and Reuchsel, D. (2007) 'Device and method from spreading a carbon fiber hank' US Patent Application Publication: 0101564 A1.
 143. Peters, S.T. and McLarty, J.L. (2001) 'Filament winding', ASM Handbook, 21, ASM.
 144. Duflou, J.R., De Moor, J., Verpoest, I. and Dewulf, W. (2009) 'Environmental impact analysis of composite use in car manufacturing' *Journal of Manufacturing Technology*, Vol 58, pp. 9-12.
 145. Stewart, R. (2010) 'Legislation for recycling waste composites', *Management, Recycling and Reuse of Waste Composites*, Woodhead Publishing in Materials, Chapter 2, pp. 20-38.
 146. The Environmental permitting (England and Wales) Regulations (2010).

-
147. European composite recycling services company, (2010) 'The green FRP recycling label'.
 148. Directive 2008/98/EC of the European Parliament and of the Council, (2008), *Official Journal of the European Union*.
 149. Directive 2003/33/EC of the European Parliament and of the Council, (2003) *Official Journal of the European Union*.
 150. Directive 2005/673/EC of the European Parliament and of the Council on end-of-life vehicles, (2005) *Official Journal of the European Union*.
 151. The Environmental permitting (England and Wales) Regulations (2007).
 152. Stewart, R. (2010) 'Waste management' *Management, Recycling and Reuse of Waste Composites*, Woodhead Publishing in Materials, Chapter 3, pp. 39-62.
 153. Council directive 96/61/EC concerning integrated pollution prevention and control, (1996) *EC Regulation*.
 154. Pickering, S.J. (2006) 'Recycling technologies for thermoset composite materials – current status' *Journal of Composites: Part A*, Vol 37, pp. 1206-1215.
 155. Otheguy, M.E., Gibson, A.G., Findon, E., Cripps, R.M., Ochoa Mendoza, A. and Aguinaco Castro, M.T. (2009) 'Recycling of end-of-life thermoplastic composite boats', *Journal of Plastics, Rubber and Composites*, Vol 38, No 9/10, pp. 406-411.
 156. Pickering, S.J., Kelly, R.M., Kennerley, J.R., Rudd, C.D. and Fenwick, N.J. (2000) 'A fluidized-bed process for the recovery of glass fibres from

-
- scrap thermoset composites' *Journal of Composites Science and Technology*, Vol 60, pp. 509-523.
157. Lester, E., Kingman, S., Wong, K.H., Rudd, C., Pickering, S. and Hilal, N. (2004) 'Microwave heating as a means for carbon fibre recovery from polymer composites: a technical feasibility study' *Materials Research Bulletin*, Vol 39, pp. 1549.
158. Cunliffe, A.M., Jones, N. and Williams, P.T. (2003) 'Recycling of fibre-reinforced polymeric waste by pyrolysis: thermo-gravimetric and bench-scale investigations' *Journal of Analytical and Applied Pyrolysis*, Vol 70, pp. 315-338.
159. Torres, A., de Marco, I., Caballero, B.M., Laresgoiti, M.F., Legaretta, J.A., Cabrero, M.A., Gonzalez, A., Chomon, M.J. and Gondra, K. (2000) 'Recycling by pyrolysis of thermoset composites: characteristics of the liquid and gaseous fuels obtained' *Journal of Fuel*, Vol 79, pp. 897-902.
160. Lee, C.K., Kim, Y.K., Phirada, P., Kim, J.S., Lee, K.M. and Ju, C.S. (2010) *Journal of Transportation Research*, Part D.
161. Soh, S.K., Lee, D.K., Cho, Q., and Rag, Q. (1994) 'Low temperature pyrolysis of SMC scrap' Proceedings of 10th Annual ASM/ESD Advanced Composites Conference, pp. 47-52.
162. Pickering, S.J. (2010) 'Thermal methods for recycling waste composites', *Management, Recycling and Reuse of Waste Composites*, Woodhead Publishing in Materials, Chapter 4, pp. 63-101.
163. Kaminsky, W. (2010) 'Fluidised bed pyrolysis of waste polymer composites for oil and gas recovery', *Management, Recycling and Reuse*

of Waste Composites, Woodhead Publishing in Materials, Chapter 8, pp. 192-214.

164. Kennerley, J.R., Kelly, R.M., Fenwick, N.J., Pickering, S.J. and Rudd, C.D. (1998) 'The characterization and reuse of glass fibres recycled from scrap composites by the action of a fluidized bed process' *Journal of Composites: Part A: Applied Science and Manufacturing*, Vol 29A, pp. 839-845.
165. Yip, H.L.H., Pickering, S. and Rudd, C. (2002) 'Characterisation of carbon fibres recycled from scrap composites using a fluidised bed process' *Journal of Plastics, Rubbers and Composites*, Vol 31, pp. 278-282.
166. Fenwick, N.J. and Pickering, S.J. (1994) 'Using waste materials to reduce emissions – combustion of glass reinforced plastic with coal in a fluidized bed' Conference on Engineering Profit from Waste IV, International Mechanical Engineering, Conference C493, pp. 157-166.
167. Wong, K.H., Pickering, S.J. and Rudd, C.D. (2010) 'Recycled carbon fibre reinforced polymer composite for electromagnetic interference shielding' *Journal of Composites: Part A*, Vol 41, pp. 693-702.
168. Turner, T.A., Harper, L.T., Warrior, N.A. and Rudd, C.D. (2008) 'Low-cost carbon-fibre-based automotive body panel systems: a performance and manufacturing cost comparison' Proceedings of the Institution of Mechanical Engineers - Part D, *Journal of Automobile Engineering*, Vol 222(D1), pp. 53-63.

-
169. Ushikoshi, K., Komatsu, N. and Sugino, M. (1995) 'Recycling of CFRP by pyrolysis method', *Journal of the Society of Materials Science*, Vol 44, pp. 428-431.
170. Norris, D.R. (1990) 'Development of the pyrolysis process for recycling of SMC' *Proceedings of the 8th Annual ASM/ESD Advanced Composites Conference*.
171. Meyer, L.O., Schulte, K. and Grove-Nielsen, E. (2009) 'CFRP – Recycling following a pyrolysis route: Process optimization and potentials' *Journal of Composite Materials*, Vol 43, pp. 1121-1132.
172. Blazso, M. (2010) 'Pyrolysis for recycling waste composites' *Management, Recycling and Reuse of Waste Composites*, Woodhead Publishing in Materials, Chapter 5, pp. 102-121.
173. Palmer, J., Ghita, O.R., Savage, L. and Evans, K.E. (2009) 'Successful closed-loop recycling of thermoset composites' *Journal of Composites: Part A*, Vol 40, pp. 490-498.
174. Recycled Carbon Fibre, Cannon Business Park, Gough Road, Coseley, West Midlands, WV14 8XR, UK.
175. Curcuras, C.N., Flax, A.M., Graham, W.D. and Hartt, G.N. (1991) 'Recycling of thermoset automotive components' SAE Technical Paper Series.
176. Jutte, R.B. and Graham, W.D. (1991) 'Recycling SMC scrap as a reinforcement' *Journal of Plastics Engineering*, Vol 47, pp. 13-16.
177. DeRosa, R., Tefeyan, E. and Mayes, S. (2004) 'Expanding the use of recycled SMC in BMC's' Global Plastics Environmental Conference 2004

-
- plastics: helping grow a greener environment, GPEC 2004, *Society of Plastics Engineers*, pp. 371-383.
178. Bledzki, A.K., Kurek, K. and Barth, C.H. (1992) 'Development of a thermoset part with SMC reclaim' Proceedings of ANTEC'92, *Society of Plastics Engineers*, pp. 1558-1560.
179. Schaefer, P. and Plowgian, A.G. (1994) 'SMC recycling: an update-ERCOM's experience in production and application' 49th Annual Conference, Composites Institute, *The Society of the Plastics Industry*.
180. Jiang, G., Pickering, S.J., Lester, E., Turner, T.A., Wong, K.H. and Warrior, N.A. (2009) 'Characterisation of carbon fibres recycled from carbon-fibre/epoxy resin composites using supercritical n-propanol' *Journal of Composites Science and Technology*, Vol 69, pp. 192-198.
181. Pinero-Hernanz, R., Dodds, C., Hyde, J., Garcia-Serna, J., Poliakoff, M., Lester, E., Cocero, M., Kingman, S., Pickering, S. and Wong, K. (2008) 'Chemical recycling of carbon fibre reinforced composites in near-critical and supercritical water', *Journal of Composites: Part A*, Vol 39, pp. 454-461.
182. Belingardi, G., Koricho, E.G. and Martorana, B. (2011) 'Design optimisation and implementation of composite and recyclable thermoplastic materials for automotive bumper', *Fifth International Conference on Advanced Computational Methods in Engineering*, Liege, Belgium.

-
183. Conroy, A., Halliwell, S. and Reynolds, T. (2006) 'Composite recycling in the construction industry', *Journal of Composites: Part A*, Vol 37, pp. 1216-1222.
184. Yuyan, L., Guohua, S. and Linghui, M. (2009) 'Recycling of carbon fibre reinforced composites using water in subcritical conditions', *Journal of Materials Science and Engineering A*, Vol 52, pp. 179-183.
185. Pinhero-Hernanz, R., Garcia-Serna, J., Dodds, C., Hyde, J., Poliakoff, M., Cocero, M., Kingman, S., Pickering, S. and Lester, E. (2008) 'Chemical recycling of carbon fibre composites using alcohols under subcritical and supercritical conditions', *Journal of Supercritical Fluids*, Vol 46, pp. 83-92.
186. Bai, Y., Wang, Z. and Feng, L. (2010) 'Chemical recycling of carbon fibres reinforced epoxy resin composites in oxygen in supercritical water' *Journal of Materials and Design*, Vol 31, pp. 999-1002.
187. Buggy, M., Farragher, L. and Madden, W. (1995) 'Recycling of composite materials' *Journal of Materials Processing Technology*, Vol 55, pp. 448-456.
188. Yoshiki, S., Yasuhiko, K., Koji, T. and Noboru, K. (2005) 'Degradation behavior and recovery of bisphenol-A from epoxy resin and polycarbonate resin by liquid-phase chemical recycling' *Journal of Polymer Degradation and Stability*, Vol 89, pp. 317-326.
189. Hyde, J.R., Lester, E., Kingman, S., Pickering, S. and Wong, K.H. (2006) 'Supercritical propanol, a possible route to composite carbon fibre

-
- recovery: A viability study' *Journal of Composites: Part A*, Vol 37, pp. 2171-2175.
190. Guinee, J.B., Gorree, M., Heijungs, R., Huppes, G., Kleijn, R., de Koning, A., van Oers, L., Sleeswijk, A.W., Suh, S., Udo de Haes, H.A., de Bruijn, H., van Duin, R. and Huijbregts, M.A.J. (2001) 'Life cycle assessment: An operational guide to the ISO standards' published report.
191. International Organization for standardization, ISO 14040, Environmental Management – Life Cycle Assessment – Principles and Framework, (1997).
192. Djekic, I. (2006) 'New approach to life cycle analysis of self-propelled agricultural machines' *Agricultural Engineering International: the CIGR Ejournal*, Invited overview No 9, Vol 8.
193. Rebitzer, G. and Buxmann, K. (2005) 'The role and implementation of LCA within life cycle management at Alcan' *Journal of Cleaner Production*, Vol 13, pp. 1327-1335.
194. ISO 14040, (1997), 'Environmental Management – Life Cycle Assessment – Principles and Framework', *International Organisation for Standardisation*.
195. ISO 14041, (1998) 'Environmental Management – Life Cycle Assessment: Goal and scope definition and inventory analysis' *International Organisation for Standardisation*.
196. ISO 14042, (2000) 'Environmental Management – Life Cycle Assessment: Life cycle impact assessment', *International Organisation for Standardisation*.

-
197. ISO 14043, (2000) 'Environmental Management – Life Cycle Assessment: Life cycle interpretation' *International Organisation for Standardisation*.
198. Joshi, S.V., Drzal, L.T., Mohanty, A.K. and Arora, S. (2004) 'Are natural fibre composites superior to glass fiber reinforced composites?' *Journal of Composites: Part A*, Vol 35, pp. 371-376.
199. Pervaiz, M. and Sain M.M. (2003) 'Carbon storage potential in natural fibre composites' *Journal of Resources, Conservation and Recycling*, Vol 39, pp. 325-340.
200. Kasai, J. (1999) 'Life cycle assessment, evaluation method for sustainable development' *JSAE Review*, Vol 20, pp. 387-393.
201. Song, Y.S., Youn, J.R. and Gutowski, T.G. (2009) 'Life cycle energy analysis of fibre-reinforced composites' *Journal of Composites: Part A*, Vol 40, pp. 1257-1265.
202. Keoleian, G.A. and Kar, K. (2003) 'Elucidating complex design and management tradeoffs through life cycle design: air intake manifold demonstration project' *Journal of Cleaner Production*, Vol 11, pp. 61-77.
203. Wotzel, K., Wirth, R. and Flake, R. (1999) 'Life cycle studies on hemp fibre reinforced components and ABS for automotive parts' *Angew Makromol Chem*: Vol 272, pp. 121-127.
204. Schmidt, W.P. and Beyer, H.M. (1998) 'Life cycle study on a natural fibre reinforced component, SAE Technical paper 982195, *SAE total life cycle conference*, Graz, Austria.

-
205. Ardente, F., Beccali, M., Cellura, M. and Mistretta, M. (2008) 'Building energy performance: A LCA case study of kenaf-fibres insulation board' *Journal of Energy and Buildings*, Vol 40, pp. 1-10.
206. Corbiere-Nicollier, T., Gfeller-Laban, B., Lundquist, L., Leterrier, Y., Manson, J.A.E. and Jolliet, O. (2001) 'Life Cycle Assessment of Biofibers Replacing Glass Fibers as Reinforcement in Plastics' *Resources, Conservation, Recycling*, Vol 33, pp. 267-287.
207. Luz, S.M., Caldeira-Pires, A. and Ferrao, P.M.C. (2010) 'Environmental benefits of substituting talc by sugarcane bagasse fibres as reinforcement in polypropylene composites: Ecodesign and LCA as strategy for automotive components' *Journal of Resources, Conservation and Recycling*, Vol 54, pp. 1135-1144.
208. Vidal, R., Martinez, P. and Garrain, D. (2009) 'Life cycle assessment of composite materials made of recycled thermoplastics combined with rice husks and cotton linters' *International Journal of Life Cycle Assessment*, Vol 14, pp. 73-82.
209. Alves, C., Ferrao, P.M.C., Silva, A.J., Reis, L.G., Freitas, M., Rodrigues, L.B. and Alves, D.E. (2010) 'Ecodesign of automotive components making use of natural jute fibre composites', *Journal of Cleaner Production*, Vol 18, pp. 313-327.
210. White, N.M. and Ansell, M. (1983) 'Straw reinforced polyester composites', *Journal of Materials Science*, Vol 18, pp. 1549-1556.

-
211. Zah, R., Hischer, R., Leao, A.L. and Braun, I. (2007) 'Curaua fibres in the automobile industry – a sustainability assessment', *Journal of Cleaner Production*, Vol 15, pp. 1032-1040.
212. Marsh, G. (2004), 'The green guide to composites: An environmental profiling system for composite materials and products', *Reinforced Plastics*, pp. 18-26.
213. Suzuki, T. and Takahashi, J. (2005) 'Prediction of energy intensity of carbon fibre reinforced plastics for mass-produced passenger cars' *Ninth Japan International SAMPE Symposia*.
214. Tonn, B.E., Schexnayder, S.M., Peretz, J.H., Das, S. and Waidley, G. (2003) 'An assessment of waste issues associated with the production of new, lightweight, fuel-efficient vehicles' *Journal of Cleaner Production*, Vol 11, pp. 753-765.
215. Shotton-Gale, N., Harris, D., Pandita, S.D., Paget, M.A., Allen, J.A. and Fernando, G.F. (2010) 'Clean and environmentally friendly wet-filament winding' *Management, Recycling and Reuse of Waste Composites*. Woodhead Publishing in Materials, Chapter 13, pp. 329-368.
216. Shotton-Gale, N., Pandita, S.D., Paget, M., Wait, C., Allen, J.A., Harris, D. and Fernando, G.F. (2009), 'An environmentally friendly modified wet-filament winding process', *ICCM Conference*.
217. Liu, T. and Fernando, G.F. (2001) 'Processing of polymer composites: an optical fibre-based sensor system for on-line amine monitoring', *Journal of Composites: Part A*, Vol 32, pp. 1561-1572.

-
218. Ghani, J., Choudhury, I. and Hassan, H., (2004) 'Application of Taguchi method in the optimisation of end milling parameters' *Journal of Materials Processing Technology*, Vol 145, pp. 84-92.
219. ASTM D2584, (2002) 'Standard test methods for ignition loss of cured reinforced plastics'.
220. ASTM D2734, (2003) 'Standard test methods for void content of reinforced plastics'.
221. ASTM D2290, (2004) 'Apparent tensile strength of ring or tubular plastics by split disk method'.
222. ASTM D2344, (2006) 'Short-beam strength of polymer matrix composite materials and their laminates'.
223. Gupta, N.K. and Abbas, H. (2000) 'Lateral collapse of composite cylindrical tubes between flat platens' *International Journal of Impact Engineering*, Vol 24, pp. 329-346.
224. Liu, T., Mohamed, R. and Fernando, G.F. (1998) 'Optical sensor system for monitoring the extent of mixing in thermosetting resins' *Smart Structures and Materials*, SPIE, San Diego, USA, pp. 154-162.